The Archaean of the Karelia Province in Finland
Edited by Pentti Hölttä
Geological Survey of Finland, Special Paper 54, 74–175, 2012

THE AGE OF THE ARCHAEAN GREENSTONE BELTS IN FINLAND

by
Hannu Huhma[1)], Irmeli Mänttäri[1)], Petri Peltonen[1,4)], Asko Kontinen[2)], Tapio Halkoaho[2)], Eero Hanski[5)], Tuula Hokkanen[1)], Pentti Hölttä[1)], Heikki Juopperi[3)], Jukka Konnunaho[3)], Yann Lahaye[1)], Erkki Luukkonen[2)], Kimmo Pietikäinen[3)], Arto Pulkkinen[1)], Peter Sorjonen-Ward[2)], Matti Vaasjoki[1,a)] and Martin Whitehouse[6)]

Huhma, H., Mänttäri, I., Peltonen, P., Kontinen, A., Halkoaho, T., Hanski, E., Hokkanen, T., Hölttä, P., Juopperi, H., Konnunaho, J., Layahe, Y., Luukkonen. E., Pietikäinen. K., Pulkkinen, A., Sorjonen-Ward, P., Vaasjoki, M. & Whitehouse, M. 2012. The age of the Archaean greenstone belts in Finland. *Geological Survey of Finland, Special Paper 54*, 74−175, 69 figures, 1 table and 4 appendices.

Reliable concordant U-Pb zircon data obtained for volcanic rocks in the Archaean greenstone belts in Finland indicate distinct age groups for each belt: Suomussalmi 2.94, 2.87 and 2.82 Ga; Kuhmo-Tipasjärvi 2.84–2.80 Ga; Ilomantsi-Kovero 2.88 and 2.75 Ga; and Oijärvi 2.82–2.80 Ga. The relative abundance of rocks within these age groups still remains unclear. Results from the Kuhmo belt indicate that the age of felsic and gabbroic rocks in the central part of the belt (Kellojärvi area) is 2798 ± 2 Ma, which is also the minimum age for the local mafic-ultramafic magmatism, including komatiites. Tholeiitic mafic rocks in the Kuhmo belt, as represented by the Moisiovaara gabbro, are 2823 ± 6 Ma in age, which is considered the maximum age for the komatiites.

Both the Kuhmo and Tipasjärvi belts contain sedimentary rocks that were deposited after 2.75 Ga, and thus at least 50 Ma after the volcanism. Still younger sediments have been found in the Arola area of the Kuhmo belt, where a deformed quartzite contains detrital zircon as young as 2.70 Ga. The sediments in the paragneiss belts were deposited ca. 2.72 Ga ago.

Sm-Nd isotopic results show that volcanic rocks in the Kuhmo and Tipasjärvi belts largely represent newly mantle-derived material. The bulk of the granitoids surrounding the belt postdate the volcanic rocks, and the isotope results as a whole suggest that the contribution of older crustal material was negligible and does not support the existence of continental basement during the formation of the supracrustal rocks within these belts. In contrast, in the Suomussalmi belt, Sm-Nd and Pb isotope results indicate a major involvement of significantly older crustal material (>3 Ga). A minor contribution of older crustal material is also evident in the Ilomantsi belt, where some igneous rocks contain xenocrystic zircon up to 3.3 Ga in age. Altogether, the isotope results suggest that the schist belts store a long-lived (>200 Ma), fragmentary record of geological evolution, possibly in various geodynamic settings, including an oceanic plateau (Kuhmo, Tipasjärvi), island arc (Ilomantsi), back arc/intra-arc (paragneiss belts) and intra-continental rift (Suomussalmi).

Keywords (GeoRef Thesaurus, AGI): schist belts, greenstone belts, absolute age, U/Pb, Sm/Nd, isotopes, lead, Archean, Finland

[1)] *Geological Survey of Finland, P.O. Box 96, FI-02151 Espoo, Finland*
[2)] *Geological Survey of Finland, P.O. Box 1237, FI-70211 Kuopio, Finland*
[3)] *Geological Survey of Finland, P.O. Box 77, FI-96101 Rovaniemi, Finland*
[4)] *Present address: First Quantum Minerals Ltd, Kaikukuja 1, FI-99600 Sodankylä, Finland*
[5)] *Department of Geosciences, P.O. Box 3000, FI-90014 University of Oulu, Finland*
[6)] *Swedish museum of Natural History, P.O. Box 50007, SE-10405 Stockholm, Sweden*
[a)] *deceased*

E-mail: hannu.huhma@gtk.fi

INTRODUCTION

The age and other characteristics of the Archaean volcano-sedimentary belts, especially their relationship with the surrounding granitic-gneissic terrains, are essential in modelling the evolution of the Archaean lithosphere. From the Finnish Archaean bedrock, multi-grain zircon U-Pb TIMS analyses have been available for decades (e.g. Kouvo 1958, Wetherill et al. 1962, Hyppönen 1983). Although often being imprecise, these data have provided useful constraints for the geological evolution of the Archaean crust. Precise multi-grain dating has often been difficult because of the presence of xenocrystic zircon and/or effects of metamorphism. A frequent problem is also that suitable materials for dating are scarce, and the identification of their protoliths may also be difficult because of strong metamorphic effects. The Sm-Nd and Rb-Sr methods have turned out to be even more problematic in the dating of Archaean volcanic rocks. Primary igneous minerals are commonly unavailable, and the very strict assumptions required for whole-rock dating are usually difficult to verify.

Recently, a large amount of new U-Pb data has been obtained from the Archaean schist/ greenstone belts in Finland, including the Suomussalmi, Kuhmo, Tipasjärvi, Ilomantsi (Hattu), Kovero and Oijärvi belts (Fig. 1). The aim of this paper

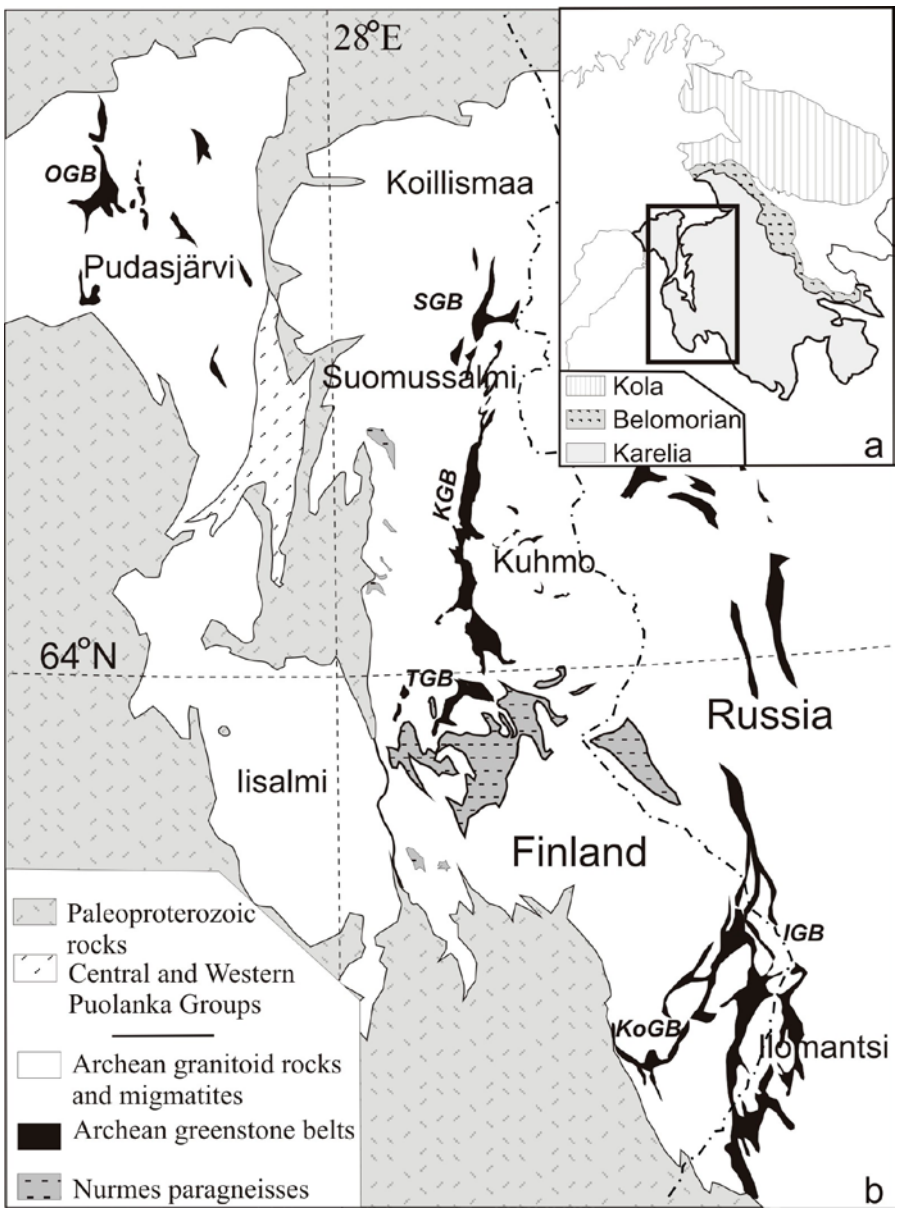

Fig. 1. (a) Major Archaean tectonic provinces of the central part of Finland and adjacent Russian Karelia. (b) Generalized geological map of central Finland (from Kontinen et al. 2007) showing the main Archaean units. OGB/SGB/KGB/TGB/IGB/ KoGB = Oijärvi/ Suomussalmi/ Kuhmo/ Tipasjärvi/ Ilomantsi/ Kovero greenstone belt.

is to present these results together with some new data on Archaean granitoids and paragneisses outside the greenstone belts. The U-Pb results from ca. 60 samples consist of ca. 600 analyses by SIMS, 200 analyses by LA-MC-ICPMS and 170 analyses using TIMS. These results construct a much-improved basis for constraining the Archaean evolution in Finland and the entire Fennoscandian Shield. As practically all samples are from deformed and metamorphosed rocks, mostly metamorphosed under amphibolite facies conditions, the "meta" prefix is not generally used. Sample sites are shown on bedrock maps (e.g. Fig. 4), which are based on GTK's database (1:1 000 000, DigiKP 200) (http://www.geo.fi/en/bedrock.html). Sample co-ordinates are given in the associated paper on Sm-Nd isotopes (Huhma et al. this volume; also http://geomaps2.gtk.fi/activemap/).

METHODS

Sampling for the present isotope studies was mostly carried out in conjunction with extensive mapping projects, and the samples should thus be well chosen and relevant in solving major geological problems. Samples for the isotope studies were washed, crushed, washed again using a Wilfley table, and treated with methylene iodide and Clerici® solutions to separate the heavy minerals. Non-magnetic heavy fractions were separated with a Frantz isodynamic separator. Zircons were selected for analysis by hand-picking. Some of the fractions were air-abraded (Krogh 1982) for TIMS (thermal ionization mass spectrometer) U-Pb analyses, and for some recent analyses, zircons were treated using the chemical abrasion method by Mattinson (2005). When applying the CA-TIMS technique, we largely followed the steps described by Schoene et al. (2006), in which zircon was placed in a furnace at 900 °C for 60 hours in beakers before being transferred to Teflon microcapsules, placed in high-pressure vessels, and leached in 29M HF for 12 hours. The decomposition of minerals and extraction of U and Pb for multi-grain TIMS analyses mainly followed the procedure described by Krogh (1973). ^{235}U-^{208}Pb-spiked and unspiked isotopic ratios were measured using a VG Sector 54 or non-commercial mass-spectrometers at the Geological Survey of Finland, Espoo. The measured lead and uranium isotopic ratios were normalized to the accepted values of SRM 981 and U500 standards. Common-lead corrections were carried out using the age-related Pb isotope composition of the Stacey and Kramers (1975) model and errors of 0.2 (for $^{206}Pb/^{204}Pb$ and $^{208}Pb/^{204}Pb$) and 0.1 ($^{207}Pb/^{204}Pb$). The measured Pb blank was 10–50 pg. The U-Pb age calculations were performed using the PbDat and the Isoplot/Ex programs (Ludwig 1991, 2003).

For SIMS and LA-MC-ICPMS analyses, zircon grains were hand-picked under a binocular microscope, mounted in epoxy resin, sectioned approximately in half and polished. Back-scattered electron images (BSE) and cathodoluminescence (CL) pictures of the zircons were taken using SEM to target the analysis spots. Most of the *in situ* SIMS (secondary ion mass spectrometry) U-Pb analyses were performed on the Nordic Cameca IMS 1270 at the Swedish Museum of Natural History, Stockholm (Nordsim facility). The spot diameter for the 4-8 nA primary O_2^- ion beam was 25-15 µm (latter values apply for recent data) and oxygen flooding in the sample chamber was used to increase the production of Pb^+ ions. Three counting blocks, each including four cycles of the Zr, Pb, Th, and U species of interest, were measured from each spot. The mass resolution (M/ΔM) was 5400 (10%). The raw data were calibrated against a zircon standard (91500; Wiedenbeck et al. 1995) and corrected for modern common lead (T=0; Stacey & Kramers 1975). For the detailed analytical procedure, see Whitehouse et al. (1999) and Whitehouse and Kamber (2005). All the errors in age reported in the text and figures are given at the 2σ level.

The measurements by LA-MC-ICPMS were performed utilizing the Nu Plasma HR multicollector ICPMS at the Geological Survey of Finland in Espoo. A technique very similar to that described by Rosa et al. (2009) was applied, with the exception that a New Wave UP193 Nd:YAG laser microprobe was used. Samples were ablated in He gas (gas flow = 0.2–0.3 l/min) using a low-volume teardrop-shaped (< 2.5 cm3) laser ablation cell (Horstwood et al. 2003). The He aerosol was mixed with Ar (gas flow = 1.2 l/min) in a teflon mixing cell prior to entry into the plasma. The gas mixture was optimized daily for maximum sensitivity. All analyses were carried out in static ablation mode. Ablation conditions were the following: beam diameter generally 25 µm, pulse frequency 10 Hz, beam energy density

1.4 J/cm^2. A single U–Pb measurement included 30 s of on-mass background measurement, followed by 60 s of ablation with a stationary beam. Masses 204, 206 and 207 were measured in secondary electron multipliers, and 238 in an extra high-mass Faraday collector. The geometry of the collector block does not allow simultaneous measurement of ^{208}Pb and ^{232}Th. Ion counts were converted and reported as volts by the Nu Plasma time-resolved analysis software. ^{235}U was calculated from the signal at mass 238 using a natural ^{238}U/^{235}U ratio of 137.88. Mass number 204 was used as a monitor for common ^{204}Pb. In ICPMS analysis, ^{204}Hg mainly originates from the He supply. The observed background counting rate on mass 204 was ca. 1200 (ca. 1.3×10^{-5} V), and had been stable at that level during the year prior to the measurements. The contribution of ^{204}Hg from the plasma was eliminated by on-mass background measurement prior to each analysis. Age-related common-lead (Stacey & Kramers 1975) correction was used if the analysis showed common-lead contents above the detection limit. Signal strengths on mass 206 were typically $>10^{-3}$ V, depending on the uranium content and age of the zircon. Two calibration standards were run in duplicate at the beginning and end of each analytical session, and at regular intervals during sessions. Raw data were corrected for the background, laser-induced elemental fractionation, mass discrimination and drift in ion counter gains and reduced to U–Pb isotope ratios by calibration to concordant reference zircons of known age, using protocols adapted from Andersen et al. (2004) and Jackson et al. (2004). Standard zircons GJ-01 (609 ± 1 Ma; Belousova et al. 2006) and an in-house standard, A1772 (2711 ± 3 Ma/TIMS; 2712 ± 1 Ma/SIMS, see below), were used for calibration. The calculations were performed off-line, using an interactive spreadsheet program written in Microsoft Excel/ VBA by T. Andersen (Rosa et al. 2009). To minimize the effects of laser-induced elemental fractionation, the depth-to-diameter ratio of the ablation pit was kept low, and isotopically homogeneous segments of the time-resolved traces were calibrated against the corresponding time interval for each mass in the reference zircon. To compensate for drift in instrument sensitivity and Faraday vs. electron multiplier gain during an analytical session, a correlation of signal vs. time was assumed for the reference zircons. A description of the algorithms used is provided in Rosa et al. (2009). Plotting of the U-Pb isotopic data and age calculations were performed using the Isoplot/Ex 3 program (Ludwig 2003). All the ages were calculated with 2σ errors and without decay constants errors.

For a few samples the dating was carried out at VGESEI in St Petersburg using SHRIMP II and methods described by Williams (1998) and Larionov et al. (2004).

U-Pb ON IN-HOUSE ZIRCON STANDARDS

Zircon grains from two rock samples are used at GTK as an in-house standard for LA-MC-ICPMS analysis. These samples are a Proterozoic pyroxene-bearing granite, A382 (Voinsalmi, Rantasalmi; Patchett & Kouvo 1986), and an Archaean gabbro, A1772 (Änäkäinen, Lieksa), which have both yielded relatively concordant multi-grain TIMS Pb/U results. Both samples contain euhedral, oscillatory-zoned, prismatic zircon, but in A382 some grains have distinct core domains.

Multi-grain TIMS analyses on A382 have yielded concordant or nearly concordant data (Appendix 2). Excluding the CA-TIMS data, four concordant analyses give an age of 1877 ± 2 Ma. The two CA-TIMS analyses on coarse-grained zircon grains give a slightly older ^{207}Pb/^{206}Pb age of ca. 1885 Ma, whereas CA-TIMS analysis on fine-grained zircon is not distinct from the original data. Fifty-six analyses on 49 grains were performed using SIMS (Nordsim) in Stockholm (Appendix 1). The common-lead content is low and most analyses are concordant within error. Regression of all 56 analyses yields an age of 1879 ± 2 Ma. Concordant data points give an age of 1877 ± 2 Ma (Fig. 2a), which is considered the age of magmatic zircon.

Isotopic compositions of a few analyses from A382 are slightly off the concordia, and considering only these data, an average ^{207}Pb/^{206}Pb age of 1882 ± 3 Ma can be calculated (Fig. 2b). These include analyses on high-U core domains, but no age difference was obtained between cores and rims. Although no distinctly older cores were found in the SIMS study, the larger database acquired by LA-MC-ICPMS contains a few analyses that give ages well above 1.9 Ga. This may explain the slightly older age obtained for the CA-TIMS data above. Consequently, there are potential problems in using sample A382 as a standard. However, it has been observed that optically good-quality,

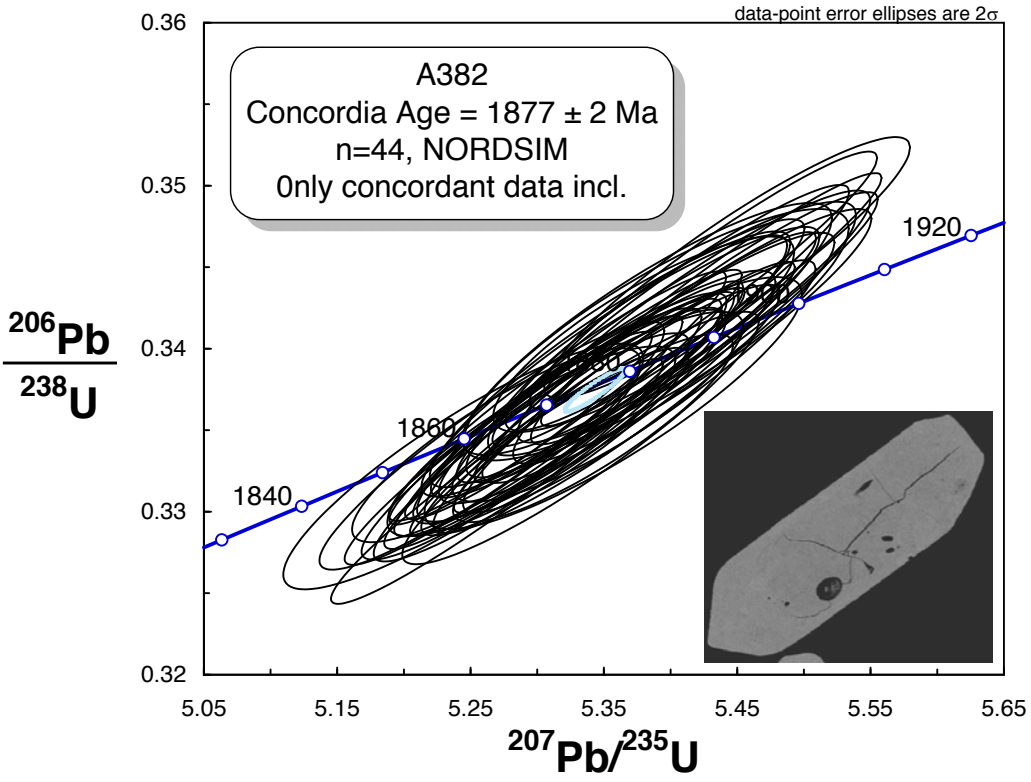

Fig. 2a. Concordia diagram of zircon analyses from the Voinsalmi granite A382.
Concordant SIMS data give an age of 1877 ± 2 Ma.

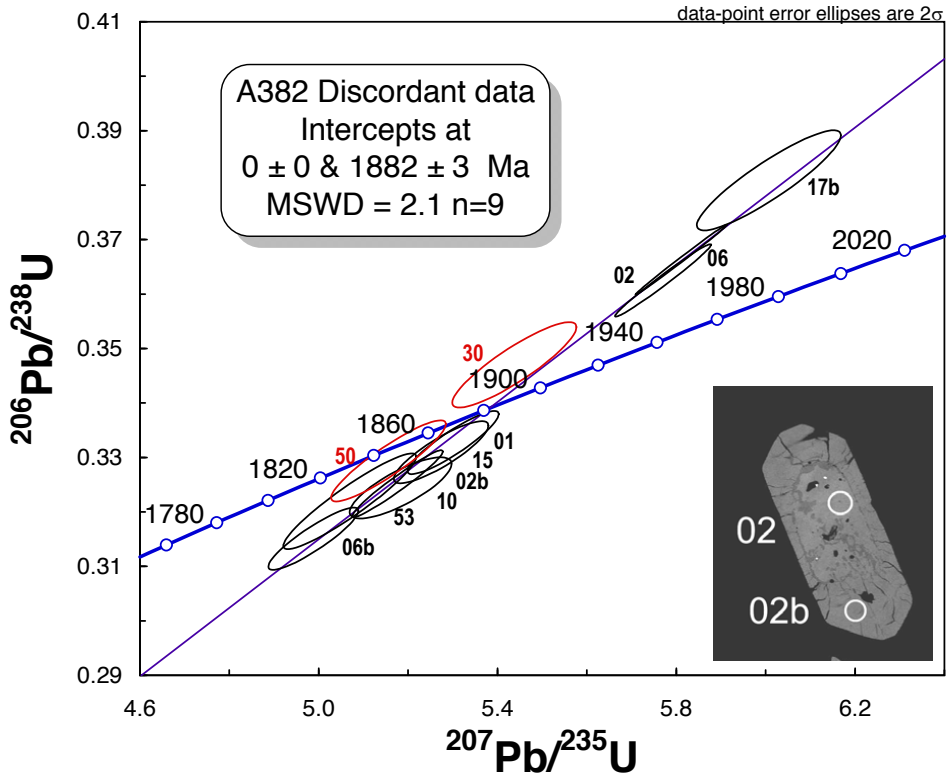

Fig. 2b. Concordia diagram of discordant zircon analyses from the Voinsalmi granite A382.

simple prismatic zircons in A382 are devoid of these problems.

The three TIMS analyses on sample A1772 are slightly discordant and yield an upper intercept age of 2711 ± 3 Ma and a lower intercept at 421 ± 200 Ma (Appendix 2). The age obtained by the ion probe (Nordsim) is 2712 ± 1 Ma and is based on 54 concordant or nearly concordant U-Pb analyses on 46 zircon grains (Appendix 1, Fig. 3). Only two analyses of the whole data set are distinct and provide slightly younger ages (n3565-44, n3565-48). The data reveal that the U content in zircon is relatively high (average 700 ppm) and the amount of common lead extremely low. Despite the high U content, most analyses are concordant within error. However, strictly taken there are still several data points slightly below the concordia, which should not appear in a perfect Pb/U standard. Heterogeneity is also evident in the Th/U ratio, which ranges from 0.01 to 1.2 (Appendix 1). For dating of Archaean zircons, it is, however, most critical to reliably measure the $^{207}Pb/^{206}Pb$ ratio, and in this respect zircon A1772 is very useful.

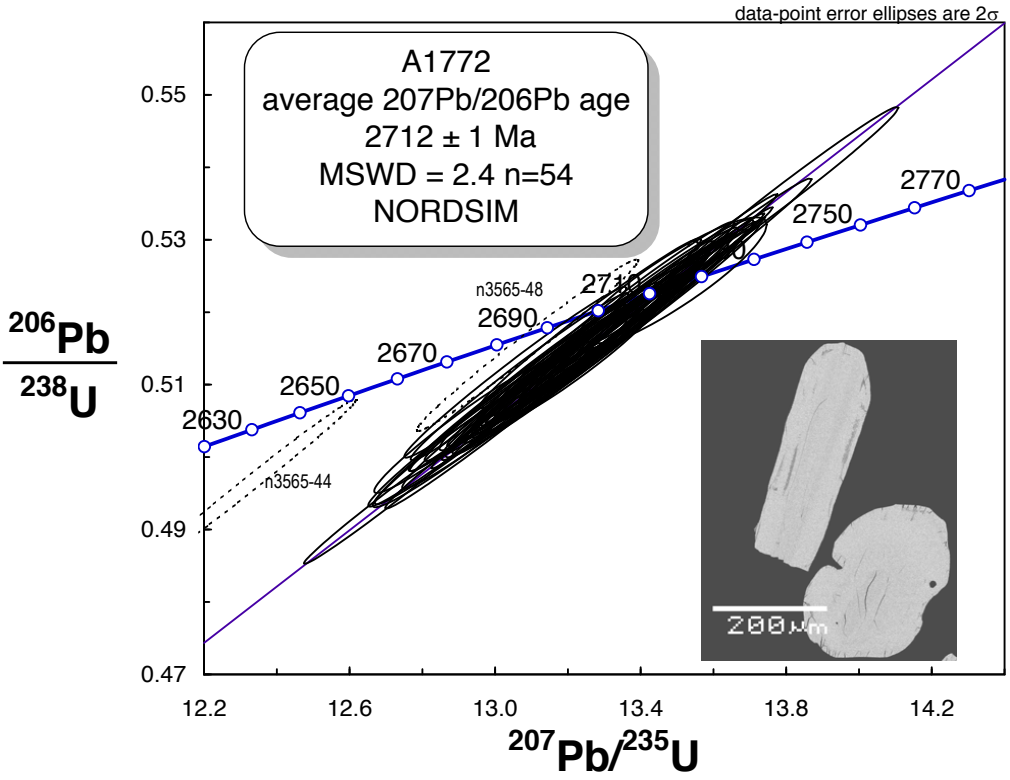

Fig. 3. Concordia diagram of zircon SIMS analyses from the Änäkäinen gabbro A1772.

SUOMUSSALMI GREENSTONE BELT

The Suomussalmi greenstone belt forms the northern part the discontinuous Tipasjärvi-Kuhmo-Suomussalmi (TKS) greenstone complex, running as a ca. 200-km-long, N–S-trending zone of supracrustal rocks in eastern Finland (Fig. 1). Although the Archaean age of these belts has been known since the early work of Kouvo and Tilton (1966), there have still been problems in constraining the detailed evolution of the supracrustal sequences within the belt and their relationship with the adjacent granitoid rocks. Based on Rb-Sr and Pb-Pb studies, Vidal et al. (1980) and Martin and Querré (1984) argued that the Suomussalmi greenstone belt was ca. 2.65–2.5 Ga old. However, U-Pb ages on zircon have shown that the volcanic rocks from the Kuhmo and Tipasjärvi greenstone belts are ca. 2.79–2.80 Ga in age (Hyppönen 1983, Vaasjoki et al. 1999), whereas even a much older age of ca. 2.97 Ga was obtained for felsic volcanic rocks from the Suomussalmi greenstone belt in the Saarikylä-Luoma area (Vaasjoki et al. 1999).

Traditionally, the Suomussalmi greenstone belt has been divided into the Luoma and Saarikylä Groups (Piirainen 1988, Engel & Dietz 1989, Luukkonen et al. 2002, Sorjonen-Ward & Luukkonen 2005), which in the Saarikylä area were thought to be separated predominantly by a N–S-trending mylonitic zone with intense albite-sericite alteration. The Luoma Group in the west mainly consists of sedimentary and volcanic rocks of andesitic-dacitic composition, while in the Saarikylä Group (= Saarikylä Formation of the Suomussalmi Group in the current geological map), mafic-ultramafic volcanic rocks are more dominant. Small mineralizations (Ag-Zn-Pb, Au, Ni, PGE) have been the reason for more detailed work in the Saarikylä-Luoma area (Kopperoinen & Tuokko 1988, Luukkonen et al. 2002). All rocks in the Suomussalmi belt are metamorphosed and deformed at amphibolite facies, but primary structures are still visible in places.

Field observations in the Saarikylä-Luoma area suggest that some rocks that were previously regarded as volcanic are rather of mixed volcanic-sedimentary in origin. The age of 2.97 Ga obtained by Vaasjoki et al. (1999) may thus represent that of detrital zircon. In order to unravel the problems related to the distincly old age of the Luoma Group, ion-microprobe dating was conducted on the original and three other related samples. The new SIMS data and additional U-Pb data obtained by TIMS and LA-MC-ICPMS, together with Sm-Nd results, are presented in this paper.

U-Pb geochronology of the Suomussalmi greenstone belt

This study concentrates on the Saarikylä-Luoma area, from where the original sample (A1191 Ala-Luoma, Vaasjoki et al. 1999) representing the Luoma Group was obtained. Three samples (A1192, A1467, A1593), originally thought to belong to the Saarikylä Group, were picked ca. 1 km east of the sampling site of A1191. According to the current understanding of the local stratigraphy, these samples also represent the Luoma Group (Fig. 4B). Two further samples from the area (A1428, A260) were collected ca. 2 km south of the sampling site of A1191. We also report data on two samples from the eastern Tormua branch of the Suomussalmi belt (A1429, A1821), and results from the volcanogenic country rock of the Kuikkapuro Au prospect in Kiannanniemi (A1701x) (Fig. 4).

A1191 Ala-Luoma volcanogenic sediment

Sample A1191-Ala-Luoma was originally interpreted as a felsic volcanic rock from the Luoma Group, but subsequent field observations have demonstrated a volcanoclastic sedimentary origin for this lithology. Sample A1191 is a fine-grained grey rock with metamorphic mineralogy.

The zircon grains are pale brown and translucent and under the binocular microscope, appear euhedral with simple prismatic surfaces dominating. The crystal edges are somewhat abraded, which is in accordance with the sedimentary nature of the rock, but does not suggest a particularly long distance of transport prior to deposition. Practically all crystals contain cracks, faint oscillatory zoning occurs occasionally, and a few crystals contain metamict zones within the crystals (Fig. 5).

The ion probe analyses obtained are relatively few (analysed in 2000, n759, Appendix 1) and form two groups. The U-Pb data on seven grains suggest an age of ca. 2.95 Ga, while two grains seem to be younger with an age of ca. 2.82 (Fig. 6a). As these two grains show magmatic oscillatory zoning and therefore are not metamorphic in origin, they should constrain the age of deposition to be significantly younger than the bulk of zircon.

In order to further study the significance of the youngest zircon grains in A1191, we also per-

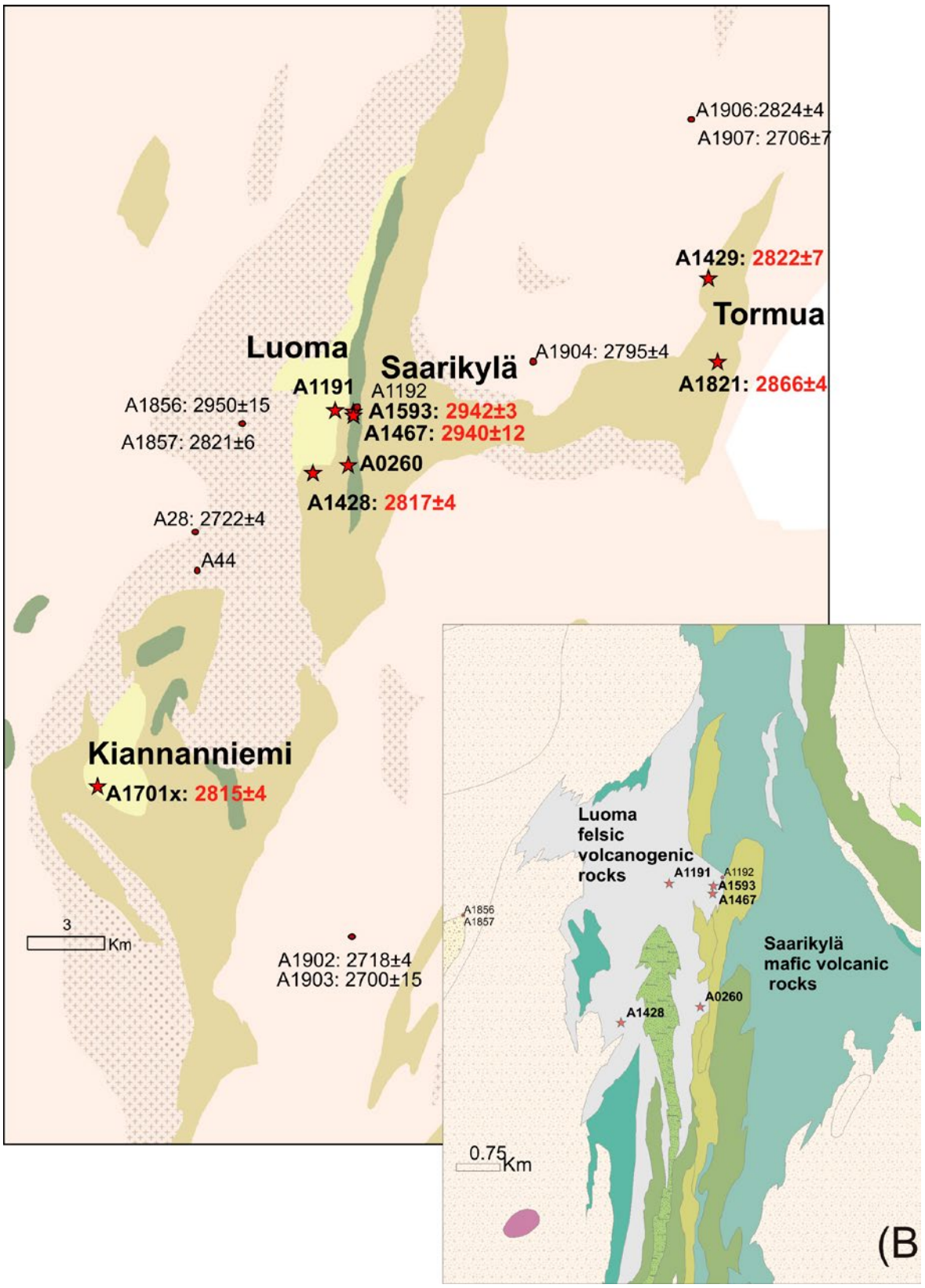

Fig. 4. Geological map of the Suomussalmi area showing the locations of the samples used for U-Pb dating (red star – this study; other samples are granidoids, published by Mikkola et al. 2011a). Igneous ages with 2-sigma errors are given in Ma after the sample number. The large map is based on the 1:1 000 000 geological map (Korsman et al. 1997), where the greenstone belt consists of three main rock types: mafic metavolcanic rocks (brown), ultramafic metavolcanic rocks (green) and intermediate-felsic metavolcanic rocks (yellow). Granitoids surrounding the greenstone belts are divided into TTGs and intrusive rocks (stippled). The inset map is based on GTK DigiKP 200. For a more detailed legend see: Bedrock of Finland – DigiKP. Digital map database [Electronic resource]. Espoo: Geological Survey of Finland [referred 31.5.2011]. Version 1.0. Available at: http://www.geo.fi/en/bedrock.html.

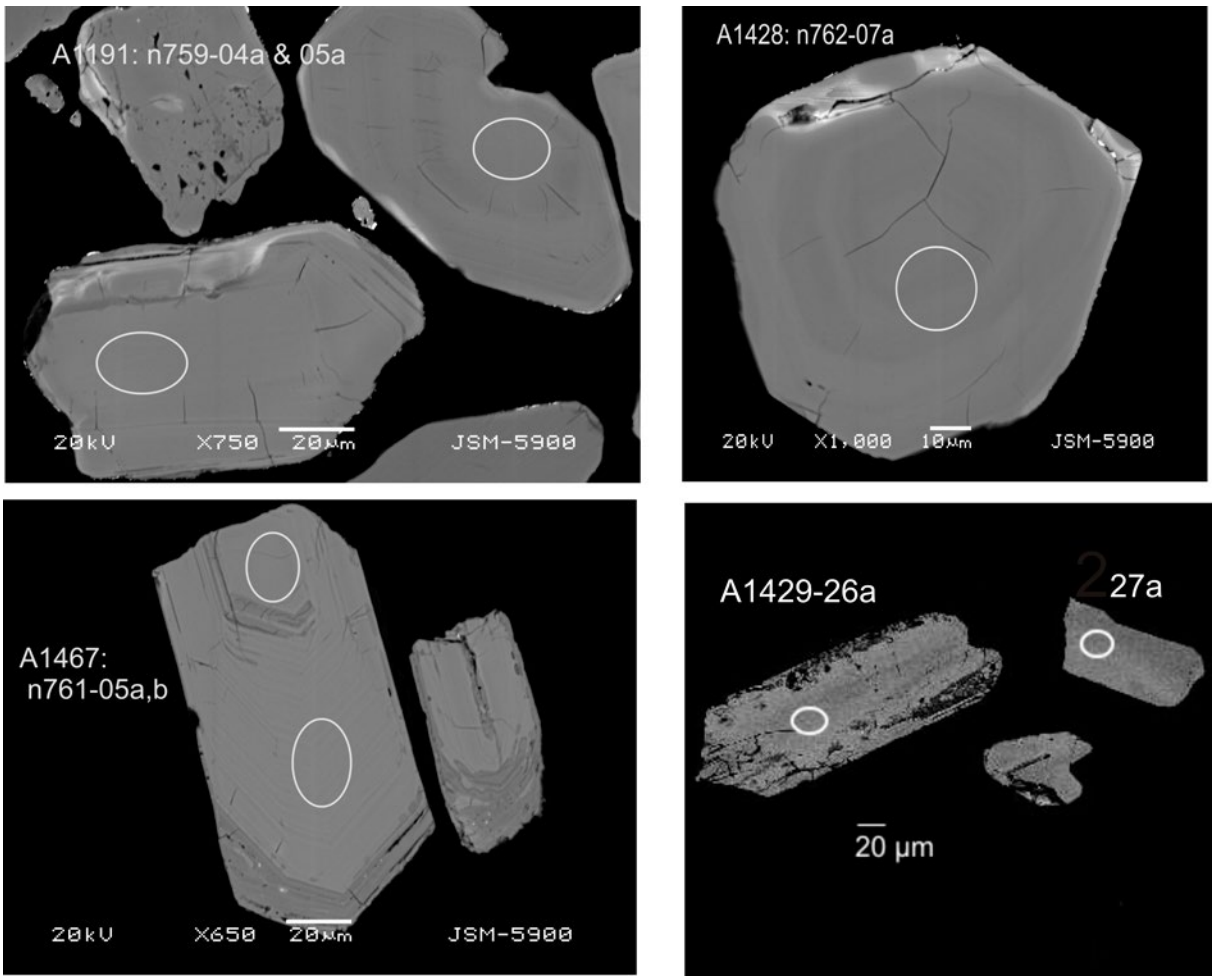

Fig. 5. BSE images of zircon A1191 (2.95 Ga), A1428 (2.82 Ga), A1429 (2.82 Ga) and A1467 (2.94 Ga).

formed LA-MC-ICPMS analyses on the original SIMS mount. The new U-Pb data show that only the two grains, originally observed by SIMS, give ages of ca. 2.82 Ga, whereas all other grains yield dates ca. 2.95 Ga (Appendix 3, Fig. 6b). Thus, considering both the SIMS and LA-MC-ICPMS data, there are only two grains out of 33 that yielded an age of ca. 2.82 Ga. As the multi-grain TIMS age estimate is also close to 2.95 Ga, we consider it is possible that the presence of 2.82 Ga grains is due to contamination during sample processing, and thus should not be used for constraining the age of deposition, unless further studies prove otherwise. In any case, the bulk of the material in the Ala-Luoma rock A1191 is from ca. 2.95 Ga sources.

A260 Haaponen greywacke

Sample A260-Haaponen is an old greywacke sample from the GTK archives, which was collected ca. 2 km south of A1191 and is also regarded as a representative of the Luoma Group. The exact coordinates of the sample are not known. In hand specimen, the rock is fine-grained and grey, similar to A1191. Mineral separation yielded abundant brown, mostly euhedral zircon grains. The population is fairly homogeneous and signs of abrasion are limited. Two multi-grain TIMS analyses carried out in 1983 (at GTK by O. Kouvo and coworkers) are discordant and plot roughly on the chord defined by the TIMS data on sample A1191, suggesting a common main source of zircon for these volcanogenic sedimentary rocks (Fig. 6a).

A1428 Mesa-aho quartz porphyry

Sample A1428-Mesa-aho is from a quartz-plagioclase porphyry, located ca. 2.5 km SSW of the site of sample A1191 (Fig. 12). Based on field evidence, the Mesa-aho rock is considered as an almost concordant, foliated felsic dyke within the volcanoclastic sediments of the Luoma Group. The rock is coarser-grained than the samples treated above, containing deformed quartz and plagioclase phenocrysts in a fine-grained matrix.

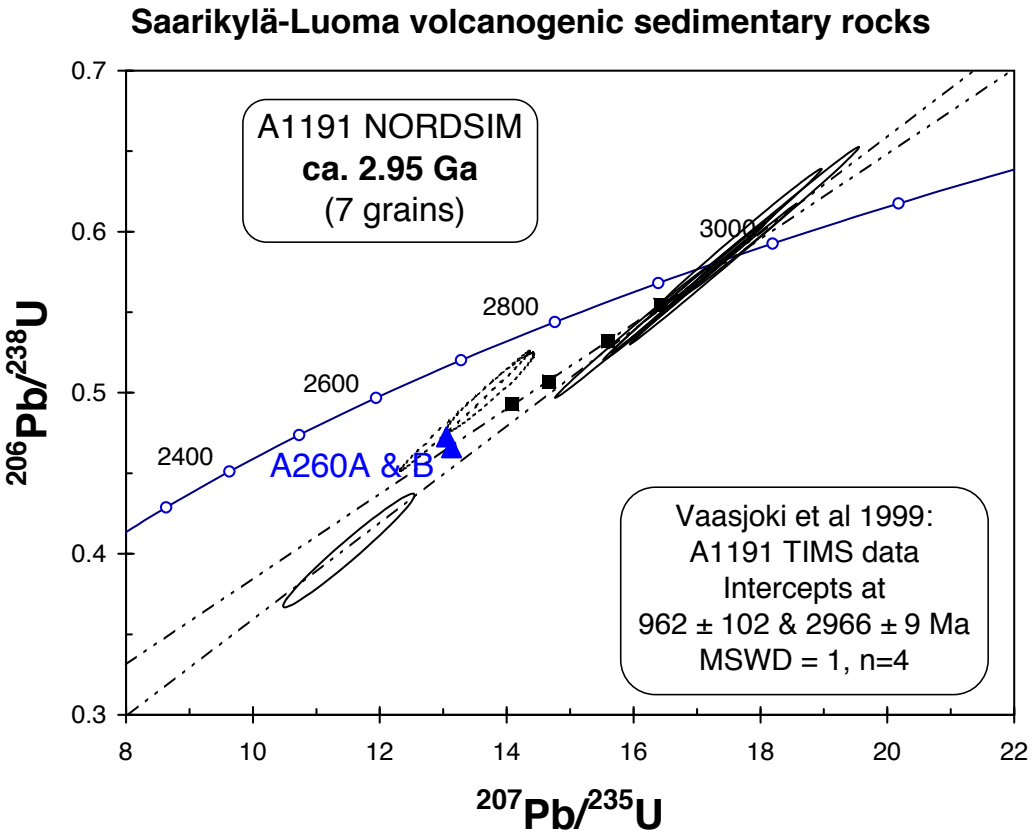

Fig. 6a. Concordia diagram of zircon analyses from the volcanosedimentary rocks of the Saarikylä-Luoma area: Error ellipses – SIMS data on A1191, squares – TIMS data on A1191 (Vaasjoki et al. 1999), triangles – TIMS data on A260.

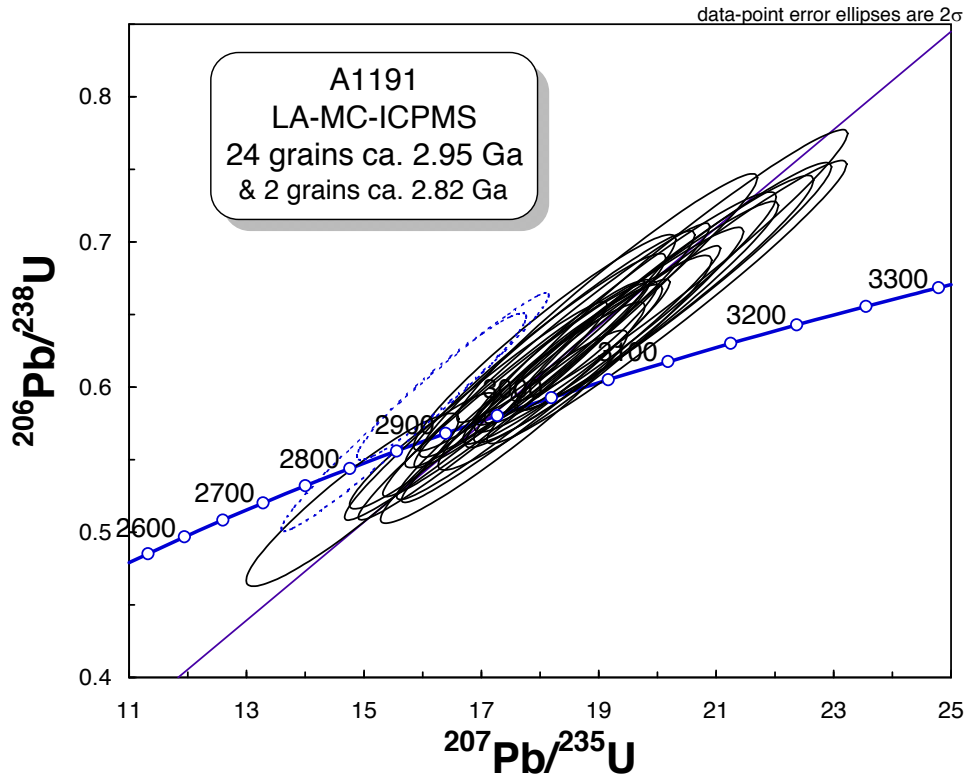

Fig. 6b. Concordia diagram of LA-MC-ICPMS analyses on zircon A1191. The two analyses at ca. 2.82 Ga are from the same grains that were measured by SIMS and yielded similarly younger ages than the other grains.

Sample A1428 yielded abundant zircon grains, which are pale brown-reddish in colour, mostly short and small (<100 μm) in size. Many grains have sharp crystal edges. SEM study showed no inner structures apart from a relatively faint zoning (Fig. 5).

The results of three TIMS U-Pb analyses on A1428 are fairly close to the concordia and provide an upper intercept age of 2817 ± 4 Ma (Appendix 2, Fig. 7). Ion microprobe analyses (n762, Appendix 1) on eight crystals are also nearly concordant and define an upper intercept at 2816 ± 12 Ma (Fig. 7). Uranium concentrations are rather low, and there is only small variation in the apparent Th/U ratios. It should be noted, however, that all isotope analyses for this sample were performed using the heaviest fraction (density > 4.3), and that zircon in the other samples in this study generally also consists of less dense material. Typically, there is a good negative correlation between density and the U content (and the degree of metamictization and discordancy).

A1467 felsic volcanic rock

Sample A1467 was collected ca. 200 m east of the shear zone that was formerly considered to mark the tectonic contact between the Luoma and Saarikylä Groups. Originally, A1467 was thought to represent the Saarikylä Group felsic volcanic rocks and correlate with the earlier sample A1192, which has yielded very discordant zircon U-Pb results (Vaasjoki et al. 1999, also Fig. 8). According to the current understanding of the local stratigraphy, these samples also represent the Luoma Group (Fig. 4B). In hand specimen, the samples are pale grey, strongly altered schists. Thin section studies reveal that they contain quartz and feldspar phenocrysts or aggregates in a sheared matrix of fine-grained quartz and sericite.

The zircon grains in the sample are turbid, brownish in colour and principally consist of simple prismatic-pyramidal, euhedral, elongated crystals. Backscatter electron images demonstrate a clear oscillatory zoning within most crystals, but in some cases this is missing, and it seems that in some crystals such unzoned domains may form ill-defined "cores" surrounded by areas with oscillatory zoning (Fig. 5). Virtually all crystals also contain numerous cracks and corroded areas. Part of these domains lie on the fringes of the crystals, but they also occur within their core parts, and the corrosion seems to advance not only along cracks but also along seemingly undisturbed

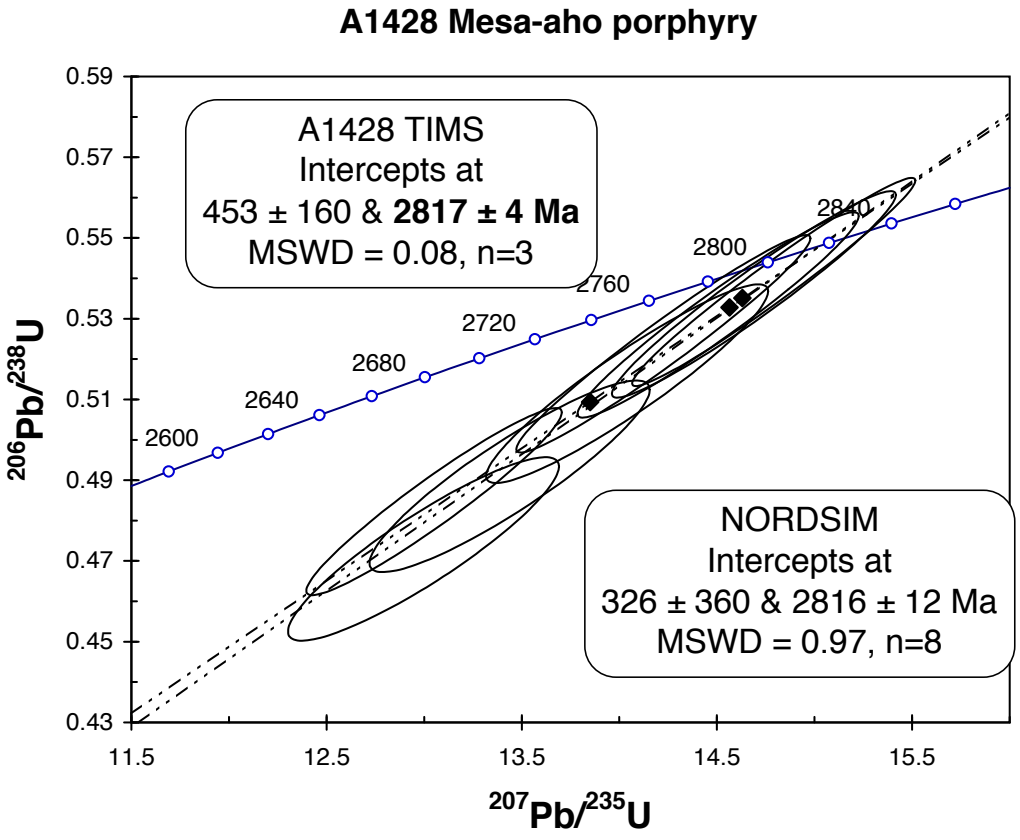

Fig. 7. Concordia diagram of zircon analyses from the Mesa-aho felsic porphyry (A1428): Error ellipses – SIMS data, diamonds – TIMS data.

crystallographic zones.

Five TIMS analyses of the zircon grains (Appendix 2) are very discordant and show a relatively high amount of common lead. They form a poorly defined, linear trend on the concordia diagram (Fig. 8) and suggest an upper intercept age of ca. 2.95 Ga. The obtained ion microprobe data (n761, Appendix 1) confirm this estimate. Excluding one analysis, the eight data points available define an age of 2940 ± 12 Ma. One analysis (n761-01) was deliberately carried out on a metamict area and is grossly discordant, and has high common lead, thus giving an obvious reason for the large discordances observed in the multi-grain TIMS analyses. If this discordant analysis is rejected, the remaining seven analyses give intercepts at 2943 ± 20 and 320 ± 480 Ma (MSWD = 4.7). One grain (n761-02) is clearly older than the others (ca. 3.2 Ga), but SEM observations do not show any obvious differences with the rest of the grains. It should be noted that analyses of the "cores" with negligible oscillatory zoning plot within the main group.

A1593 felsic porphyry

Sample A1593 (KJP-96-105) is from a quartz porphyry outcrop located ca. 150 m south of the sampling site of A1467 (Fig. 4). Based on field relationships, A1593 should represent the same association as A1467, but compared to A1467 or A1192, the rock is clearly less altered. It is characterized by bluish quartz phenocrysts 2–5 mm in diameter and occurs as a more coarse-grained foliated felsic layer (perhaps altered ash-flow) within the volcanoclastic sediments of the Luoma Group.

The sample yielded very little zircon, and no attempt was made to date this mineral. However, a few grains of monazite were obtained from the sample. A TIMS U-Pb analysis on monazite gave a nearly concordant result with a $^{207}Pb/^{206}Pb$ age of 2942 ± 3 Ma (Appendix 2). This is compatible with the zircon U-Pb results from the other two samples (Fig. 8) and, in fact, is by far the oldest monazite age obtained on any rock from Finland.

A1429 Kilpasuo andesite, Tormua

The Kilpasuo sample represents the fine-grained, intermediate volcanic rocks found in the eastern branch of the Suomussalmi belt, also known as the Tormua belt (Fig. 4). Only a small number of small, brown, euhedral zircon grains were obtained from this sample. The three TIMS analy-

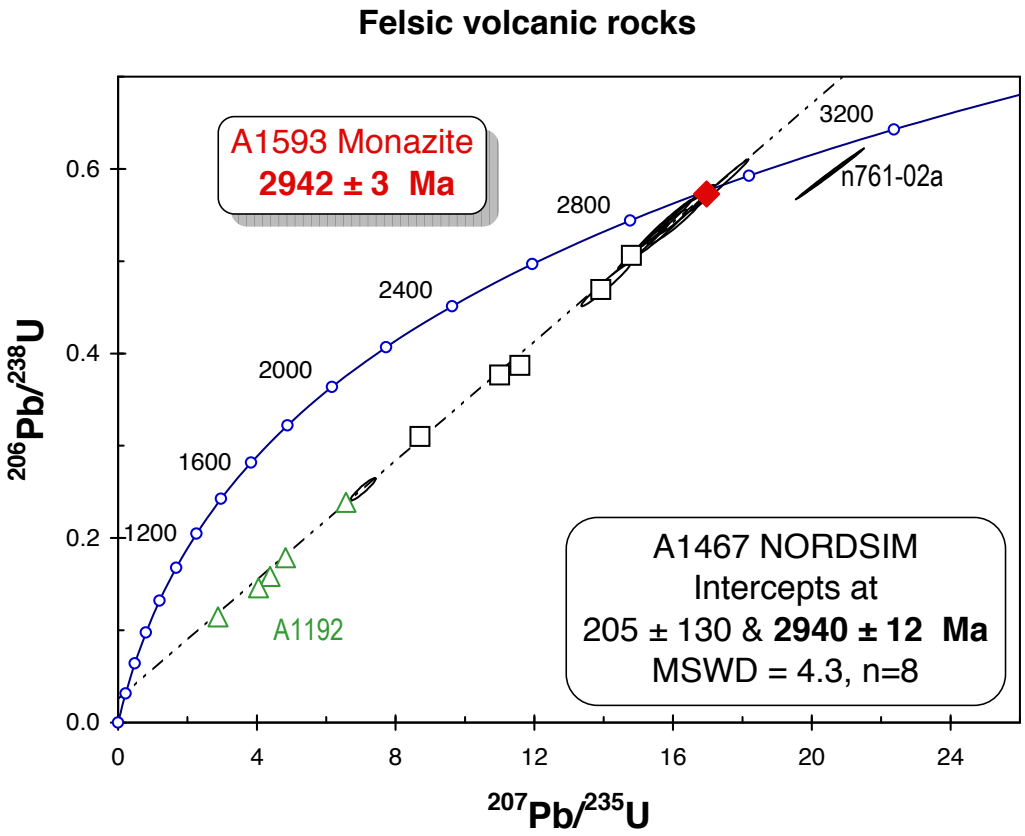

Fig. 8. Concordia diagram of zircon and monazite analyses from the felsic volcanic rocks of the Saarikylä-Luoma area: Error ellipses – SIMS data A1467 zircon, squares – TIMS data on A1467 zircon, triangles – TIMS data on A1192 zircon (Vaasjoki et al. 1999), diamond – A1593 monazite.

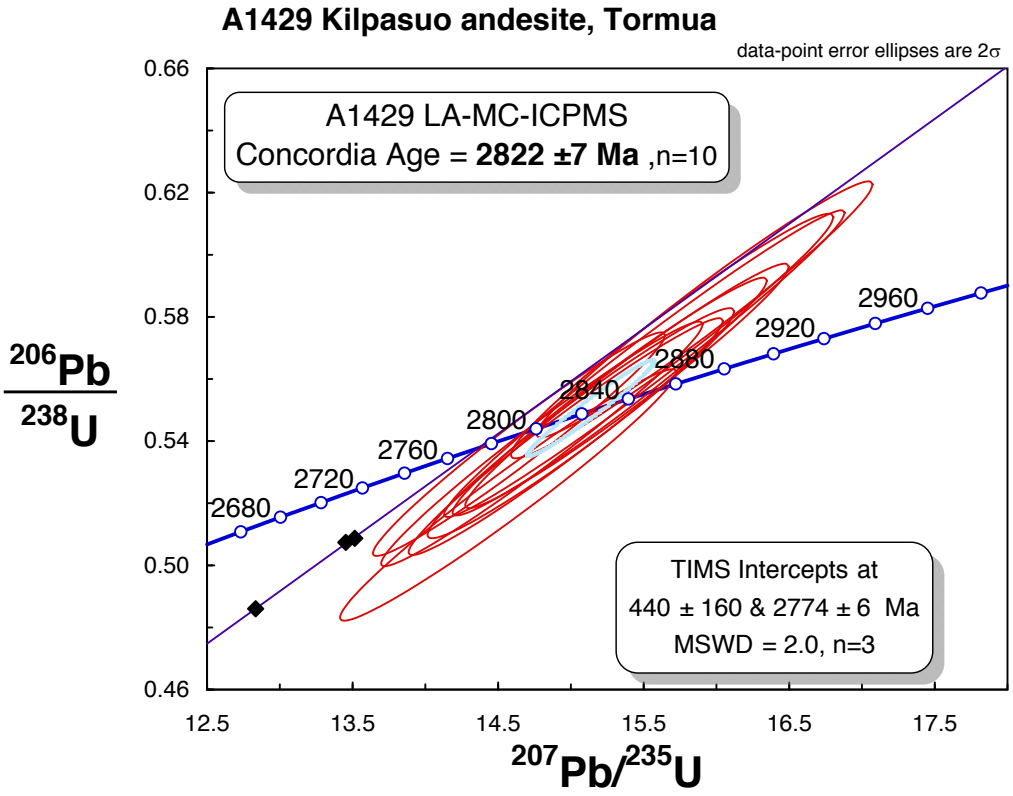

Fig. 9. Concordia diagram of zircon LA-MC-ICPMS (error ellipses) and TIMS analyses on zircon from the Kilpasuo andesite (A1429).

ses are discordant and yield intercepts at 2774 ± 6 and 440 ± 160 Ma. An analysis using chemical abrasion was not successful, since hardly any zircon was left after the treatment. The U-Pb analyses by LA-MC-ICPMS are, however, concordant and give an age of 2822 ± 7 Ma (Appendix 3, Fig. 9). The result, based on analyses utilizing the Archaean in-house standard (A1772), is considered a reliable age estimate for zircon and the Kilpasuo volcanic rocks in the Tormua belt.

A1821 Tormua gabbro

Sample A1821 was collected from a gabbroic rock that is thought to represent the coarse-grained inner part of a tholeiitic lava flow within the Tormua belt (Fig. 4). Only a small amount of zircon was obtained from this sample. In the density fraction d > 4.2 g cm^{-3}, most grains are weakly brownish and translucent. They have forms varying from long to short with prismatic faces (l:w 2-4) (zircon 07 in Fig. 14J) or more ragged and formless surfaces in more equant grains (zircon 06 in Fig. 14J). The density fraction 4.0-4.2 g cm^{-3} also includes a few transparent and more roundish zircon crystals. In BSE images, the zircon grains frequently show pale inner domains with voids and/or dense, white spots potentially resulting from exsolution. The grains are corroded, and the rims have irregular boundaries, dark BSE and frequent microcracks. In places darker, faint spots or bands also occupy the pale inner zircon domains. Zircon grain #07 represents the least corroded/altered zircon example of the long prism type (Fig. 14J).

A total of 16 zircon domains were analysed by SIMS from the Tormua gabbro (Appendix 1). Four analyses were rejected because of the high common-lead contents. In spite of the variety of analysed zircon domain types, ten of the 12 data points cluster at 2866 ± 4 Ma, which is considered the age of magmatic zircon and the age of the gabbro (Fig. 10).

A1701x Kuikkapuro

In connection with the research on the Kuikkapuro Au-prospect in the Kiannanniemi area, two samples were collected from drill-core R361 from host rocks below the mineralized zone (Fig. 4). Sample #1 (=A1701x) from the depth interval 44.50–45.50 m is a biotite-plagioclase-amphibole schist and sample #2 from the depth interval 97.00–99.70 m a biotite-garnet-amphibole schist. Both samples yielded mostly fine-grained zircon, which is generally dark brown, translucent and euhedral. In sample #2, some grains are turbid and pale.

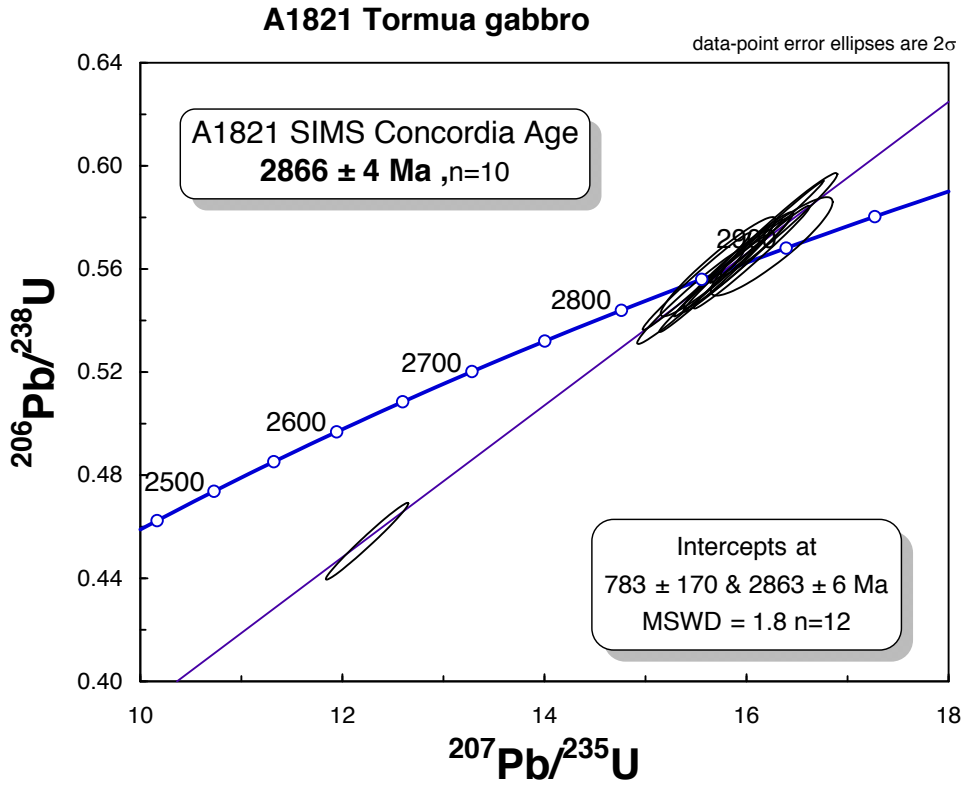

Fig. 10. Concordia plot showing zircon SIMS U-Pb isotopic results from the Tormua gabbro sample A1821, Suomussalmi, eastern Finland.

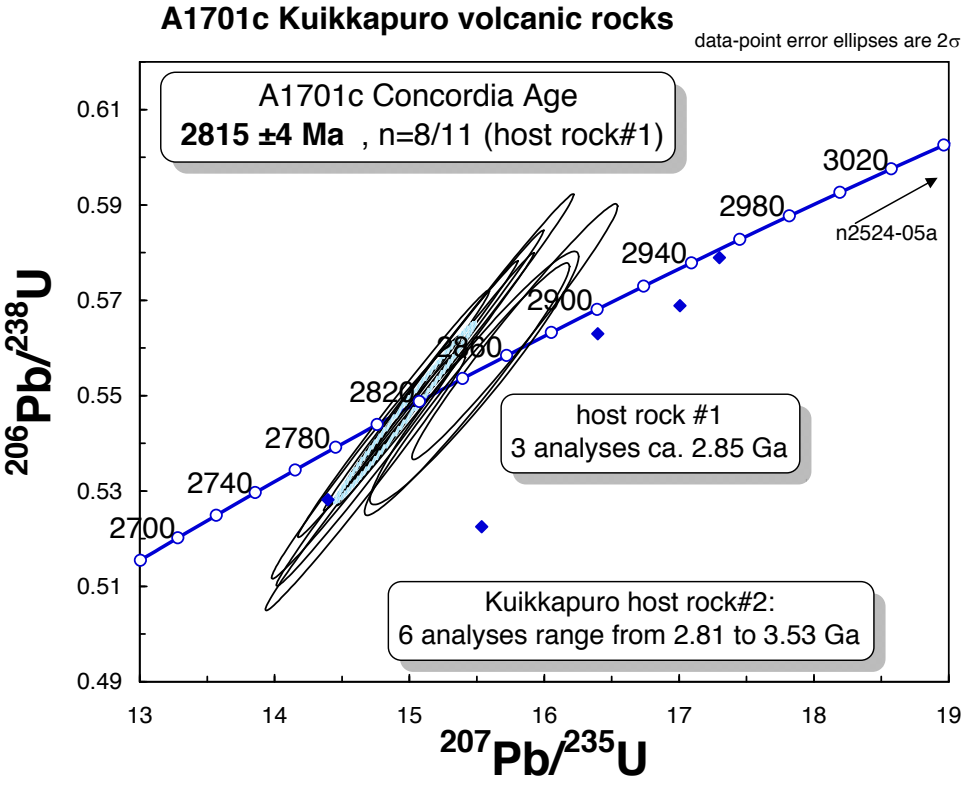

Fig. 11. Concordia plot showing zircon SIMS U-Pb isotopic results from Kuikkapuro rocks in Kiannanniemi. Error ellipses – sample 4511/98/R361/44.50-45.50, diamonds – sample 4511/98/R361/97.00-99.70 (analysis n2524-05a plots outside the figure).

Eight SIMS analyses from sample #1 are concordant and give an age of 2815 ± 4 Ma, but three analyses are slightly older at 2.85 Ga (Appendix 1, Fig. 11). The six analyses carried out on sample #2 scatter from 2.81 to 3.53 Ga. Four of these suggest an age of ca. 2.96 Ga.

Due to alteration, it is difficult to judge the ultimate origin of these schists, but the rocks in the Kiannanniemi area are mostly volcanogenic. We are inclined to think that the youngest, apparently magmatic zircons define the age of volcanism at 2815 ± 4 Ma. The older zircons are considered xenocrystic and thus suggest an involvement of older crustal material in the petrogenesis of the Kiannanniemi volcanic rocks.

Discussion on the Suomussalmi greenstone belt data

As mentioned earlier, the supracrustal rocks of the Luoma Group have been considered older than the rocks of the Saarikylä Group/Formation (Piirainen 1988, Engel & Dietz 1989, Vaasjoki et al. 1999, Sorjonen-Ward & Luukkonen 2005, Papunen et al. 2009). In the Saarikylä-Luoma area, the boundary between these two units was thought to be principally along the N–S-trending mylonitic zone with intense albite-sericite alteration. According to the current view presented on the geological map of the Saarikylä-Luoma area, the boundary is now adjusted so that the bulk of the felsic rocks in the west are considered part of the Luoma Group, and the mafic-ultramafic rocks eastwards are assigned to the Saarikylä Formation (formerly Group) of the Suomussalmi Group (Fig. 4B). Accordingly, the Luoma Group contains felsic volcanogenic rocks, which are ca. 2.94 Ga old. This is strongly supported by the U-Pb age of 2942 ± 3 Ma obtained from monazite in sample A1593.

The Suomussalmi belt also contains significantly younger felsic volcanogenic rocks, which formed ca. 2.82 Ga. These include the Mesa-aho porphyry (A1428), a volcanogenic rock in the Kiannanniemi area (A1701x), and the Kilpasuo andesite (A1429) in the Tormua branch, ca. 15 km ENE of

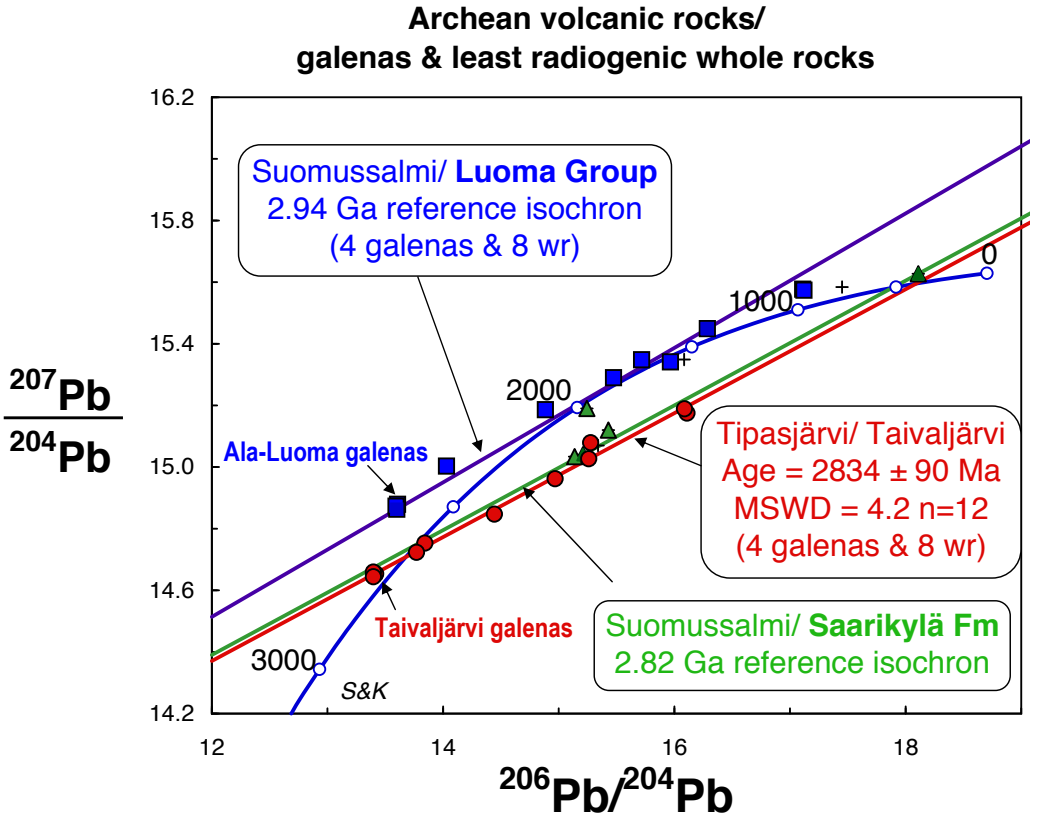

Fig. 12. Diagram showing the Pb isotope composition for galenas and whole rock samples from the Luoma Group (blue squares) and Saarikylä Formation (green triangles) from the Suomussalmi belt, compared with Pb isotope results from the Tipasjärvi belt (red dots). Data are from Vaasjoki et al. (1999), and with only the least radiogenic whole rock analyses ($^{206}Pb/^{204}Pb < 19$) plotted. The evolution of the average terrestrial lead isotope composition by Stacey and Kramers (1975) is shown for reference (S&K).

the Saarikylä area (Fig. 4). The 2866 ± 4 Ma gabbro from Tormua (A1821) represents the third age group obtained in the belt. The relative abundance of these age groups remains unclear. The two age groups obtained in the Saarikylä-Luoma area are also found in granitoids west of the greenstone belt (A1856 and A1857 in Fig. 4, Mikkola et al. 2011a).

In any case, the contribution of material at least as old as 2.94 Ga in the Suomussalmi greenstone belt is significant. In addition to U-Pb results, this becomes evident from the Sm-Nd data presented by Huhma et al. (this volume). This old age is also supported by lead isotope results (Vidal et al. 1980, Vaasjoki 1981, Vaasjoki et al. 1999). This is shown in Fig. 12, where lead isotope compositions of galena from the Ala-Luoma sulphide mineralization together with associated Luoma Group whole-rocks samples seem to plot roughly on a 2.94 Ga reference isochron. This suggests that the isotopic composition measured from galena ($^{206}Pb/^{204}Pb$ = 13.60, $^{207}Pb/^{204}Pb$ = 14.87, $^{208}Pb/^{204}Pb$ = 33.47) records the initial composition for the felsic rocks at 2.94 Ga. As this plots far above the average terrestrial evolution curve by Stacey and Kramers (1975), it means that the source for lead had an extended evolution in a high-U/Pb environment before 2.94 Ga. The diagram also shows isotope compositions for a few mafic rocks from the Saarikylä Formation. Four of them plot below the Luoma chord and suggest that the initial Pb isotope composition was clearly distinct from Luoma, and in fact similar to the composition obtained for galena from the VMS-type Taivaljärvi deposit in the 2.8 Ga Tipasjärvi greenstone belt (Vaasjoki et al. 1999). As is shown in Figure 12, the isotopic composition of associated whole-rocks samples plots roughly on a 2.8 Ga isochron, suggesting that galena ($^{206}Pb/^{204}Pb$ = 13.41, $^{207}Pb/^{204}Pb$ = 14.65, $^{208}Pb/^{204}Pb$ = 33.13) records the initial isotope composition for the Tipasjärvi volcanic rocks. As is shown by Huhma et al. (this volume), these volcanic rocks have yielded positive, depleted mantle-type initial $\varepsilon_{Nd(2800)}$ values. It is thus possible that the Pb isotope composition measured from the Taivaljärvi galena could represent a depleted mantle value at 2.8 Ga, or at least gives the maximum value, provided that some old upper crustal lead was involved. High Pb concentrations in crust-derived compared to mantle-derived materials make Pb very sensitive to crustal contamination compared to Nd. In fact, the Pb isotope composition of the Taivaljärvi galenas is more radiogenic than the composition of 2.8 Ga model mantle (Stacey & Kramers 1975, Zartman & Doe 1981).

It should be noted that in this discussion we have used only the results of the least radiogenic analyses ($^{206}Pb/^{204}Pb < 19$), which should be more important when evaluating the initial isotope composition of the system. More radiogenic data scatter considerably, which is obviously due to metamorphic effects, and the data as a whole yield younger age estimates for the Luoma Group samples (Vaasjoki et al. 1999). Based on the isotope results presented here, it is conceivable that crust as old as 3.5-3.6 Ga may have existed in the area.

KUHMO AND TIPASJÄRVI GREENSTONE BELTS

The Kuhmo greenstone belt forms the central part of the N–S-trending Tipasjärvi-Kuhmo-Suomussalmi greenstone complex in eastern Finland (Fig. 1). The geology and geochemistry of the belt has been summarized by Papunen et al. (2009), who also provide references to previous studies. One of the key localities is the Kellojärvi-Siivikkovaara area (Fig. 13), where relatively abundant komatiitic lava flows and cumulates occur and have been extensively studied.

Previous U-Pb zircon data suggest that the volcanic rocks in the Kuhmo and Tipasjärvi greenstone belts are ca. 2.79-2.80 Ga old, while the surrounding granitoids are generally younger (Hyppönen 1983, Luukkonen 1988, Vaasjoki et al. 1999, Käpyaho et al. 2006). However, due to discordant and slightly heterogeneous data, the errors in the ages of greenstone belt samples are often fairly large. Therefore, new analyses using up-to-date methods have also been performed on samples utilized in previous studies. New data including U-Pb analyses by SIMS, TIMS and LA-MC-ICPMS are presented in this paper. The Sm-Nd isotope results are discussed in the associated paper by Huhma et al. (this volume).

Fig. 13. Geological map of the Kuhmo greenstone belt showing the locations of the samples used for U-Pb dating (red star – this study; other samples – Hyppönen 1983, Luukkonen 2001, Käpyaho et al. 2006, 2007, Kontinen et al. 2007, Heilimo et al. 2011; also: http://geomaps2.gtk.fi/activemap/). Igneous ages with 2-sigma errors are given in Ma after the sample number (red – volcanic rocks of the main belt). The map is based on the 1:1 000 000 geological map (Korsman et al. 1997), where the greenstone belt consists of four main rock types: mafic metavolcanic rocks (brown), ultramafic metavolcanic rocks (green), intermediate-felsic metavolcanic rocks (yellow) and metasediments (blue). Granitoids surrounding the greenstone belts are divided into TTGs and intrusive rocks (stippled).

We present new U-Pb results on eighteen samples from the Kuhmo greenstone belt, including samples from the Ruokojärvi and Pitkäperä belts, which are located slightly east of the main Kuhmo belt (Fig. 13). The samples include ten felsic-intermediate volcanic, three gabbroic and four sedimentary rocks.

A1346 Lampela andesite

Sample A1346-Lampela represents a fine- to medium-grained volcanic unit of an intermediate composition, which occurs in the Kellojärvi area in the middle part of the Kuhmo greenstone belt and is assigned to the Mäkisensuo Formation on the geological map (Fig. 13). The sample yielded a small amount of fine-grained, pale zircon. The fraction d > 4.5 g/cm^3 contains a few small, weakly reddish, transparent and some large, turbid grains. In the density fraction 4.3–4.5 g/cm^3, the zircon population is homogeneous and mostly consists of equant (~100 μm), translucent grains. In BSE images, most zircon grains reveal weak oscillatory zoning (Fig. 14C). Inclusions are very common.

The previous multi-grain U-Pb TIMS analyses show a relatively high amount of common lead and provide fairly discordant results (Appendix 2). However, in the analysis using chemical abrasion (Mattinson 2005), the common-lead content was very low and the result nearly concordant with a ^{207}Pb/^{206}Pb age of 2797 ± 2 Ma. The six TIMS analyses are on a chord, giving an upper intercept age of 2801 ± 4 Ma and a lower intercept at 766 ± 31 Ma (Fig. 15).

A total of 13 zircon domains from the coarser-grained fraction were analysed using secondary ion mass spectrometry (Appendix 1). From these analyses, one was rejected due to a high amount of common lead. On a concordia diagram (Fig. 15), ten analyses largely from faintly zoned zircon grains plot in a cluster with a concordia age of 2798 ± 4 Ma. The distinct core and rim domains are coeval. Analysis #12 from a structurally homogeneous zircon domain indicates a marginally younger age of ca. 2.76 Ga. Zircon from this sample was also analysed by MC-ICPMS using a laser with a spot diameter of 35 μm and the GJ and in-house A382 standards. Ten analyses provide practically similar and, within 2-sigma error, mostly concordant results, which give an average ^{207}Pb/^{206}Pb age of 2794 ± 8 Ma (Appendix 3, Fig. 15). All three methods thus give consistent results, and the age of 2798 ± 4 Ma may be used as an eruption age of this volcanic rock.

A1560 Huuhilonkylä felsic rock

Sample A1560-Huuhilonkylä was collected ca. 2 km south of the Lampela andesite and represents a medium-grained, felsic rock that occurs in the middle of the Kellojärvi ultramafic complex (Fig. 13). In hand specimen, sample A1560 looks fairly similar to sample A1346 from Lampela. According to Papunen et al. (2009), the age relationship between the Kellojärvi ultramafic complex and this felsic rock has only been observed in a drill-core, where a felsic rock is seen to intrude a marginal pyroxenite of the Kellojärvi complex as dykes.

A large amount of euhedral zircon was obtained from the Huuhilonkylä sample. Most grains are translucent and reddish, with zoning typical of magmatic zircon grains. In the fine-grained, heavy fraction (+4.3/ < 75 μm), some grains are colourless and clear (analysis A1560F). The six previous multi-grain TIMS analyses give scattered and discordant U-Pb results with ^{207}Pb/^{206}Pb ages up to 2.78 Ga. Instead, the result using the CA-TIMS method is concordant at 2798 ± 2 Ma (Fig. 16). The scatter of the data is not due to zircon inheritance but obviously due to metamorphic effects, which are most prominent in analysis #A1560F.

The concordant zircon analysis is considered to date the magmatic event at 2798 ± 2 Ma. Provided that the age relationships referred to above are valid, the obtained date would give the minimum age for the Kellojärvi ultramafic complex.

A1418 Niittylahti gabbro

Sample A1418-Niittylahti was collected from a gabbro-anorthosite body also located in the middle of the Archaean Kellojärvi ultramafic complex (Fig. 13). It has been considered to be the latest magmatic phase in the Kellojärvi complex, but as it is chemically distinct from the associated ultramafic rocks, it may instead represent a distinctly later intrusive phase. The gabbro yielded a large amount of principally long (l:w ~3-8), weakly yellowish brown, mostly turbid zircon with ragged surfaces. The grain size varies from large (300 μm) to fine (<100 μm), and the morphology of the zircon is typical for zircon grains in gabbroic rocks, with abundant resorption features (Fig. 14A). Some grains show weak longitudinal compositional zoning and some have fairly diffuse pale and darker domains in BSE.

From the Niittylahti gabbro, a total of 21 zircon domains were dated by SIMS (Appendix 1).

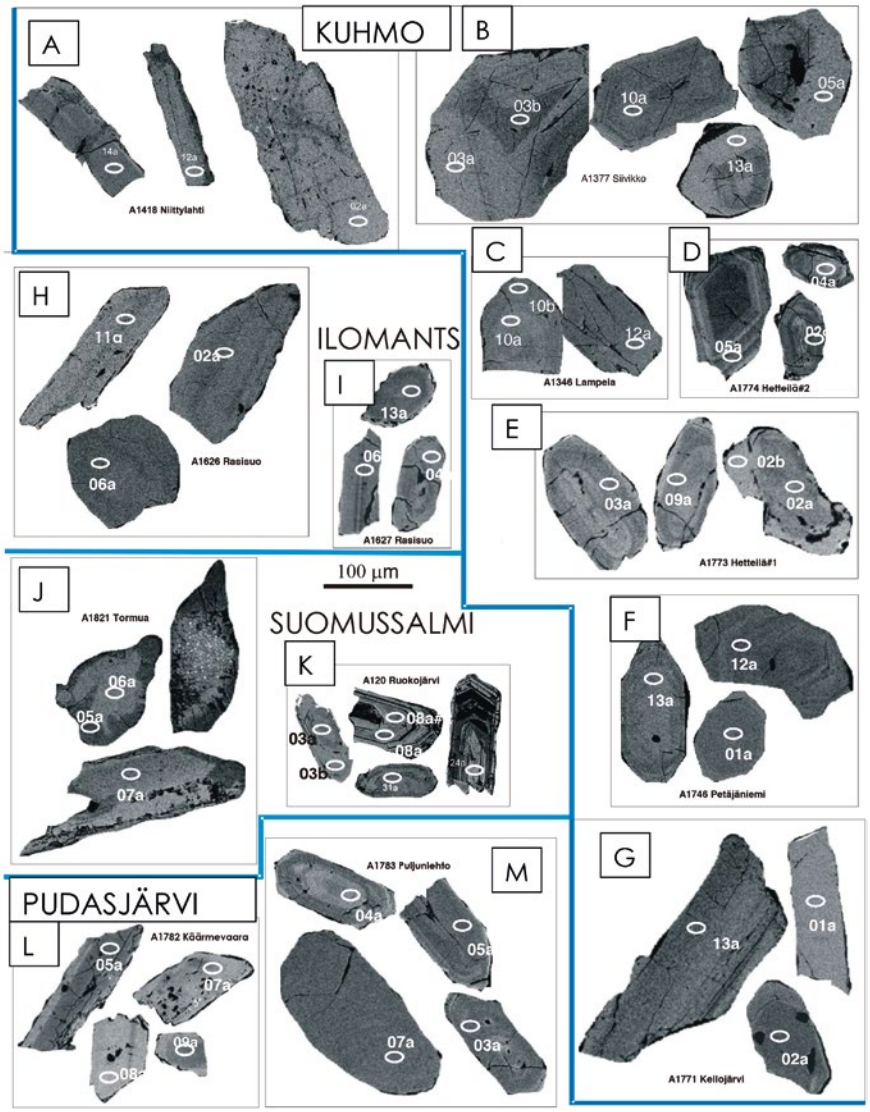

Fig. 14. BSE images of selected zircon crystals and grains. Analysis numbers and spot sites are marked in the figures.
A) Kuhmo, A1418 Niittylahti gabbro: Rather unaltered (14a) and altered (02a) 2.79 Ga gabbroic zircon and gabbroic zircon giving a younger age of 2.74 Ga.
B) Kuhmo, A1377 Siivikko felsic xenolith in komatiite: ~2.80–2.79 Ga analyses from a sector zoned grain 03 (a and b) and oscillatory-zoned crystal (10a) from the coarser grain-size faction. BSE pale, homogeneous rim zircon phases with a mean age of 2.77 Ga.
C) Kuhmo, A1346 Lampela andesite: Magmatic 2.80 Ga zircon with a pale, quite homogeneous inner domain (10b) and a weakly zoned outer domain (10a). An age of 2.76 Ga was measured from a structurally homogeneous grain (12a).
D) Kuhmo, A1774 Hetteilä#2 mica schist: ~2.74 Ga magmatic zircon (05a and 02 a) and an older rounded 2.79 Ga core (04a).
E) *Kuhmo, A1773 Hetteilä#1 intermediate volcanic rock:* ~2.83 Ga rounded cores and zoned grains (02a, 09a, and 03a) and a 2.67 Ga metamorphic rim.
F) Kuhmo, A1746 Petäjäniemi metasediment: An oscillatory zoned magmatic (13) and a probable metamorphic zircon (01) plotting on the same discordia line with an upper intercept age of 2847 ± 9 Ma. A younger age of 2.74 Ga was measured from a low-U zoned zircon 12.
G) Kuhmo, A1771 Kellojärvi gabbro-norite: ~2.81 Ga typical gabbroic zircon (13) and a BSE pale and homogeneous slightly younger, recrystallized (?) grain with an age of 2.78 Ga. Zircon core 02a was dated at 1.1 Ga.
H) Ilomantsi, A1626 Rasisuo gabbro: 06 represents an equidimensional grain with a rather homogeneous internal structure and 02 and 11a are from weakly zoned gabbroic zircon. Both types are coeval and plot in the same 2756 ± 4 Ma cluster.
I) *Ilomantsi, A1627 Rasisuo felsic tuff:* 2.88–2.87 Ga zoned (longitudinal and oscillatory) zircon 04a and 06a, 13a homogeneous grain with rim remnants.
J) Suomussalmi, A1821 Tormua gabbro: 05a BSE dark irregular rim without reasonable U-Pb data and the 2.87 Ga BSE pale core domain (06a), 2.85 Ga darker domain of an euhedral grain, and an example of phase separation (no analysis).
K) Suomussalmi, A120 Ruokojärvi dacite: 08 and 24 examples of rejected analyses on another major zircon type (~2.83 Ga?). 3.13–3.12 Ga cores (31a and 03a) and a 2.98 Ga weakly zoned rim (03b).
L) *Ranua, A1782 Käärmevaara gabbro:* 2.81–2.80 Ga gabbroic zircon (05, 07 and 08) representing the most unaltered types and a younger ~2.70 Ga metamorphic grain (09a).
M) Ranua, A1783 Puljunlehto dacite: 2.83–2.82 Ga magmatic grains (04a and 05a) and a younger 2.79 Ga metamorphic (07a) grain. An age of 2.78 Ga was also measured from the weakly zoned zircon 03 (contamination or ancient lead loss?).

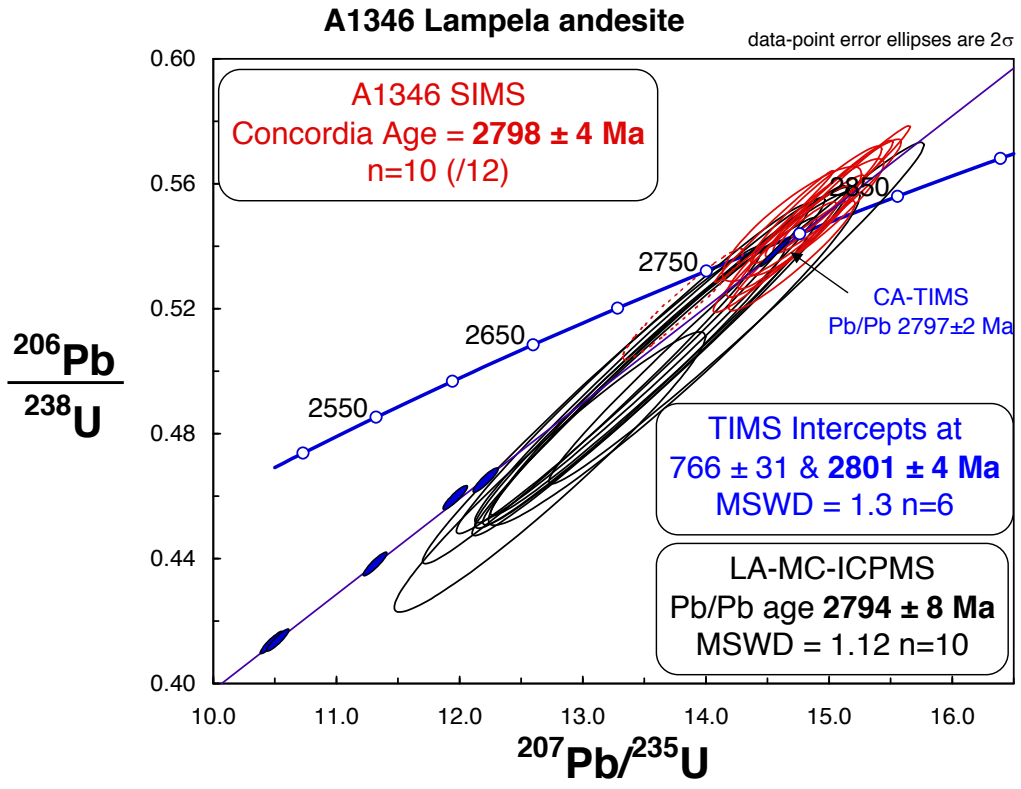

Fig. 15. Concordia diagram of zircon analyses from the Lampela andesite (A1346): Red error ellipses – SIMS data, blue filled ellipses – TIMS data, black error ellipses – ICPMS data.

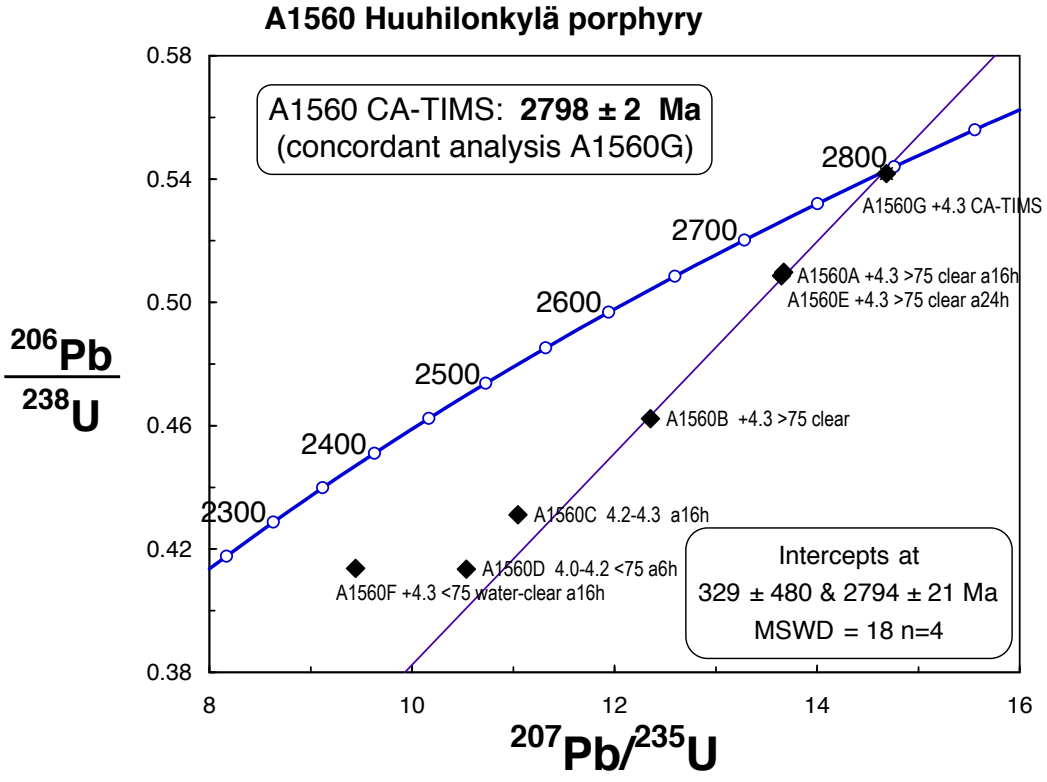

Fig. 16. Concordia diagram of zircon U-Pb TIMS analyses from the Huuhilonkylä felsic porphyry (A1560).

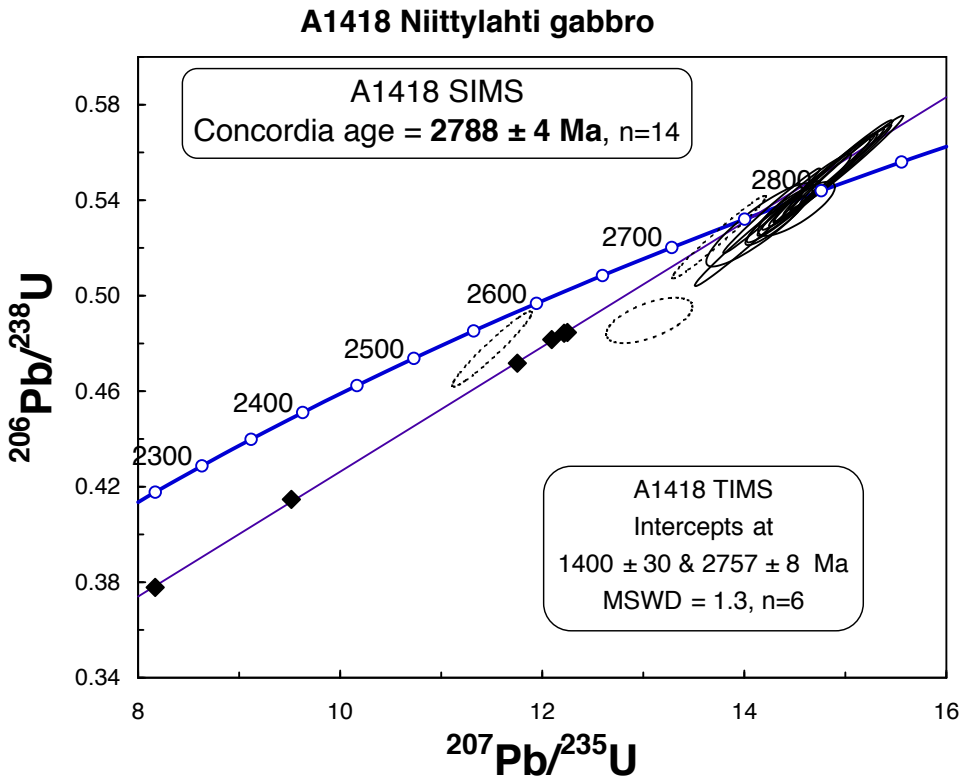

Fig. 17. Concordia diagram of zircon analyses from the Niittylahti gabbro (A1418): Error ellipses – SIMS data, diamonds – TIMS data.

Two of the analyses were rejected because of high common-lead proportions. Fifteen analyses plot in a tight cluster and 14 of them determine a concordia age of 2788 ± 4 Ma (Fig. 17).

One analysis (12a, Fig. 14A) from a structurally homogeneous, long grain enveloped by an alteration rim is concordant at 2.74 Ga, and analysis n2251-19a is quite distinct, suggesting an age of ca. 1.9 Ga. The latter analyses probably register metamorphic effects. This interpretation receives some support from the relatively old lower intercept age obtained by the TIMS analyses (see below).

The six TIMS analyses show a fairly high amount of common lead and provide discordant results (Appendix 2). The data plot on a chord that gives intercepts at 2757 ± 8 Ma and 1400 ± 30 Ma. Chemical abrasion of this turbid zircon was not successful, since hardly any material was left after the treatment. The analysis has high common lead and yielded reversely discordant result. The available isotope data thus suggest that this gabbro could be marginally younger than the ultramafic Kellojärvi complex.

A1771 Kellojärvi gabbro

The gabbroic sample A1771-Kellojärvi was collected from a drill-core in the middle of the Kellojärvi ultramafic complex (M52/4411/03/R315/286.95-293.0) (Fig. 13). The gabbro-norite belongs to the heterogeneous sequence composed of gabbro, pyroxenite and anorthosite with peridotite interlayers. These rocks may represent a "hybrid" sequence, which developed from komatiitic magma via contamination with older felsic crustal material.

Mineral separation yielded a large amount of fairly coarse-grained, mostly turbid, grey-pigmented, long, subhedral to anhedral zircon with ragged surfaces. In BSE images (Fig. 14G), the zircon grains show either compositional zoning or a homogeneous internal structure. Many larger and long grains show signs of corrosion and alteration.

From the Kellojärvi gabbronorite, a total of 13 zircon domains were analysed by SIMS (Appendix 1). All data are concordant and their radiogenic lead proportions are high enough for U-Pb ages. However, most data range between 2.80 and 2.74 Ga and do not allow precise age calculation. There are also three grains with distinct ages, one at 3.23 Ga and two ca. 1.0 Ga. The 1.0 Ga grains are dark and homogeneous in BSE images. They have low U and probably represent unusual metamorphic zircon. One multi-grain U-Pb analysis was also carried out using the TIMS technique

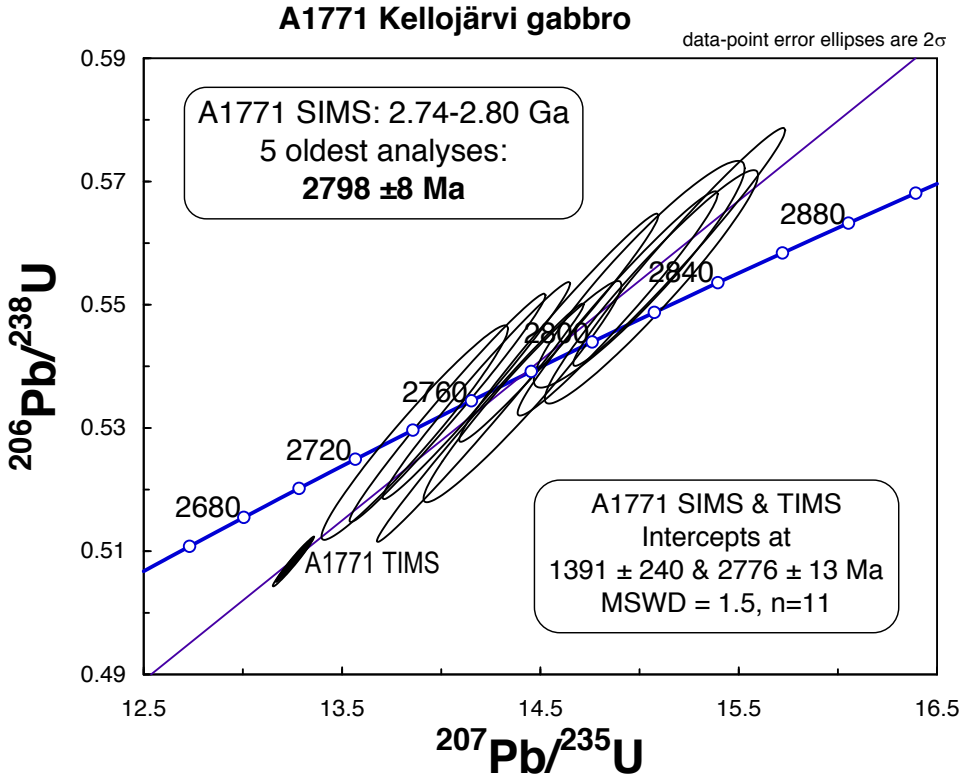

Fig. 18. Concordia diagram of zircon analyses from the Kellojärvi gabbro (A1771): Open error ellipses – SIMS data.

and yielded a discordant result, although consistent with the bulk of the SIMS data. Combining all data, intercepts with concordia at 2776 ± 13 and 1391 ± 240 Ma can be calculated (Fig. 18). It is conceivable that metamorphic effects are significant in this sort of turbid zircon, and in fact, there is a good negative correlation between the calculated age and U content. Thus, the real magmatic age of zircon could be closer to the oldest obtained dates, which give a concordia age of 2798 ± 8 Ma (n = 5).

A1377 Siivikko felsic rock

Sample A1377-Siivikko represents felsic rock fragments of a granodioritic composition, up to a few metres in diameter, which occur as inclusions within komatiitic lava flows in the Siivikko area south of the Kellojärvi ultramafic complex (Fig. 13). The outcrops containing these inclusions were shortly described by Papunen et al. (1998). Papunen et al. (2009) interpreted the felsic bodies as large xenoliths captured from wall rocks by the komatiitic magma. Another interpretation is that they represent fragments of boudinaged felsic dykes. The Siivikko sample yielded a reasonable amount of pale, transparent to translucent zircon grains varying in morphology from long prismatic to equant. In BSE images (Fig. 14B), the zircon crystals typically show longitudinal or oscillatory zoning and less frequently sector zoning. Equant grains typically have pale, homogeneous, non-fractured rims enveloping darker BSE cores.

A total of 15 zircon domains were analysed by SIMS from sample A1377 (Appendix 1). Excluding three discordant analyses, the U-Pb data plot in a cluster and give an average $^{207}Pb/^{206}Pb$ age of 2786 ± 8 Ma (Fig. 19). The high MSWD of 8 suggests, however, a scatter in excess of analytical error. The darker BSE, zoned zircon domains tend to give older apparent ages, and their U concentrations are frequently the lowest in the data set. Four of these define a concordia age of 2797 ± 4 Ma, and combined with the remaining three, give an average $^{207}Pb/^{206}Pb$ age of 2795 ± 7 Ma. Four of the structurally homogeneous pale BSE domains, which are mostly obvious rims, yield a concordia age of 2771 ± 8 Ma, but one similar pale domain (n2248-03a) has a $^{207}Pb/^{206}Pb$ age of 2800 ± 6 Ma, being the same age as obtained from the inner part of this same grain (n2248-03b). Three previous TIMS U-Pb analyses on multigrain zircon samples are very discordant (Appendix 2, Fig. 19).

Our best interpretation is that the age of 2797 ± 4 Ma records the timing of the primary crys-

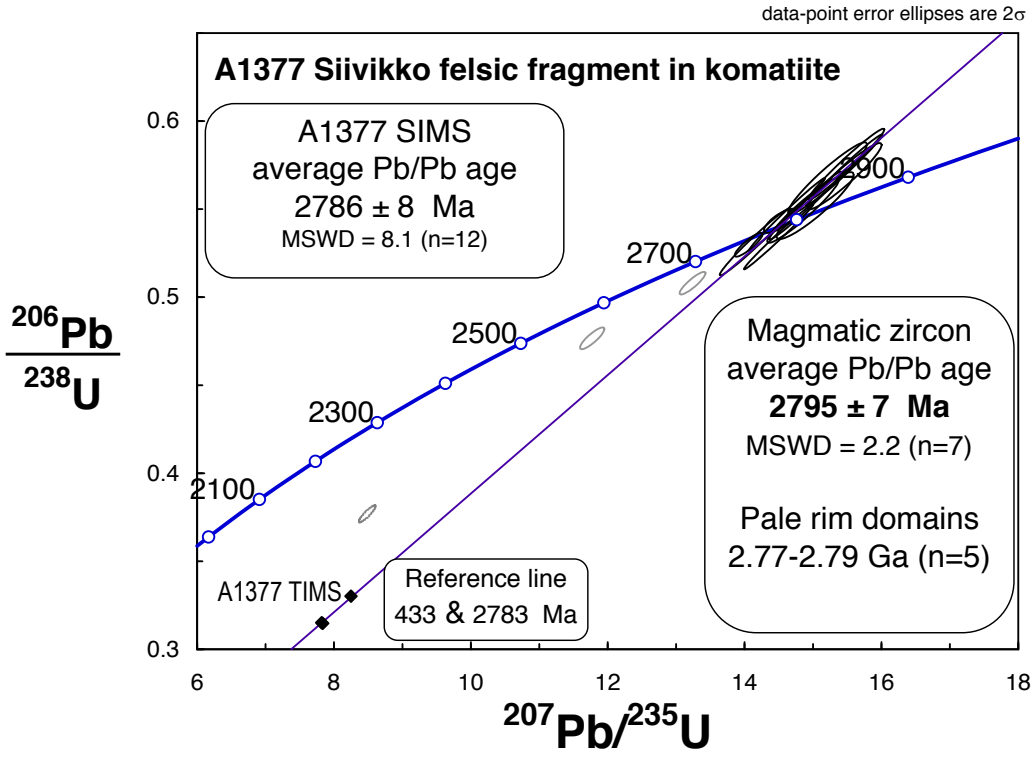

Fig. 19. Concordia diagram of zircon analyses from the Siivikko felsic fragment (A1377): Error ellipses – SIMS data, diamonds – TIMS data.

tallization of the felsic rock A1377, and the pale zircon domains were affected by a later metamorphic event. In principle, the metamorphic effect could have been related to the capture by the komatiitic magma, but more likely it is related to general metamorphic events in the area, which are also recorded by many other samples dealt with in this study. This interpretation would also be consistent with the discordant analyses from this sample. In fact, the results from the samples discussed above suggest that the komatiites cannot be younger than 2798 ± 2 Ma. The initial $\varepsilon_{Nd(2797)}$ of +2.0 shows that the felsic rock represents juvenile mantle-derived material (Huhma et al. this volume).

A2027 Siivikkovaara quartz porphyry dyke

Sample A2027 represents a felsic dyke intruding the komatiites in the Siivikkovaara area (Hanski 1980). The sample yielded abundant zircon grains, which are light-coloured, fairly transparent, euhedral to subhedral prisms or fragments. Both TIMS and LA-MC-ICPMS have been used for U-Pb dating (Appendices 2 and 3).

An analysis carried out using the chemical abrasion TIMS method is practically concordant at 2795 ± 2 Ma, and together with other two slightly discordant analyses plot on a chord, which gives intercepts at 2797 ± 5 Ma and 1082 ± 110 Ma. The LA-MC-ICPMS data are also concordant, and using all data an age of 2800 ± 5 Ma can be calculated. Although within the error quoted, two analyses (8a, 13a) seem to give marginally older ages. Rejecting these, the age would be 2795 ± 5 Ma (Fig. 20). In BSE or CL images, no distinct cores were found. Combining all data available, an age of 2795 ± 3 Ma is considered as the best estimate for zircon and the porphyry dyke, providing a minimum age for the country rock komatiites.

A511 Katerma rhyolite

Sample A511-Katerma represents a large rhyolitic rock formation located several km south of the Kellojärvi ultramafic complex (Fig. 13). Based on seven discordant multi-grain TIMS analyses, a U-Pb age of 2798 ± 15 Ma was reported by Hyppönen (1983). Zircon grains in this sample are euhedral, pale and mostly turbid crystals, which typically have resorbed surfaces. An analysis using the CA-TIMS technique provides a nearly concordant result with a $^{207}Pb/^{206}Pb$ age of 2797 ± 2 Ma (Appendix 2). The common-lead content in this analysis is very low compared to the older data. All eight analyses available are roughly on a

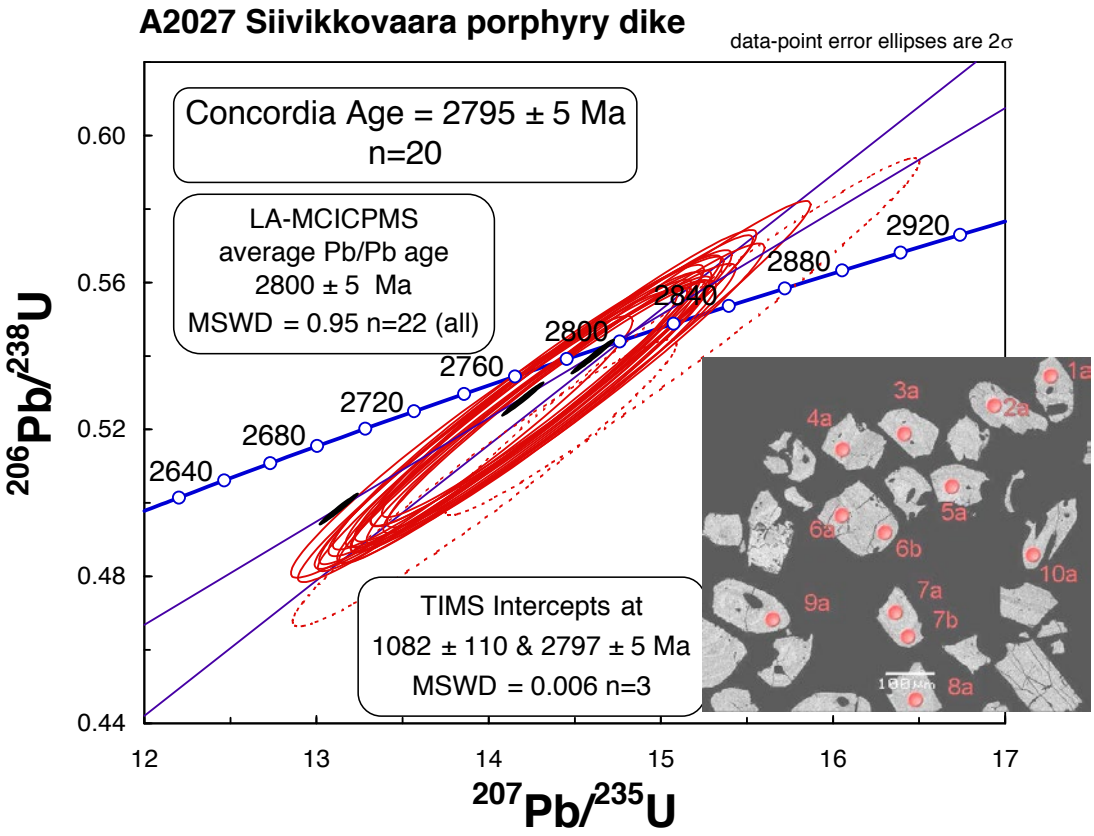

Fig. 20. Concordia diagram of zircon analyses from the Siivikkovaara felsic dyke (A2027): Large red error ellipses – LA-MC-ICPMS data, small black error ellipses – TIMS data.

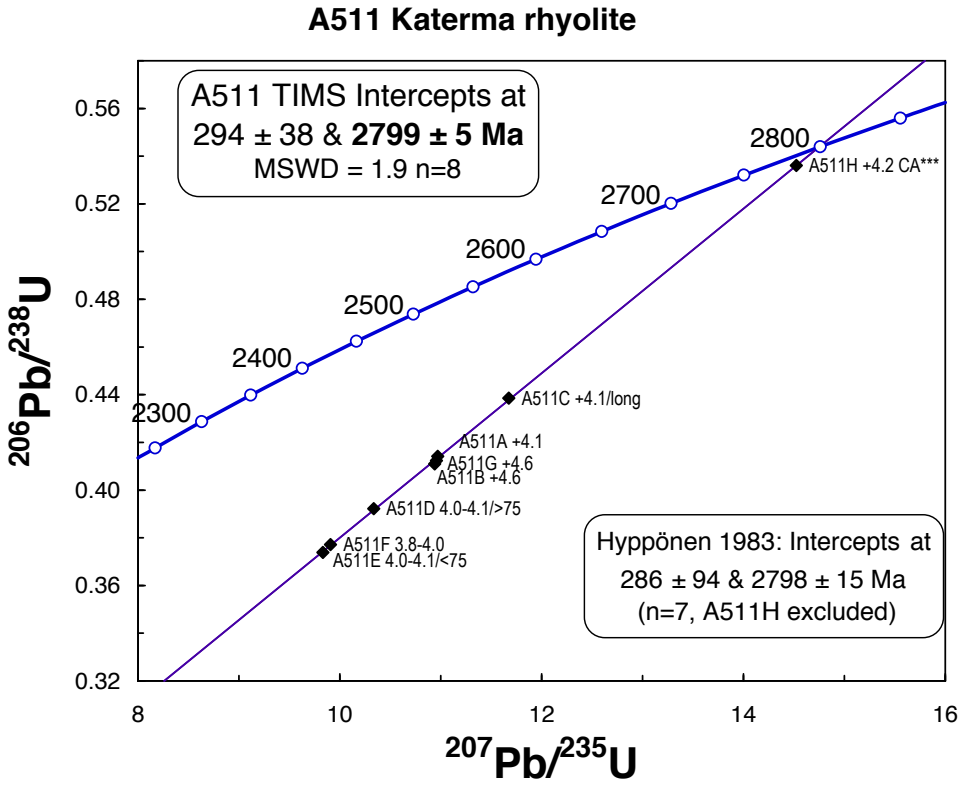

Fig. 21. Concordia diagram of zircon U-Pb TIMS analyses from the Katerma rhyolite (A511).

chord, which gives intercept ages at 2799 ± 5 and 294 ± 38 Ma (Fig. 21). The upper intercept age can be considered a reliable eruption age for the Katerma rhyolite.

A788 Polvilampi rhyolite

Sample A788-Polvilampi represents a large felsic volcanic unit located several kilometres north of the Kellojärvi complex (Fig. 13). Hyppönen (1983) called this rock quartz-feldspar schist and reported an age of 2810 ± 48 Ma, which was based on four discordant U-Pb TIMS analyses on zircon. Abundant zircon in this rock consists of euhedral grains often showing sharp crystal edges and well-developed zoning, which are typical features of zircon grains in igneous rocks.

A CA-TIMS analysis on zircon from A788 yielded a nearly concordant result with a $^{207}Pb/^{206}Pb$ age of 2795 ± 2 Ma (Appendix 2). Combining all TIMS U-Pb analyses, an upper intercept age of 2800 ± 11 Ma can be calculated (Fig. 22).

Zircon from this sample was also analysed using SIMS (SHRIMP) at VSEGEI, St. Petersburg (Appendix 4). Sixteen U-Pb analyses are nearly concordant and yield an upper intercept age of 2788 ± 14 Ma. Combining all SIMS and TIMS data produces intercepts with concordia at 2799 ± 5 and 397 ± 50 Ma. The date of 2799 ± 5 Ma can be considered as the age of sample A788, and gives the timing of the related felsic volcanism.

A976 Moisiovaara gabbro

Sample A976-Moisiovaara is a coarse-grained, tholeiitic mafic rock, which was taken from a sill intruding banded tholeiitic amphibolites in the northern part of the Kuhmo greenstone belt, ca. 30 km north of the Kellojärvi complex (Fig. 13). According to Luukkonen (1988), these voluminous layered tholeiitic mafic-ultramafic sills predominate in the lower stratigraphic part of the greenstone belt and may be 10 km long and up to 800 m thick.

Based on discordant and slightly heterogeneous TIMS analyses on zircon, Luukkonen (1988) reported a U-Pb age of 2790 ± 18 Ma for the Moisiovaara gabbro. Abundant zircon grains available from sample A976 mostly consist of turbid, grey, subhedral-anhedral crystals, being fairly typical igneous zircon from a gabbroic rock. In the heavy fraction, translucent, simple euhedral zircon prisms were also found. The CA-TIMS analyses on zircon are not perfectly concordant, but the $^{207}Pb/^{206}Pb$ ages of 2811 ± 3 Ma and 2806 ± 3 Ma should provide an absolute minimum age. Using all ten TIMS analyses, the intercept ages are 2815 ± 16 and 1102 ± 150 Ma, but the scatter is rather large (Fig. 23). A special feature of the zircon in A976 is the high Th/U ratio (inferred from radiogenic $^{208}Pb/^{206}Pb$, Appendix 2).

Zircon from sample A976 was also analysed using laser MC-ICPMS. All 16 data points are practically condordant within 2-sigma error, and fifteen of them give an average $^{207}Pb/^{206}Pb$ age of 2823 ± 6 Ma. One analysis (A976-10a) gives a slightly younger Pb/Pb age and is close to the bulk of the TIMS data (Appendix 3, Fig. 23). The data as a whole suggest that the scatter in TIMS analyses is more likely due to metamorphic effects than older xenocrystic zircon. The Th/U ratio in the CA-TIMS data is lower than in the other analyses (Luukkonen 1988), and it is thus conceivable that these CA-TIMS analyses do not record the age of solely magmatic zircon. It should be noted that the MC-ICPMS analyses were carried out during the same session using the same standards as with sample A1346, on which the TIMS and SIMS analyses confirm the accuracy of the MC-ICPMS $^{207}Pb/^{206}Pb$ ages. We are inclined to consider the average $^{207}Pb/^{206}Pb$ age of 2823 ± 6 Ma as the best available estimate for the age of magmatic zircon and emplacement of the Moisiovaara gabbro.

A1773 Hetteilä intermediate volcanic rock

Sample A1773-Hetteilä is a fine-grained felsic rock from the Vuosanka area, where supracrustal rocks seem to form a separate N–S-trending belt just east of the main Kuhmo greenstone belt. The sample was collected from a drill core (M52/4412/02/R416/6.20-8.80).

Partly due to the small sample size, mineral separation yielded only a few medium to fine-grained, pale coloured, transparent to translucent zircon grains with a rather rounded morphology. Short prismatic crystals are uncommon. In BSE images (Fig. 14E), the zircon is mostly rounded and/or corroded and shows a diffuse compositional structure/zoning. Only some zircon grains display clear oscillatory zoning or a rather homogeneous internal structure. A thin pale outer rim surrounds almost all zircon grains. Some titanite grains were also obtained from this sample, suggesting an igneous origin for the rock.

A total of 15 zircon domains were analysed (Appendix 1) from A1773 using the secondary ion microprobe (Nordsim). One analysis was rejected because of its high degree of reverse discordancy. The U-Pb data cluster in two groups with a good correlation with the analysed zircon domain type. The cores and zoned grains have ages around

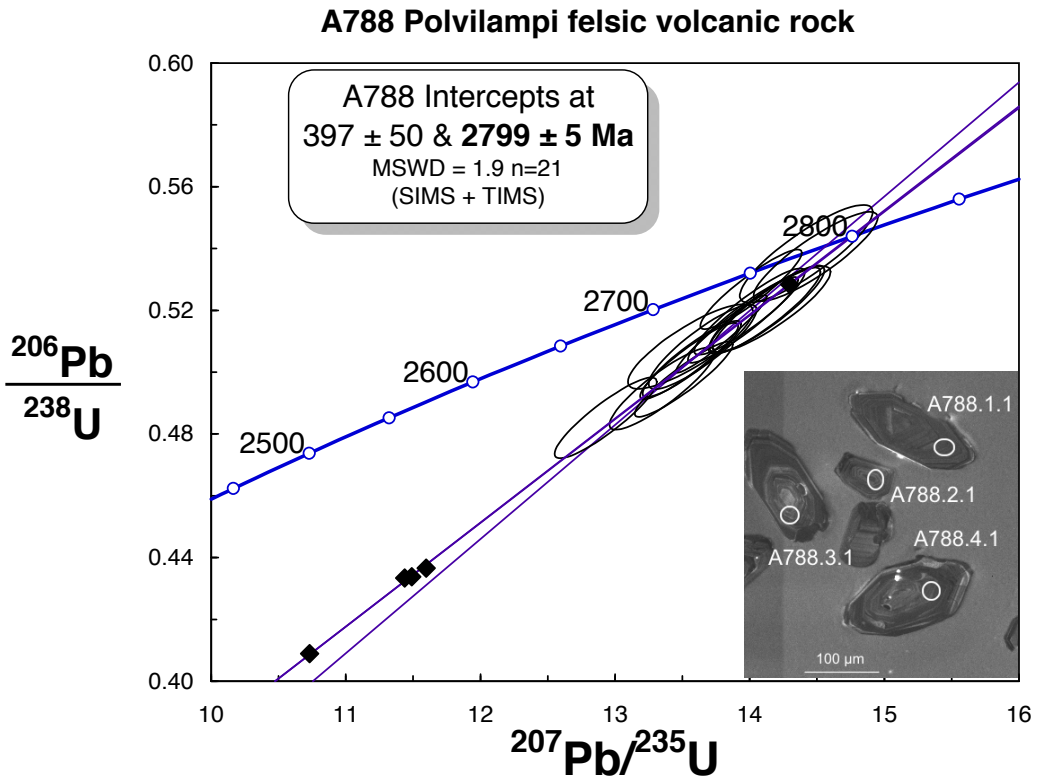

Fig. 22. Concordia diagram of zircon analyses from the Polvilampi rhyolite (A788): Error ellipses – SIMS data (SHRIMP), diamonds – TIMS data.

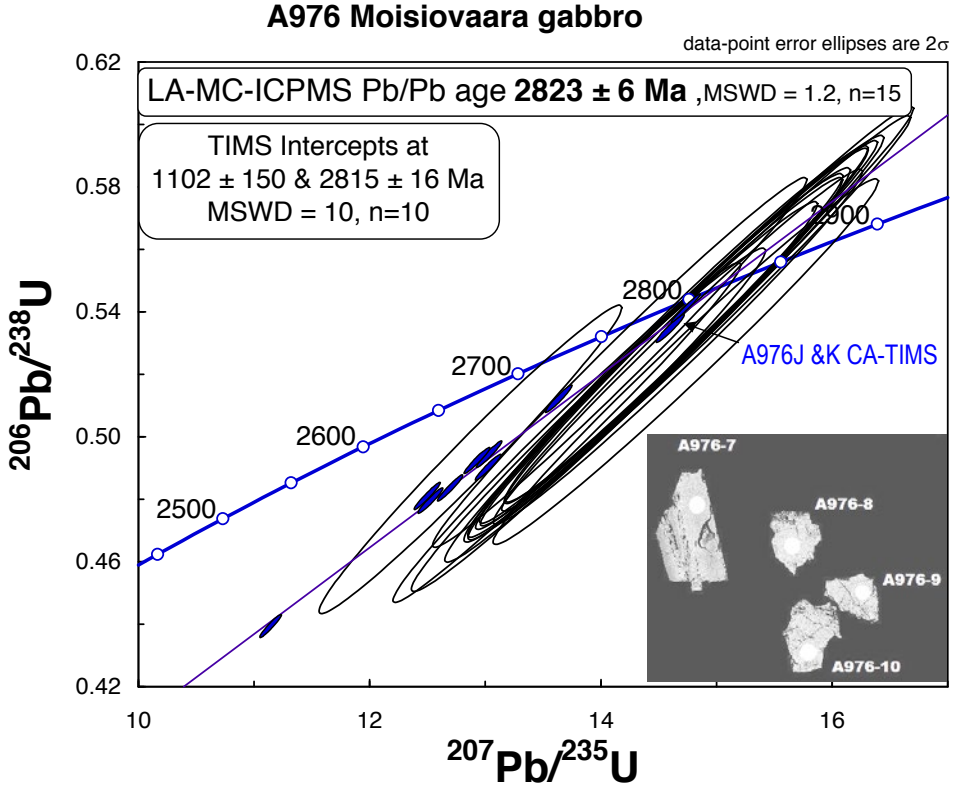

Fig. 23. Concordia diagram of zircon U-Pb TIMS (solid error ellipses) and LA-MC-ICPMS (open ellipses) analyses from the Moisiovaara gabbro (A976). The length of grain 7 is ca. 200 µm.

2.85–2.80 Ga and the outermost pale rims with low Th/U determine an age of 2678 ± 3 Ma (Fig. 24). A wide pale rim (01a) with a very high U content (6600 ppm) gives an age of ca. 530 Ma.

Provided that the rock is of a purely igneous origin, the average Pb/Pb age of 2836 ± 6 Ma obtained from the zoned magmatic zircon probably gives the age of the felsic rock A1773, and the younger rims register a metamorphic event at 2.68 Ga. The rounded morphology of these zircon grains probably originates from postmagmatic resorption, which is common in Archaean zircon in eastern Finland.

A1774 Hetteilä mica schist

Sample A1774-Hetteilä represents a fine-grained mica schist unit from the same drill core (M52/4412/02/R416, depth 94.80–96.65) from which the other Hetteilä sample (A1773) was taken. Rocks in the drill-cores between these two samples are mostly amphibolites.

The sample yielded a small amount of pale, typically fine-grained (75–100µm), short prismatic to round and equant zircon grains. In general, the population looks homogeneous, and the rounded morphology of some grains is compatible with their assumed detrital origin. In BSE images (Fig. 14D), the majority of the zircon grains are dark and show different types of oscillatory zoning (broad and smooth or narrow and sharp). Some grains have separate cores and rims, while others show rather homogeneous internal structures. Several zircon grains are surrounded by remnants of a thin pale rim. Inclusions are common.

Ten zircon domains were analysed from A1774 using the SIMS (Nordsim) (Appendix 1). Most of the data show minor discordance and moderate to low U concentrations. Analyses from the oscillatory-zoned zircon grains plot on the same chord, suggesting an age of ca. 2.74 Ga (Fig. 25). Zircon core n2557-04a (see Fig. 14D) and grain n2557-10a are ca. 2.79 Ga old. Provided that the rock sampled by A1774 is of a sedimentary origin, the data constrain the deposition after 2.74 Ga, which would imply a considerably younger time of formation than what was obtained for the 2.84 Ga rock above (A1773), and a tectonic break between the two sequences.

In fact, this would be consistent with the presence of 2.75 Ga detrital zircons in the sedimentary samples in the Ronkaperä Formation discussed

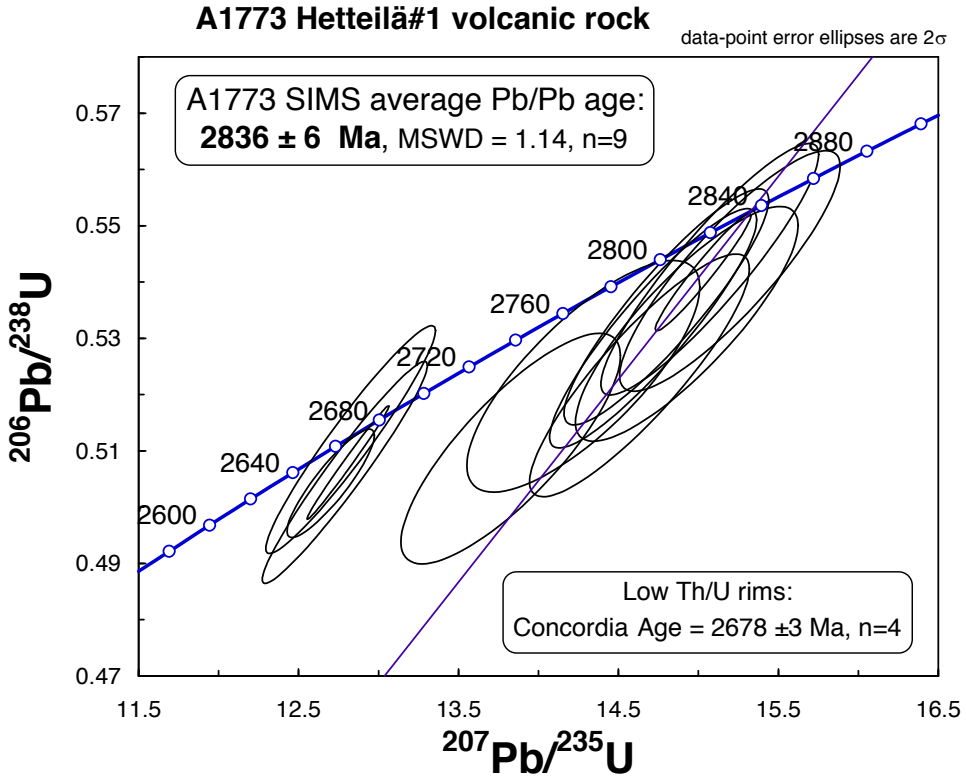

Fig. 24. Concordia diagram of zircon SIMS analyses from the Hetteilä intermediate volcanic rock A1773. Analysis n2556-01a is outside the range of the figure.

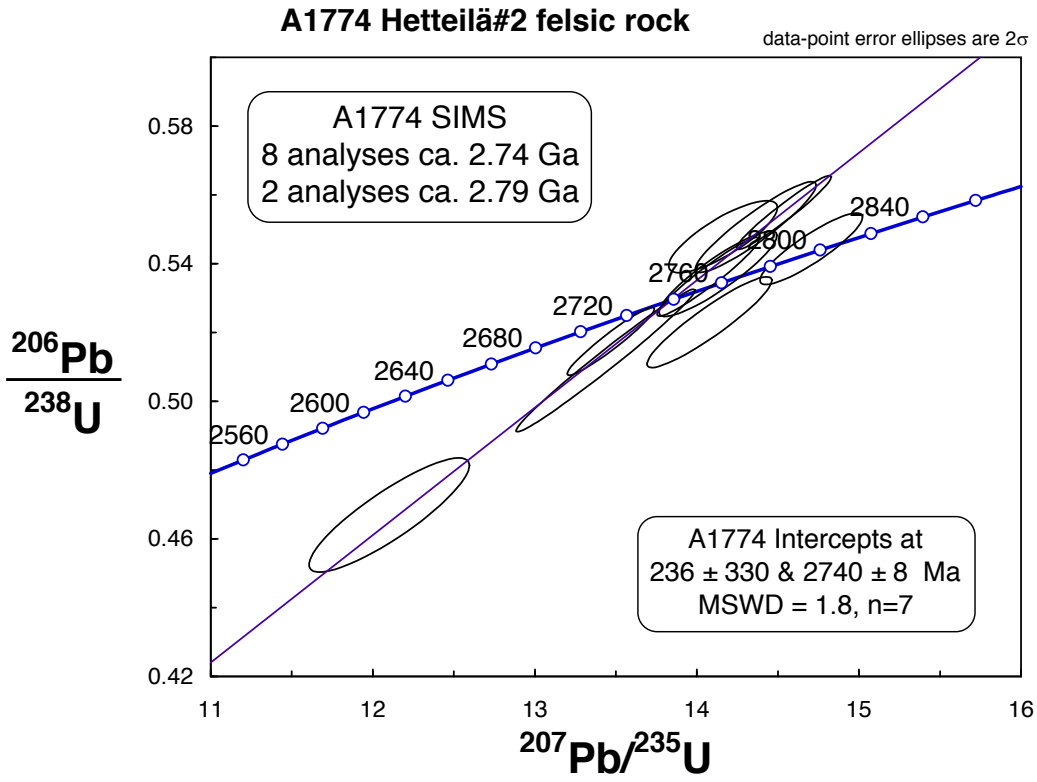

Fig. 25. Concordia diagram of zircon SIMS analyses from the Hetteilä felsic rock A1774.

below. A similar situation was also observed in the Tipasjärvi schist belt, where a sedimentary rock from the Kokkoniemi Formation contains abundant 2.74 Ga zircons, while the volcanic rocks lower in the lithostratigraphy of the belt are ca. 2.8 Ga old.

A1746 Petäjäniemi sedimentary rock

Fine-grained, laminar metasediments occur at Petäjäniemi, north-east of Lake Ontojärvi. In the stratigraphy these rock are above the mafic-ultramafic volcanic rocks. Two samples for isotope studies were collected from the same outcrop (AAK-03-109). Of these, A1746 represents a fairly homogeneous felsic layer and A1747 was taken from a heterolithic exposure consisting of alternating, thin (few mm to few cm) felsic and mafic mica rich layers. However, no zircon grains were recovered from A1747.

A very small amount of mainly colourless to red-tinted, transparent to translucent zircon grains was separated from sample A1746. These grains are either short prismatic or oval-shaped (w:l~1.5-2.5; 100-200 µm) without distinct crystal faces. Although homogeneous under a stereomicroscope, the population is heterogeneous in BSE images (Fig. 14F). Several short zircon grains are clear and show weak, smooth zoning (metamorphic grains?), whereas some longer prismatic crystals show evident magmatic oscillatory zoning with occasional zone-controlled alteration (magmatic grains). A few distinct cores were detected. Signs of abrasion are generally minor. However, some grains have a slightly rounded morphology compatible with a detrital origin.

A total of 18 zircon domains were dated from the Petäjäniemi sediment sample A1746 (Appendix 2). One analysis was rejected due to a high common-lead content. The U-Pb analyses define two age groups, at ca. 2.85 Ga and 2.74 Ga (Fig. 26). Assuming that the 14 older grains have a common origin, an upper intercept age of 2847 ± 9 Ma can be calculated (together with a lower intercept of 582 ± 270 Ma, MSWD = 3.5). The 2.74 Ga ages were measured from a weakly oscillatory-zoned, euhedral grain n2246-12a (Fig. 14F) and from a BSE-darker, homogeneous, metamorphic rim phase of zircon 09 having a 2.86 Ga core. The ages obtained register both igneous and metamorphic events that are considered to predate the deposition of the Petäjäniemi sediment.

Before drawing broader inferences, one should remember that only very few zircons were found

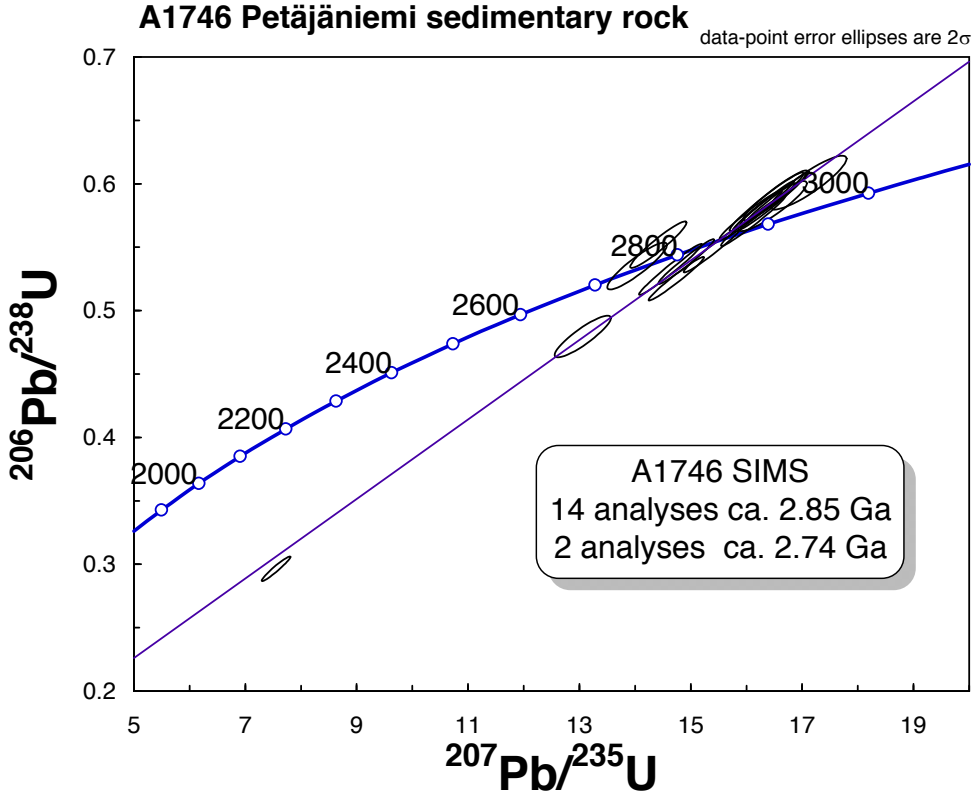

Fig. 26. Concordia diagram of zircon SIMS analyses from the Petäjäniemi sediment sample A1746.

in this rock and the number of analyses is also small. Nevertheless, deposition of this sediment after the main volcanic phase in the Kuhmo greenstone belt is possible, being reminiscent of the case observed at Vuosanka (A1744-Hetteilä), Rakennuslahti (83-PGN-90 below) and Tipasjärvi (A1748-Aarreniemi below), and also consistent with the stratigraphic scheme (e.g. Papunen et al. 2009).

83-PGN-90 (A2102) Rakennuslahti greywacke

A fairly large area of the southern part of the Kuhmo greenstone belt is dominated by the metasedimentary rocks assigned to the Ronkaperä Formation. In this work, this predominantly metaturbidite unit is represented by the metagreywacke sample 83-PGN-90 from Rakennuslahti (Fig. 13). The sample was collected from a sandy layer in an outcrop of metaturbidite schist dominated by 5–15-cm-thick, gray-coloured, massive sandy layers. The rock has a blastoclastic-schistose texture, in which the largest obvious relict clastic grains are up to 0.5 mm in size and mainly consist of monocrystalline quartz. The present mineral composition is quartz, plagioclase, biotite and chlorite with minor ilmenite, apatite, tourmaline and zircon.

Zircon in this sample mainly consists of euhedral crystals, which show clear magmatic zoning. Signs of abrasion are generally limited. The MC-ICPMS U-Pb data on 45 zircon grains were originally obtained utilizing only the GJ1 and Proterozoic (A382) in-house standards. Later, ten of these grains were re-analysed using the Archaean in-house standard (A1772) for calibration. It turned out that the data on these two sessions are indistinguishable (Appendix 3). The ages range from ca. 2.74 Ga up to 3.2 Ga, and nearly half of the analysed grains are close to 2.75 Ga in age (Fig. 27). It seems evident that the deposition of this sedimentary rock took place after the main volcanic phases of the Kuhmo greenstone belt and subsequent to ca. 2.75 Ga.

A1753 Arola quarzite

Sample A1753 (55-PTP-03) represents the quartzites that occur as a relatively narrow, ca. 1- km-long, apparently fault-bound sliver in the central part of the Kuhmo greenstone belt (Fig. 13). The rock is a reddish, sericite-bearing, blastoclastic, laminar and deformed quartzite. A fair amount of zircon obtained from a relatively small sample consists of mostly euhedral, slightly rounded, brownish grains.

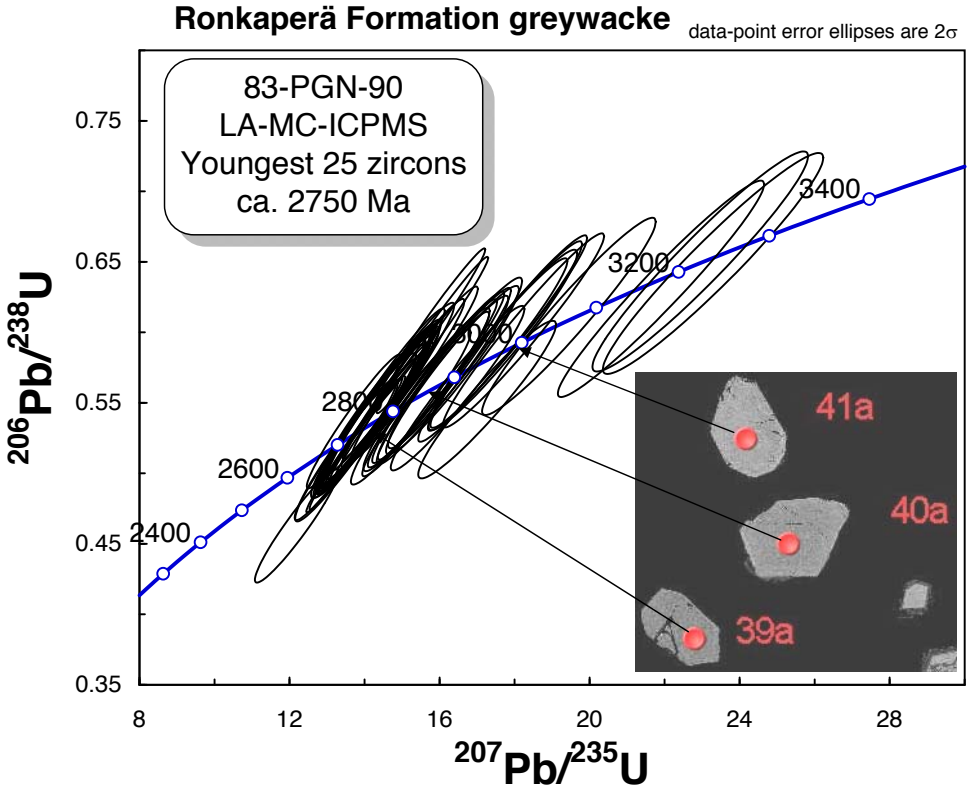

Fig. 27. Concordia diagram of zircon LA-MC-ICPMS analyses from the Rakennuslahti greywacke sample 83-PGN-90. The length of grain 39a is ca. 100µm.

Zircon in this sample was analysed using SIMS (SHRIMP) at VSEGEI, St. Petersburg. Most of the 22 U-Pb analyses are concordant within error and show a large range of ages from 2.70 to 3.45 Ga (Appendix 1, Fig. 28). Half of the dates concentrate on ca. 2.70 Ga and were obtained from oscillatory zoned zircon domains. They probably derive from felsic magmatic rocks, and the data thus suggest that the deposition of the Arola quartzite took place after ca. 2.70 Ga. Granitoids and felsic dykes crosscutting the volcanic rocks of the greenstone belt in the Arola area have yielded U-Pb zircon age of ca. 2.74–2.73 Ga and are thus significantly older (samples A402, A572, A1702, A1707, Hyppönen 1983, Käpyaho et al. 2006, Heilimo et al. 2011) than the Arola quartzite. Evidently, the Arola quartzite is much younger than any other supracrustal unit in the Kuhmo greenstone belt.

It is notable that the Arola quartzite is clearly deformed. However, observing that most Proterozoic metadiabase dykes just west of the Kuhmo greenstone belt are pervasively schistose, even a Proterozoic age of this quartzite could be speculated. The presence of 2.22 Ga gabbro-wehrlite sills within the middle part of the Kuhmo belt (Hanski et al. 2010) suggests that the 2.2 Ga erosion level was not much higher than the present erosion level. Over the whole Karelia Province, these sills are restricted to <1–2 km below the Palaeoproterozoic Kainuu-Jatuli quartzites.

A1213, A1254 Pitkäperä meta-andesites

The Pitkäperä samples A1213 and A1254 represent andesitic rocks in a location ca. 10 km east of the main Kuhmo greenstone belt, where they form a 4-km-long, NE-trending belt (Fig. 13). The geology and geochemistry of the rocks in the Pitkäperä area have been described by Luukkonen (2001). The samples collected for dating are fine- to medium-grained rocks mainly consisting of plagioclase, quartz and biotite.

Mineral separation yielded only a small amount of fine-grained zircon grains, which are short, pale, fairly transparent and euhedral. Abundant titanite was also obtained from these samples. The previous conventional TIMS results are discordant, but data after chemical abrasion are fairly close to concordia and yield 207Pb/206Pb ages of ca. 2.83 Ga (Appendix 2).

The MC-ICPMS analyses on zircon A1254 provide a concordant age at 2847 ± 8 Ma (Fig. 29), which is close to the upper intercept age of

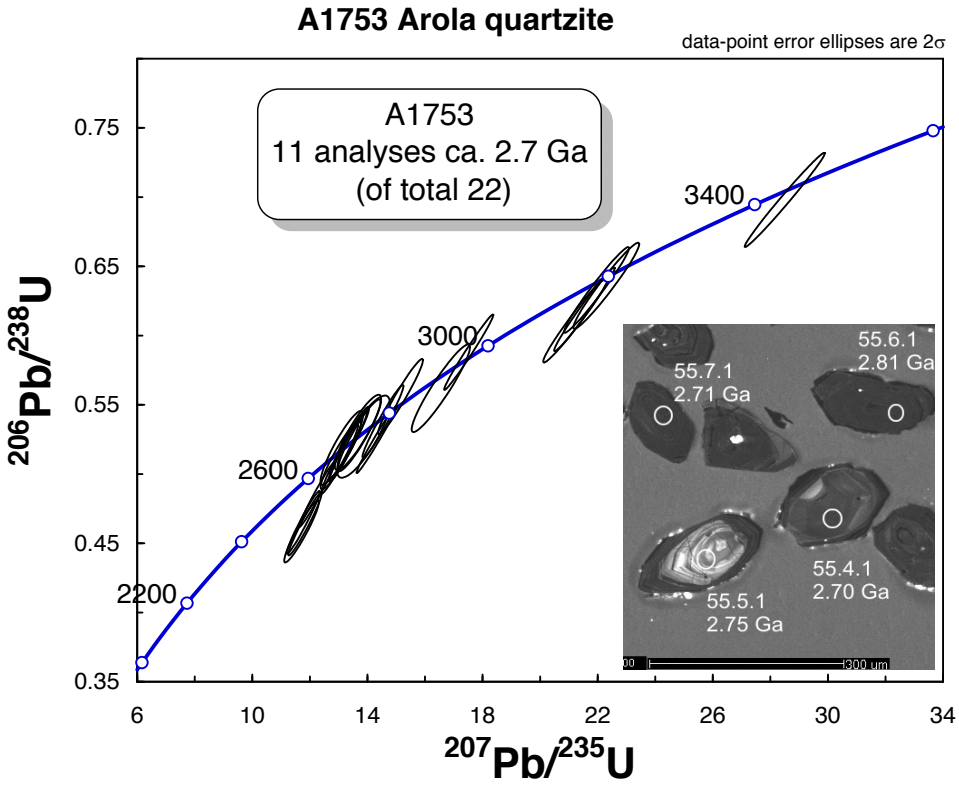

Fig. 28. Concordia diagram of zircon SIMS analyses from the Arola quartzite A1753.

2842 ± 5 Ma obtained from the TIMS data on sample A1213 (only two analyses). These are the best estimates for the age of magmatic zircon of the Pitkäperä volcanic rocks.

The TIMS data on the two samples do not plot exactly on the same chord (Fig. 29). In particular, the two CA-TIMS data points fairly close to concordia are slightly distinct in terms of the Pb/Pb age, which calls for some explanation. It is conceivable that some metamorphic effects are responsible for this scatter, involving different discordia patterns for different samples. This interpretation receives some support from a TIMS analysis carried out on zircon from a third sample N5, giving results clearly distinct from the other data (Appendix 2, Fig. 29). Another possibility could be that A1213 contains a minor inherited component or some unconstrained fractionation took place during the CA treatment. The third potential explanation appeared after MC-ICPMS analyses, since two Proterozoic magmatic grains with an age of ca. 1.75 Ga were observed in sample A1254 during the first analytical session (data not shown in Appendix 2). It is very likely that their presence is due to contamination during sample crushing, which fits well with the laboratory log book records, showing that the previous sample in the crushing line was a 1.75 Ga granite.

A120 & A1000 Ruokojärvi felsic volcanic rocks

The Ruokojärvi samples A120 and A1000 represent a small felsic volcanic unit in the northern part of the Kuhmo belt (Fig. 13). These rocks are situated in a small, granitoid-surrounded enclave ca. 1 km east of the main schist belt and consist of tuffs and pyroclastic breccias, which are strongly tectonized and cataclasized (Luukkonen 1988).

A large amount of fine-grained zircon is available from sample A120. For the most part, it is prismatic (l:w ~3-4), brownish and transparent to translucent. In the density fraction 3.8–4.0 g/cm^3, zircon grains tend to be more turbid, have a tint of brown colour and occur as shorter grains than in other fractions. In BSE images, many zircon crystals show clear oscillatory zoning with strong zone-controlled alteration patterns (Fig. 14K). Distinct cores are also common.

The previous multi-grain zircon U-Pb TIMS data from A120 are discordant, and the low-density, turbid zircon grains have a very high amount of common lead (Appendix 2). The data are clearly scattered but suggest an age of ca. 3 Ga (Fig. 30).

To improve our basis for interpretation, a total of 40 zircon domains were analysed from the Ruokojärvi sample A120 using SIMS (Appendix 1). Nine analyses mainly from the clearly zoned grains had to be rejected from further evaluation

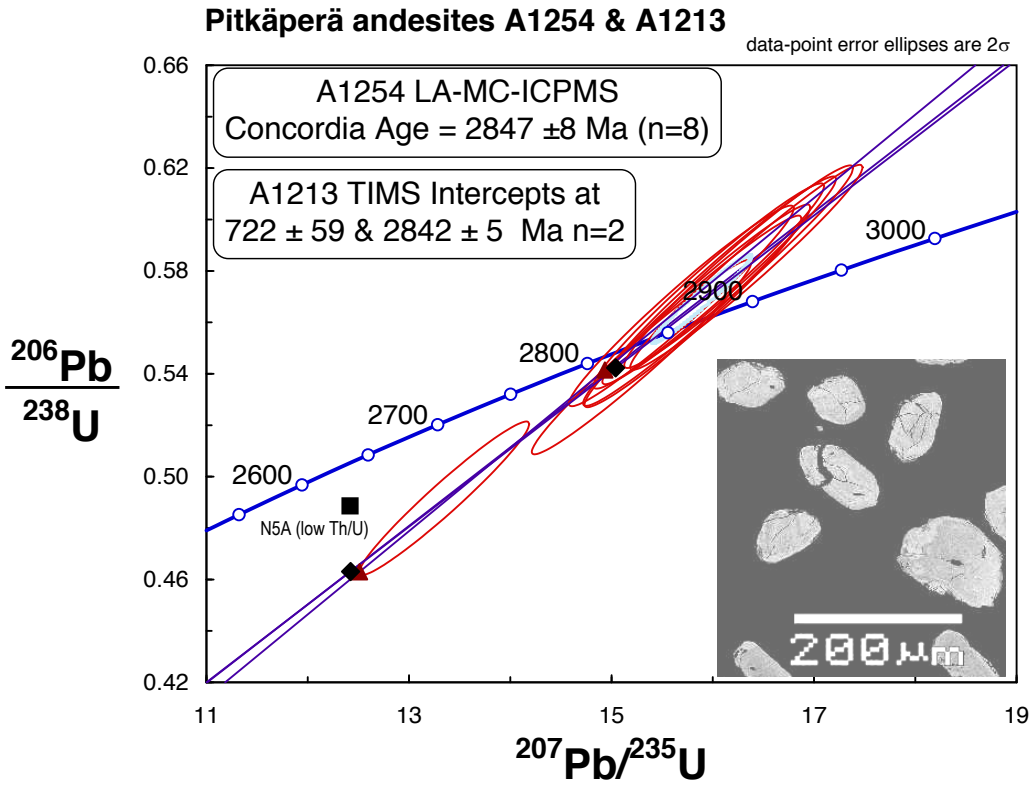

Fig. 29. Concordia diagram of zircon U-Pb analyses from the Pitkäperä andesites: Error ellipses - LA-MC-ICPMS on A1254, red triangles – TIMS on A1254, black diamonds – TIMS on A1213, black square – TIMS on N5. The inset shows a BSE image of zircon from A1254.

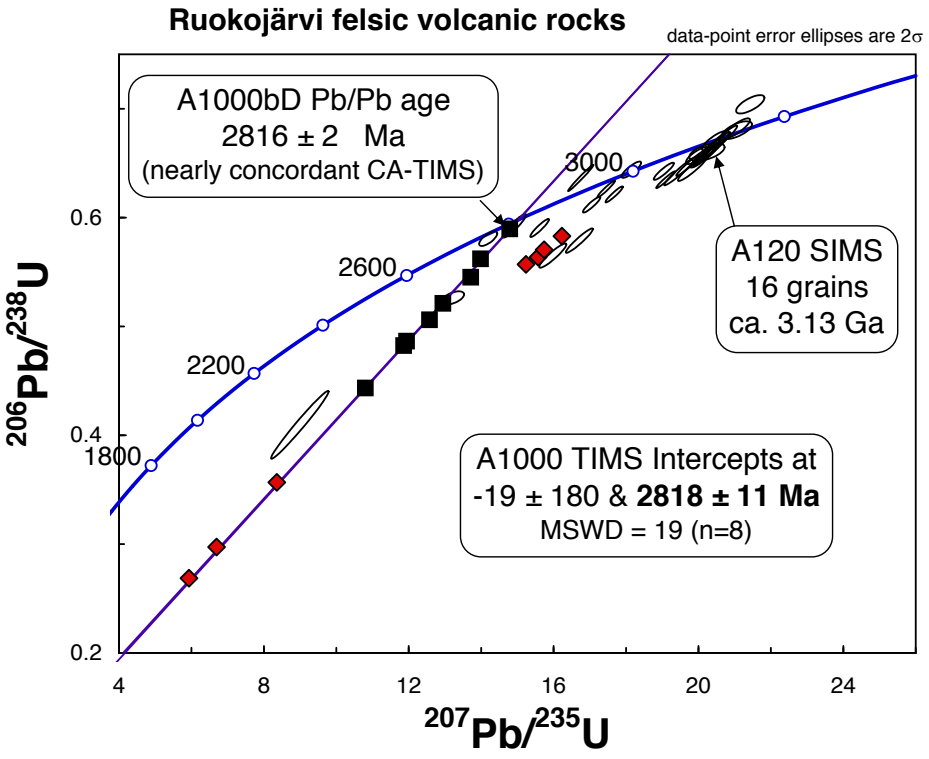

Fig. 30. Concordia diagram of zircon analyses from the Ruokojärvi felsic volcanics. Error ellipses – SIMS data on A120, red diamonds – TIMS data on A120, squares – TIMS data on A1000.

due to an unusually high amount of common lead. The remaining SIMS data scatter considerably, but most analyses from both zoned and homogeneous zircon domains plot at around 3.13 Ga (Fig. 30). Some weakly zoned grains give ages close to 2.99 Ga. The youngest ages of ca. 2.8 Ga were measured from structurally homogeneous zircon domains. The data also reveal a wide range in Th/U ratios from 0.03 to 1.4 (Appendix 1), but there seems to be no correlation with age and Th/U.

The other sample, A1000, collected later from the same rock unit as A120 seems to represent a more homogeneous variety, but evaluation of the primary nature of the rocks in the area is difficult due to strong tectonic strain. Zircon in sample A1000 consists of euhedral, brown to reddish and translucent crystals.

Seven multi-grain TIMS analyses yield discordant results, and mostly contain abundant common lead (Appendix 2). Instead, the CA-TIMS analysis carried out on the highest density zircon fraction gives a nearly concordant result with a $^{207}Pb/^{206}Pb$ age of 2816 ± 2 Ma, which should be the minimum age for the material analysed. Regression of all TIMS data gives an upper intercept age of 2818 ± 11 Ma, but the scatter is considerable and the lower intercept is set to the origin.

The results allow us to conclude that the Ruokojärvi felsic volcanic rocks are ca. 2.82 Ga in age and some samples, like the breccia A120, contain abundant xenocrystic zircon mostly derived from 3.13 Ga crustal sources.

U-Pb geochronology of the Tipasjärvi greenstone belt

A few kilometres SSW of the southern end of the Kuhmo greenstone belt, Archaean supracrustal rocks form an approximately 25-km-long, NE–SW-trending Tipasjärvi greenstone belt (Figs. 1 and 31). An age of ca. 2.79 Ga was reported for felsic volcanic rock A1174 by Vaasjoki et al. (1999). In conjunction with subsequent mapping and research, three additional samples were collected from felsic volcanic rocks.

A1922 Tipasjärvi intermediate volcanic rock

Sample A1922 collected from a drill core (4322-2006-R337/138.55-139.75) represents the intermediate, pyroclastic volcanic unit along the western margin of the Tipasjärvi belt. These volcanic rocks are considered older than the associated ultramafic volcanism.

Sample A1922 yielded a small number of light-coloured, euhedral, fairly transparent zircon grains. The population looks homogeneous and magmatic in origin. Only two U-Pb TIMS analyses were carried out on this sample, one using a lengthy air-abrasion treatment (analysis A) and the other with chemical abrasion (CA, analysis B, Appendix 2). They show that the common-lead content is low and provide nearly concordant data, with an average Pb/Pb age of 2828 ± 3 Ma (Fig. 32). Analyses by LA-MC-ICPMS were carried out in two stages, but here only the data from the last session (August 2010) utilizing the Archaean in-house standard are included in calculations (Appendix 3). Isotopic results for zircon A1922 are concordant and provide an age of 2826 ± 8 Ma (Fig. 32). Including the analytical results from the first session, no significant heterogeneity is observed in the data on 30 zircons, which suggests that the date of the nearly concordant TIMS analyses is the best age estimate for magmatic zircon of this intermediate volcanic rock.

A1921 Tipasjärvi felsic volcanic rock

Sample A1921 collected from a drill core (4322-2006-R324/16.25-17.40) represents a felsic volcanic unit at the eastern margin of the Tipasjärvi belt. These felsic rocks are thought to postdate the main ultramafic magmatic phase.

Only a small number of zircon grains were obtained from sample A1921 consisting of small, euhedral, transparent crystals. A U-Pb analysis using the chemical abrasion technique gave a concordant result and an age of 2781 ± 3 Ma (Appendix 2, Fig. 32). However, concordant analyses by LA-MC-ICPMS yielded an older age of 2810 ± 10 Ma (Appendix 3). In addition to these 11 analyses, this sample was also analysed in an earlier session, but due to some uncertainties with the calibration, these data are excluded from the final age calculations. Nevertheless, all analyses on 31 zircon grains give the same age within error, suggesting that zircon is of magmatic origin without significant inherited domains. It appears that few grains in the zircon mount prepared of sample A1921 are actually monazite, which is optically very similar to zircon. According to an LA-MC-ICPMS analysis, this monazite is ca. 1.9 Ga in age (A1921-18a, Appendix 3). It is very likely that a minor amount of such monazite could have been included in the multi-grain TIMS analysis, which

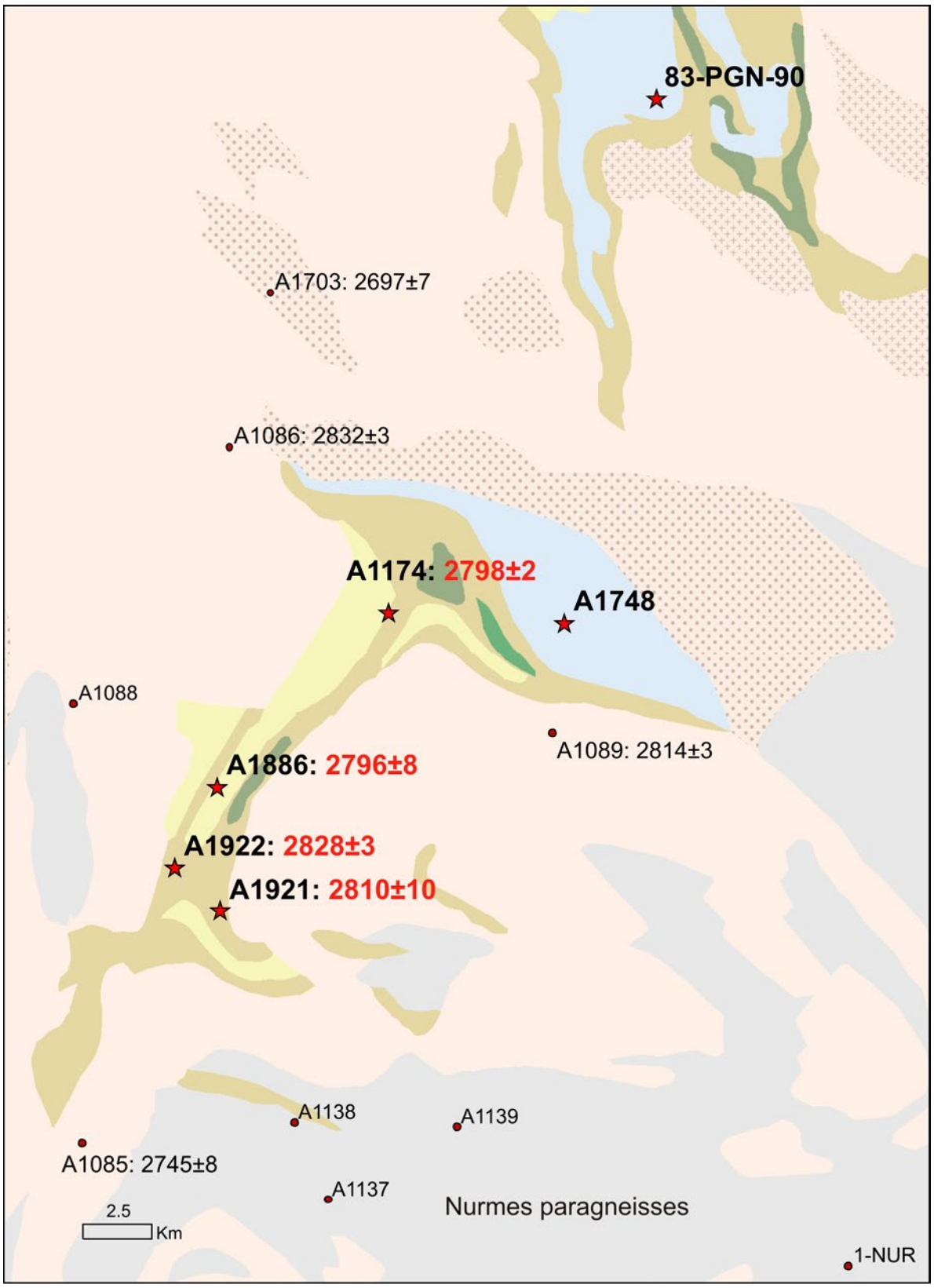

Fig. 31. Geological map of the Tipasjärvi greenstone belt showing sample sites (red star – this study, other samples – Vaasjoki et al. 1999, Käpyaho et al. 2006; see also http://geomaps2.gtk.fi/activemap/). Igneous ages with 2-sigma errors are given in Ma after the sample number. The map is based on the 1:1 000 000 geological map (Korsman et al. 1997), where the greenstone belt consists of four main rock types: mafic metavolcanic rocks (brown), ultramafic metavolcanic rocks (green), intermediate-felsic metavolcanic rocks (yellow) and metasediments (blue). Granitoids surrounding the greenstone belts are divided into TTGs and intrusive rocks (stippled), and (Nurmes) paragneisses are shown in grey.

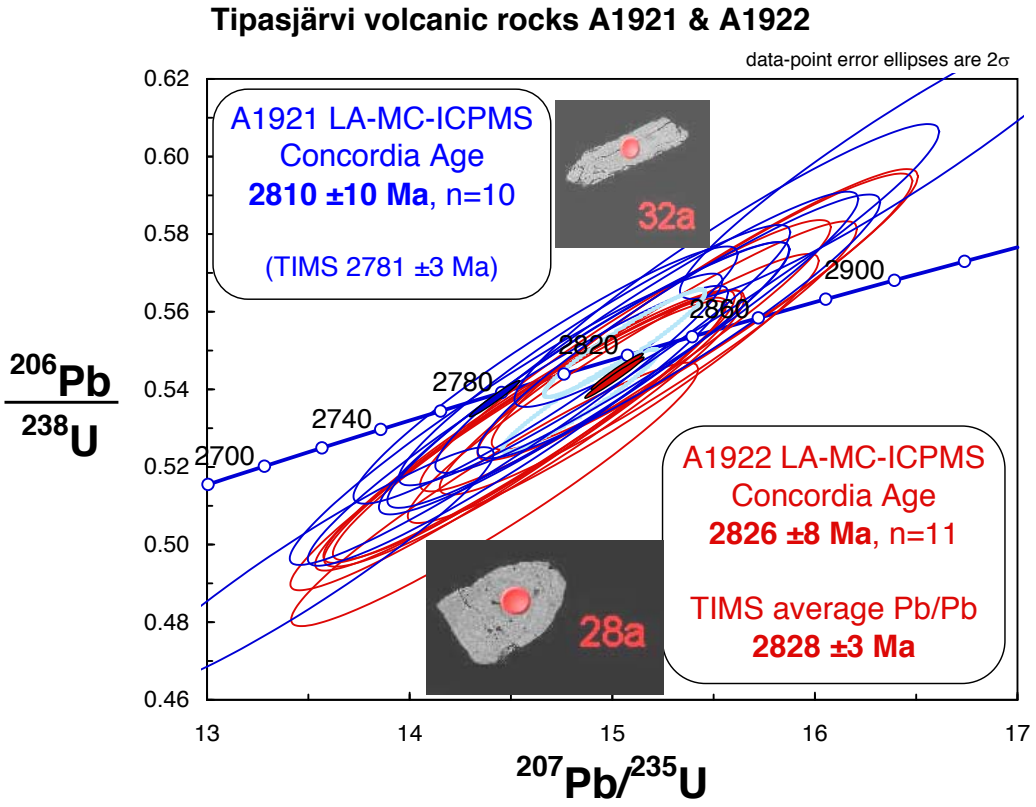

Fig. 32. Concordia diagram of zircon U-Pb TIMS (solid error ellipses) and LA-MC-ICPMS analyses from the Tipasjärvi volcanic rocks (A1922-red, A1921-blue). The length of zircon grains is approximately 100 µm.

thus would explain the younger age. This is supported by the elevated $^{208}Pb/^{206}Pb$ ratio measured by the TIMS analysis.

Although the error ellipses in the laser MC-ICPMS analyses on A1921 and A1922 are overlapping, there is a clear tendency of A1922 giving slightly older ages than A1921. These data were obtained during the same session using the same calibration.

A1174 Taivaljärvi rhyolite

Sample A1174 represents the felsic volcanic rocks hosting the Taivaljärvi Ag-Zn deposit and was collected from the mine incline (Vaasjoki et al. 1999). Abundant zircon available at the GTK storage consists of clear, euhedral, mostly elongate crystals. A U-Pb analysis using the chemical abrasion technique gave a concordant result and an age of 2798 ± 2 Ma (Appendix 2, Fig. 33). This age is slightly older than the date (2790 ± 3 Ma) published by Vaasjoki et al. (1999), who also reported some analytical problems with their data. Compared to our new result (A1174E), the old data show much higher levels of common lead and were also obtained using separate U and Pb spikes, which may yield accidental Pb/U errors during weighing.

The CA-TIMS age of 2798 ± 2 Ma obtained in this work is strongly supported by the LA-MC-ICPMS results. Excluding two analyses, the amount of common lead is negligible in all other 26 analyses, which give an average $^{207}Pb/^{206}Pb$ age of 2800 ± 6 Ma (Appendix 3, Fig. 33). It seems evident that there is no xenocrystic zircon in sample A1174, and thus the age of 2798 ± 2 Ma can be considered as a reliable estimate for the timing of the felsic volcanism.

A1886 Tipasjärvi felsic tuff

Sample A1886 represents a large, fairly homogeneous felsic unit, which occurs in the middle part of the Tipasjärvi belt (Fig. 31). According to the geological map, it may correlate with sample A1174 discussed above. Sample A1886, collected from a drill core (4322-2005-R305/235-239), is a rhyolitic tuff mainly consisting of quartz and sericite.

Sample A1886 yielded a good amount of light-coloured, euhedral, fairly transparent zircon. The zircon population looks quite homogeneous and magmatic in origin. Some rutile was also observed in the heavy fraction.

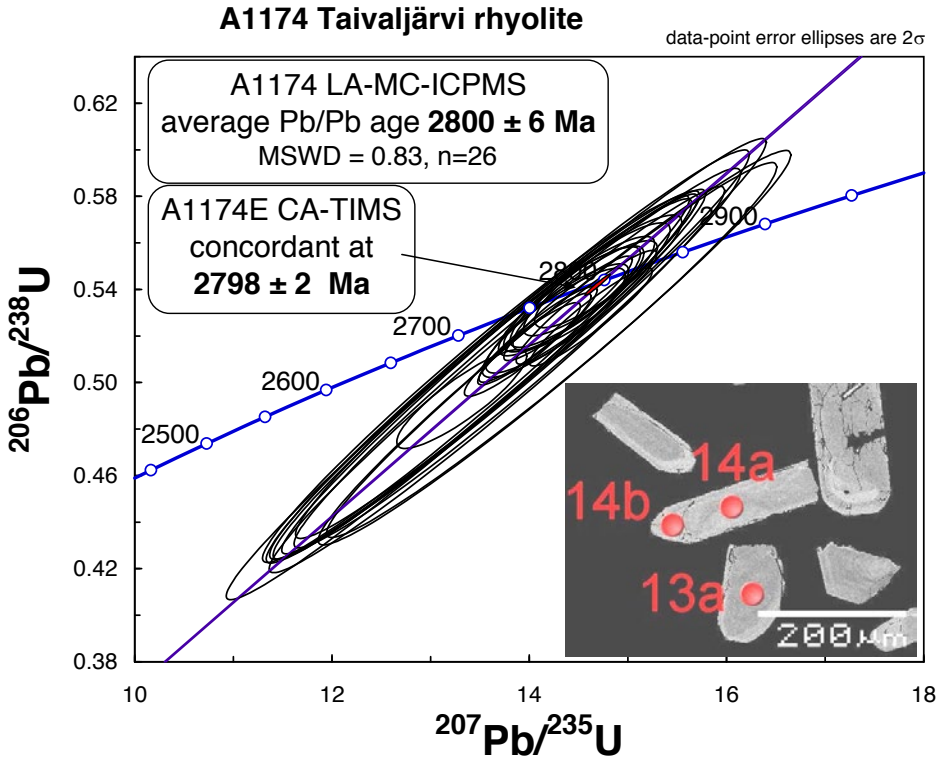

Fig. 33. Concordia diagram of zircon U-Pb analyses from the Tipasjärvi volcanic rock A1174 collected from the Taivaljärvi mine. Small red error ellipse – CA-TIMS analysis A1174E, large error ellipses – LA-MC-ICPMS analyses.

The five U-Pb TIMS analyses yield intercepts with the concordia at 2792 ± 5 and 1191 ± 150 Ma (MSWD = 1.6, Appendix 2). The upper intercept age is consistent with analysis #A1886I, which was carried out using the CA-TIMS method and gave a concordant age of 2794 ± 2 Ma.

All ten LA-MC-ICPMS analyses yielded concordant results and an age of 2796 ± 8 Ma (Appendix 3, Fig. 34). The date of 2796 ± 8 Ma may be considered as the crystallization age of zircon and felsic tuff A1886.

A1748 Aarreniemi greywacke

The metagreywacke-dominated Kokkoniemi Formation is considered to be the uppermost unit in the volcanic-metasedimentary succession preserved in the Tipasjärvi greenstone belt (Taipale 1983). The sampled outcrop (A1748 Aarreniemi) at the SE corner of Tipasjärvi Lake consists mainly of schistose, medium-grained, grey-coloured metawacke with a few bands of slightly finer-grained, darker grey metawacke that contains some graphite and iron sulphide. Although distinctly schistose, the Aarreniemi metawacke still shows clear remains of a clastic texture with flattened sand-size clasts up to 0.5 mm in their longest dimension. The larger, still identifiable clasts consist either of mono- or polycrystalline quartz or granoblastic plagioclase plus quartz, presumably from felsic volcanic or subvolcanic sources. The matrix between the sand-size clasts is recrystallised to a granoblastic-lepidoblastic mass of plagioclase, quartz and biotite with minor sulphide, and zircon. The separation yielded a fair amount of predominantly distinctly euhedral, long-prismatic oscillatory zoned zircon grains, for the most part without signs of abrasion.

Thirteen domains of 12 different zircon grains were analysed using SHRIMP II at VSEGEI, St. Petersburg (Appendix 4). Excluding one analysis, the data define an upper intercept age of 2746 ± 8 Ma (Fig. 35). Although the number of analyses is small and calculation assumes a common origin, and is thus not fully justified for detrital zircon, the data nevertheless strongly suggest that zircon grains in A1748 were predominantly from a source approximately 2.75 Ga in age. This is supported by one multi-grain TIMS analysis carried out at GTK (Appendix 2, Fig. 35) and the uniform appearance of the zircon population.

The results suggest that the maximum age of deposition of the Kokkoniemi Formation is ca. 2.75 Ga. A minimum age for the deposition is provided by the leucogranites cross-cutting the Kokkoniemi Formation along its NE border, dated at 2697 ± 7 Ma at Katajavaara 10 km N of Tipasjärvi (A1703, Fig. 31, Käpyaho et al. 2006).

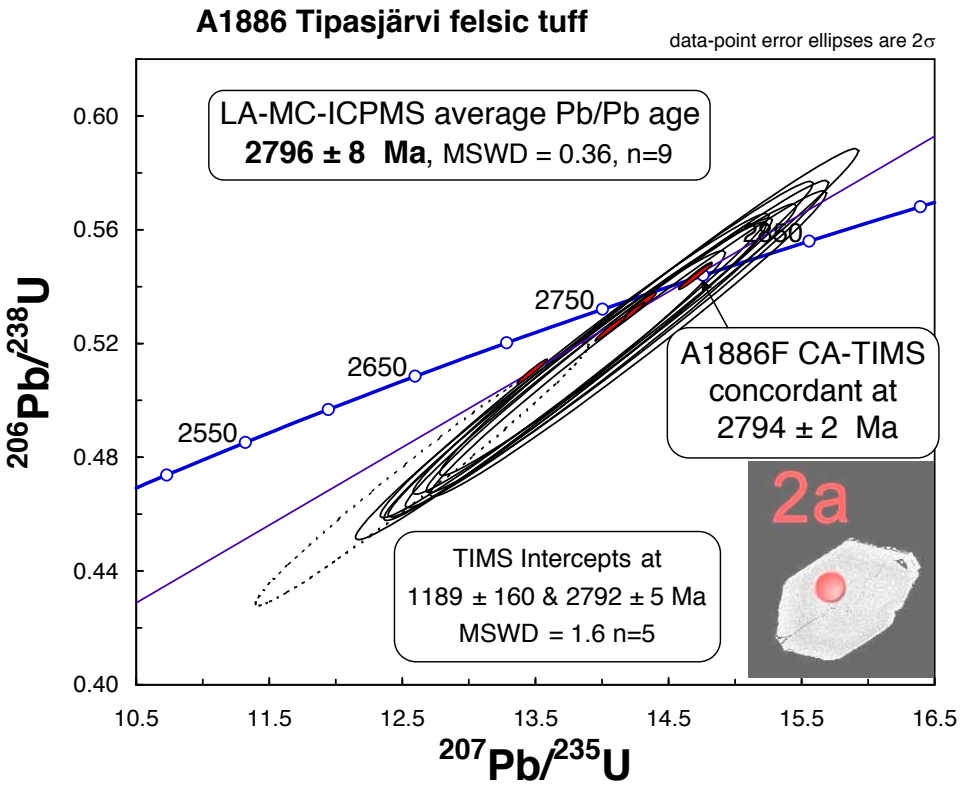

Fig. 34. Concordia diagram of zircon U-Pb analyses from the Tipasjärvi felsic tuff A1886 (TIMS data – small red error ellipses, MC-ICPMS data – open error ellipses). Length of zircon is 150 µm.

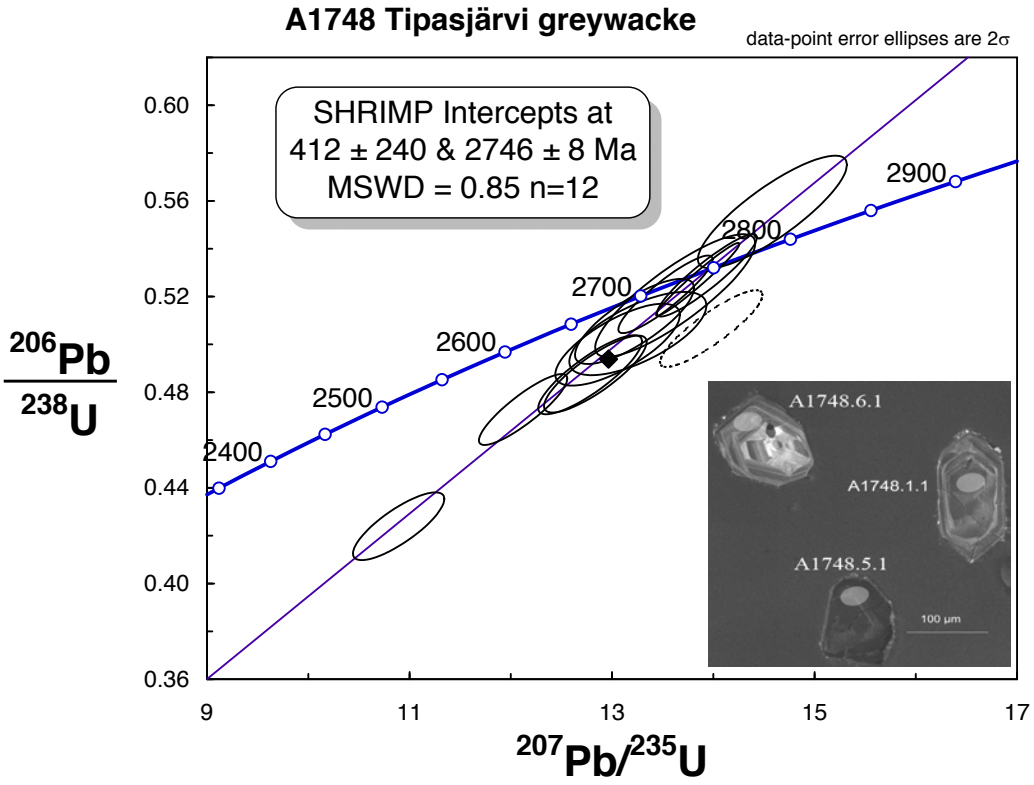

Fig. 35. Concordia diagram of zircon U-Pb analyses from the Aarreniemi, Tipasjärvi greywacke A1748 (SIMS/SHRIMP data – open error ellipses, TIMS analysis – filled diamond). Only one grain is clearly older than 2.75 Ga.

Discussion on the Kuhmo-Tipasjärvi greenstone belt

The results presented in this paper provide an improved basis for constraining the evolution of the Kuhmo and Tipasjärvi greenstone belts. According to the stratigraphic scheme of the Kuhmo greenstone belt, komatiites, most voluminous in the Siivikko Formation, are younger than the tholeiitic basalts of the Pahakangas Formation, for which an age of 2790 ± 18 Ma has previously been applied. This age was based on discordant TIMS zircon data from the Moisiovaara mafic-ultramafic sill considered to intrude and be coeval with the Pahakangas tholeiites (Luukkonen 1992, Papunen et al. 2009). The new data on the Moisiovaara sample (A976) suggest a slightly older age of 2823 ± 6 Ma, which, according to the stratigraphy, should give the upper age limit for the komatiites.

The age of dated igneous rocks in the Kellojärvi area, in the central part of the Kuhmo belt, is close to 2800 Ma (Fig. 36). Four of these samples are felsic rocks belonging to the Mäkisensuo Formation and give an average age of 2798 ± 2 Ma. According to the geological field relations, some of these rocks are considered intruding the komatiites of the Siivikko Formation and should thus provide the minimum age for the associated mafic-ultramafic magmatism. Particularly strong evidence is provided by the felsic porphyry dyke A2027 with an age of 2795 ± 3 Ma, which clearly intrudes the komatiites in the Siivikkovaara area. The results call for a revision of the stratigraphic position of the Mäkisensuo Formation, which was previously thought to be located below the Pahakangas Formation (Papunen et al. 2009).

The igneous ages obtained from the four samples of the felsic volcanic units in the Tipasjärvi greenstone belt range from 2828 ± 3 Ma to 2796 ± 8 Ma and thus resemble those measured from the Kuhmo belt. The revised age of 2798 ± 2 Ma from the felsic volcanic host rock of the Taivaljärvi ore deposit is equal to that obtained for the felsic rocks in the Kellojärvi area. In terms of age constraints, the komatiitic volcanism in the Tipasjärvi belt resembles that in the Kuhmo belt.

A major adjustment concerns the age of the Ruokojärvi Formation, which has been thought to be as old as ca. 3 Ga (Papunen et al. 2009). This was based on multi-grain TIMS data and the position of these rocks in the marginal zone of the greenstone belt. The new U-Pb data on two felsic volcanic rocks suggest that the magmatic age actually is ca. 2.82 Ga, but the presence of abundant

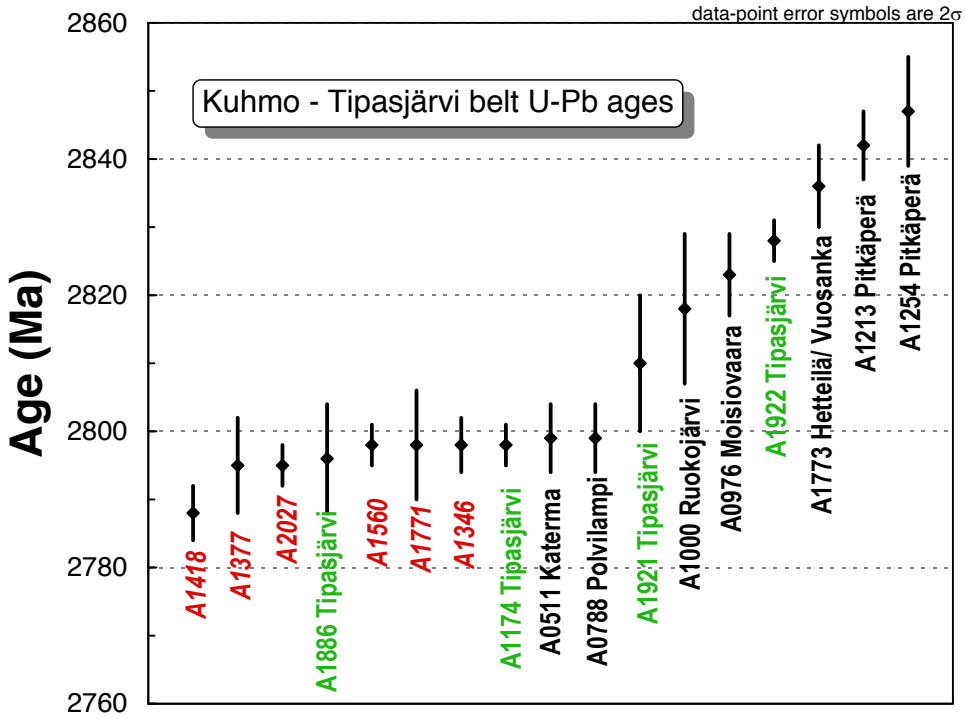

Fig. 36. Summary of the U-Pb ages (Ma) of the Kuhmo and Tipasjärvi greenstone belts. Red labels in italics refer to samples from the Kellojärvi area.

xenocrystic zircon up to 3.13 Ga in age is also evident. Rocks with ages of ca. 2.84 Ga observed in the Vuosanka (Hetteilä) and Pitkäperä areas (Fig. 13) on the eastern side of the main Kuhmo belt seem to represent volcanic activity preceding the main magmatic phases of volcanism recorded in the Kuhmo belt (Fig. 36).

Both the Kuhmo and Tipasjärvi belts contain sedimentary rocks that were deposited after 2.75 Ga and thus at least 50 Ma after the associated volcanism. These rocks have been assigned to the Ronkaperä and Kokkoniemi Formations. Still younger sediments have been found at Arola, in the Kuhmo belt, where a quartzite sliver contains detrital zircon as young as 2.7 Ga.

The new ages from the greenstone belts also imply that many felsic plutons, including the 2785 ± 7 Ma Viitavaara tonalite close to Kellojärvi, are clearly younger than the volcanic rocks within the belt. However, the 2830 ± 2 Ma Haasiavaara and 2814 ± 3 Ma Huuskonvaara tonalites flanking the Tipasjärvi belt are coeval with the oldest volcanic rocks in this belt.

One of the main conclusions from the Sm-Nd (Huhma et al. this volume) and U-Pb results is that the bulk of the Kuhmo and Tipasjärvi belt igneous rocks represent juvenile, 2.8 Ga materials from mantle, and the contribution of older crust is very limited. This is consistent with Patchett et al. (1981), who reported an $\varepsilon_{Hf(2800)}$ of +6 for zircon in the rhyolite A511 (Katerma), and is also seen in trace element compositions of the mafic volcanic rocks of these greenstone belts, as they are systematically characterized by low Th/Yb and LREE/Yb coupled with low Nb/Yb (ref). Many granitoids surrounding the belt, e.g. those at Viitavaara and Haasiavaara, also represent juvenile additions to the crust (Huhma et al. this volume).

ILOMANTSI AND KOVERO SCHIST BELTS

The geology of the Ilomantsi area and the Ilomantsi (Hattu) schist belt, in particular, was dealt with in great detail in the Ilomantsi gold project (Nurmi & Sorjonen-Ward 1993). The region consists of an Archaean plutonic dominated terrain, in which mostly tonalitic and granodioritic intrusions penetrated and deformed a sediment-dominated supracrustal sequence. No depositional basement for the volcano-sedimentary rock successions has been found or any obvious unconformities within the successions. All contacts between the granitoid and volcanic-sedimentary rocks are intrusive or tectonic. Primary depositional features such as graded and cross-bedding are commonly preserved and have enabled a fairly confident assessment of the regional structural framework (Sorjonen-Ward 1993).

The Ilomantsi (Hattu) schist belt proper (Fig. 37) was formed ~2.75 Ga ago (Vaasjoki et al. 1993), and granitoids intruded immediately after or during the volcanic activity. Some conglomerate clasts in flanking sediments exhibit ages close to those of the greenstone belt volcanics and the intruding granitoid rocks. Multi-grain TIMS U-Pb data available on some greywackes also suggest relatively rapidly evolving crustal generation (Vaasjoki et al. 1993). In order to obtain a better picture of the geochronological relationships, zircons from a sedimentary rock (A221) and porphyry dyke (A282, A301) were analysed using the ion microprobe (Nordsim).

A221 Hattuvaara greywacke in Ilomantsi

Sample A221 represents a fine-grained, schistose, lower-amphibolite-facies greywacke from Hattuvaara, on which multi-grain U-Pb TIMS analyses were published by Vaasjoki et al. (1993, Fig. 37). Abundant zircon available at GTK storage consists of a light-coloured, fairly homogeneous population. Many grains are stubby and translucent prisms showing oscillatory zoning typical for zircon of felsic plutonic rocks. The signs of sedimentary abrasion are evident but relatively minor.

SIMS U-Pb analyses were carried out on 35 zircon grains, mostly from inner, oscillatory-zoned domains (Appendix 1). The bulk of the data plots in a cluster, which suggests an age of ca. 2.75 Ga (Fig. 38). Only two dates are significantly older and two slightly younger at ca. 2.7 Ga. Considering only the concordant data, the youngest Pb/Pb ages are 2700 ± 6 Ma (n2494-15, 2-sigma error) and 2711 ± 14 Ma (n2494-24). Several analyses yield ages of ca. 2.75 Ga, which can be considered as a reliable upper age limit for the deposition. The ages of the granitoids and dykes that intrude the Ilomantsi schists represented by sample A221 are also close to 2.75 Ga (samples A1094 Tasanvaara,

A1095 Kivisuo, A285 Kuittila, A284 Lehtovaara, Vaasjoki et al. 1993, Sorjonen-Ward & Claoué-Long 1993, Heilimo et al. 2011). These ages are based on both TIMS and SIMS U-Pb analyses and thus confirm the rapid crustal generation and uniform sedimentary source. Consequently, the two younger dates obtained in A221 cannot represent crystallization ages of the source rocks, but are either due to metamorphic disturbance or contamination during sample processing. In fact, analysis n2494-15 shows distinctly higher Th/U and total Th+U, making a case for metamorphic lead loss very plausible. In the available BSE images, these two grains are not distinct from the other zircons. The Sm-Nd model age T_{DM} for this sample is 2.82 Ga (O'Brien et al. 1993), which is also consistent with a relatively juvenile provenance.

U-Pb geochronology of the Vehkavaara dykes in Ilomantsi

The age data from the Vehkavaara porphyritic dykes presented a vexing problem (Vaasjoki et al. 1993). Based on well-exposed field relations, there is no doubt that these dykes cut across mafic host rocks, which closely resemble those of the Ilomantsi schist belt exposed to the north and east of the Silvevaara granodiorite. Within the framework of the Ilomantsi data discussed above, an age of around 2.75 Ga or less would thus be anticipated. However, results of conventional bulk analyses suggested an upper intercept age of ca. 3 Ga for zircons in sample A282, and the least discordant, air-abraded zircon fractions from two other samples (A301 and A338) registered $^{207}Pb/^{206}Pb$ ages of 2.93 and 3.01 Ga, respectively (Vaasjoki et al. 1993). Although the conventional data were heterogeneous, the option that the mafic volcanic rocks in this western part of the Ilomantsi belt were as old as 3 Ga was considered a possibility. Thus, an ion-probe investigation of zircon from the Vehkavaara dykes seemed warranted and was carried out in 2000 at the NORDSIM laboratory.

Plagioclase-phyric dykes at Vehkavaara intrude a NE-trending zone of mafic volcanic rocks exposed near the western margin of the Silvevaara granodiorite (Fig. 37, Vaasjoki et al. 1993). Contacts against the host greenstones are sharp. The dykes range in width from 0.2 to 60 m and are strongly deformed and metamorphosed. The existing zircon separates from samples A282 and A301 were used for the isotopic analyses. The zircon grains from both samples are rather similar, euhedral or subhedral, with simple prismatic and pyramidic faces dominant. A striking feature is the frequent occurrence of a thin, darker, crack-filled layer within the crystals, which seems to define an interface between cores and outer domains. The latter often display oscillatory zoning, while zonation in the cores is less frequent but wider (Fig. 39).

The U-Pb data from both samples are similar. Analyses from the zircon cores yield, with one exception, significantly older ages than the outer domains (Appendix 1). Four nearly concordant data points from the outer domains of A301 define an average $^{207}Pb/^{206}Pb$ age of 2755 ± 8 Ma, and the results of three further analyses from the outer zircon domains in A282 are consistent with this age (Fig. 40). Seven analyses of cores from A282 provide ages close to 3.0 Ga, while the $^{207}Pb/^{206}Pb$ ages of other core analyses range from 2.9 to 3.3 Ga. The few nearly concordant TIMS data points from both samples plot within the field determined by the ion probe analyses.

Discussion on the Vehkavaara dykes

The ion-microprobe results from the Vehkavaara porphyry samples record, beyond any doubt, a complex history for these rocks. The oscillatory-zoned zircon domains surrounding distinct cores are considered to represent growth within felsic magma. Thus, the age of 2755 ± 8 Ma obtained from these outer domains should also record the emplacement of the Vehkavaara dykes. Although some grains are nearly devoid of such enveloping zircon, in several grains from sample A301, in particular, these domains make up a significant proportion of the zircon grain volumes (Fig. 39). One analysis (n760-08a) suggests a slightly younger age (Fig. 40), which is probable due to a post-magmatic open-system behaviour of this high-U zircon.

The analyses from the cores do not record any specific older event, as the ages range from 2.9 to 3.3 Ga (Fig. 40). It is conceivable that some of the scatter could be due to partial resetting of the U-Pb system, but it more likely originates from a heterogeneous protolith.

An origin predominantly from a much older (e.g. 3.3 Ga) crustal source is not supported by the Sm-Nd

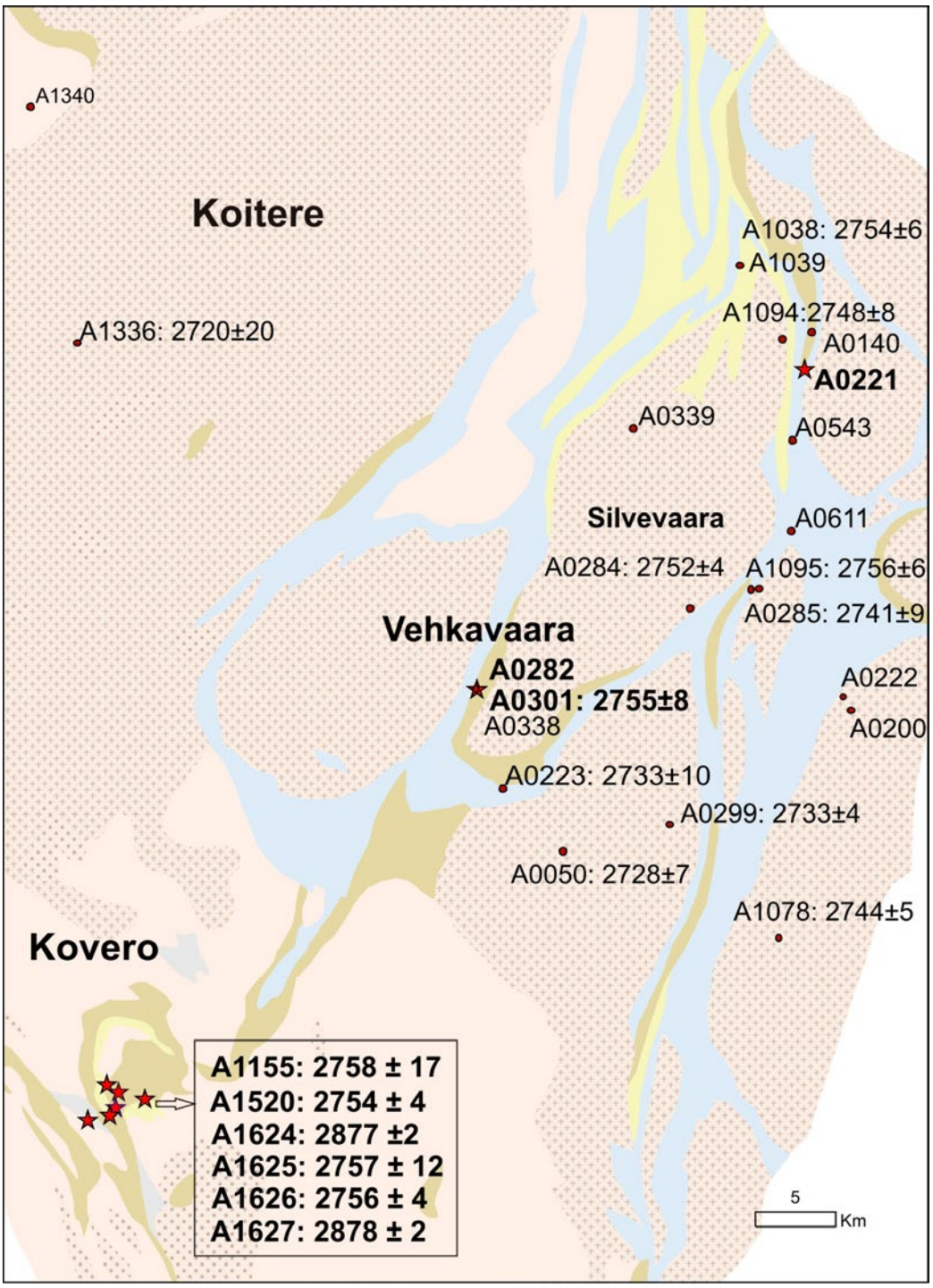

Fig. 37. Geological map of the Ilomantsi-Kovero area showing sample sites (red star – this study, other samples – Vaasjoki et al. 1993, Heilimo et al. 2011). Igneous ages with 2-sigma errors are given in Ma after the sample number. The map is based on the 1:1 000 000 geological map (Korsman et al. 1997), where the greenstone belt consists of three main rock types: mafic (and minor ultramafic) metavolcanic rocks (brown), intermediate-felsic metavolcanic rocks (yellow) and metasediments (blue). Granitoids surrounding the greenstone belts are divided into TTGs and intrusive rocks (stippled).

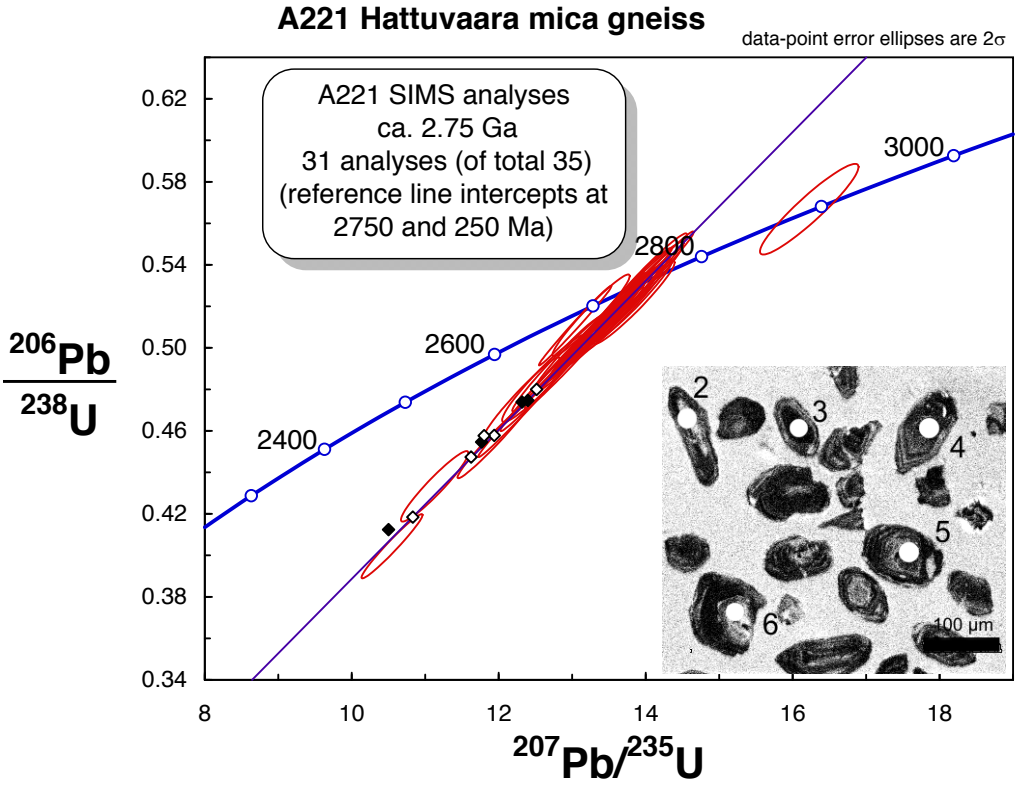

Fig. 38. Concordia diagram of zircon U-Pb SIMS analyses from the Hattuvaara greywacke A221 (error ellipses). The multi-grain TIMS analyses on A221 (solid diamonds) and another greywacke A543 (open diamonds) are shown for reference (Vaasjoki et al. 1993).

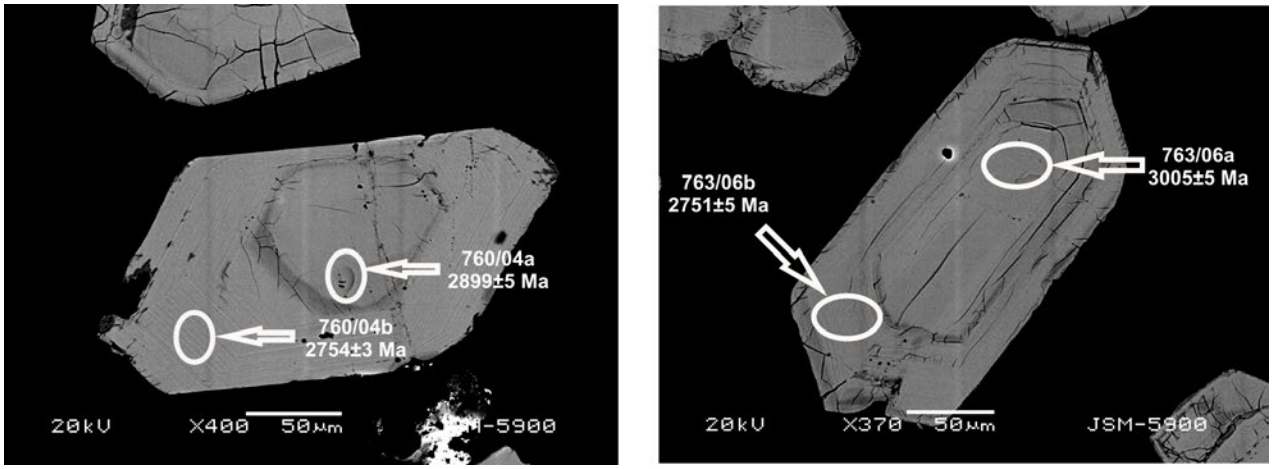

Fig. 39. Scanning electron microscope (SEM) backscatter electron (BSE) images of grain 4 from sample A301 (left) and grain 6 from sample A282 (right) showing analysis spots and $^{207}Pb/^{206}Pb$ ages with 1-sigma errors. Note the darker, fractured zone between the old cores and ca. 2.75 Ga oscillatory zoned outer domains.

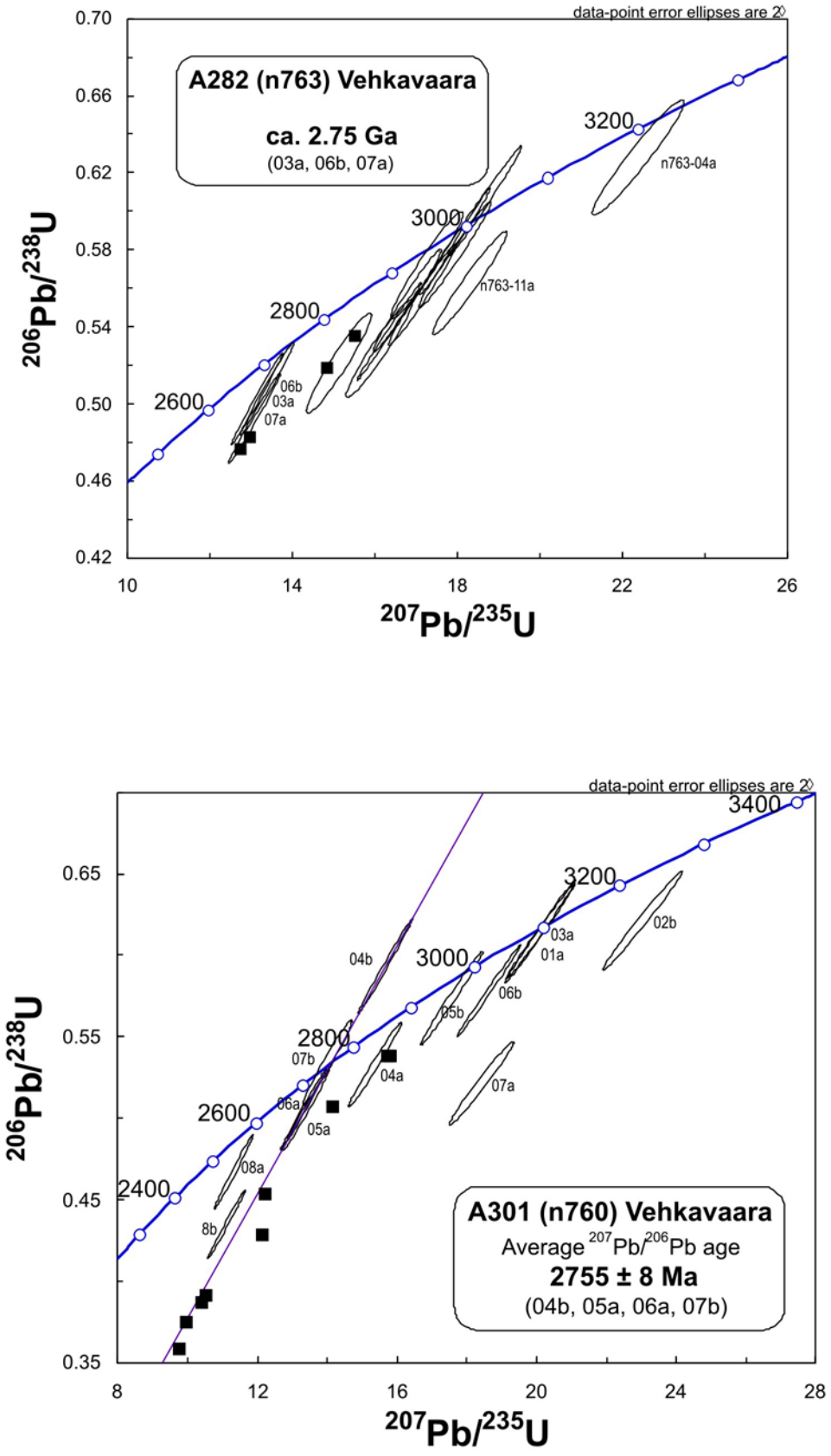

Fig 40. U-Pb concordia plot of zircon data from the Vehkavaara porphyry dyke samples A282 and A301. The black squares denote TIMS data points by Vaasjoki et al. (1993).

data, which provide slightly negative $\varepsilon_{Nd}(2750)$ values and T_{DM} model ages slightly exceeding 3.0 Ga (Fig. 41). In any case, the Vehkavaara porphyry contains abundant inherited zircon, which survived well through the melting process that formed the felsic magma, and typically acted as nuclei for new zircon growth at 2.75 Ga.

Accepting the age of ca. 2.75 Ga as the timing of emplacement of the dykes also removes stratigraphic difficulties, as this age is practically identical to the intrusion ages of the granitoid domes deforming the Hattu schist belt. Moreover, this interpretation agrees with the titanite U-Pb data from the Vehkavaara samples A301 and A338 (Vaasjoki et al. 1993). The ages of the plutons intruding the belt include 2748 ± 8 Ma (A1094-Tasanvaara) and 2741 ± 9 Ma (A285-Kuittila), which are also indistinguishable from the age of volcanism dated at 2754 ± 6 Ma in the Hattu schist belt (A1038-Poikapää, Vaasjoki et al. 1993). These conventional results are supported by the U-Pb zircon age of 2757 ± 4 Ma determined by SIMS (SHRIMP) for the Silvevaara granodiorite (A284, Sorjonen-Ward & Claoué-Long 1993). In addition to this magmatic population, the granodiorite sample also contains few older grains up to 3.19 Ga in age. This heterogeneity was expected based on the scattered conventional data (Vaasjoki et al. 1993).

The conventional U-Pb zircon ages available for other felsic dykes dated from the Ilomantsi area are also close to 2.75 Ga (Vaasjoki et al. 1993). These include 2756 ± 6 Ma from the porphyry (A1095-Kivisuo) near Kuittila on the eastern side of the Silvevaara pluton and 2733 ± 10 Ma from a dyke (A223-Iknonvaara) on the southern margin of the Silvevaara pluton (Fig. 37). Although the data from A223 are slightly scattered, there is no evidence for major old inheritance in either of these dykes.

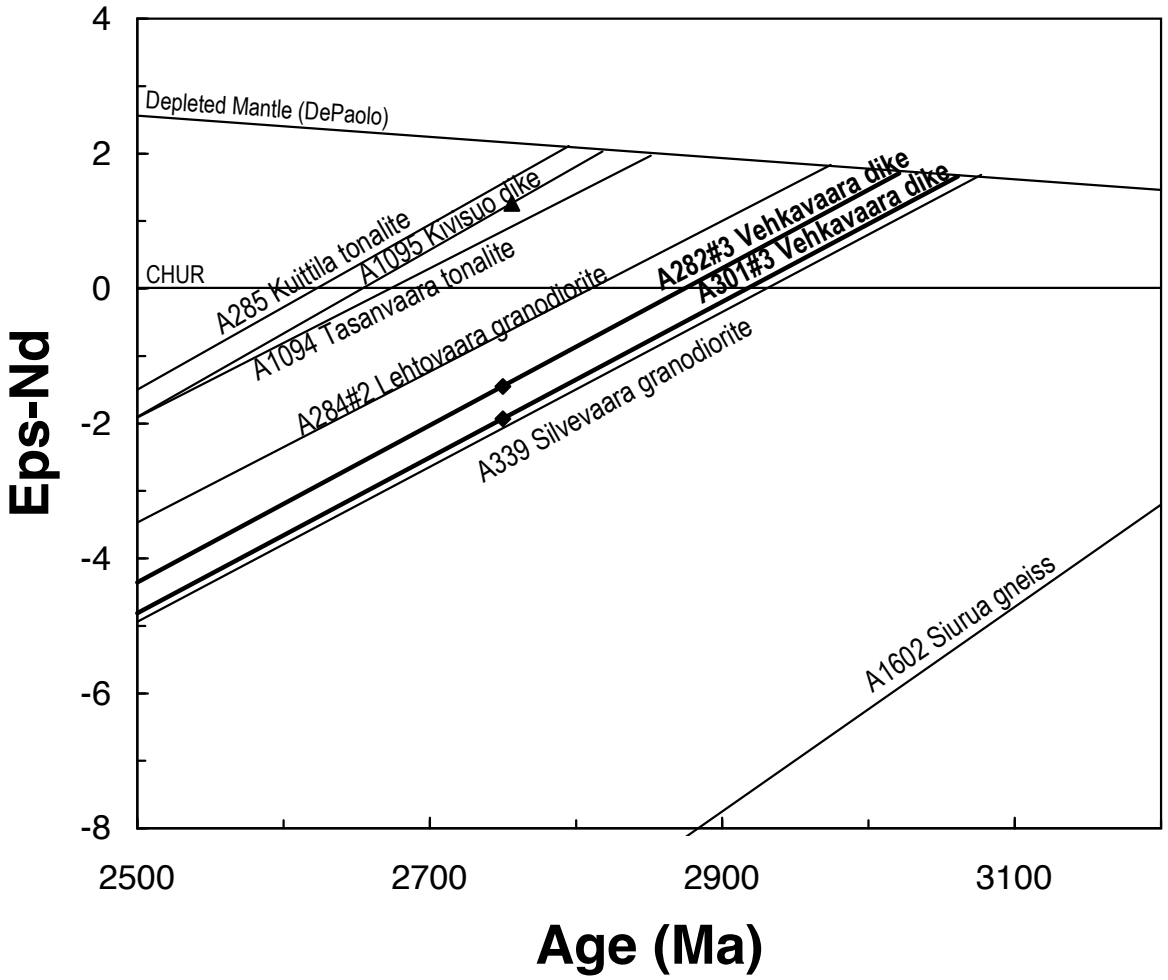

Fig. 41. Epsilon-Nd vs. age diagram of Vehkavaara porphyries and selected samples from the Ilomantsi area (data from Huhma et al. this volume, O'Brien et al. 1993). In addition to evolution lines, initial ratios are shown for Vehkavaara (diamonds) and Kivisuo porphyries (triangle). The evolution of chondritic uniform reservoir (CHUR, DePaolo & Wasserburg 1976), depleted mantle (DePaolo 1981) and the 3.5 Ga Siurua gneiss (Mutanen & Huhma 2003) are shown for reference.

The Sm-Nd data support the pattern observed from the U-Pb zircon studies (Fig. 41). The results from the Vehkavaara porphyries (initial epsilon of -1.5 and -1.9) are similar to that from the 2.75 Ga Silvevaara granodiorite (A284 and A339, O'Brien et al. 1993), which also contains some older (3.1–3.2 Ga) zircon crystals (Sorjonen-Ward & Claoué-Long 1993), suggesting a significant contribution from old crustal sources. In contrast, the Sm-Nd data from the Kivisuo dyke and Kuittila tonalite provide clearly positive initial epsilon values, suggesting a short crustal prehistory for the source material of these rocks.

U-Pb geochronology of the Kovero greenstone belt

From the Vehkavaara area discussed above, the Ilomantsi (Hattu) schist belt continues to the southwest and at a distance of ca. 30 km, joins a wider domain of volcanic rocks called the Kovero greenstone belt (Fig. 37). The Kovero greenstone belt has been subdivided into three stratigraphic sections: 1) Keskijärvi (western part), 2) Kuusijärvi (middle part) and 3) Sonkaja (eastern part) (Tuukki 1991). The belt mostly consists of tholeiitic volcanic rocks, komatiites, komatiitic basalts, felsic volcanic rocks and sedimentary rocks (Tuukki 1991, Konnunaho 1999). The research carried out on the ore potential and related mapping of the area has provided the framework and goals for the isotope studies (Konnunaho 1999). Eight samples were collected from representative felsic and mafic lithologies, and four of these have yielded zircon for U-Pb analyses. Zircon from three previously studied samples was also included in this study and analysed using the CA-TIMS method.

A1624 Hämäläniemi felsic volcanic rock

The Hämäläniemi sample A1624 is a fine-grained, felsic volcanic rock. The rock seems to form a thin tuffaceous interlayer within the tholeiitic Kontiokangas Formation of the Kuusijärvi section. Felsic volcanic interlayers and banded iron formations within mafic units at the Kovero greenstone belt are quite common manifestations of the bimodal volcanism in the area (Tuukki 1991, Konnunaho 1999).

Mineral separation yielded a fair number of zircon grains, which are small (<70 µm), fairly turbid, subhedral and slightly rounded due to resorption. The colour of the grains ranges from reddish to pale or colourless. The U-Pb zircon

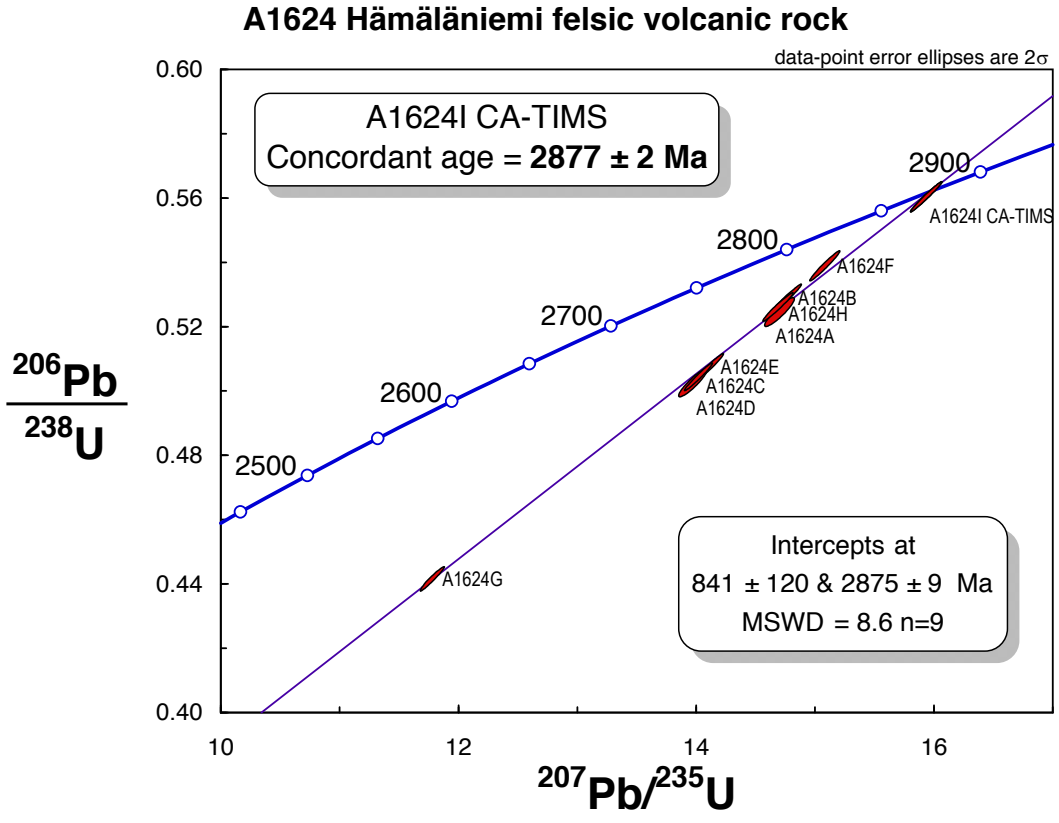

Fig. 42. Concordia diagram of zircon U-Pb TIMS analyses from the Hämäläniemi felsic rock (A1624), which is considered as a tuffaceous interlayer within tholeiitic volcanic rocks of the Kovero greenstone belt.

data including one CA-TIMS analysis define a chord with intercepts on the concordia at 2875 ± 9 and 841 ± 120 Ma (MSWD = 8.6, Appendix 2, Fig. 42). Some scatter is evident, but no distinction in the isotopic composition was observed between the analysed red and pale zircon grains. The analytical result obtained using chemical abrasion (A1624I) is concordant at 2877 ± 2 Ma and is considered the age of zircon and the host felsic rock as well.

A1627 Rasisuo felsic tuff

A 30-metre-thick zone of felsic pyroclastic rock occurs in the upper part of the Kuuspuro Formation in the Kuusijärvi section of the Rasisuo area. The felsic rock occurs between mafic and ultramafic volcanics. Some primary textures are also visible on the outcrops of felsic tuffaceous rocks in the Rasisuo area. Sample A1627 from this exposure is very fine-grained and mainly consists of plagioclase, quartz and biotite and minor amounts of chlorite and amphibole.

A fair number of zircon grains were obtained from this sample. They consist of euhedral, short prismatic (l:w ~2) to more equant, brownish and translucent crystals. The population is homogeneous, and the grain-size is predominantly fine to medium (~100 µm). In BSE images, the grains commonly show weak oscillatory, magmatic zoning (Fig. 14I). A few grains have distinct core and mantle domains, and thin, obviously metamorphic rims are common (Fig. 14I, zircon 13).

Both TIMS and SIMS analyses on zircon are available from the Rasisuo felsic tuff. A total of 18 zircon domains were analysed by SIMS from the sample (Appendix 1). Two of these have high common-lead content and are useless for age calculations. Two data points are marginally above concordia, but as a whole, the data are concordant and yield an age of 2875 ± 4 Ma (Fig. 43). There are no age differences between various zircon domains.

Before access to the SIMS facility, TIMS U-Pb analyses yielded a chord with concordia intercepts at 2868 ± 22 and 1232 ± 250 Ma (Fig. 43). The data are, however, slightly scattered along the line (MSWD = 17), very likely due to metamorphic effects, which are pronounced in Archaean terrains in Finland.

A CA-TIMS analysis carried out on the high density zircon fraction provides a concordant result at 2878 ± 2 Ma. As no heterogeneity was observed in the SIMS data and the Th/U ratio (deduced from the radiogenic $^{208}Pb/^{206}Pb$ ratio, Appendix 2) in chemically abraded zircon is the

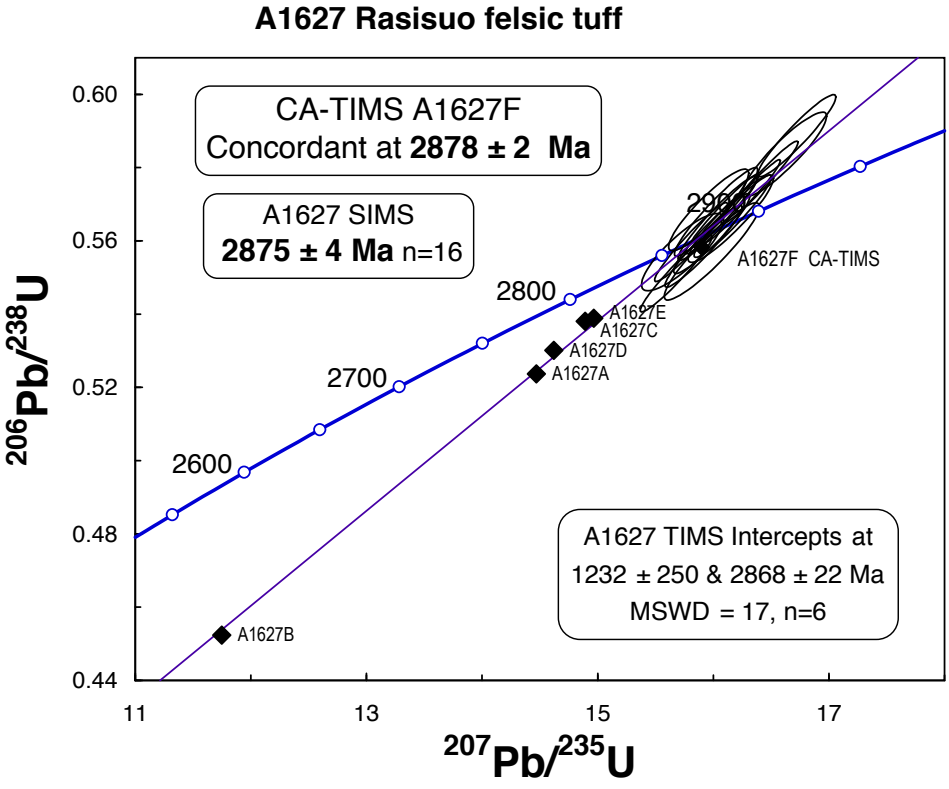

Fig. 43. Concordia diagram of zircon U-Pb SIMS (error ellipses) and TIMS (diamonds) analyses from the Rasisuo felsic tuff (A1627), Kovero greenstone belt.

same as in untreated material, the age of 2878 ± 2 Ma is considered to date the felsic volcanism of the Rasinsuo area.

A1625 Rasisuo plagioclase porphyry dyke

Dykes of andesitic to dacitic compositions are common in the Kovero greenstone belt. Sample A1625 was collected from a plagioclase porphyry dyke approximately 1 km south of the sampling site of the felsic tuff A1627 discussed above. The dyke crosscuts tholeiitic volcanic rocks of the Kuuspuro Formation in the Kuusijärvi section. The groundmass consists of fine-grained plagioclase, quartz and biotite and minor amounts of titanite, ilmenite, chlorite, sericite, apatite and zircon. The phenocrysts are mainly oligoclase and also hornblende in some andesitic dykes (Tuukki 1991, Konnunaho 1999).

Sample A1625 yielded abundant subhedral zircon grains, which are translucent, brown and mostly larger than 75 µm (+200 mesh). Crystal edges are commonly sharp, and the population looks homogeneous. The five U-Pb TIMS analyses carried out on zircon define a chord, which has intercepts at 2757 ± 12 Ma and 921 ± 260 Ma (Appendix 2, Fig. 44). Some scatter presumably due to metamorphic effects is evident (MSWD = 5), but the nearly concordant CA-TIMS analysis #A1625F and the homogeneity of the zircon population strongly suggest that the upper intercept age can be considered a good estimate for the crystallization time of zircon and the dyke as well. In fact, the $^{207}Pb/^{206}Pb$ age of 2756 ± 2 Ma should provide the minimum age, constraining the lower error limit of the regression calculation.

A1626 Rasisuo gabbro

Sample A1626 represents the most evolved variety of gabbroic amphibolites in the Rasisuo area. These amphibolites comprise a series of variable fractionated mafic to intermediate, coarse-grained gabbroic rocks. Sample (A1626) is a variety of intermediate, coarse-grained, plagioclace- and quartz-rich rock. Tuukki (1991) suggested that the gabbroic rocks are stratigraphically associated with the Kuuspuro Formation of the Kuusijärvi section. However, the stratigraphical situation and genesis of the gabbroic amphibolites are still open.

Zircon separated from the Rasisuo gabbro A1626 consists of dark brown, transparent to translucent, coarse grained (<75 µm grain-size fraction largely comprises zircon fragments), mainly subhedral, long to more equant crystals.

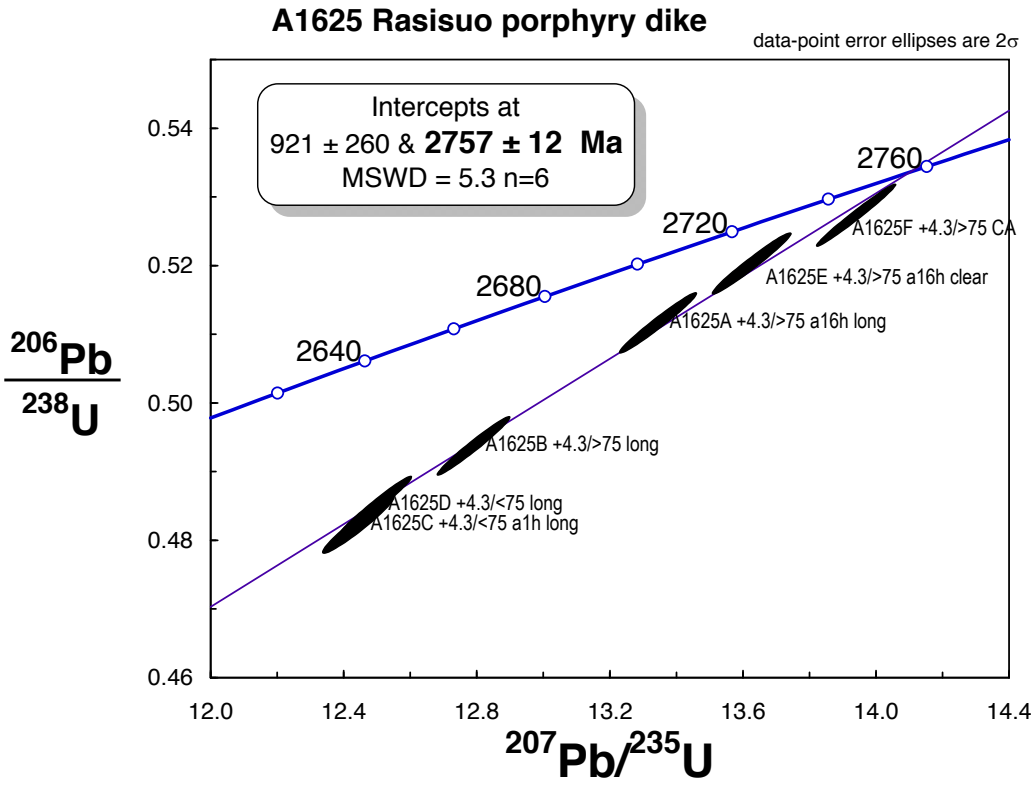

Fig. 44. Concordia diagram of zircon U-Pb TIMS analyses from the Rasisuo porphyry dyke (A1625), which crosscuts mafic volcanic rocks in the Kovero greenstone belt.

The fraction 4.0–4.2 g/cm^3 also contains pale and smaller grains with varying, mostly subhedral to anhedral forms. Generally, the zircon population is rather homogeneous and typical for gabbroic rocks.

In BSE images (Fig. 14H), the zircon grains commonly show either weak, longitudinal compositional zoning or homogeneous internal structures. Few grains show separate core and rim structures, and some grains have suffered from a varying degree of alteration.

A total of 18 zircon domains were analysed by ion microprobe from the Rasisuo gabbro. Two of these analyses were rejected due to high common-lead contents (Appendix 1). All other U-Pb data plot in a tight cluster and define a concordia age of 2756 ± 4 Ma (Fig. 45). The previous multi-grain TIMS U-Pb determinations on zircon produced discordant and heterogeneous data, but are roughly compatible with the age obtained by SIMS (Appendix 2, Fig. 45). It is clear from the BSE images that many zircon grains contain metamict domains, which are the major source for discordance in the TIMS analyses. As Archaean rocks, especially near the Proterozoic boundary, have undergone a complex metamorphic history, lead loss may have had taken place in several stages and with a variable intensity depending on the zircon domains and fractions, resulting in heterogeneous U-Pb data.

A1520 Kiukoinvaara felsic dyke

A granodioritic dyke crosscuts andalusite-bearing mica schist at Kiukoinvaara (Luukkonen et al. 2002). The dyke is deformed, and on the geological map this location (A1520) is clearly west of the main Kovero volcanic belt discussed above.

Zircon separated from sample A1520 consists of euhedral, brown, short and resorbed grains.

Five previously performed TIMS analyses on zircon revealed a large amount of common lead and yielded discordant U-Pb data (Appendix 2) plotting along a chord with concordia intercepts at 2724 ± 6 and 423 ± 48 Ma (MSWD=1.6; not shown in Fig. 46). In contrast, the composition obtained by CA-TIMS analysis has very high $^{206}Pb/^{204}Pb$ (28500) and yields a nearly concordant date of 2750 ± 2 Ma, significantly older than the upper intercept obtained from the discordant data (Fig. 46). Six data points yield intercepts at 2748 ± 16 and 585 ± 150 Ma, and an obviously large MSWD of 16. It is clear that discordant analyses with high common lead should have a minor weight in determining the real age of magmatic zircon. The CA-TIMS analysis together with two

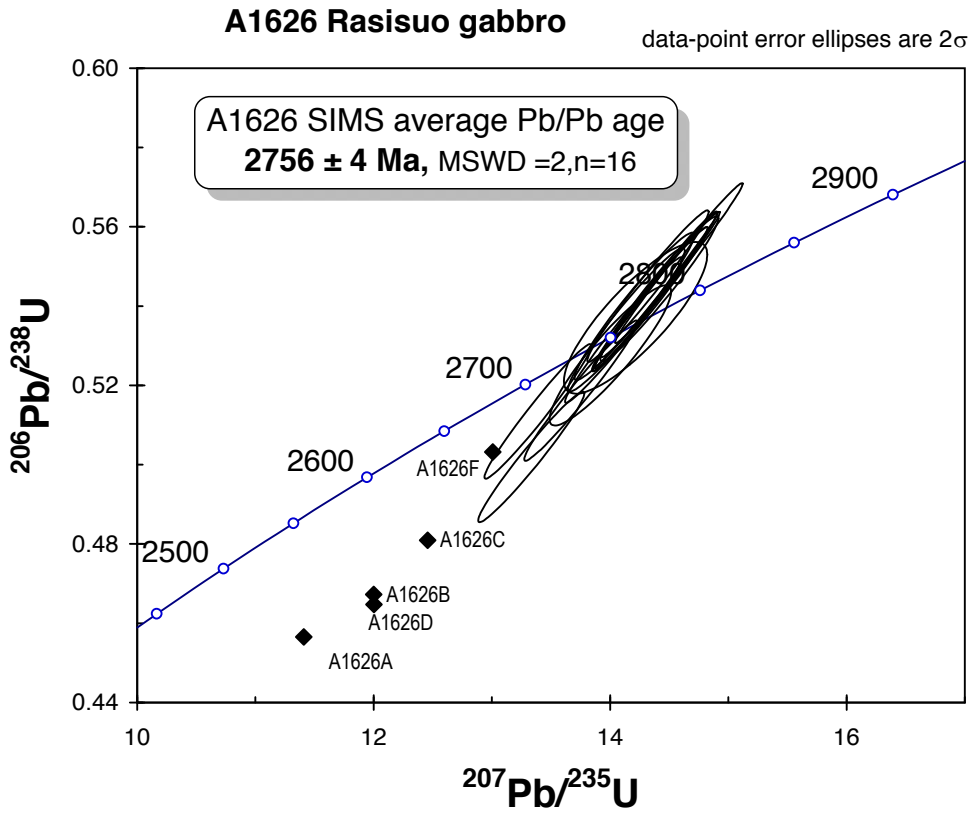

Fig. 45. Concordia diagram of zircon U-Pb SIMS (error ellipses) and TIMS (diamonds) analyses from the Rasisuo gabbro (A1626), Kovero greenstone belt.

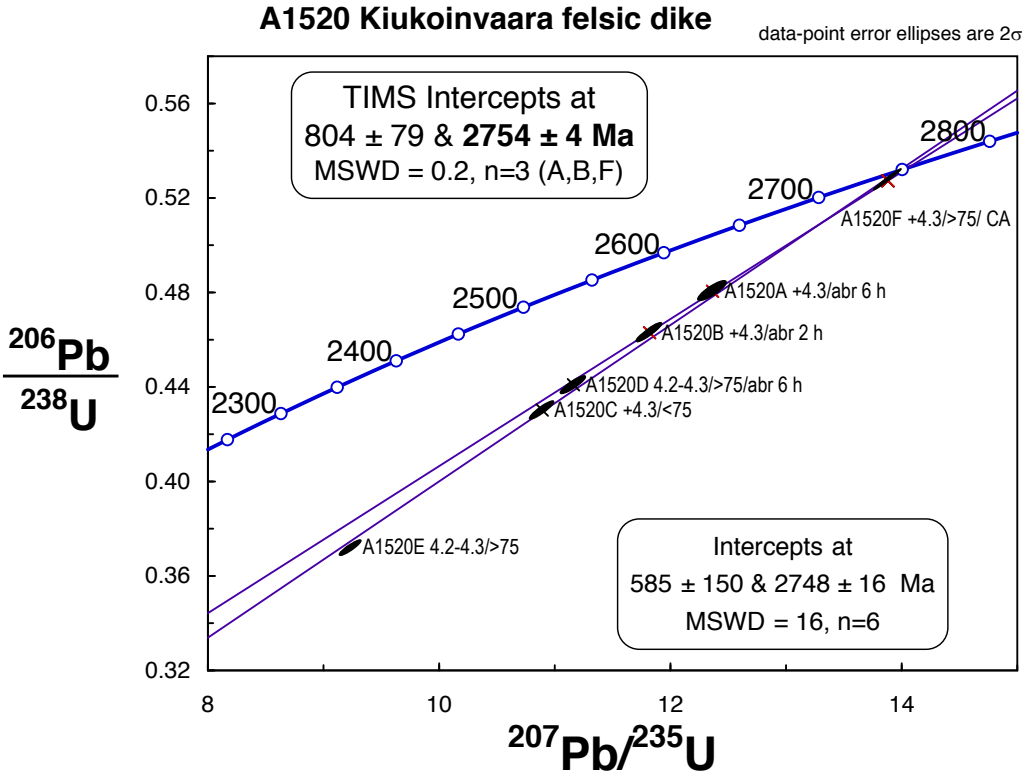

Fig. 46. Concordia diagram of zircon U-Pb TIMS analyses from the Kiukoinvaara felsic dyke (A1520), Kovero greenstone belt (analyses A1520A-E from Vaasjoki et al. 1993).

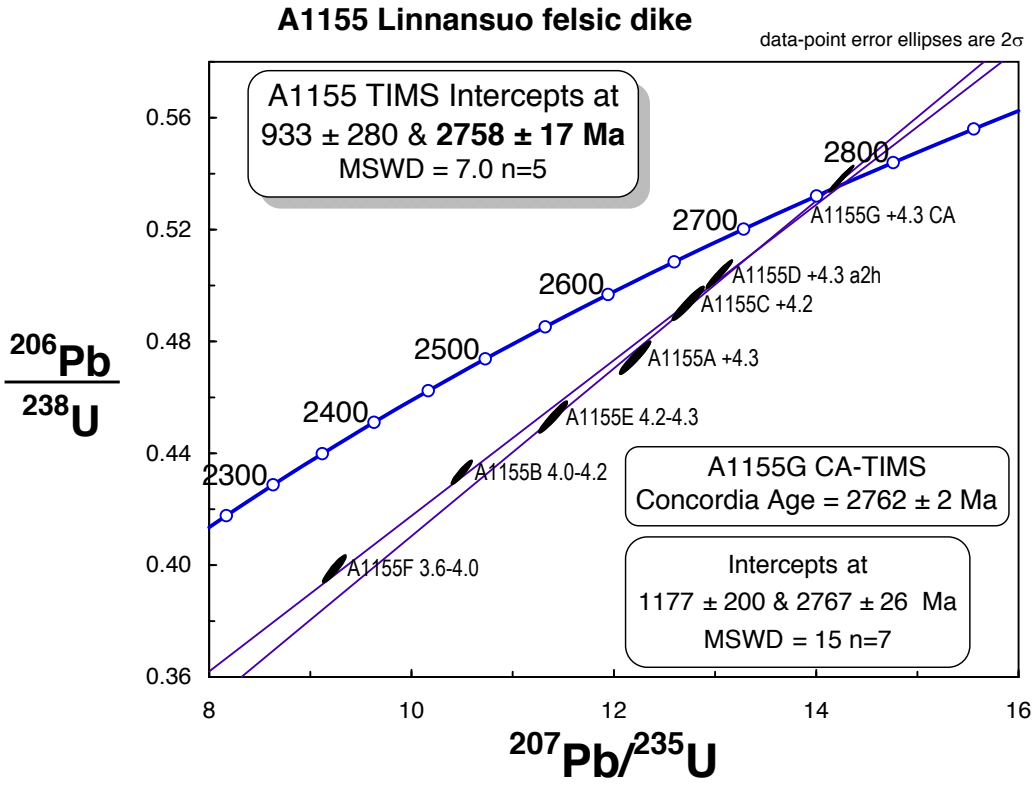

Fig. 47. Concordia diagram of zircon U-Pb TIMS analyses from the Linnansuo felsic dyke (A1155), Kovero belt (analyses A1155A-F from Vaasjoki et al. 1993).

other TIMS analyses on high density, air-abraded zircon fractions yield an upper intercept age of 2754 ± 4 Ma, which we consider to be the best estimate for the crystallization age of the Kiukoinvaara dyke.

A1155 Linnansuo felsic dyke

The Linnansuo plagioclase-phyric, tonalitic dyke crosscuts sedimentary rocks of the Kovero belt. On the aeromagnetic map, the location is at the southern edge of a magnetic high, which seems to follow the mafic rocks. Discordant and slightly heterogeneous U-Pb data were reported by Vaasjoki et al. (1993). The CA-TIMS analysis on high density zircon gives a concordant result at 2762 ± 2 Ma (Appendix 2, Fig. 47). Including all analyses on high density zircon, an upper intercept age of 2758 ± 17 Ma can be calculated. The homogeneous nature of the zircon population in the high density fraction, consisting of euhedral, brown, fairly transparent and short grains, implies that the age obtained can be considered the magmatic age of the dyke. The slight scatter in the data is likely to be due to metamorphic effects. The dyke is deformed and probably predates the major deformations in the area.

Discussion on the Kovero greenstone belt

Two Archaean age groups are evident in the Kovero greenstone belt: 1) the felsic volcanic rocks at 2878 ± 2 Ma and 2) felsic dykes and gabbroic rocks at 2.75–2.76 Ga. The relative abundance of rocks in each age group is, however, impossible to evaluate from the information available.

Sample A1624 (felsic volcanic rock) represents a thin interlayer within tholeiitic basalts, which would suggest that the associated mafic volcanic rocks are also ca. 2.88 Ga old.

Unfortunately, the samples north along the strike (A1622 Otravaara and A1623) were devoid of separable zircon and the extent of these old rocks, as well as the age of one of the main stratigraphic horizons with the Kovero belt (Otravaara formation), remains open.

If the age of the dated gabbro A1626 represents significant volumes of the mafic volcanics, then the rocks of the Kovero greenstone belt would be predominantly 2.75–2.76 Ga in age, which is also the age of the volcanism recorded in the Ilomantsi schist belt. However, the correlation between the Kovero and the Ilomantsi belt is not obvious, since there are differences in their lithologies and geochemistry (O'Brien et al. 1993, Tuukki 1991, Hölttä et al. this volume).

The Ipatti belt ca. 75 km NNW of Kovero contains felsic volcanic rock, which has yielded an age of 2811 ± 4 Ma (Appendix 2, Pekkarinen et al. 2006), and therefore is not directly related to the Kovero belt. The age of 2.88 Ga is unique within the Archaean bedrock in Finland. In Russian Karelia, similar zircon ages have been measured from the Sumozero-Kenozero greenstone belt (2875 ± 2 Ma, Puchtel et al. 1999).

OIJÄRVI GREENSTONE BELT AND PUDASJÄRVI AREA

The Oijärvi greenstone belt is located in the central part of the Archaean Pudasjärvi area (Fig. 48). Due to limited outcrop, the area is relatively poorly known, and much of the current understanding of the geology is based on aeromagnetic data. The few published age results available from the Pudasjärvi area reveal that the oldest rocks in the Fennoscandian Shield, i.e. the 3.5 Ga Siurua gneisses, are found in this region (Mutanen & Huhma 2003). However, the geographical extent of these old gneisses seems to be quite limited. The N–S-trending Oijärvi greenstone belt consists of typical components of Archaean greenstone belts, including mafic, ultramafic, intermediate and minor felsic volcanic rocks and sediments. No age determinations have previously been published from the greenstone belt. The belt is surrounded by granitoids, which are also the subject of the isotope studies reported here.

U-Pb geochronology of the Oijärvi greenstone belt and adjacent areas

This paper presents U-Pb data on 13 samples from the Pudasjärvi area (Fig. 48). Most of these samples are granitoids collected from exploration drill-cores and only two samples are from the supracrustal rocks of the greenstone belt. Results on two paragneisses outside the Oijärvi belt are given in a separate chapter below, and Sm-Nd analyses for most samples are given in Huhma et al. (this volume).

A1783 Puljunlehto dacite

The Puljunlehto sample A1783 was collected from a small outcrop in the northern part of the belt (Fig. 48), where felsic rocks occur among mafic volcanic rocks. The sampled dacitic rock is pale and fine-grained. Mineral separation yielded only a small number of zircon grains, which were all (appr. 50) mounted in epoxy for ion microprobe measurements. The population is slightly heterogeneous in terms of size and morphology. Some grains are prismatic (l:w ~2.5), but more rounded forms also occur. In BSE images, both magmatic, oscillatory-zoned (grains 04, 05) and homogeneous crystals without a distinct internal structure (grain 07) are available (Fig. 14M).

Ten zircon domains were analysed by ion microprobe (Nordsim) from sample A1783 (Appendix 1). The U-Pb data are mostly concordant, low in U and plot in a cluster on a concordia diagram (Fig. 49). Using all data, an average $^{207}Pb/^{206}Pb$ age of 2820 ± 11 Ma can be calculated. The slight scatter may result from metamorphic effects, although the age differences are quite marginal.

A1782 Käärmevaara gabbro

The sampled outcrop of the Käärmevaara gabbro is located at the northern edge of the Oijärvi greenstone belt (Fig. 48). Sample A1782 represents a medium-grained, fairly homogeneous gabbro surrounded by mafic volcanic rocks and may be part of a subvolcanic sill. The main minerals are amphibole and plagioclase.

Only a small amount of zircon was obtained from this sample with all grains found in the density fraction d > 4.2 gcm^{-3}. They are mostly medium- to fine-grained (75–150 μm), weakly yellowish and transparent to translucent. The morphology varies from short subhedral to long prismatic (l:w >3). In BSE images (Fig. 17), almost all zircon grains are pale and show a varying degree of fluid corrosion ("holes") with occasional phase separation (white, dense spots. Only a few grains show clear variation in internal composition (grain 05 in Fig. 14L). Some have pale, quite homogeneous or corroded core domains surrounded by thin dark BSE rims.

Only ten zircon domains were analysed by SIMS (Nordsim, Appendix 1). Most data are marginally above concordia, which is obviously related to the U/Pb calibration. In SIMS analyses, this calibration has no effect on the lead isotope ratios, and thus ages based on Pb isotopic composition on nearly concordant data are reliable. Seven of the ten data points cluster around 2.8 Ga and the corresponding weighted average $^{207}Pb/^{206}Pb$ age is 2802 ± 5 Ma (Fig. 50). Analysis #09a from a dark BSE core of a tiny, presumably metamorphic grain yields an age of 2.70 Ga, #03a from a darker BSE domain has an age of 1.85 Ga, and the youngest grain (#10a) is dated at 0.86 Ga. The Th/U ratio for the 2.8 Ga zircon grains is high, which is common for zircon in mafic rocks. Although the data are relatively sparse, the age of 2802 ± 5 Ma is considered a reliable crystallization age for magmatic zircon and the Käärmevaara gabbro.

Fig. 48. Geological map of the Pudasjärvi area showing sampling sites (red star – this study, other samples – Mutanen & Huhma 2003, Lauri et al. 2011, Perttunen & Vaasjoki 2001).
Igneous ages with 2-sigma errors are given in Ma after sample number. The map is based on the 1:1 000 000 geological map (Korsman et al. 1997), where the main units are the Oijärvi greenstone belt (brownish) and granitoid areas.

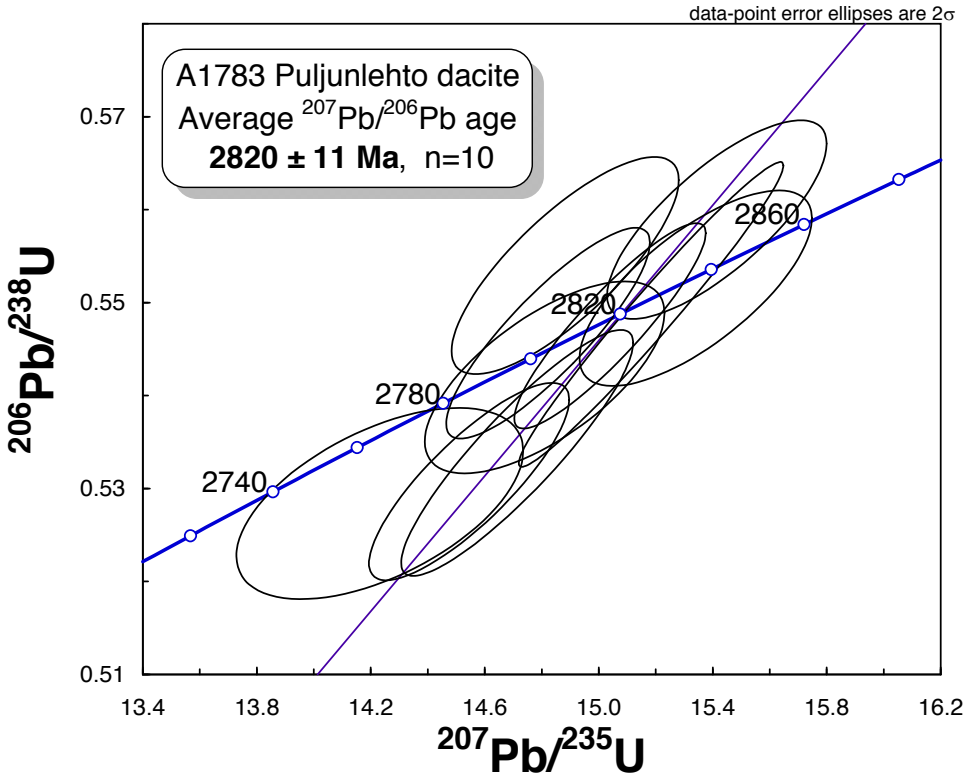

Fig. 49. Concordia diagram showing zircon SIMS U-Pb isotopic data from A1783 Puljunlehto dacite, Oijärvi greenstone belt.

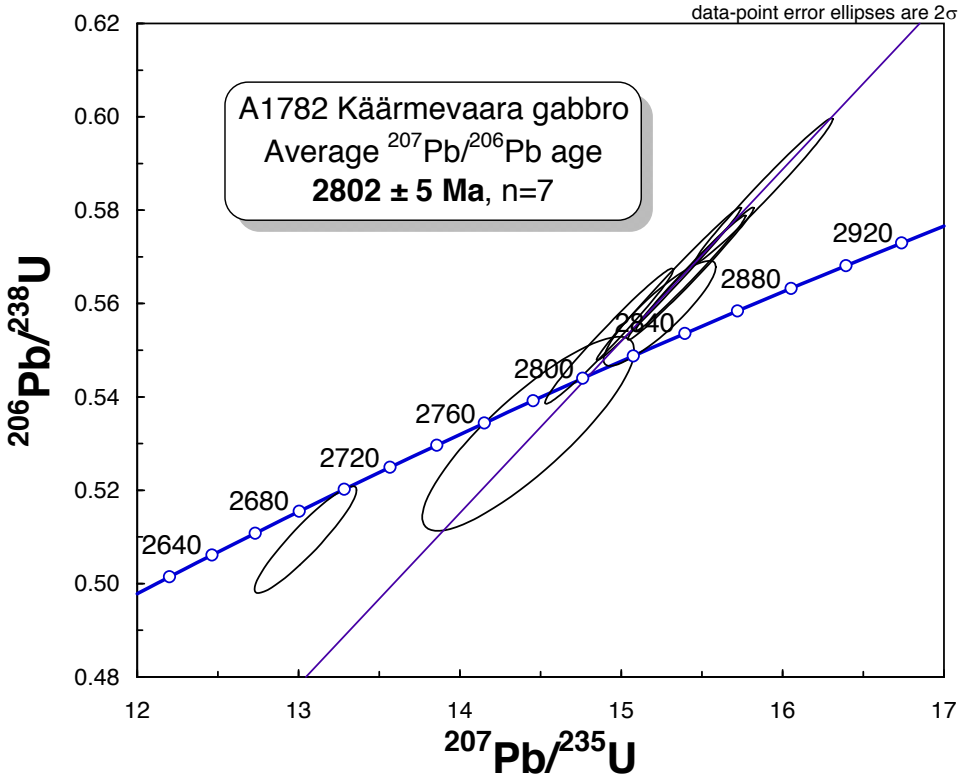

Fig. 50. Concordia diagram showing zircon SIMS U-Pb isotopic data from the Käärmevaara gabbro (A1782), Oijärvi greenstone belt.

A1533 Surmakumpu porphyry dyke

The Surmakumpu-type porphyries occur as crosscutting or conformable dykes within the mafic and ultramafic volcanic rocks in central part of the Oijärvi greenstone belt (Fig. 48). Sample A1533 (TPT-96-80), which was collected from a 20-m-thick dyke, is a reddish and sheared rock containing phenocrysts of quartz and altered plagioclase. The matrix minerals include quartz, plagioclase, K-feldspar, carbonate, sericite, biotite, opaque and zircon.

Mineral separation yielded abundant zircon, which consists of euhedral prisms with well-developed pyramids and typically sharp crystal edges. Zircon is generally dark reddish, and many crystals, especially in the low-density fraction, have distinct, turbid inner domains. The isotopic data reveal a very wide range in Pb/U ratios consistent with microscopic observations on the presence of metamict domains (Appendix 2, Fig. 51). The common-lead content is high in the domains, producing discordant data. In contrast, the CA-TIMS analysis #A1533F shows very low common lead and provides a nearly concordant result with a $^{207}Pb/^{206}Pb$ age of 2690 ± 2 Ma.

Recently, a few analyses were carried out using LA-MC-ICPMS. The data on fresh zircon are concordant and yield an age of 2670 ± 9 Ma, but turbid cores are strongly discordant (e.g. #8a, Appendix 3, Fig. 51). Both methods give roughly consistent results, although the age obtained by CA-TIMS is slightly older than the age obtained by ICPMS. As the ICPMS session was stable and analyses were carried out using the in-house Archaean standard, we consider the age of 2670 ± 9 Ma the best estimate for the crystallization time of magmatic zircon and the dyke. It is conceivable that some older inherited zircon was included in the CA-TIMS analysis.

A1553 Pitkäkumpu tonalite

Sample A1553 collected from a drill core (3521/97/R590/33.60–56.10) is from a reddish, medium-grained and homogeneous tonalite intrusion crosscutting volcanic rocks in the central part of the Oijärvi belt (Fig. 48). The main minerals are fairly coarse, euhedral plagioclase and more fine-grained quartz and biotite. The accessory minerals include apatite, zircon and pyrite, and sericite, carbonate and chlorite as alteration

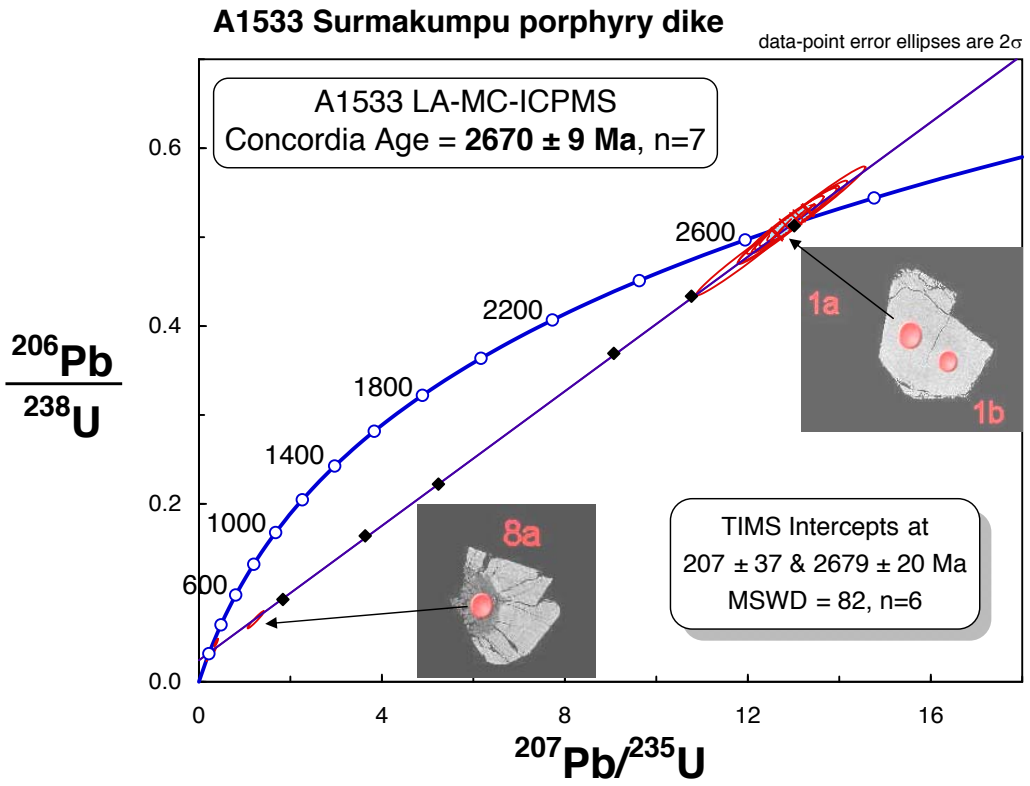

Fig. 51. Concordia diagram of zircon U-Pb TIMS (diamonds) and LA-MC-ICPMS (error ellipses) analyses from the Surmakumpu porphyry dyke (A1533), which crosscuts volcanic rocks of the Oijärvi greenstone belt.

products of plagioclase and biotite. Inclusions of volcanic rocks are observed near the margin of the intrusion.

Zircon obtained from the Pitkäkumpu tonalite consists of euhedral, long prisms, which are mostly pale and fairly clear. The six U-Pb TIMS analyses on zircon show a range of Pb/U ratios and are scattered along a chord, which gives intercepts with the concordia at 2728 ± 14 and 48 ± 92 Ma (MSWD = 42, Appendix 2 and Fig. 52). The CA-TIMS analysis #A1553F has a very low common-lead content and gives a nearly concordant result with a $^{207}Pb/^{206}Pb$ age of 2735 ± 2 Ma. Although there are no detailed images of zircon or spot analyses at hand, the morphology of the zircon grains suggests that this result is close to the age of zircon and magmatic crystallization of the Pitkäkumpu tonalite.

A1490 Tuore Ristisuonpalo granodiorite

Sample A1490 represents granodioritic gneiss close to the western margin of the Oijärvi greenstone belt (Fig. 48). The sample was collected from an exploration drill core (M52/3521/96/R511, depth 65.50-75.20). Based on drill-core observations, the rock is strongly deformed and seems to cross cut a mica schist of the Oijärvi belt. The main minerals of the sample are altered plagioclase, K-feldspar, quartz and biotite. The accessory minerals include titanite, apatite, opaque and zircon. Mineral separation yielded a relatively small number of zircon grains, which are euhedral and prismatic but in transmitted light are fairly turbid.

The four conventional U-Pb TIMS analyses provide discordant results and define a chord with an upper intercept at 2699 ± 22 Ma (Appendix 2, Fig. 53). However, the analysis #A1490E using chemical abrasion is closer to concordia and yields a $^{207}Pb/^{206}Pb$ age of 2801 ± 2 Ma, which is the minimum age for the material analysed. The data as a whole are thus scattered, which is due to zircon inheritance and/or multistage metamorphic effects resulting in variable discordia patterns. As the Th/U ratio (calculated from radiogenic $^{208}Pb/^{206}Pb$) in the CA-treated zircon fraction #A1490E and the other heavy (>4.2 g/cm3) zircon fractions are similar, it is likely that the CA-TIMS analysis registers the composition of the same magmatic domains. Using these two analyses, an upper intercept age of 2815 ± 5 Ma can be calculated. Without further studies, the precise age of this sample remains unclear but may well be close to 2.8 Ga.

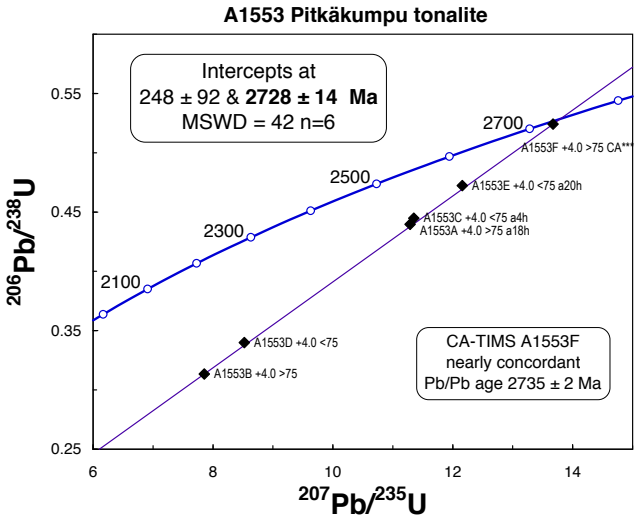

Fig. 52. Concordia diagram of zircon analyses from the Pitkäkumpu tonalite (A1553), which crosscuts volcanic rocks in the Oijärvi greenstone belt.

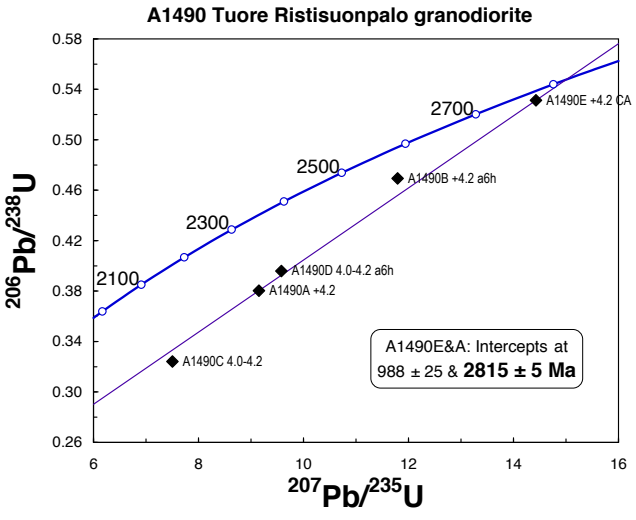

Fig. 53. Concordia diagram of zircon analyses from the Tuore Ristisuonpalo granodiorite (A1490) occurring close to the western margin of the Oijärvi greenstone belt.

A1534 Keväpalo tonalite

Sample A1534 (TPT-96-61) from Keväpalo represents tonalites occurring on the eastern side of the Oijärvi greenstone belt (Fig. 48). The rock is medium grained and light-coloured and mostly consists of altered plagioclase, quartz and biotite. Titanite, apatite, opaque and zircon are the main accessory minerals. Zircon forms euhedral, long magmatic crystals, which are pale in colour and typically fairly transparent.

The U-Pb data on zircon, including one CA-TIMS analysis define a chord and intercepts at 2781 ± 6 and 330 ± 100 Ma (MSWD = 3; Appendix 2, Fig. 54). The upper intercept age is younger than the age of 2830 ± 20 Ma interpreted from laser MC-ICPMS analyses carried out in Oslo (Lauri et al. 2011). The U-Pb analysis on sphene gives an age of 2717 ± 3 Ma, which probably registers the timing of a metamorphic event.

A1739 Veskanmaa granodiorite

The Veskanmaa granodiorite represents felsic plutonic rocks occurring west of the Oijärvi greenstone belt (Fig. 48). Sample A1739 collected from a drill core (3521/00/R677/ 170.70–192.90) is fine-grained, only slightly deformed and has plagioclase, quartz and K-feldspar as the main minerals. Plagioclase is partly altered to epidote, sericite and carbonate. Other minor minerals are biotite, apatite, titanite and opaque. Only a small number of zircon grains was obtained from this sample. They are mostly clear, euhedral and slightly rounded on edges due to resorption.

The U-Pb data are discordant and do not yield a coherent chord on the concordia diagram (Appendix 2, Fig. 55). The CA-TIMS analysis #A1739E is also somewhat discordant, but the Pb/Pb age of 2.76 Ga can be taken as a minimum age for the analysed material. As the Th/U ratios (based on radiogenic $^{208}Pb/^{206}Pb$) are the same in all analysed fractions, it is likely that the CA-TIMS analysis registers the composition of the primary magmatic domains. The scatter of the data is due to zircon inheritance and/or multiple metamorphic effects, which are pronounced in many Archaean rocks in Finland. In this sample, these effects are also shown by the U-Pb analysis on titanite, which gives a Pb/Pb age of 2.63 Ga. Without further studies, the exact age of this rock remains unclear, but may well be close to 2.77 Ga.

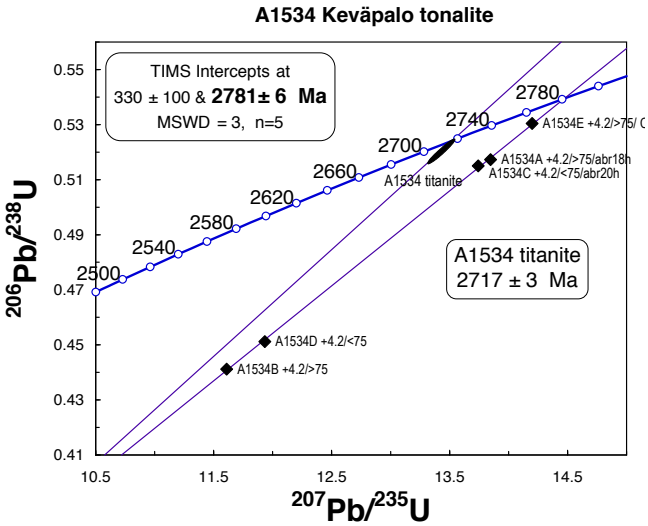

Fig. 54. Concordia diagram of zircon and titanite analyses from the Keväpalo tonalite (A1534), east of the Oijärvi greenstone belt.

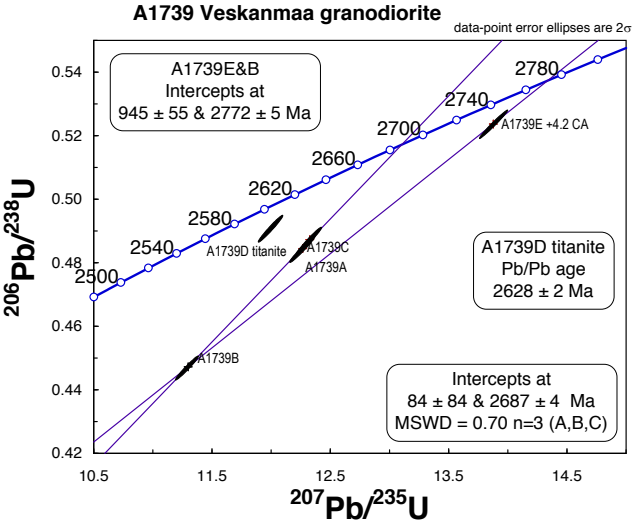

Fig. 55. Concordia diagram of zircon and titanite analyses from the Veskanmaa granodiorite (A1739) occurring on the western side of the Oijärvi greenstone belt.

A1731 Palomaa granite

The Palomaa sample A1731 was collected from a drill core (3514/01/R410/41.55–51.50) recovered ca. 12 km west of the 3.5 Ga Siurua gneisses (Fig. 48). The main minerals are plagioclase, K-feldspar and quartz, and the accessory minerals include biotite, titanite and opaque phases. Although the rock is now chemically and mineralogically granite, it is possible that it has been granitized and was originally a tonalite.

Zircon in sample A1731 consists of euhedral, brownish and fairly long, translucent prisms. Five U-Pb TIMS analyses are slightly scattered along a chord, which has an upper intercept at 2702 ± 16 Ma (MSWD = 8.9; Appendix 2, Fig. 56). The scatter is likely to be due to complex metamorphic effects, which have taken place in several stages during Archaean and Proterozoic times or even later. Compared to the CA-TIMS data #A1731E, the three most discordant fractions have a fairly high amount of common lead and should be weighted less in determining the zircon age. Rejecting them, the remaining two analyses indicate an upper intercept age of 2708 ± 6 Ma.

A1740 Palomaa monzonite

The Palomaa monzonite sample A1740 was collected from a drill core (3514/01/R406/ 146.00–151.10) approximately 600 m west of the site of the previous sample. The rock is medium-grained and homogeneous with plagioclase and K-feldspar as the main minerals. The accessory minerals include biotite, brown amphibole, orthopyroxene, clinopyroxene, quartz, apatite, zircon and opaque phases. Pyroxenes are partly altered to light-coloured amphibole. The Palomaa monzonite shows up on the aeromagnetic maps as a pronounced positive anomaly.

Mineral separation yielded abundant zircon grains, which are mainly euhedral, brown and fairly transparent. Crystal surfaces are shiny probably due to resorption. Most grains are larger than 75 µm. In spite of the relatively high content of U in zircon, the TIMS U-Pb data are only mildly discordant (Appendix 2, Fig. 57). The effects of air abrasion are negligible, consistent with the morphology of zircon. All seven data points including the concordant CA-TIMS analysis #A1740G define a chord with concordia intercepts at 2682 ± 15 Ma and 970 ± 380 Ma (MSWD = 5.7). Analysis A1740G gives a concordant result at 2672 ± 2 Ma, but has a clearly lower Th/U ratio (deduced from radiogenic $^{208}Pb/^{206}Pb$) than in the other data. It is thus feasible that, compared to the other data, the latter contained a larger metamorphic zircon component distinct from the main magmatic population.

A1741 Pahkakoski granodiorite

Sample A1741 was collected from a drill core (3512/02/R339/ 20.20-27.70), which was drilled in Pahkakoski on the southern margin of the Pudasjärvi area close to the Proterozoic Kiiminki schist belt (Fig. 48). On the geological map, the rock unit is named as Tannila granodiorite. The rock is massive, medium-grained granodiorite, which has altered plagioclase, quartz and K-feldspar as the

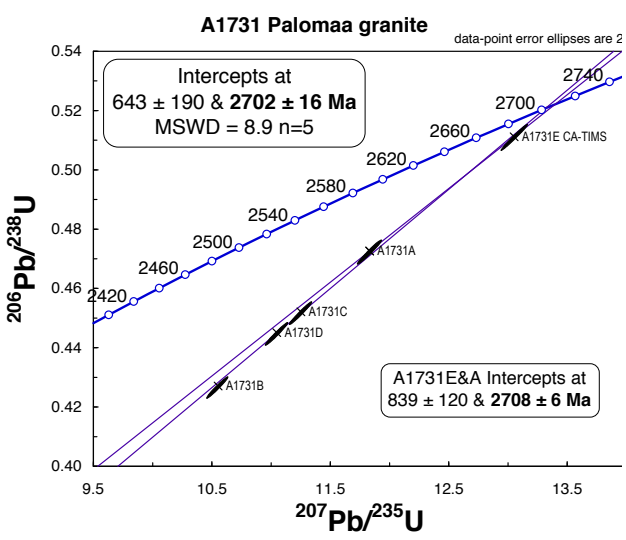

Fig. 56. Concordia diagram of zircon analyses from the Palomaa granite (A1731).

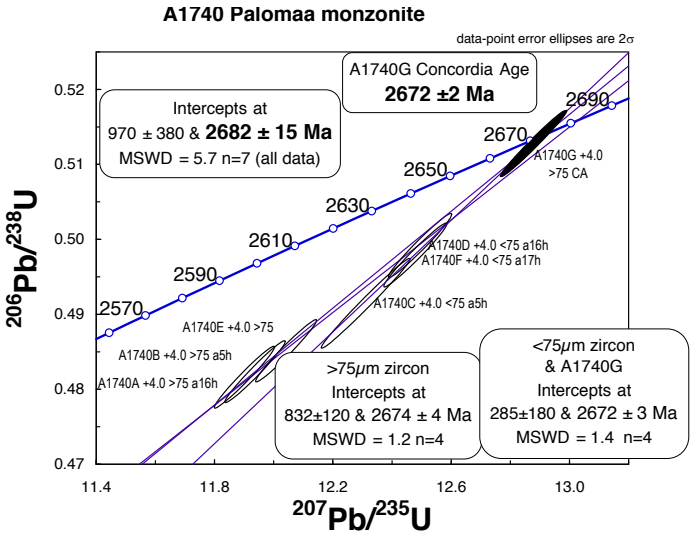

Fig. 57. Concordia diagram of zircon analyses from the Palomaa monzonite (A1740).

main minerals. Among the accessory minerals are biotite, epidote, apatite and opaque.

Sample A1741 yielded only a small number of zircon grains, which are mostly reddish and turbid. The conventional U-Pb data reveal that the common-lead content is very high, and the results are strongly discordant. In contrast, the CA-TIMS analysis #A1741E shows only a small amount of common lead and provides Pb/U ratios reasonably close to the concordia curve (Appendix 2, Fig. 58). All data define a chord with concordia intercepts at 2758 ± 13 and 140 ± 35 Ma. The data do not fit perfectly with the regression line (MSWD =18), which may partly be due to an underestimate of analytical errors for the low $^{206}Pb/^{204}Pb$ analyses. Nevertheless, due to the CA-TIMS analysis, the date of 2758 ± 13 Ma may be considered a reasonable estimate for the crystallization age of the Pahkakoski (Tannila) granodiorite.

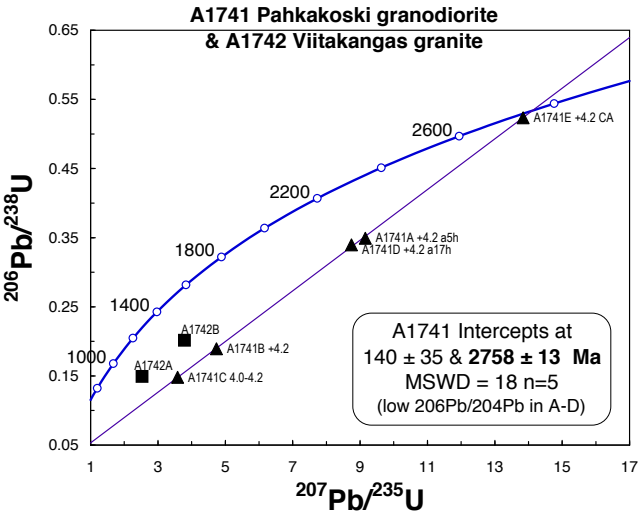

Fig. 58. Concordia diagram of zircon analyses from the Pahkakoski granodiorite (A1741) and Viitakangas granite (A1742).

A1742 Viitakangas granite

The Viitakangas granite is also located on the southern margin of the Pudasjärvi area ca. 20 km west of the Pahkakoski locality discussed above (Fig. 48). Sample A1742 was collected from an outcrop (SIR-02-1.1) and has K-feldspar, plagioclase and quartz as the main minerals. The rock is fairly coarse-grained, grey and sheared, and plagioclase is partly altered.

Zircon grains obtained from sample A1742 are short, grey and turbid prisms. Only two U-Pb TIMS analyses were carried out on this sample, resulting in very discordant data with high concentrations of uranium and common lead (Appendix 2, Fig. 58). Consequently, no age estimate can be made from these data.

Discussion on the age of the Oijärvi greenstone belt and adjacent areas

SIMS U-Pb analyses on two samples, A1782 and A1783, suggest that the age of the Oijärvi greenstone belt is ca. 2.82–2.80 Ga. Provided that the gabbroic rock A1782 represents a primary, undisturbed composition, an origin from time-integrated depleted mantle with clearly positive initial ε_{Nd} (+2.7) is indicated for the mafic lithologies (Huhma et al. this volume).

Many of the granitoids and dykes in close association with the greenstone belt provide discordant and heterogeneous U-Pb zircon data. The age estimates for these samples presented above are largely based on concordant or nearly concordant isotopic compositions obtained by CA-TIMS analysis, but some of these may still represent mixtures of various age components. Nevertheless, most of these estimates suggest that the surrounding granitoids are younger than the greenstone belt, which is consistent with the crosscutting relationship whenever the contact is observed. The Sm-Nd model ages (T_{DM}) for these felsic rocks range from 2.7 to 3.0 Ga and suggest that many lithologies are relatively juvenile and thus do not represent much older reworked crust, in contrast to the 3.5 Ga Siurua gneisses east of the greenstone belt (Fig. 48, Huhma et al. this volume). The Sm-Nd model ages from the Siurua gneisses are mostly ca. 3.5–3.7 Ga, and distinctly old crustal signatures are also evident from Lu-Hf results on zircon from these rocks (Lauri et al. 2011).

SIMS AGES ON ZIRCON IN PARAGNEISSES

In addition to metasediments within the greenstone belts discussed above, ion microprobe datings have been performed on four samples taken from sedimentary rocks in Archaean paragneiss belts. In their previous study on the Archaean Nurmes paragneisses in eastern Finland, Kontinen et al. (2007) concluded that the deposition of the protolith wackes took place close to 2.7 Ga. Their trace element and U–Pb data suggest that the source terrains mainly comprised 2.75–2.70 Ga TTG gneisses and sanukitoid-type plutons and mafic volcanic rocks. Most zircon grains in the few studied metasediment samples from the Central Puolanka Group of the Kainuu belt (Fig. 1) are also ca. 2.73 Ga (Huhma et al. 2000).

A1814 Pitkäpalo mica gneiss in the Pudasjärvi area

Sample A1814 (56-PSH-04) represents a slightly migmatized sedimentary rock occurring ca. 15 km west-northwest of the Oijärvi greenstone belt (Fig. 48). The zircon grains obtained from this sample are mostly euhedral with slightly rounded edges, typical for zircon in many paragneisses.

SIMS U-Pb analyses were carried out on 26 zircon grains, but many analyses provided discordant age results (Appendix 1). However, most data plot on a chord which intercepts the concordia at ca. 2.74 Ga and 0.2 Ga (Fig. 59). The rest of the analyses suggest older ages up to 3.17 Ga. The results imply that the deposition of this sediment took place after 2.73–2.74 Ga. The relatively young average provenance is consistent with the Sm-Nd T_{DM} model age of 2.81 Ga (Huhma et al. this volume).

A1842 Jäkälämaa mica gneiss in the Pudasjärvi area

Sample A1842 (PSH$-2004-79) was collected 7 km NE of the 3.5 Ga Siurua gneiss (Fig. 48). The rock is medium-grained, grey, mica-rich banded gneiss containing ca. 5–10% granitic leucosome. Zircon grains obtained from this sample are mostly light grey and rounded, showing internal oscillatory zoning. In addition to zircon, separation yielded abundant garnet and monazite.

SIMS U-Pb analyses were carried out on 32 zircon grains from inner, mostly oscillatory-zoned domains (Appendix 1). One-third of the data provide discordant ages and as a whole, the ages range from ca. 2.7 up to ca. 3 Ga (Fig. 60). Considering only concordant data, most ages are between 2.70 and 2.76 Ga. The key question also here is whether these ages represent real

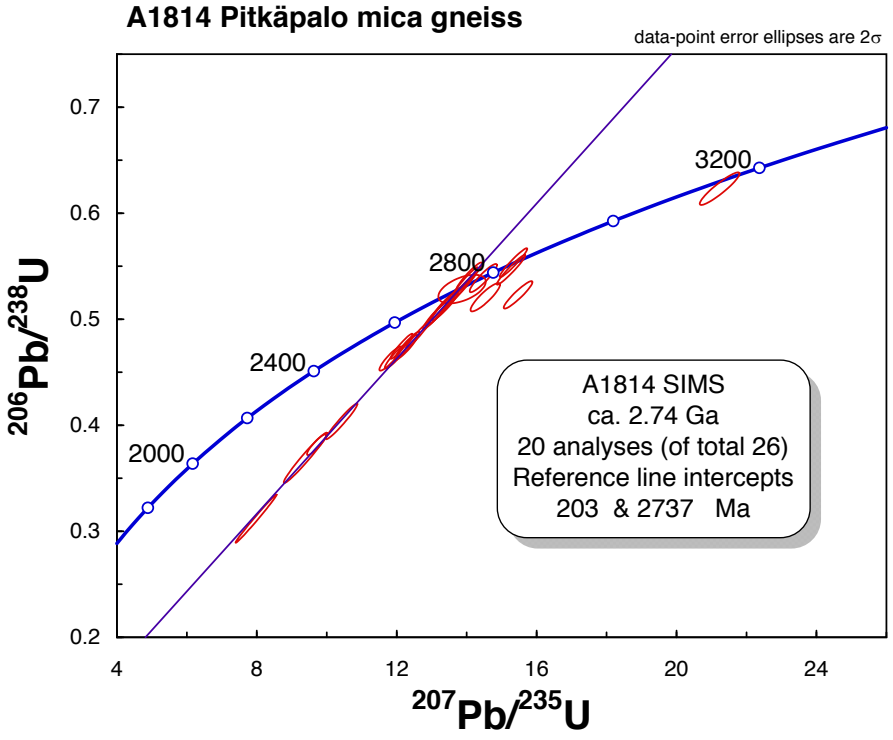

Fig. 59. Concordia diagram of zircon SIMS analyses from the Pitkäpalo (Ranua) mica gneiss A1814.

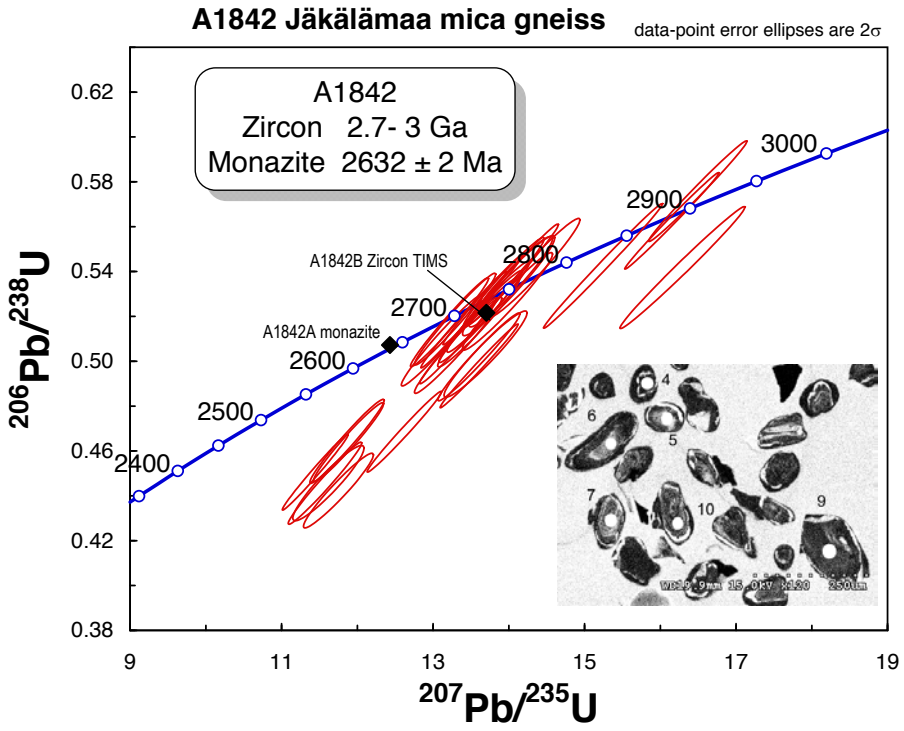

Fig. 60. Concordia diagram showing U-Pb analyses from the Jäkälämaa mica gneiss A1842 from Pudasjärvi. Error ellipses – SIMS analyses, diamonds – multi-grain TIMS analyses on zircon and monazite.

magmatic ages from the source rocks or whether there are any metamorphic effects that might produce younger ages. Some constraint for the timing of metamorphism in the case of sample A1842 is provided by the U-Pb TIMS analysis on monazite, which is concordant at 2632 ± 2 Ma (Appendix 2, Fig. 60). In terms of the morphology and Th/U ratio, the youngest zircons do not notably differ from the other grains. For example, zircon n2497-29 is a large (200 µm), oscillatory zoned grain, and the analysis carried out on the core yielded a date of 2701 ± 10 Ma. Although there are no obvious reasons to interpret the several dates between 2.70 and 2.73 Ga as representing metamorphic events, one may still speculate whether the zircon grains have been partly affected by metamorphism, since the rock is migmatitic.

In any case, the results obtained from sample A1842 are similar to those reported by Kontinen et al. (2007) for Archaean paragneisses in eastern Finland. It is also evident that no 3.5 Ga zircons were found in the sample, even though the sampling site is located only 6.7 km from the 3.5 Ga Siurua gneisses (Mutanen & Huhma 2003). This indicates that either the Siurua gneiss was not exposed at the time of sedimentation or that the paragneiss and the Siurua gneiss were later juxtaposed by tectonic movements. The relatively young average provenance of the mica gneiss is consistent with the Sm-Nd T_{DM} model age of 2.74 Ga (Huhma et al. this volume).

A1840 Riihivaara mica gneiss

Sample A1840 (PIM$-2003-497-N7) represents migmatitic mica gneisses located ca. 40 km WSW of the Suomussalmi greenstone belt and ca. 20 km east of the Palaeoproterozoic Kainuu schist belt. The rock is a medium-grained, pale to dark grey and banded gneiss containing 10–15% granitic leucosome. Zircon grains are moderately rounded, fairly dark and oscillatory-zoned.

SIMS U-Pb analyses were carried out on 32 zircon grains from inner, mostly oscillatory-zoned domains (Appendix 1). Due to a high content of common lead, three analyses were rejected. Most data are concordant and give dates from 2.72 up to 2.97 Ga (Fig. 61). Provided that these register the ages of igneous protoliths, several analyses suggest that the deposition took place after 2.72-2.73 Ga. This is consistent with the results obtained from a tonalitic vein crosscutting the mica gneiss, which has yielded a U-Pb zircon age of 2702 ± 14 Ma (Mikkola et al. 2011a). The Sm-Nd T_{DM} model age for this sample is 2.87 Ga (Huhma et al. this volume).

A1243 Susi-Kervinen mica gneiss in the Iisalmi complex

Sample A1243 is a migmatitic mica gneiss from Rautavaara, belonging to the Iisalmi complex (Fig. 1). The rocks in the Susi-Kervinen area comprise mica gneisses, amphibolites and strongly altered lithologies including garnet-cordierite-rocks and migmatites (Paavola 1999). Zircon grains in sample A1243 are grey, turbid, rounded and shiny on surfaces.

SIMS U-Pb analyses were carried out on 30 zir-

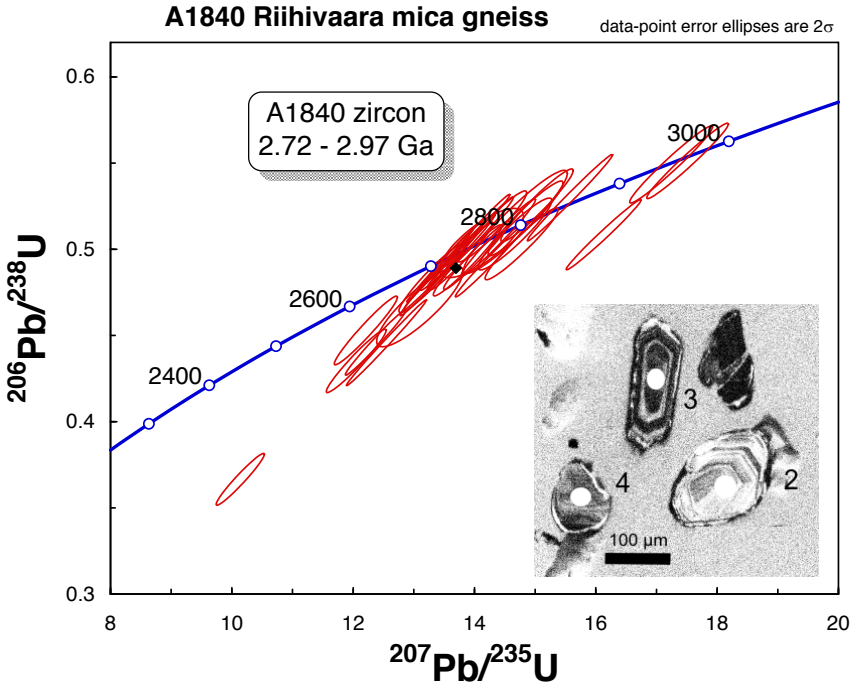

Fig. 61. Concordia diagram showing U-Pb zircon analyses from the Riihivaara mica gneiss (A1840) from Suomussalmi. Error ellipses – SIMS analyses, diamond – multi-grain TIMS analysis.

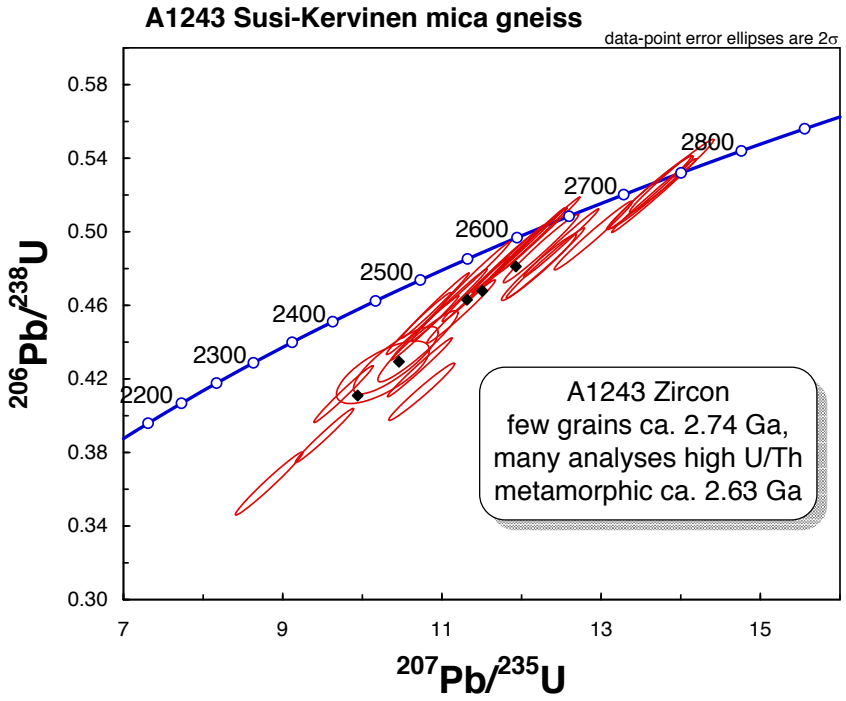

Fig. 62. Concordia diagram showing U-Pb zircon analyses from the Susi-Kervinen mica gneiss (A1243) from Rautavaara, Iisalmi complex. Error ellipses – SIMS analyses, diamonds – multi-grain TIMS analyses.

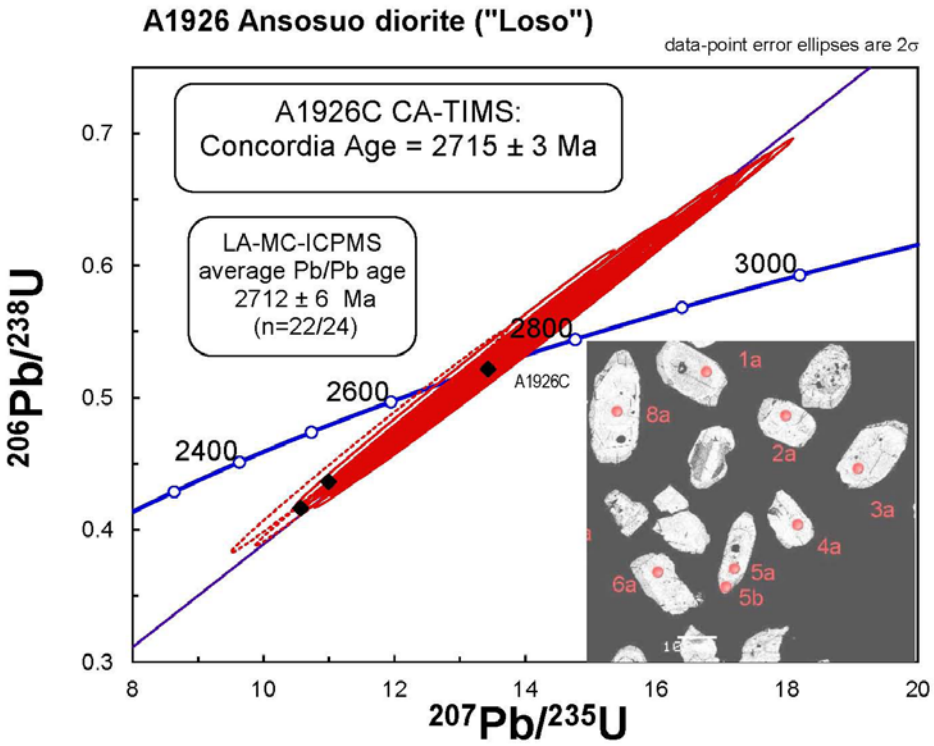

Fig. 63. Concordia diagram showing U-Pb zircon analyses from the Ansosuo diorite A1926. Error ellipses – LA-MC-ICPMS analyses, diamonds – multi-grain TIMS analyses.

con grains (Appendix 1). The data reveal that the U content in most analyses is high and the compositions tend to be discordant (Fig. 62). Most analyses suggest ages of ca. 2.6–2.7 Ga with a cluster around 2.63–2.64 Ga, which is the age of the granulite facies metamorphism in the Iisalmi complex (Hölttä et al. 2000, Mänttäri & Hölttä 2002). A few analyses with a moderate U content are concordant at ca. 2.74 Ga and are thought to represent the ages of the source rocks. The youngest zircon grains in sample A1243 are evidently metamorphic, which is also indicated by their high U concentrations and low Th/U ratios compared with the other, older zircon grains (Appendix 1).

A1926 Ansosuo diorite (Loso)

Important age constraints for the deposition of Archaean paragneisses are provided by crosscutting granitoids. One of these rocks is the Loso quartz diorite of sanukitoid affinity, for which an age of 2719 ± 19 Ma was reported by Kontinen et al. (2007). The relatively large error was due to slight heterogeneity in the SIMS (SHRIMP) U-Pb data on zircon (sample A331). In order to improve this result, a new sample was taken from the most mafic variety of the Loso intrusion. Sample A1926 from Ansosuo is a homogeneous gneissic diorite with the main minerals being plagioclase, hornblende and biotite. Other minerals include quartz, titanite, apatite and zircon. Plagioclase and biotite are relatively fresh, indicating only mild Proterozoic effects. Abundant zircon grains obtained from this sample are mostly euhedral, 100–200-µm-long crystals showing internal oscillatory zoning.

Both TIMS and LA-MC-ICPM analyses were carried out on zircon. The two conventional TIMS analyses yield discordant results and have an unusually high amount of common lead (Appendix 2). However, after chemical abrasion the amount of common lead became negligible and the result concordant at 2715 ± 2 Ma (Fig. 63). All data obtained by laser MC-ICPMS are consistent with this age and give an average Pb/Pb age of 2712 ± 6 Ma (Appendix 3, Fig. 63).

We have also carried out additional U-Pb analyses on zircon from the original Loso quartz diorite sample A331 (Fig. 64). Again, the CA-TIMS analysis gives concordant results, but the age of 2703 ± 3 Ma is younger than that obtained from sample A1926. In contrast to A1926, it also appears that the LA-MC-ICPMS data from sample A331 are heterogeneous. Most analyses yield dates close to 2.7 Ga, but one is older at ca. 2.8 Ga and a few analyses are clearly younger than 2.7 Ga. It seems likely that metamorphic effects have disturbed the U-Pb system in zircon, which

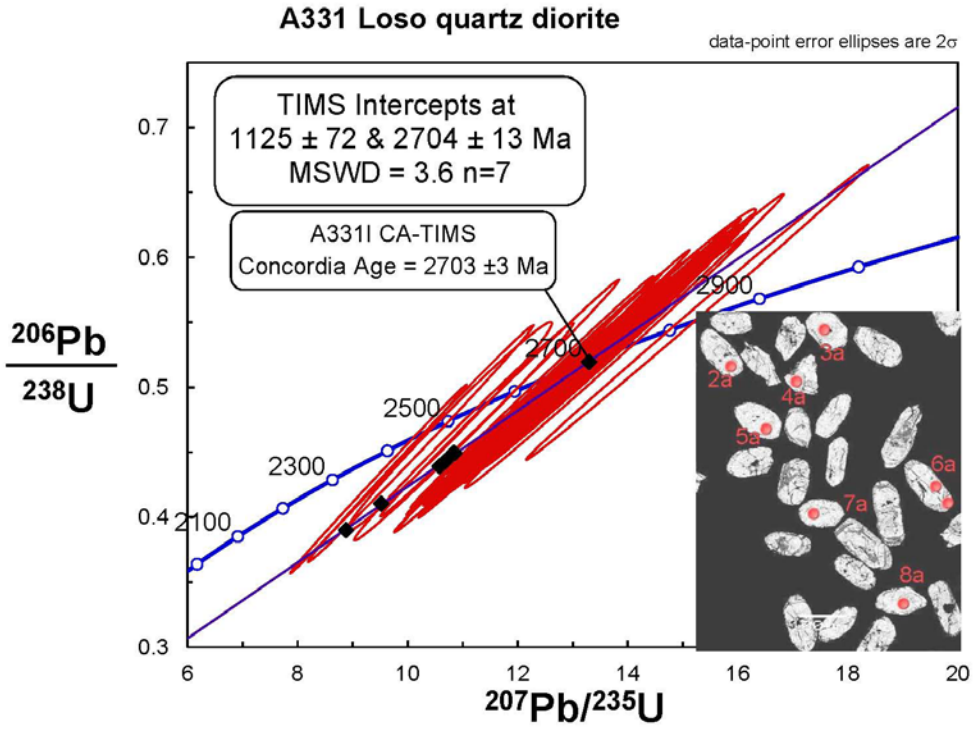

Fig. 64. Concordia diagram showing U-Pb zircon analyses from the Loso quartz diorite A331. Error ellipses – LA-MC-ICPMS analyses, diamonds – multi-grain TIMS analyses from Kontinen et al. (2007), except A331I.

also explains the slightly younger CA-TIMS result. It should be noted that 90% of zircon was lost in the CA pretreatment, and the analysis may well represent zircon, which contains a significant proportion of the annealed material. The heterogeneity obtained is consistent with previous results by Kontinen et al. (2007), and it remains impossible to precisely determine the age of sample A331.

It can be concluded that the emplacement age of the Loso sanukoid intrusion is 2715 ± 2 Ma, the age of sample A1926. This gives the minimum age for the deposition of the sedimentary rocks within the Nurmes paragneisses.

Discussion on Archaean paragneisses

The results of this study are similar to those of Kontinen et al. (2007) and Huhma et al. (2000). The majority of zircon grains in most samples have an age of ca. 2.73–2.75 Ga, which suggests that Neoarchaean granitoid intrusions of this age probably produced most of the detritus of the sediments (Fig. 65). The relatively young provenance is also supported by the Sm-Nd results obtained on whole-rock samples (Kontinen et al. 2007, Huhma et al. this volume) and average U-Pb TIMS analyses from some other localities (Vaasjoki et al. 1993, 1999, 2001).

The U-Pb results also provide important constraints on the age of deposition. However, as was discussed above, there are serious problems in reliably determining the age of the youngest detrital zircon population due to common post-depositional metamorphic reworking of these mostly migmatite-grade rocks. Figure 65 shows zircon dates from 13 sedimentary samples collected both from greenstone and paragneiss belts. Sample A1243 from the Iisalmi complex is distinct, since it contains many 2.6–2.7 Ga zircon grains clustering around 2.63–2.64 Ga, which is the age of the granulite facies metamorphism in that area (Hölttä et al. 2000, Mänttäri & Hölttä 2002). The youngest zircon grains in sample A1243 are evidently metamorphic, which is also indicated by their high U contents and low Th/U ratios compared to the other zircon grains (Table 1). As was discussed above, the 2.7 Ga zircons in the Arola quartzite (A1753) are all considered detrital and thus constrain the time of deposition to be younger than that of other sediments in the Kuhmo greenstone belt.

In all mica gneisses analysed from the Kuhmo, Tipasjärvi and Ilomantsi greenstone belts, the youngest grains seem to be close to 2.74 Ga in age.

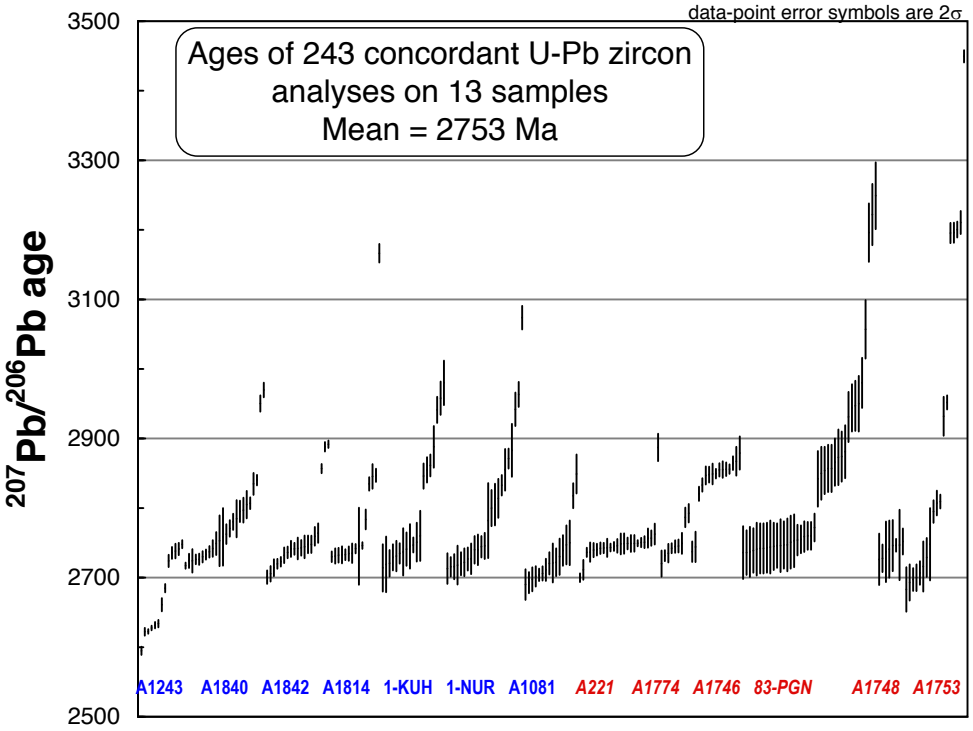

Fig. 65. U-Pb ages of concordant SIMS or LA-MC-ICPMS (83-PGN) analyses on zircon grains in seven Archaean paragneisses (left) and six metasedimentary rocks from the Kuhmo, Tipasjärvi and Ilomantsi greenstone belts. Data for each sample are organized according to nominal age, increasing from left to right. Data on paragneisses 1-KUH, 1-NUR and A1081 are from Kontinen et al. (2007).

In contrast, most samples in the paragneiss belts contain a small population of slightly younger zircon grains in the range 2.72–2.73 Ga, which we believe constrains the time of deposition. This is supported by the new U-Pb zircon age of 2715 ± 2 Ma obtained from the Loso sanukitoid (sample A1926 Ansosuo), which crosscuts the paragneisses.

The minimum age of 2715 ± 2 Ma for the deposition of paragneisses requires that the few dates of ca. 2.70 Ga obtained from mica gneisses in this terrain (Kontinen et al. 2007) do not solely represent detrital zircon grains but rather post-depositional metamorphic effects. It is also likely that the deposition of greywackes in the paragneiss belts took place slightly later than the deposition of greywackes in the greenstone belts. There also seems to be a slight difference in the average provenance, although the effects of metamorphism may have had some contribution to the age distribution obtained (Fig. 66).

CONCLUSIONS

This paper reports U-Pb analyses on 60 samples from the Archaean schist belts and associated granitoids in Finland. The data were obtained using TIMS, SIMS and LA-MC-ICPMS techniques. When samples were characterised by a single age population, consistent results were obtained using all the different methods applied during this study. For LA-MC-ICPMS analyses, we have utilized the Archaean in-house standard A1772, which has yielded relatively concordant multi-grain TIMS Pb/U results and an age of 2711 ± 3 Ma. The analyses by ion probe (Nordsim) show that in terms of age, the zircon standard is homogeneous and gives an age 2712 ± 1 Ma.

The U-Pb ages for igneous supracrustal and closely related rocks dated so far from the Archaean schist belts in central Finland are summarized in Table 1 and Figure 67.

In Figures 68A–D, the ages of volcanic rocks are compared with ages from surrounding granitoids in each belt, and a summary of the Sm-Nd results from the Tipasjärvi-Kuhmo-Suomussalmi greenstone complex is given in Figure 69.

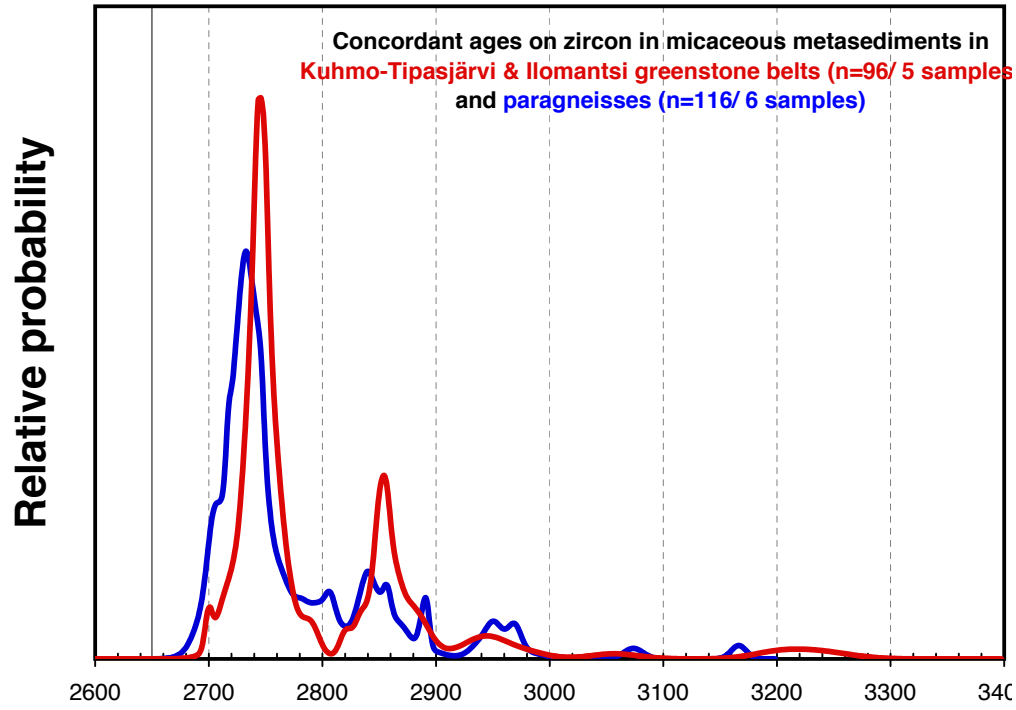

Fig. 66. Distribution of concordant zircon U-Pb ages in Archaean mica gneisses from paragneiss belts (blue) and greenstone belts (red). The data are the same as in Fig. 70, except that samples A1243 (abundant metamorphic zircon) and A1753 (quartzite) are excluded. Age population distributions of the two groups are similar but differ in detail.

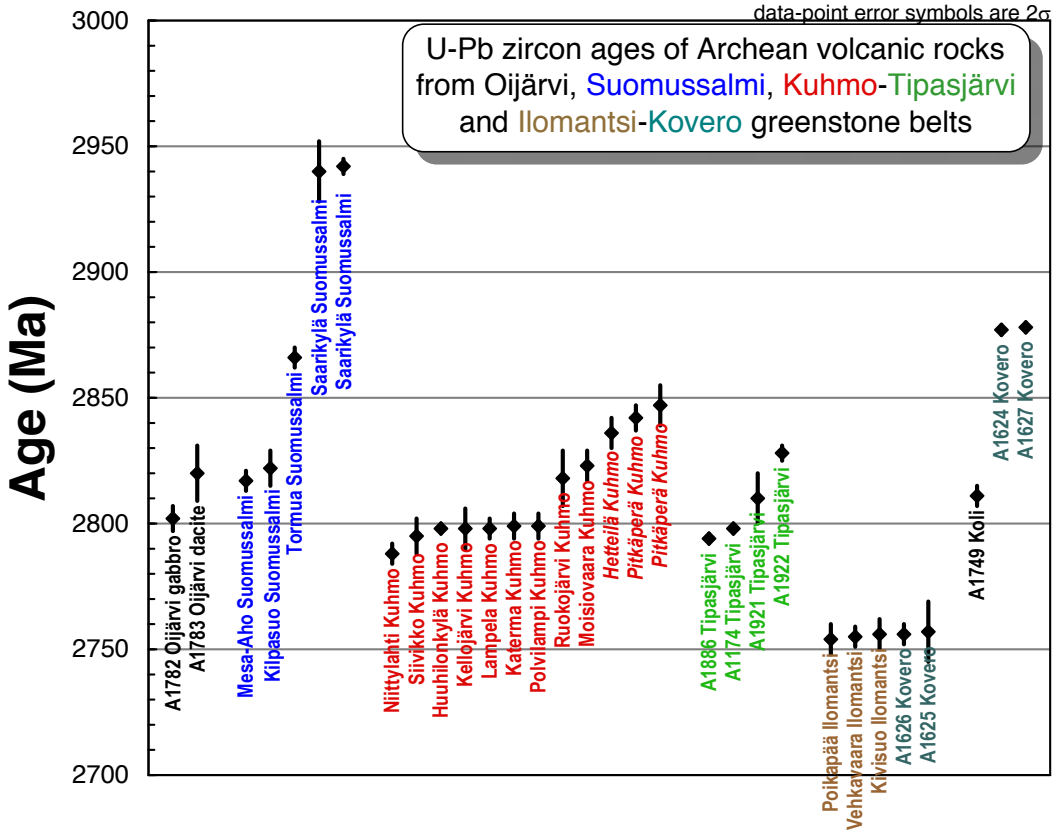

Fig. 67. U-Pb zircon ages of Archaean volcanic rocks in Finland.

Table 1. Summary of U-Pb ages of Archaean schist belts with remarks on stratigraphy.

Tipasjärvi			Kuhmo			Suomussalmi			Ilomantsi-Kovero (& Ipatti)			Oijärvi		
Sample	**Age (Ma)**	**Rock type stratigraphy**	**Sample**	**Age (Ma)**	**Rock type stratigraphy**	**Sample**	**Age (Ma)**	**Rock type stratigraphy**	**Sample**	**Age (Ma)**	**Rock type stratigraphy**	**Sample**	**Age (Ma)**	**Rock type**
			A1753	<2700	quartzite (Arola)									
												A1553	2728±14	tonalite, crosscut volc. rocks
									A221	ca. 2750	mica gneiss Hattuvaara	A1814	<2740	mica gneiss
									A1038	2754±6	andesite Poikapää			
A1748	<2750	mica gneiss, Kokkoniemi Fm	83-PGN	<2750	mica gneiss, Ronkaperä Fm				A1520	2754±4	dyke cutting mica gneiss, Kovero			
			A1746	<2750	mica gneiss, Ronkaperä Fm				A1625	2757±12	dyke cutting mica gneiss, Kovero			
			A1774	<2750	mica gneiss, Ronkaperä Fm				A1626	2756±4	gabbro, Kovero			
			A1418	2788±4	gabbro intruding Kellojärvi cplx/Siivikko Fm									
			A1771	2798±8	gabbro intruding Kellojärvi cplx/Siivikko Fm									
			A2027	2795±3	porphyry dyke intruding komatiites of Siivikko Fm									
A1886	2796±8	felsic tuff, Koivumäki Fm?	A1377	2795±7	felsic fragment (dike?) in Kellojärvi cplx									
A1174	2798±2	rhyolite, Koivumäki Fm	A1346	2798±4	andesite, Mäkisensuo Fm									
			A1560	2798±2	porphyry, Mäkisensuo Fm, intr. Kellojärvi cplx?									
A1921	2810±10	rhyolite, Koivumäki Fm?	A511	2799±5	rhyolite, Mäkisensuo Fm									
			A788	2799±5	rhyolite, Mäkisensuo Fm							A1782	2802±5	gabbro
			2798 ±2 <komatiites < 2823 ±6											
									A1749	2811±4	**Ipatti belt** felsic volcanic rock			
			A1000	2818±11	rhyolite, Ruokojärvi Fm	A1701	2815±4	volc, Kiannanniemi				A1490	2815±20	granodiorite, crosscut volc. rocks
						A1428	2817±4	porphyry, Mesa-aho				A1783	2820±11	dacite
A1922	2828±3	dacite	A976	2823±6	gabbro, Moisiovaara, Pahakangas Fm	A1429	2822±7	andesite, Tormua						
			A1773	2836±6	dacite?, Vuosanka belt									
			A1213	2842±5	andesite, Pitkäperä belt									
			A1254	2847±8	andesite, Pitkäperä belt									
						A1821	2866±4	gabbro, Tormua						
									A1624	2877±2	felsic volc. rock, Kovero			
									A1627	2878±2	felsic volc. rock, Kovero			
						A1467	2940±12	felsic volc. rock						
						A1593	2942±3	felsic porphyry						
						A1191	<2950	sediment, Luoma						

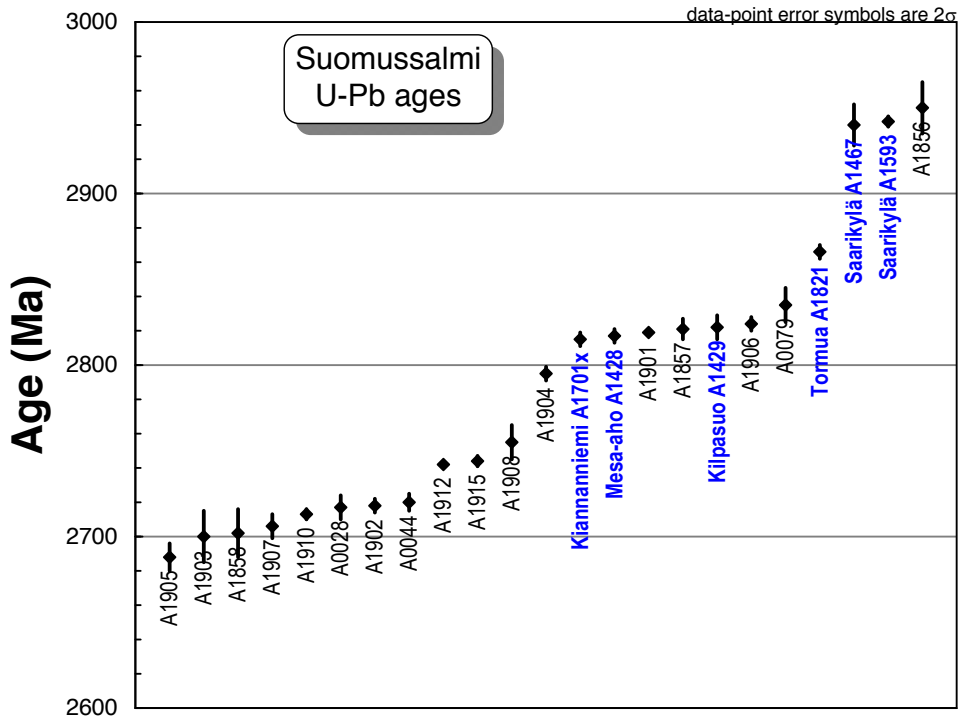

Fig. 68A. U-Pb ages on six volcanic rocks from the Suomussalmi greenstone belt (blue bold labels) compared with the ages of surrounding granitoids. Data from this study, Mikkola et al. (2011a, b), Käpyaho et al. (2007) and Heilimo et al. (2011).

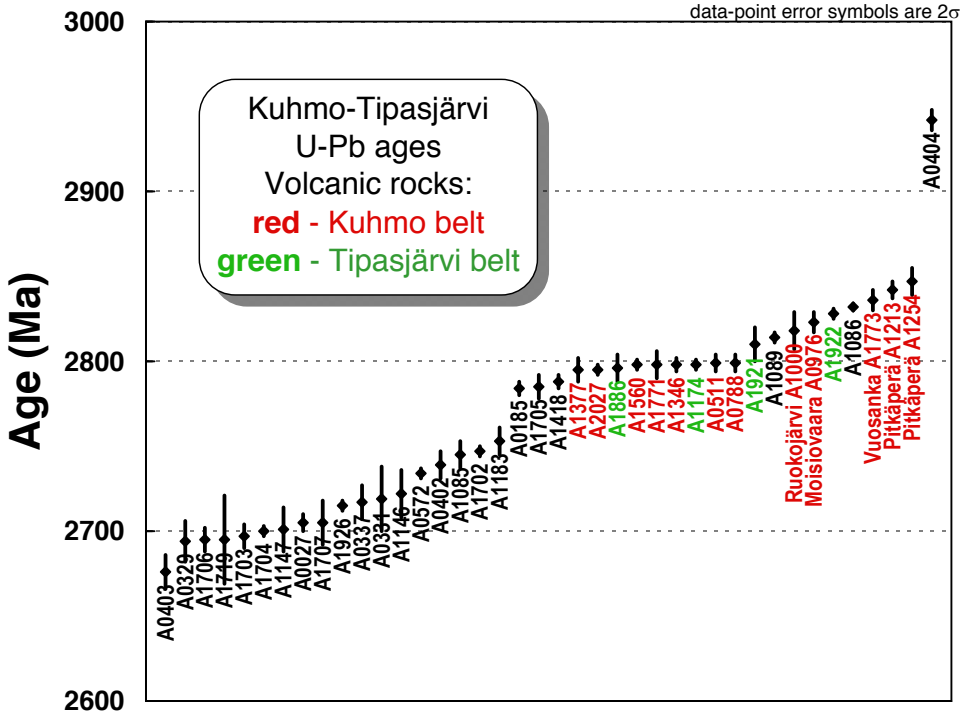

Fig. 68B. U-Pb ages on 16 volcanic rocks from the Kuhmo (red labels) and Tipasjärvi (green labels) greenstone belts compared with the ages of surrounding granitoids. Data from this study, Hyppönen (1983), Käpyaho et al. (2006, 2007), Luukkonen (1985, 2001), Vaasjoki et al. (1999) and Heilimo et al. (2011).

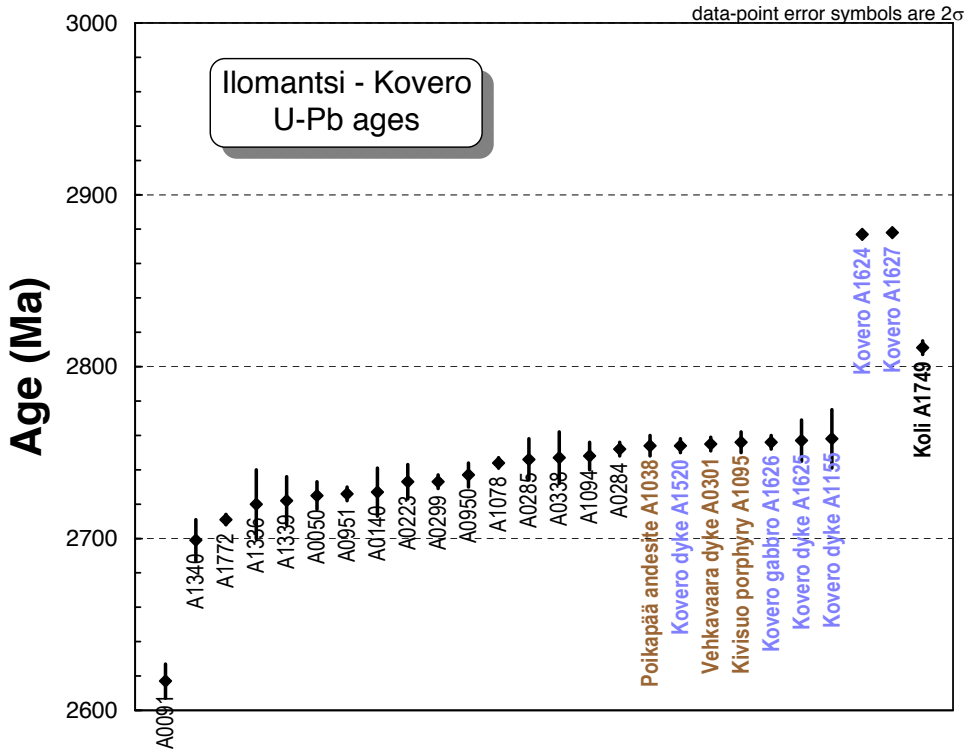

Fig. 68C. U-Pb ages on nine volcanic or dyke rocks from the Ilomantsi-Kovero greenstone belt (bold coloured labels) compared with the ages of surrounding granitoids. Data from this study, Vaasjoki et al. (1993), Sorjonen-Ward and Claoué-Long (1993) and Halla (2002). The age of 2811 ± 4 Ma for the volcanic rock A1749 from the Ipatti belt is also shown (Pekkarinen et al. 2006; the age is updated utilizing the CA-TIMS analysis given in Appendix 2).

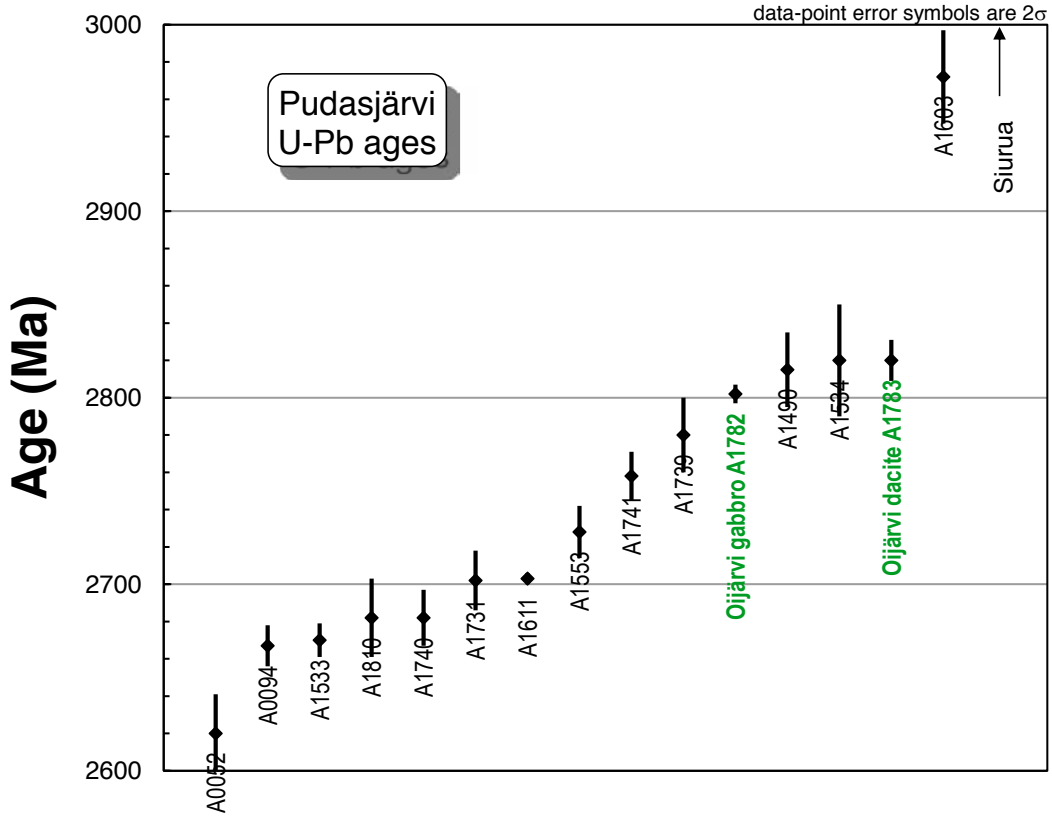

Fig. 68D. U-Pb ages on two volcanic rocks from the Oijärvi greenstone belt (green labels) compared with the ages of surrounding granitoids. Data from this study, Perttunen and Vaasjoki (2001), Mutanen and Huhma (2003) and Lauri et al. (2011). The age of Siurua gneisses is ca. 3500 Ma (Mutanen & Huhma 2003).

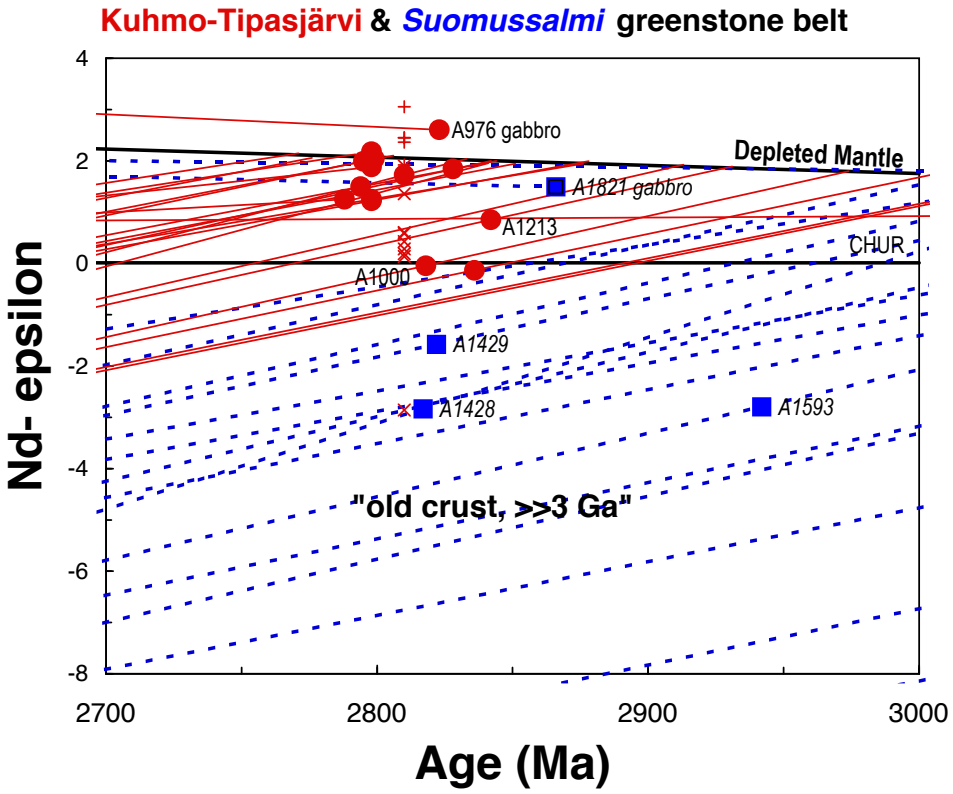

Fig. 69. Epsilon-Nd vs. age diagram showing evolution lines for mostly felsic samples from the Tipasjärvi-Kuhmo-Suomussalmi greenstone complex (data from Huhma et al. this volume). Initial values using filled symbols are shown for samples for which the age is based on U-Pb zircon dating. Suomussalmi: blue squares and dotted blue evolution lines. Kuhmo-Tipasjärvi: red dots and solid red evolution lines. Komatiites and komatiitic basalts from the Pahakangas-Siivikkovaara area in Kuhmo: red x at 2810 Ma, basalts from other sites in Kuhmo belt: red +. Depleted mantle evolution is according to DePaolo (1981).

The results obtained call for the revision of some traditional views on these belts and allow the following conclusions to be made:

1. Mafic rocks of the **Kuhmo belt** represented by the Moisiovaara gabbro are 2823 ± 6 Ma old, which according to the stratigraphic scheme (e.g. Papunen et al. 2009) should give the upper age limit for komatiites.

2. Felsic rocks in the Kellojärvi area, the central part of the Kuhmo belt, formed 2798 ± 2 Ma ago and provide the minimum age for the local mafic-ultramafic magmatism, including komatiites.

3. The igneous ages obtained for the four volcanic rocks from the **Tipasjärvi belt** range from 2828 ± 3 Ma to 2796 ± 8 Ma and thus resemble the geochronological data from the Kuhmo belt. The revised age of 2798 ± 2 Ma determined for the host rock of the Taivaljärvi Ag-Zn ore deposit is exactly the same as the age obtained for the felsic rocks in the Kellojärvi area.

4. Felsic rocks in the Kuhmo and Tipasjärvi belts represent new crustal materials ultimately derived from depleted mantle-type sources with $\varepsilon_{Nd(2.8\,Ga)}$ about +2. The bulk of the surrounding granitoids postdate the volcanism, and the isotope results as a whole suggest that the contribution of older crustal material is negligible and do not support the concept of formation of the Kuhmo belt in a rift basin on an ancient sialic basement.

5. Volcanic rocks with ages of ca. 2.84 Ga, occurring in the Vuosanka (Hetteilä) and Pitkäperä areas on the eastern side of the main Kuhmo belt, represent an event of volcanic activity preceding the major magmatic phase in the Kuhmo belt.

6. A major re-appraisal concerns the age of the Ruokojärvi Formation east of the main Kuhmo belt, which has previously been regarded to be as old as ca. 3 Ga (Papunen et al. 2009). The new U-Pb data on two felsic volcanic rocks suggest that the magmatic age is ca. 2.82 Ga, but abundant xenocrystic zircon suggests the involvement of ca. 3.1 Ga crust in the genesis of these rocks.

7. Both the Kuhmo and Tipasjärvi greenstone belts contain sedimentary rocks that were deposited after 2.75 Ga and thus at least 50 Ma after the recorded volcanism. Still younger sediments have been found in the Arola area, the Kuhmo belt, where a deformed quartzite contains detrital zircon grains as young as 2.7 Ga.

8. The **Suomussalmi belt** contains at least three age groups of volcanic rocks erupted at 2.94, 2.87 and 2.82 Ga, but the relative proportions of these units remain unclear. Compared to the Kuhmo and Tipasjärvi belts, the Sm-Nd crustal residence ages in the Suomussalmi belt are significantly older, mostly exceeding 3 Ga.

9. The supracrustal rocks in the **Ilomantsi belt** and many surrounding/intruding granitoids formed within a short period of time at ca. 2.75 Ga ago, but signs of older crustal contribution are evident in the form of xenocrystic zircon up to 3.3 Ga in age. In the **Kovero belt** SW of Ilomantsi, two age groups are evident at 2.75 and 2.88 Ga, but the relative proportions of these units remain unclear. Involvement of older crustal material is consistent with models suggesting a continental arc setting for the Ilomantsi belt (O'Brien et al. 1993).

10. The age of the supracrustal rocks exposed in the **Oijärvi belt** in the Pudasjärvi area is ca. 2.80–2.82 Ga. No contribution from such old sources as the nearby 3.5 Ga Siurua gneisses was found in igneous rocks within or surrounding the belt.

11. The sediments in the **paragneiss belts** were deposited ca. 2.72 Ga ago, which in the case of the Nurmes belt, according to Kontinen et al. (2007), took place in a back arc or intra-arc setting.

Altogether, the isotope results suggest that the greenstone belts store a long-lived (>200 Ma), fragmentary record of geological evolution. The interpretation and modelling of the tectonic framework of this evolution remains a major challenge.

ACKNOWLEDGEMENTS

The Nordic geological ion-microprobe facility (Nordsim) is operated and funded under an agreement between the respective research funding agencies of Denmark, Norway and Sweden, the Geological Survey of Finland, and the Swedish Museum of Natural History. This paper is NORDSIM contribution No. 313. The staff of the NORDSIM laboratory, and the separation laboratory at GTK are acknowledged for skilled technical assistance. We thank the staff of CIR, VSEGEI, St. Petersburg for SHRIMP analyses of three samples, and are deeply grateful to Tom Andersen for providing his excellent program to handle the ICPMS data. Discussions and comments by Perttu Mikkola and review comments by Hugh O'Brien are greatly acknowledged. We want to express our gratitude to Olavi Kouvo for initiating the isotope research in Finland and the Geological Survey of Finland for providing facilities and support for these studies.

REFERENCES

Andersen T., Griffin W. L., Jackson S. E., Knudsen T.-L. & Pearson N. J. 2004. Mid-Proterozoic magmatic arc evolution at the southwest margin of the Baltic Shield. Lithos 73, 289–318.

Belousova E. A., Griffin W. L. & O'Reilly S. Y. 2006. Zircon crystal morphology, trace element signatures and Hf isotope composition as a tool for petrogenetic modeling: examples from Eastern Australian granitoids. J Petrol 47, 329–353.

DePaolo, D. J. 1981. Neodymium isotopes in the Colorado Front Range and crust-mantle evolution in the Proterozoic. Nature 291, 684−687.

DePaolo, D. J. & Wassenburg, G. J. 1976. Nd isotopic variations and petrogenetic models. Geophys. Res. Lett. 3, 249−252.

Engel, W. & Dietz, G.-J. 1989. A modified stratigraphic and tectonomagmatic model for the Suomussalmi greenstone belt, eastern Finland, based on the remapping of the Ala-Luoma area. Bulletin of the Geological Society of Finland 61, 143−160.

Gruau, G., Tourpin, S., Fourcade, S. & Blais, S. 1992. Loss of isotopic(Nd, O) and chemical (REE) memory during metamorphism of komatiites: new evidence from eastern Finland. Contributions to Mineralogy and Petrology 112, 66–82.

Halla, J. 2002. Origin and Paleoproterozoic reactivation of

Neoarchean high-K granitoid rocks in eastern Finland. Annales Academiae Scientiarum Fennicae. Geologica - Geographica 163. Helsinki: Suomalainen Tiedeakatemia. 103 p.

Hanski, E. J. 1980. Komatiitic and tholeiitic metavolcanic rocks of the Kellojärvi group in the Siivikkovaara area of the Archaean Kuhmo greenstone belt, eastern Finland. Bulletin of the Geological Society of Finland 52, 67–100.

Hanski, E., Walker, R.J., Huhma, H. & Suominen I. 2001. The Os and Nd isotopic systematics of c. 2.44 Ga Akanvaara and Koitelainen mafic layered intrusions in northern Finland. Precambrian Research 109, 73–102.

Hanski, E., Huhma, H. & Vuollo, J. 2010. SIMS zircon ages and Nd isotope systematics of the 2.2 Ga mafic intrusions in northern and eastern Finland. Bulletin of the Geological Society of Finland 82, 31−62.

Heilimo, E., Halla, J. & Huhma, H. 2011. Single-grain zircon U-Pb age constraints of the western and eastern sanukitoid zones in the Finnish part of the Karelian Province. Lithos 121, 87−99.

Hölttä, P., Huhma, H., Mänttäri, I. & Paavola J. 2000. P-T-t development of Archaean granulites in Varpaisjärvi, Central Finland II. Dating of high-grade metamorphism with the U-Pb and Sm-Nd methods. Lithos 50, 121−136.

Hölttä, P., Heilimo, E., Huhma, H., Kontinen, A., Mertanen, S., Mikkola, P., Paavola, J., Peltonen, P., Semprich, J., Slabunov, A. & Sorjonen-Ward, P. 2012. The Archean of the Karelia Province in Finland. In: Hölttä, P. (ed.) The Archaean of the Karelia Province in Finland. Geological Survey of Finland, Special Paper 54.

Horstwood, M. S. A., Foster, G. L., Parrish, R. R., Noble, S. R. & Nowell, G. M. 2003. Common-Pb corrected in situ U–Pb accessory mineral geochronology by LA-MC-ICP-MS. Journal of Analytical Atomic Spectrometry 18, 837–846.

Huhma, H., Kontinen, A. & Laajoki, K. 2000. Age of the metavolcanic-sedimentary units of the Central Puolanka Group, Kainuu schist belt, Finland. In: 24. Nordiske Geologiske Vintermøte, Trondheim 6.−9. januar 2000. Geonytt (1), 87−88.

Huhma, H., Kontinen, A., Mikkola, P., Halkoaho, T., Hokkanen, T., Hölttä, P., Juopperi, H., Konnunaho, J., Luukkonen, E., Mutanen, T. Peltonen, P., Pietikäinen, K. & Pulkkinen, A. 2012. Nd isotopic evidence for Archean crustal growth in Finland. In: Hölttä, P. (ed.) The Archaean of the Karelia Province in Finland. Geological Survey of Finland, Special Paper 54.

Hyppönen, V. 1983. Ontojoen, Hiisijärven ja Kuhmon karttaalueiden kallioperä. Summary: Pre-Quaternary Rocks of the Ontojoki, Hiisijärvi and Kuhmo Map-Sheet areas. Geological Map of Finland 1:100 000, Explanation to the Maps of Pre-Quaternary Rocks, Sheets 4411, 4412, 4413. Geological Survey of Finland. 60 p.

Jackson S. E., Pearson N. J., Griffin W. L. & Belousova E. A. 2004. The application of laser ablation-inductively coupled plasma-mass spectrometry to in-situ U–Pb zircon geochronology. Chemical Geology 211, 47–69.

Jahn, B.-M., Vidal, P. & Kröner, A. 1984. Multi-chronometric ages and origin of Archaean tonalitic gneisses in Finnish Lapland: a case for long crustal residence time. Contributions to Mineralogy and Petrology 86, 398−408.

Käpyaho, A., Mänttäri, I. & Huhma, H. 2006. Growth of Archaean crust in the Kuhmo district, eastern Finland: U-Pb and Sm-Nd isotope constraints on plutonic rocks. Precambrian Research 146, 95−119.

Käpyaho, A. Hölttä, P. & Whitehouse, M. J. 2007. U-Pb zircon geochronology of selected Archaean migmatites in eastern Finland. Bulletin of the Geological Society of Finland 79 (1), 95−115.

Konnunaho, J. 1999. Kuusijärven jakson komatiitit ja niiden malmipotentiaali Koveron arkeeisella vihreäkivivyöhykkeellä. M.Sc. thesis, University of Oulu, Department of Geology, 73 p. (in Finnish)

Kontinen, A., Käpyaho, A., Huhma, H., Karhu, J., Matukov, D., Larionov, A. & Sergeev, S. 2007. Nurmes paragneisses in eastern Finland, Karelian craton: Provenance, tectonic setting and implications for Neoarchaean craton correlation Precambrian Research 152, 119–148.

Kopperoinen, T. & Tuokko, I. 1988. The Ala-Luoma and Taivaljärvi Zn-Pb-Ag-Au deposits, eastern Finland. In: Marttila, E. (ed.) Archaean geology of the Fennoscandian Shield. Geological Survey of Finland, Special Paper 4, 131−144.

Korsman, K., Koistinen, T., Kohonen, J., Wennerström, M., Ekdahl, E., Honkamo, M., Idman, H. & Pekkala, Y. (eds.)1997. Suomen kallioperäkartta – Berggundskarta över Finland – Bedrock map of Finland 1:000 000. Espoo: Geological Survey of Finland.

Kouvo, O. 1958. Radioactive age of some Finnish Precambrian minerals. Bulletin de la Commission Géologique de Finlande 182.

Kouvo, O. & Tilton, G. 1966. Mineral ages from the Finnish Precambrian. Journal of Geology 74, 421−442.

Krogh, T. E. 1973. A low-contamination method for hydrothermal decomposition of U and Pb for isotopic age determinations. Geochim. Cosmochim. Acta 37, 485−494.

Krogh, T. E. 1982. Improved accuracy of U–Pb zircon ages by the creation of more concordant systems using an air abrasion technique. Geochim. Cosmochim. Acta 46, 637–649.

Larionov, A. N., Andreichev, V. A. & Gee, D. G. 2004. The Vendian alkaline igneous suite of northern Timan: ion microprobe U–Pb zircon ages of gabbros and syenite. In: Gee, D. G. & Pease, V. L. (eds.) The Neoproterozoic Timanide Orogen of Eastern Baltica, vol. 30. Geol. Soc., London Mem, 69–74.

Lauri, L. S., Rämo, O. T., Huhma, H., Mänttäri, I. & Räsänen, J. 2006. Petrogenesis of silicic magmatism related to the ~ 2.44 Ga rifting of Archean crust in Koillismaa, eastern Finland. Lithos 86, 137−166.

Lauri, L. S., Andersen, T., Hölttä, P., Huhma, H. & Graham, S. 2011. Evolution of the Archaean Karelian province in the Fennoscandian Shield in the light of U–Pb zircon ages and Sm–Nd and Lu–Hf isotope systematics. Journal of the Geological Society 168, 201–218.

Ludwig, K. R. 1991. PbDat 1.21 for MS-dos: A computer program for IBM-PC Compatibles for processing raw Pb-U-Th isotope data. Version 1.07. U.S. Geological Survey. Open File Report, 88−542. 35 p.

Ludwig, K. R. 2003. User's manual for Isoplot/Ex, Version 3.00. A geochronological toolkit for Microsoft Excel. Berkeley Geochronology Center Special Publication No.4.

Luukkonen, E. 1985. Structural and U-Pb isotopic study of late Archaean migmatitic gneisses of the Presvecokarelides, Lylyvaara, eastern Finland. Transactions of the Royal Society at Edinburgh, Earth Sciences 76, 401−410.

Luukkonen, E. 1988. Moisiovaaran ja Ala-Vuokin karttaalueiden kallioperä. Summary: Pre-Quaternary Rocks of the Moisiovaara and Ala-Vuokki Map-Sheet areas. Geological Map of Finland 1:100 000, Explanation to the Maps of Pre-Quaternary Rocks, Sheets 4421 and

4423+4441. Geological Survey of Finland. 90 p.

Luukkonen, E. J. 1992. Late Archaean and early Proterozoic structural evolution Kuhmo–Suomussalmi terrain, eastern Finland. Ann. Univ. Turkuensis, Ser. A. Biol. Geogr. Geol. 78.

Luukkonen, E. J. 2001. Lentiiran kartta-alueen kallioperä. Summary: Pre-Quaternary Rocks of the Lentiira Map-Sheet area. Geological Map of Finland 1:100 000,Explanation to the Maps of Pre-Quaternary Rocks, Sheet 4414 + 4432. Geological Survey of Finland. 51 p., 1 app.

Luukkonen, E., Halkoaho, T., Hartikainen, A., Heino, T., Niskanen, M., Pietikäinen, K. & Tenhola, M. 2002. Itä-suomen arkeeiset alueet–hankkeen (12201 ja 210 5000) toiminta vuosina 1992–2001 Suomussalmen, Hyrynsalmen, Kuhmon, Nurmeksen, Rautavaaran, Valtimon, Lieksan, Ilomantsin, Kiihtelysvaaran, Enon, Kontiolahden, Tohmajärven ja Tuupovaaran alueella. Geological Survey of Finland, archive report M19/4513/2002/1. (in Finnish)

Mänttäri, I. & Hölttä, P. 2002. U-Pb dating of zircons and monazites from Archean granulites in Varpaisjärvi, Central Finland: - Evidence for multiple metamorphism and Neoarchean terrane accretion. Precambrian Research 118(1−2), 101−131.

Martin, H. & Querré, G. 1984. A 2.5 Ga reworked sialic crust: Rb-Sr ages and isotopic geochemistry of late Archaean volcanic and plutonic rocks from E. Finland. Contributions to Mineralogy and Petrology 85, 292−299.

Mattinson, J. M. 2005. Zircon U-Pb chemical abrasion ("CA-TIMS") method: Combined annealing and multi-step partial dissolution analysis for improved precision and accuracy of zircon ages. Chemical Geology 220, 47−66.

Mikkola, P., Huhma, H., Heilimo, E. & Whitehouse, M. 2011a. Archean crustal evolution of the Suomussalmi district as part of the Kianta Complex, Karelia: Constraints from geochemistry and isotopes of granitoids. Lithos 125, 287−307.

Mikkola, P., Salminen, P., Torppa, A. & Huhma H. 2011b. The 2.74 Ga Likamännikkö complex in Suomussalmi, East Finland: Lost between sanukitoids and truly alkaline rocks? Lithos 125, 716−728.

Miller, R. G., O'Nions, R. K., Hamilton, P. J. & Welin, E. 1986. Crustal residence ages of clastic sediments, orogeny and continental evolution. Chemical Geology 57, 87−99.

Mutanen, T. & Huhma, H. 2003. The 3.5 Ga Siurua trondhjemite gneiss in the Archaean Pudasjärvi Granulite Belt, northern Finland. Bull. Geol. Soc. Finland 75, 51−68.

O'Brien, H., Huhma, H. & Sorjonen-Ward, P. 1993. Petrogenesis of the late Archean Hattu schist belt, Ilomantsi, eastern Finland : geochemistry and Sr, Nd isotopic composition. In: Nurmi, P. & Sorjonen-Ward, P. (eds.) Geological development, gold mineralization and exploration methods in the late Archean Hattu schist belt, Ilomantsi, eastern Finland. Geological Survey of Finland, Special Paper 17, 147−184.

Paavola, J. 1999. Rautavaaran kartta-alueen kallioperä. Summary: Pre-Quaternary Rocks of the Rautavaara Map-Sheet area. Geological Map of Finland 1:100 000, Explanation to the Map of Pre-Quaternary Rocks, Sheet 3343. Geological Survey of Finland. 53 p.

Papunen, H., Halkoaho, T., Tulenheimo, T. & Liimatainen, J. 1998. Excursion to the Kuhmo greenstone belt. In: Hanski, E. & Vuollo, J. (eds.) International Ophiolite Symposium and Field Excursion: Generation and Emplacement of Ophiolites Through Time, August 10 15, 1998, University of Oulu, Oulu, Finland. Abstracts and Excursion Guide. Geological Survey of Finland, Special Paper 26, 91–106.

Papunen, H., Halkoaho, T. & Luukkonen, E. 2009. Archaean evolution of the Tipasjärvi-Kuhmo-Suomussalmi Greenstone Complex, Finland. Geological Survey of Finland, Bulletin 403. 68 p.

Patchett, J., Kouvo, O., Hedge, C. & Tatsumoto, M. 1981. Evolution of continental crust and mantle heterogeneity: evidence from Hf isotopes. Contributions to Mineralogy and Petrology 78, 279−297.

Patchett, J. & Kouvo, O. 1986. Origin of continental crust of 1.9-1.7 Ga age: Nd isotopes and U-Pb zircon ages in the Svecokarelian terrain of south Finland. Contributions to Mineralogy and Petrology 92, 1−12.

Pekkarinen, L., Kohonen, J., Vuollo, J. & Äikäs, O. 2006. Kolin kartta-alueen kallioperä. Summary: Pre-Quaternary Rocks of the Koli Map-Sheet area. Geological Map of Finland 1:100 000, Explanation to the Map of Pre-Quaternary Rocks, Sheet 4313. Geological Survey of Finland. 116 p. + 3 app. maps.

Peltonen, P., Mänttäri, I., Huhma, H. & Whitehouse, M. J. 2006. Multi-stage origin of the lower crust of the Karelian craton from 3.5 to 1.7 Ga based on isotopic ages of kimberlite-derived mafic granulite xenoliths. Precambrian Research 147, 107−123.

Perttunen, V. & Vaasjoki, M. 2001. U-Pb geochronology of the Peräpohja Schist Belt, northwestern Finland. In: Vaasjoki, M. (ed.) Radiometric age determinations from Finnish Lapland and their bearing on the timing of Precambrian volcano-sedimentary sequences. Geological Survey of Finland, Special Paper 33, 45−84.

Piirainen, T. 1988. The geology of the Archaean greenstone - granitoid terrain in Kuhmo, eastern Finland. In: Marttila, E. (ed.) Archean geology of the Fennoscandian Shield. Geological Survey Finland, Special Paper 4, 39−51.

Puchtel, I. S., Hofmann, A. W., Amelin, Yu, V., Garbe-Schonberg, C. D., Samsonov, A. V. & Shchipansky, A. A. 1999. Combined mantle plume-island arc model for the formation of the 2.9 Ga Sumozero-Kenozero greenstone belt, SE Baltic Shield: isotope and trace element constraints. Geochimica et Cosmochimica Acta 63(21), 3579−3595.

Rosa D. R. N., Finch A. A., Andersen T. & Inverno C. M. C. 2009. U-Pb geochronology and Hf isotope ratios of magmatic zircons from the Iberian pyrite belt. Miner. Petrol. 95, 47−69.

Schoene B., Crowley J. L., Condon D. J., Schmitz M. D. & Bowring, S. A. 2006. Reassessing the uranium decay constants for geochronology using ID-TIMS U–Pb data. Geochimica et Cosmochimica Acta 70, 426–445.

Sorjonen-Ward, P. 1993. An overview of structural evolution and lithic units within and intruding the late Archean Hattu schist belt, Ilomantsi, eastern Finland. In: Nurmi, P. & Sorjonen-Ward, P. (eds.) Geological development, gold mineralization and exploration methods in the late Archean Hattu schist belt, Ilomantsi, eastern Finland. Geological Survey of Finland, Special Paper 17, 9−102.

Sorjonen-Ward, P. & Claoué-Long, J. 1993. Preliminary note on ion probe results for zircons from the Silvevaara granodiorite, Ilomantsi, eastern Finland. In: Autio, S. (ed.) Geological Survey of Finland, Current Research 1991−1992. Geological Survey of Finland, Special Paper 18, 25−29.

Sorjonen-Ward, P. & Luukkonen, E. J. 2005. Archean rocks. In: Lehtinen, M., Nurmi, P. A., & Rämö, O. T. (eds.) Precambrian Geology of Finland – Key to the Evolution of the Fennoscandian Shield. Amsterdam: Elsevier B.V., 19−99.

Stacey, J. S. & Kramers, J. D. 1975. Approximation of terrestrial lead isotope evolution by a two-stage model. Earth and Planetary Science Letters 26, 207−221.

Taipale, K. 1983. The geology and geochemistry of the Archaean Kuhmo greenstone-granite terrain in the Tipasjärvi area, eastern Finland. Acta Univ. Oul., Ser. A 151.

Tuukki, P. 1991. Arkeeinen Koveron liuskejakso ja sen mafisten ja ultramafisten kivien geokemia ja petrogenesis. Pohjois-Karjalan malmiprojekti. University of Oulu. Report 28. 129 p.

Vaasjoki, M. 1981. The lead isotopic composition of some Finnish galenas. Geological Survey of Finland Bulletin 316. 32 p.

Vaasjoki, M., Sorjonen-Ward, P. & Lavikainen, S. 1993. U-Pb age determinations and sulfide Pb-Pb characteristics from the late Archean Hattu schist belt, Ilomantsi, eastern Finland. In: Nurmi, P. & Sorjonen-Ward, P. (eds.) Geological development, gold mineralization and exploration methods in the late Archean Hattu schist belt, Ilomantsi, eastern Finland. Geological Survey of Finland. Special Paper 17, 103−131.

Vaasjoki, M., Taipale, K. & Tuokko, I. 1999. Radiometric ages and other isotopic data bearing on the evolution of Archaean crust and ores in the Kuhmo-Suomussalmi area, eastern Finland. Bulletin of the Geological Society of Finland 71, 155−176.

Vaasjoki, M., Kärki, A, & Laajoki, K. 2001. Timing of Paleaeoproterozoic crustal shearing in the central Fennoscandian Shield according to U-Pb data from associated granitoids, Finland. Bulletin of the Geological Society of Finland 73, 87−101.

Vidal, P., Blais, S., Jahn, B.-M., Capdevila, R. & Tilton, G. 1980. U-Pb and Rb-Sr systematics of the Suomussalmi Archaean greenstone belt (eastern Finland). Geochimica et Cosmochimica Acta 44, 2033−2044.

Wetherill, G., Kouvo, O., Tilton, G. & Gast, P. 1962. Age measurements of rocks from the Finnish Precambrian. Journal of Geology 70, 74−88.

Whitehouse, M. J., Kamber, B. & Moorbath, S. 1999. Age significance of U-Th-Pb zircon data from early Archaean rocks of west Greenland – a reassessment based on combined ion-microprobe and imaging studies. Chemical Geology 160, 201−224.

Whitehouse, M. J. & Kamber, B. S. 2005. Assigning dates to thin gneissic veins in high-grade metamorphic terranes – a cautionary tale from Akilia, southwest Greenland. Journal of Petrology, 46, 291−318.

Wiedenbeck, M., Allé, P., Corfu, F., Griffin, W. L., Meier, M., Oberli, F., Von Quadt, A., Roddick, J. C. & Spiegel, W. 1995. Three natural zircon standards for U–Th–Pb, Lu–Hf, trace elements and REE analyses. Geostandards Newsletter 19, 1–23.

Williams, I. S. 1998. U–Th–Pb geochronology by ion microprobe. In: McKibben, M. A., Shanks III, W. C. & Ridley, W. I. (eds.) Applications of Microanalytical Techniques to Understanding Mineralizing Processes, vol. 7. Rev. Econ. Geol., 1–35.

Zartman, R. E & Doe, B. R. 1981. Pumbotectonics – the model. Tectonophysics 75, 135−162.

Appendix 1. Ion microprobe U-Pb data on zircons (NORDSIM).

		Derived ages						*Corrected ratios*					*Elemental data*				
Sample/	**Zircon domain**	^{207}Pb	±σ	^{207}Pb	±σ	^{206}Pb	±σ	^{207}Pb	±σ	^{206}Pb	±σ	ρ [1]	**Disc. %** [2]	**[U]**	**[Pb]**	**Th/U**	f_{206} % [3]
spot #		^{206}Pb		^{235}U		^{238}U		^{235}U	%	^{238}U	%			**ppm**	**ppm**	**meas**	
Suomussalmi greenstone belt																	
A1191 Ala-Luoma metasediment. Suomussalmi (n759)																	
n759-01a	zoned inner	2810	5	2704	30	2565	66	13.34	3.1	0.4886	3.1	1.00	-4.9	161	104	0.41	0.19
n759-01a2	zoned inner	2810	10	2725	20	2613	43	13.64	2.1	0.4998	2.0	0.96	-4.1	184	121	0.48	0.27
n759-02a	zoned inner	2953	3	2931	30	2900	73	16.94	3.1	0.5682	3.1	1.00		622	453	0.22	0.07
n759-03a	zoned inner	2967	2	2949	30	2923	74	17.25	3.1	0.5736	3.1	1.00		649	644	1.69	0.02
n759-04a	zoned inner	2948	4	2876	30	2774	71	15.98	3.1	0.5378	3.1	1.00	-1.4	340	258	0.75	0.20
n759-05a	zoned inner	2945	4	2969	30	3005	75	17.62	3.1	0.5939	3.1	1.00		512	406	0.44	0.15
n759-06b	zoned inner	2887	13	2566	35	2179	67	11.51	3.7	0.4021	3.6	0.98	-22.9	523	284	0.71	0.92
n759-08a	zoned inner	2960	4	2999	30	3056	76	18.17	3.1	0.6065	3.1	1.00		385	383	1.48	0.04
n759-09a	homog. inner	2955	3	2924	30	2879	73	16.80	3.1	0.5630	3.1	1.00		408	362	1.62	0.07
n759-10a	zoned inner	2816	3	2759	30	2680	69	14.13	3.1	0.5155	3.1	1.00	-0.0	316	224	0.60	0.16
n759-10a2	zoned inner	2820	8	2732	20	2614	43	13.74	2.1	0.5001	2.0	0.97	-4.7	390	271	0.66	0.38
A1428 Mesa-aho porphyry. Suomussalmi (n762)																	
n762-01a	zoned inner	2820	15	2679	21	2497	41	13.00	2.2	0.4730	2.0	0.90	-8.8	45	36	1.94	* 0.06
n762-02a	zoned inner	2814	15	2711	21	2575	42	13.44	2.2	0.4910	2.0	0.90	-5.3	59	42	0.96	0.17
n762-03a	zoned inner	2811	9	2783	19	2745	44	14.51	2.0	0.5309	2.0	0.96		91	73	1.17	0.13
n762-04a	zoned inner	2801	9	2765	21	2715	47	14.23	2.2	0.5238	2.1	0.97		85	71	1.42	0.12
n762-05a	zoned inner	2811	13	2752	20	2673	43	14.04	2.1	0.5139	2.0	0.93	-1.2	58	48	1.48	0.21
n762-06a	zoned inner	2787	10	2683	20	2548	41	13.05	2.0	0.4847	2.0	0.95	-6.1	79	56	1.14	0.19
n762-07a	zoned inner	2818	7	2802	19	2780	44	14.79	2.0	0.5391	2.0	0.97		116	92	1.05	* 0.04
n762-08a	zoned inner	2816	9	2795	19	2767	44	14.69	2.0	0.5360	1.9	0.96		66	59	1.77	0.11
A1467 Saarikylä felsic volcanic rock. Suomussalmi (n761)																	
n761-01a	zoned core	2847	12	2119	19	1453	26	7.061	2.1	0.2528	2.0	0.94	-51.0	657	224	0.91	9.92
n761-02a	zoned inner	3188	2	3112	19	2996	47	20.44	2.0	0.5917	2.0	1.00	-3.8	845	679	0.45	0.13
n761-03a	zoned inner	2918	5	2863	19	2785	44	15.77	2.0	0.5405	2.0	0.99	-1.7	830	581	0.32	0.07
n761-04a	zoned core	2933	7	2899	19	2851	45	16.38	2.0	0.5561	1.9	0.98		146	108	0.45	0.28
n761-04b	zoned inner	2950	4	2954	19	2959	46	17.34	2.0	0.5825	2.0	0.99		733	540	0.19	0.02
n761-05a	zoned inner	2937	10	2881	20	2802	44	16.07	2.0	0.5444	1.9	0.95	-1.2	656	480	0.45	1.14
n761-05b	zoned inner	2926	5	2824	19	2684	43	15.15	2.0	0.5165	1.9	0.99	-6.4	349	240	0.45	0.13
n761-06a	zoned inner	2934	7	2855	19	2744	44	15.63	2.0	0.5306	1.9	0.98	-4.0	322	228	0.50	0.11
n761-07a	zoned inner	2943	8	2754	20	2503	42	14.06	2.1	0.4744	2.0	0.97	-14.3	202	125	0.33	0.37
A1821Tormua gabbro. Suomussalmi																	
~~*n2252-01a*~~	~~*pale homog.*~~	~~*2618*~~	~~*846*~~	~~*2551*~~	~~*1085*~~	~~*2468*~~	~~*342*~~	~~*11.33*~~	~~*71.4*~~	~~*0.4664*~~	~~*16.3*~~	~~*0.23*~~		~~*261*~~	~~*384*~~	~~*6.40*~~	~~*54.53*~~
n2252-02a	pale homog.	2863	2	2889	14	2926	33	16.20	1.4	0.5744	1.4	1.00		810	865	2.47	0.01
n2252-03a	pale homog.	2867	3	2857	13	2843	32	15.67	1.4	0.5543	1.4	0.99		842	983	3.42	0.01
n2252-04a	striped zoning	2867	5	2896	14	2938	33	16.32	1.4	0.5773	1.4	0.98		165	176	2.38	0.05
~~*n2252-05a*~~	~~*dark homog. rim*~~	~~*2800*~~	~~*17*~~	~~*2731*~~	~~*16*~~	~~*2640*~~	~~*30*~~	~~*13.73*~~	~~*1.7*~~	~~*0.5061*~~	~~*1.4*~~	~~*0.79*~~	~~*-2.1*~~	~~*113*~~	~~*123*~~	~~*3.43*~~	~~*5.83*~~
n2252-05b	pale homog. inner	2866	5	2872	13	2881	32	15.92	1.4	0.5634	1.4	0.97		190	262	4.51	0.10
n2252-07a	dark quite homog.	2853	8	2860	14	2870	33	15.72	1.5	0.5609	1.4	0.95		67	84	3.77	0.21
n2252-08a	pale homog.	2869	4	2871	13	2874	31	15.90	1.4	0.5618	1.3	0.99		308	358	3.17	0.02
n2252-09a		2876	4	2880	14	2886	34	16.05	1.5	0.5646	1.4	0.99		264	351	4.31	0.02
n2252-10a	dark homog.	2884	11	2892	15	2903	32	16.25	1.5	0.5688	1.4	0.90		42	45	2.45	0.57

Appendix 1. cont.

		Derived ages						Corrected ratios						Elemental data			
Sample/ spot #	Zircon domain	$^{207}Pb/^{206}Pb$	±σ	$^{207}Pb/^{235}U$	±σ	$^{206}Pb/^{238}U$	±σ	$^{207}Pb/^{235}U$	±σ %	$^{206}Pb/^{238}U$	±σ %	ρ [1]	Disc. % [2]	[U] ppm	[Pb] ppm	Th/U meas	f_{206} % [3]
A1821Tormua gabbro. Suomussalmi																	
~~*n2252-11a*~~	~~*dark homog. rim*~~	~~*2588*~~	~~*87*~~	~~*2620*~~	~~*53*~~	~~*2662*~~	~~*31*~~	~~*12.20*~~	~~*5.5*~~	~~*0.5112*~~	~~*1.4*~~	~~*0.26*~~		~~*5*~~	~~*3*~~	~~*0.23*~~	~~*13.53*~~
n2252-11b	pale homog. inner	2864	3	2866	13	2868	32	15.82	1.4	0.5604	1.4	0.99		516	567	2.84	0.01
~~*n2252-13a*~~	~~*dark homog. rim*~~	~~*2687*~~	~~*36*~~	~~*2692*~~	~~*46*~~	~~*2699*~~	~~*95*~~	~~*13.17*~~	~~*4.8*~~	~~*0.5198*~~	~~*4.3*~~	~~*0.89*~~		~~*21*~~	~~*14*~~	~~*0.50*~~	~~*7.36*~~
n2252-14a	quite homog	2858	5	2843	13	2822	31	15.45	1.4	0.5493	1.4	0.98		213	312	5.48	0.03
n2252-15a	pale homog. inner	2847	4	2847	13	2847	32	15.50	1.4	0.5552	1.4	0.99		715	916	4.18	0.02
n2252-15b	dark homog. rim	2789	4	2623	13	2415	27	12.24	1.4	0.4544	1.3	0.98	-13.6	367	301	3.20	0.34
A1701x Kuikkapuro. Kiannanniemi Suomussalmi																	
Host rock #1/ n2523 (4511/98/R361/44.40-45.40)																	
n2523-01a	weakly zoned. long	2828	4	2794	20	2748	46	14.67	2.1	0.5316	2.1	0.99		688	507	0.66	0.01
n2523-02a	weakly zoned. long	2821	4	2797	19	2765	44	14.72	2.0	0.5355	1.9	0.99		497	375	0.75	0.02
n2523-03a	weakly zoned	2812	4	2795	19	2771	44	14.68	2.0	0.5371	1.9	0.99		331	234	0.43	0.05
n2523-04a	quite homog stubby	2807	3	2808	19	2809	44	14.88	2.0	0.5462	1.9	0.99		489	350	0.41	0.01
n2523-05a	weakly zoned. long	2819	3	2827	19	2840	45	15.19	2.0	0.5535	2.0	1.00		804	637	0.86	0.01
n2523-06a	weakly zoned stubby	2811	3	2821	19	2834	45	15.08	2.0	0.5521	1.9	1.00		874	664	0.66	0.05
n2523-07a	weakly zoned stubby	2813	3	2831	19	2857	46	15.25	2.0	0.5577	2.0	1.00		676	493	0.41	0.03
n2523-08a	weakly zoned. long	2849	9	2845	20	2840	45	15.48	2.0	0.5537	2.0	0.96		132	93	0.25	0.02
n2523-09a	weakly zoned	2850	8	2842	19	2831	45	15.43	2.0	0.5514	2.0	0.97		133	93	0.27	0.05
n2523-	weakly zoned	2814	3	2845	19	2889	46	15.48	2.0	0.5653	2.0	0.99		426	329	0.64	0.03
n2523-11a	weakly zoned	2852	6	2864	19	2881	45	15.78	2.0	0.5634	1.9	0.98		165	120	0.35	0.14
Host rock #2/ n2524 (4511/98/R361/97.00-99.70)																	
n2524-01a	weakly zoned	2948	6	2849	14	2710	31	15.54	1.4	0.5225	1.4	0.96	-7.0	253	175	0.36	0.09
n2524-02a	quite homog	2807	6	2776	14	2734	31	14.39	1.4	0.5282	1.4	0.97	-0.2	165	118	0.56	0.02
n2524-03a	weakly zoned	2957	6	2952	14	2944	33	17.30	1.4	0.5789	1.4	0.96		178	141	0.54	0.03
n2524-04a	weakly zoned	2915	6	2900	14	2879	33	16.40	1.5	0.5630	1.4	0.96		107	79	0.38	0.06
n2524-05a	quite homog rounded	3528	4	3518	14	3499	37	30.95	1.4	0.7207	1.4	0.99		230	225	0.17	0.03
n2524-06a	weakly zoned	2957	4	2935	14	2903	33	17.01	1.4	0.5689	1.4	0.98		260	188	0.22	0.04
Kuhmo greenstone belt																	
A1346 Lampela andesite. Kuhmo																	
n2250-01a	zoned darker rim	2799	8	2795	14	2790	31	14.68	1.4	0.5416	1.3	0.94		77	54	0.32	0.19
n2250-01b (=02a)	homog pale core	2799	9	2809	14	2822	32	14.90	1.5	0.5493	1.4	0.92		143	102	0.38	0.25
n2250-03a	weakly zoned	2798	7	2819	14	2850	31	15.07	1.4	0.5560	1.3	0.95		88	63	0.32	0.04
n2250-04a	weakly zoned	2814	8	2796	14	2771	30	14.70	1.4	0.5370	1.3	0.94		73	52	0.48	0.19
n2250-05a	weakly zoned	2800	7	2801	14	2802	31	14.78	1.4	0.5445	1.4	0.96		96	68	0.41	0.17
n2250-06a	zoned	2793	6	2815	14	2847	32	15.00	1.4	0.5553	1.4	0.97		132	96	0.41	0.13
n2250-07a	pale inner	2770	3	2787	13	2810	31	14.55	1.4	0.5463	1.3	0.99		899	745	1.19	0.07
n2250-07b (=08a)	darker rim	2784	12	2796	15	2813	31	14.70	1.6	0.5471	1.4	0.87		47	32	0.27	0.09
n2250-09a	weakly zoned	2787	8	2809	14	2839	32	14.90	1.5	0.5533	1.4	0.95		69	50	0.37	0.07
n2250-10a	weakly zoned dark rim	2800	6	2787	13	2769	30	14.56	1.4	0.5365	1.3	0.96		150	105	0.46	0.57
n2250-10b (=11a)	weakly zoned pale center	2795	4	2823	14	2863	33	15.13	1.4	0.5592	1.4	0.99		280	210	0.53	0.03
n2250-12	quite homog.	2760	7	2737	14	2705	31	13.81	1.5	0.5215	1.4	0.96		142	95	0.37	0.47
~~*n2250-13*~~	~~*weakly zoned*~~	~~*2653*~~	~~*94*~~	~~*2625*~~	~~*63*~~	~~*2589*~~	~~*63*~~	~~*12.27*~~	~~*6.5*~~	~~*0.4942*~~	~~*2.9*~~	~~*0.45*~~		~~*700*~~	~~*459*~~	~~*0.62*~~	~~*2.98*~~

Appendix 1. cont.

		Derived ages						*Corrected ratios*						*Elemental data*			
Sample/		^{207}Pb	±σ	^{207}Pb	±σ	^{206}Pb	±σ	^{207}Pb	±σ	^{206}Pb	±σ	ρ [1]	**Disc.**	**[U]**	**[Pb]**	**Th/U**	f_{206}
spot #	**Zircon domain**	^{206}Pb		^{235}U		^{238}U		^{235}U	%	^{238}U	%		**% [2]**	**ppm**	**ppm**	**meas**	**% [3]**
A1418 Niittylahti gabbro. Kuhmo																	
n2251-01a	quite homog. pale corroded	2795	4	2819	13	2853	32	15.06	1.4	0.5568	1.4	0.99		282	232	1.01	0.11
n2251-02a	quite homog. pale (corroded)	2789	4	2812	13	2845	32	14.95	1.4	0.5548	1.4	0.98		251	202	0.97	0.02
n2251-03a	quite homog. pale (corroded)	2785	6	2786	14	2787	32	14.54	1.5	0.5409	1.4	0.97		234	181	0.89	0.66
n2251-04a	quite homog. pale (corroded)	2788	4	2799	13	2814	31	14.75	1.4	0.5473	1.4	0.98		239	191	0.98	0.22
n2251-05a	quite homog. pale (corroded)	2793	4	2812	13	2839	31	14.96	1.4	0.5534	1.3	0.99		324	267	1.08	0.06
n2251-06a	homog. pale	2787	3	2802	13	2823	31	14.80	1.4	0.5495	1.4	0.99		421	350	1.15	0.05
n2251-07a	homog. pale	2790	4	2808	13	2833	31	14.89	1.4	0.5519	1.3	0.99		418	347	1.14	0.02
n2251-08a	weak zoning (corroded)	2774	12	2760	15	2740	30	14.15	1.5	0.5297	1.3	0.88		227	180	1.16	0.74
n2251-09a	quite homog. pale (corroded)	2781	4	2753	15	2715	34	14.04	1.6	0.5236	1.5	0.99		465	363	1.09	0.48
n2251-10a	quite homog. pale (corroded)	2603	6	2565	13	2517	28	11.50	1.4	0.4777	1.4	0.97	-1.0	803	602	1.38	0.52
n2251-11a	quite homog. pale (corroded)	2770	3	2768	13	2765	31	14.27	1.4	0.5356	1.4	0.99		404	301	0.71	0.14
n2251-12a	quite homog. pale	2743	4	2733	13	2718	30	13.75	1.4	0.5246	1.4	0.98		277	211	0.95	0.43
n2251-13a	quite homog. pale	2789	5	2803	14	2822	32	14.80	1.4	0.5493	1.4	0.98		177	130	0.53	0.08
n2251-14a	dark. weak zoning	2788	6	2771	8	2747	18	14.31	0.9	0.5314	0.8	0.91		69	49	0.48	{0.03}
~~n2251-15a~~	~~*dark. weak zoning*~~	~~2771~~	~~20~~	~~2747~~	~~15~~	~~2715~~	~~22~~	~~13.96~~	~~1.6~~	~~*0.5238*~~	~~1.0~~	~~0.62~~		~~221~~	~~170~~	~~0.99~~	~~2.98~~
n2251-16a	pale weakly zoned inner	2785	4	2781	8	2775	18	14.46	0.8	0.5379	0.8	0.96		192	145	0.78	0.08
~~n2251-17a~~	~~weakly zoned~~	~~2866~~	~~162~~	~~2920~~	~~113~~	~~2998~~	~~89~~	~~16.73~~	~~11.2~~	~~*0.5922*~~	~~3.7~~	~~0.33~~		~~202~~	~~183~~	~~2.62~~	~~7.83~~
n2251-18a	quite homog	2772	17	2684	13	2569	17	13.06	1.3	0.4897	0.8	0.60	-4.4	139	95	0.69	1.33
n2251-19a	weakly zoned	1907	4	1810	7	1727	12	4.946	0.8	0.3073	0.8	0.96	-9.0	510	260	1.95	0.12
n2251-20a	quite homog dark inner	2788	4	2778	8	2764	18	14.42	0.8	0.5355	0.8	0.96		159	117	0.63	0.03
n2251-21a	dark quite homog	2796	10	2784	10	2768	19	14.52	1.1	0.5364	0.9	0.80		73	52	0.48	0.53
A1771 Kellojärvi gabbronorite. Kuhmo																	
n2249-01	homog. pale. long	2776	3	2763	14	2745	33	14.20	1.5	0.5309	1.5	0.99		513	406	1.10	0.06
n2249-02	homog. dark inner . short	1090	38	1083	16	1080	14	1.906	2.4	0.1824	1.4	0.59		26	7	1.39	{0.34}
n2249-03	homog. dark. short	970	69	1012	24	1031	13	1.709	3.7	0.1735	1.4	0.37		23	6	1.41	1.11
n2249-04	weakly zoned pale. long	2749	4	2752	14	2755	32	14.03	1.4	0.5333	1.4	0.99		384	283	0.69	0.56
n2249-05	quite homog. pale	2802	4	2828	14	2864	33	15.20	1.4	0.5594	1.4	0.98		199	153	0.69	0.03
n2249-06	weakly zoned pale	2774	4	2789	13	2810	32	14.59	1.4	0.5463	1.4	0.98		264	212	1.03	0.01
n2249-07	weakly zoned pale. long	2793	8	2815	14	2846	31	15.00	1.4	0.5549	1.4	0.94		419	345	1.08	1.61
n2249-08	weakly zoned. long	2758	4	2762	13	2767	30	14.18	1.4	0.5361	1.3	0.99		311	240	0.94	0.07
n2249-09	weakly zoned. long	2785	6	2777	14	2766	31	14.41	1.4	0.5359	1.4	0.97		117	88	0.74	0.04
n2249-10	weakly zoned. dark	3229	4	3244	14	3268	35	23.40	1.4	0.6602	1.4	0.98		166	159	0.74	0.02
n2249-11	weakly zoned. short	2795	5	2808	13	2826	31	14.89	1.4	0.5502	1.4	0.98		209	165	0.90	{0.01}
n2249-12	homog. pale. long (luid holes....)	2742	6	2741	13	2738	30	13.87	1.4	0.5293	1.3	0.97		720	549	0.93	0.02
n2249-13	weakly zoned dark. long	2806	7	2819	14	2837	32	15.06	1.5	0.5529	1.4	0.96		95	74	0.81	0.09
A1377 Siivikko felsic fragment in komatiite. Kuhmo																	
n2248-01a	zoned dark inner	2786	5	2846	14	2931	34	15.49	1.5	0.5756	1.4	0.98	3.2	163	135	0.90	0.03
n2248-02a	zoned dark inner	2794	7	2806	14	2822	31	14.86	1.4	0.5493	1.4	0.95		82	60	0.57	0.17
n2248-03a	pale	2800	3	2783	14	2760	32	14.50	1.4	0.5343	1.4	0.99		572	448	1.01	0.11
n2248-03b (=04a)	dark	2803	7	2844	14	2902	32	15.46	1.4	0.5687	1.4	0.95	1.0	76	58	0.57	0.06
n2248-05a	pale homog rim	2775	3	2791	15	2813	35	14.62	1.6	0.5470	1.5	0.99		602	479	0.97	0.03
n2248-06a	dark inner	2780	8	2829	15	2898	34	15.21	1.5	0.5676	1.5	0.94	1.6	77	58	0.48	0.09
n2248-06b (=07a)	pale outer	2769	5	2760	14	2748	33	14.16	1.5	0.5315	1.5	0.98		227	169	0.78	0.41

Appendix 1. cont.

		Derived ages						*Corrected ratios*					*Elemental data*				
Sample/		^{207}Pb	±σ	^{207}Pb	±σ	^{206}Pb	±σ	^{207}Pb	±σ	^{206}Pb	±σ	ρ [1]	**Disc.**	**[U]**	**[Pb]**	**Th/U**	f_{206}
spot #	**Zircon domain**	^{206}Pb		^{235}U		^{238}U		^{235}U	%	^{238}U	%		**% [2]**	**ppm**	**ppm**	**meas**	**% [3]**
A1377 Siivikko felsic fragment in komatiite. Kuhmo																	
n2248-08a	pale rim	2793	4	2844	14	2916	34	15.46	1.5	0.5720	1.5	0.99	2.3	299	243	0.85	0.03
n2248-08b (=9a)	weakly zoned dark inner	2806	10	2817	15	2834	32	15.03	1.5	0.5520	1.4	0.92		85	64	0.61	0.17
n2248-10a	zoned	2790	4	2808	14	2834	33	14.89	1.5	0.5520	1.4	0.98		249	193	0.80	0.04
n2248-11a	pale homog. tip	2645	5	2587	6	2513	11	11.77	0.6	0.4766	0.5	0.86	-4.4	796	570	1.33	0.05
n2248-12a	pale homog. rim	2764	5	2754	6	2740	12	14.06	0.6	0.5298	0.5	0.88		462	359	1.18	0.09
n2248-13a	pale homog. rim	2734	4	2697	6	2648	11	13.24	0.6	0.5080	0.5	0.89	-2.4	781	597	1.37	0.03
n2248-14a	pale homog. rim	2490	4	2284	5	2062	9	8.486	0.6	0.3770	0.5	0.90	-18.7	1554	973	2.09	0.30
n2248-15a	pale homog. rim	2775	7	2784	6	2798	12	14.52	0.7	0.5434	0.5	0.78		519	412	1.09	0.02
A120 Ruokojärvi dacite. Suomussalmi																	
n2554-01a	quite homog core	3127	4	3097	6	3052	13	20.13	0.6	0.6056	0.5	0.92	-1.7	513	364	0.01	0.04
n2554-01b	quite homog rim	2883	2	2921	8	2975	20	16.75	0.9	0.5864	0.8	0.99	2.1	553	454	0.70	0.32
n2554-02a	weakly zoned	3012	3	2972	5	2913	12	17.67	0.6	0.5713	0.5	0.95	-2.9	393	329	0.47	0.16
~~*n2554-02b*~~	*zoned dark rim*	~~*2794*~~	~~*18*~~	~~*2458*~~	~~*12*~~	~~*2073*~~	~~*11*~~	~~*10.25*~~	~~*1.2*~~	~~*0.3792*~~	~~*0.6*~~	~~*0.49*~~	~~*-25.9*~~	*397*	*318*	*0.47*	~~*5.41*~~
n2554-03a	dark core	3127	3	3105	6	3070	14	20.28	0.6	0.6100	0.6	0.96	-1.1	597	445	0.26	0.02
n2554-03b	weakly zoned pale rim	2978	2	2960	5	2933	13	17.45	0.6	0.5762	0.5	0.96	-0.7	391	306	0.31	0.11
n2554-04a	weakly zoned rim	3073	4	3044	6	3000	13	19.04	0.6	0.5925	0.5	0.92	-1.6	284	196	0.03	0.08
n2554-05a	zoned	2981	4	2938	6	2874	12	17.05	0.6	0.5619	0.5	0.92	-3.1	~~248~~	~~114~~	~~0.24~~	0.17
n2554-07a	zoned	3099	2	3046	5	2968	13	19.09	0.6	0.5847	0.5	0.97	-4.1	370	302	0.16	0.13
n2554-07a#2	*zoned*	*2924*	*9*	*3057*	*27*	*3263*	*69*	*19.30*	*2.7*	0.6589	*2.7*	*0.98*	*8.2*	*213*	*[123]*	*0.48*	*0.71*
~~*n2554-08a*~~	*zoned*	~~*2753*~~	~~*22*~~	~~*2279*~~	~~*13*~~	~~*1789*~~	~~*9*~~	~~*8.436*~~	~~*1.5*~~	~~*0.3199*~~	~~*0.6*~~	~~*0.39*~~	~~*-34.7*~~	~~*155*~~	~~*[107]*~~	~~*0.25*~~	~~*32.51*~~
~~*n2554-08a#2*~~	*zoned*	~~*2665*~~	~~*278*~~	~~*2454*~~	~~*192*~~	~~*2208*~~	~~*71*~~	~~*10.21*~~	~~*18.9*~~	~~*0.4085*~~	~~*3.8*~~	~~*0.20*~~		~~*194*~~	~~*95*~~	~~*0.41*~~	~~*29.48*~~
~~*n2554-09a*~~	*zoned unaltered core*	~~*2802*~~	~~*174*~~	~~*2467*~~	~~*113*~~	~~*2081*~~	~~*36*~~	~~*10.35*~~	~~*11.5*~~	~~*0.3810*~~	~~*2.0*~~	~~*0.18*~~		~~*466*~~	~~*367*~~	~~*0.47*~~	~~*19.82*~~
n2554-10a	weakly zoned	2992	5	2997	6	3006	12	18.15	0.6	0.5940	0.5	0.85		271	253	1.11	0.08
n2554-11a	quite homog-weakly zoned	3131	6	3141	7	3157	15	21.06	0.7	0.6320	0.6	0.84		127	115	0.89	0.12
n2554-12a	weakly zoned core	3135	10	3141	8	3151	13	21.06	0.8	0.6303	0.5	0.65		219	204	1.23	0.08
n2554-13a	weakly zoned	3115	7	3114	7	3112	15	20.47	0.7	0.6206	0.6	0.81		373	359	1.01	0.09
n2554-14a	weakly zoned	3104	8	3158	7	3244	13	21.43	0.7	0.6541	0.5	0.71	3.4	336	276	0.54	0.30
n2554-15a	weakly zoned	3112	7	3091	7	3059	13	19.99	0.7	0.6072	0.5	0.78	-0.2	107	91	0.77	0.14
n2554-16a	weakly zoned	3123	13	3103	10	3071	13	20.23	1.0	0.6102	0.5	0.55		860	647	0.90	0.30
n2554-17a	homog pale inner	2902	4	2853	6	2785	14	15.61	0.7	0.5404	0.6	0.93	-3.4	524	191	0.86	0.18
~~*n2554-18a*~~	~~*zoned*~~	~~*2745*~~	~~*24*~~	~~*2129*~~	~~*14*~~	~~*1551*~~	~~*7*~~	~~*7.136*~~	~~*1.6*~~	~~*0.2720*~~	~~*0.5*~~	~~*0.33*~~	~~*-42.9*~~	~~*912*~~	~~*526*~~	~~*0.34*~~	~~*15.55*~~
n2554-19a	homog pale inner	2837	13	2695	9	2511	11	13.22	1.0	0.4762	0.5	0.54	-10.6	386	245	0.03	2.74
n2554-20a	quite homog pale inner	2776	8	2763	7	2744	12	14.19	0.7	0.5306	0.5	0.72		356	233	0.03	0.81
n2554-21a	quite homog inner	2822	5	2810	8	2793	19	14.92	0.9	0.5424	0.8	0.93		373	207	1.03	0.48
~~*n2554-22a*~~	*zoned*	~~*2844*~~	~~*85*~~	~~*2601*~~	~~*54*~~	~~*2301*~~	~~*26*~~	~~*11.96*~~	~~*5.6*~~	~~*0.4289*~~	~~*1.4*~~	~~*0.24*~~	~~*-2.4*~~	~~*453*~~	~~*382*~~	~~*0.64*~~	~~*21.48*~~
n2554-23a	quite homog pale core	3111	4	3067	9	3000	21	19.49	0.9	0.5926	0.9	0.97	-2.5	586	[308]	0.68	0.63
~~*n2554-24a*~~	*zoned*	~~*2840*~~	~~*200*~~	~~*2049*~~	~~*125*~~	~~*1358*~~	~~*29*~~	~~*6.524*~~	~~*13.4*~~	~~*0.2346*~~	~~*2.4*~~	~~*0.18*~~	~~*-8.0*~~	~~*174*~~	~~*124*~~	~~*0.91*~~	~~*55.33*~~
~~*n2554-25a*~~	*darker inner*	~~*2561*~~	~~*90*~~	~~*2715*~~	~~*58*~~	~~*2928*~~	~~*53*~~	~~*13.50*~~	~~*6.0*~~	~~*0.5748*~~	~~*2.3*~~	~~*0.38*~~		~~*445*~~	~~*172*~~	~~*0.96*~~	~~*11.39*~~
~~*n2554-26a*~~	*darker inner*	~~*2918*~~	~~*83*~~	~~*2228*~~	~~*49*~~	~~*1557*~~	~~*11*~~	~~*7.973*~~	~~*5.3*~~	~~*0.2733*~~	~~*0.8*~~	~~*0.15*~~	~~*-32.1*~~	*345*	*236*	*0.46*	~~*17.89*~~
n2554-27a	quite homog	3017	6	2875	9	2678	19	15.98	1.0	0.5150	0.9	0.92	-11.6	630	318	1.42	0.52
n2554-28a	darker rim	2666	11	2337	34	1980	61	8.993	3.6	0.3595	3.6	0.98	-24.2	197	182	0.97	1.18
n2554-29a	zoned	3120	3	3102	8	3073	19	20.22	0.8	0.6108	0.8	0.98	-0.2	67	58	0.73	0.01
n2554-30a	dark homog core	3132	5	3083	8	3010	19	19.84	0.8	0.5950	0.8	0.94	-3.0	218	189	0.61	0.03

Appendix 1. cont.

		Derived ages						*Corrected ratios*						*Elemental data*			
Sample/		^{207}Pb	±σ	^{207}Pb	±σ	^{206}Pb	±σ	^{207}Pb	±σ	^{206}Pb	±σ	ρ [1]	**Disc.**	**[U]**	**[Pb]**	**Th/U**	f_{206}
spot #	**Zircon domain**	^{206}Pb		^{235}U		^{238}U		^{235}U	%	^{238}U	%		**% [2]**	**ppm**	**ppm**	**meas**	**% [3]**
A120 Ruokojärvi dacite. Suomussalmi																	
n2554-31a	weakly zoned tiny grain	3124	5	3115	11	3101	28	20.49	1.2	0.6177	1.1	0.97		216	185	0.62	0.18
n2554-32a	weakly zoned tiny grain	3125	5	3108	11	3082	25	20.35	1.1	0.6130	1.0	0.96		288	260	1.03	0.05
n2554-33a	weakly zoned tiny grain	3115	3	3080	8	3028	19	19.77	0.8	0.5996	0.8	0.97	-1.8	325	297	0.94	0.09
n2554-34a	weakly zoned tiny grain	3129	2	3106	8	3071	19	20.31	0.8	0.6102	0.8	0.99	-0.7	134	105	0.17	0.10
n2554-35a	quite homo. dark inner	3127	5	3101	8	3060	19	20.19	0.8	0.6075	0.8	0.93	-0.8	627	439	0.35	0.03
n2554-35b	pale weakly zoned	3047	5	2918	9	2736	19	16.71	0.9	0.5288	0.9	0.95	-10.6				0.07
A1773 Hetteilä#1 intermediate volcanic rock. Kuhmo																	
n2556-01a	pale homog rim	522	13	530	7	532	8	0.686	1.7	0.0860	1.6	0.94		6645	607	0.02	0.03
n2556-02a	dark core	2839	12	2820	18	2793	38	15.07	1.8	0.5423	1.7	0.91		152	117	1.02	0.07
n2556-02b	pale rim	2668	8	2667	16	2665	35	12.83	1.7	0.5120	1.6	0.96		1244	756	0.03	0.08
n2556-03a	zoned grain	2830	12	2802	17	2765	36	14.80	1.8	0.5356	1.6	0.90		118	90	1.08	0.13
n2556-04a	zoned grain	2853	15	2828	18	2792	37	15.20	1.9	0.5420	1.6	0.87		148	115	1.11	0.17
n2556-06a	quite homog tiny grain	2832	12	2797	17	2749	37	14.72	1.8	0.5318	1.6	0.91		158	116	0.85	0.28
n2556-07a	dark core	2853	17	2811	18	2752	36	14.93	1.9	0.5326	1.6	0.84		110	80	0.82	{0.13}
n2556-07b	pale rim	2683	7	2664	16	2640	35	12.79	1.6	0.5062	1.6	0.97		641	385	0.02	0.18
n2556-08a	dark quite homog	2809	21	2769	20	2713	36	14.28	2.1	0.5232	1.6	0.77		146	102	0.75	0.76
n2556-09a	dark hazy	2848	15	2792	18	2714	37	14.63	1.9	0.5234	1.7	0.88	-1.0	164	120	1.00	0.23
n2556-10a	weakly zoned grain	2797	19	2738	19	2658	36	13.83	2.0	0.5104	1.6	0.81	-0.5	91	65	1.06	0.68
n2556-11a	dark core	2836	3	2817	8	2791	18	15.03	0.8	0.5418	0.8	0.97	-0.2	207	156	0.64	0.07
n2556-11b	pale rim	2677	7	2658	8	2632	17	12.70	0.9	0.5042	0.8	0.89		1144	688	0.05	1.38
~~*n2556-12a*~~	~~*hazy*~~	~~*2820*~~	~~*3*~~	~~*2999*~~	~~*31*~~	~~*3275*~~	~~*81*~~	~~*18.18*~~	~~*3.1*~~	~~*0.6619*~~	~~*3.1*~~	~~*1.00*~~	~~*13.0*~~	~~*352*~~	~~*315*~~	~~*0.58*~~	~~*0.05*~~
n2556-13a	pale rim	2679	2	2666	8	2648	18	12.81	0.8	0.5079	0.8	0.99		1568	948	0.03	0.02
A1774 Hetteilä#2 mica schist. Kuhmo																	
n2557-01a#2	zoned	2745	5	2711	16	2665	36	13.44	1.7	0.5119	1.7	0.99	-0.2	262	196	1.02	{0.01}
n2557-02#2	zoned	2720	9	2761	9	2816	18	14.16	1.0	0.5479	0.8	0.81	1.5	114	86	0.67	{0.02}
n2557-03a#2	zoned	2724	14	2612	16	2470	30	12.10	1.7	0.4669	1.5	0.87	-7.1	217	132	0.36	0.51
n2557-04a#2	quite homogeneous core	2787	7	2755	11	2712	23	14.08	1.1	0.5230	1.0	0.92	-0.7	190	130	0.41	0.18
n2557-05a#2	zoned	2735	7	2774	10	2828	22	14.36	1.1	0.5506	1.0	0.92	1.6	307	229	0.64	0.02
n2557-06#2	zoned	2749	8	2758	10	2771	21	14.13	1.1	0.5371	0.9	0.90		97	71	0.65	{0.02}
n2557-07a#2	zoned	2745	5	2754	9	2767	20	14.07	0.9	0.5362	0.9	0.95		179	126	0.45	0.03
n2557-08a#2	zoned	2732	4	2713	8	2688	17	13.47	0.8	0.5175	0.8	0.96	-0.1	226	160	0.65	0.07
n2557-09a#2	zoned	2742	4	2785	8	2845	18	14.54	0.8	0.5549	0.8	0.96	2.8	211	163	0.75	{0.01}
n2557-10a#2	dark zoned	2793	7	2796	8	2802	18	14.71	0.9	0.5443	0.8	0.89		130	102	0.94	0.02
A1746 Petäjäniemi metasediment. Kuhmo																	
n2246-01a	weakly zoned unfractured (=metamorphic?)	2867	10	2904	15	2958	33	16.47	1.5	0.5824	1.4	0.91	0.1	47	34	0.20	{0.03}
n2246-02a	pale homog (healed?) core	2856	3	2909	14	2987	33	16.55	1.4	0.5894	1.4	0.99	2.7	356	272	0.34	0.02
n2246-03a	weakly zoned dark rim	2806	12	2684	15	2526	29	13.06	1.6	0.4796	1.4	0.89	-8.3	54	33	0.34	0.56
n2246-03b	homog. pale core	2855	5	2799	13	2721	30	14.74	1.4	0.5251	1.3	0.98	-3.0	248	177	0.70	0.20
n2246-04a	homog. core	2847	7	2898	16	2973	39	16.36	1.7	0.5858	1.6	0.97	1.7	123	97	0.54	{0.01}
n2246-05a	zoned	2821	5	2792	15	2752	35	14.63	1.6	0.5325	1.5	0.98		174	116	0.19	0.12
n2246-06a	weakly zoned	2879	12	2941	16	3033	35	17.12	1.6	0.6009	1.4	0.89	2.4	32	25	0.43	{0.06}
n2246-07a	dark weakly zoned rim	2849	7	2908	14	2993	33	16.52	1.4	0.5909	1.4	0.95	2.9	78	61	0.41	0.04

Appendix 1. cont.

Sample/ spot #	Zircon domain	Derived ages $^{207}Pb/^{206}Pb$	±σ	$^{207}Pb/^{235}U$	±σ	$^{206}Pb/^{238}U$	±σ	Corrected ratios $^{207}Pb/^{235}U$	±σ %	$^{206}Pb/^{238}U$	±σ %	ρ [1]	Disc. % [2]	Elemental data [U] ppm	[Pb] ppm	Th/U meas	f_{206} % [3]
A1746 Petäjäniemi metasediment. Kuhmo																	
n2246-08a	homogenized core	2850	3	2895	13	2961	32	16.31	1.4	0.5830	1.4	0.99	1.9	419	341	0.74	0.02
n2246-09a	dark quite homog rim	2737	7	2778	14	2834	31	14.42	1.4	0.5520	1.4	0.95	1.0	85	61	0.41	0.04
n2246-09b	pale homog. core	2855	6	2896	13	2954	32	16.32	1.4	0.5813	1.3	0.96	1.2	126	99	0.58	{0.02}
n2246-10a	weak hazy zoning	2848	6	2881	14	2929	32	16.07	1.4	0.5752	1.4	0.97	0.4	177	140	0.64	0.02
n2246-11a	dark weakly zoned inner (thin pale zones around)	2865	5	2884	14	2913	34	16.13	1.5	0.5712	1.4	0.98		170	127	0.37	0.02
n2246-12a	weakly zoned	2744	11	2752	15	2763	32	14.04	1.6	0.5351	1.4	0.90		39	27	0.35	0.09
n2246-13a	zoned	2856	5	2840	13	2818	31	15.39	1.4	0.5482	1.4	0.98		221	158	0.42	0.05
n2246-14a	weakly zoned core	2833	5	2810	13	2778	30	14.92	1.4	0.5387	1.3	0.98		225	160	0.44	0.03
n2246-14b (=15a)	weakly zoned rim	2696	6	2179	13	1674	20	7.553	1.4	0.2965	1.3	0.96	-40.8	240	95	1.29	0.12
~~*n2246-16*~~	~~*dark homog. outer*~~	~~*2826*~~	~~*54*~~	~~*2239*~~	~~*34*~~	~~*1656*~~	~~*21*~~	~~*8.072*~~	~~*3.7*~~	~~*0.2928*~~	~~*1.4*~~	~~*0.39*~~	~~*-33.6*~~	~~*11*~~	~~*4*~~	~~*0.82*~~	~~*7.82*~~
Ilomantsi greenstone belt																	
A221 Hattuvaara Ilomantsi mica gneiss (= n2494). all analyses on mostly oscillatory zoned inner domains																	
n2494-01		2740	5	2657	20	2549	45	12.69	2.1	0.4850	2.1	0.99	-4.4	265	183	0.81	0.83
n2494-02		2736	3	2706	18	2666	42	13.37	1.9	0.5122	1.9	0.99		264	196	0.85	0.54
n2494-03		2749	2	2711	16	2660	36	13.44	1.7	0.5107	1.7	1.00	-0.7	679	502	0.85	0.09
n2494-04		2743	4	2635	21	2496	46	12.39	2.2	0.4728	2.2	0.99	-6.8	201	132	0.67	0.61
n2494-05		2740	4	2696	17	2638	38	13.23	1.8	0.5055	1.7	0.99	-1.1	278	194	0.65	0.53
n2494-06		2747	5	2680	19	2591	43	13.00	2.0	0.4947	2.0	0.99	-3.0	149	102	0.70	0.74
n2494-07		2745	3	2714	18	2672	42	13.48	1.9	0.5135	1.9	0.99		391	294	0.98	0.14
n2494-08		2743	3	2732	18	2716	41	13.73	1.8	0.5239	1.8	1.00		485	360	0.80	0.02
n2494-09		2749	4	2723	17	2689	39	13.62	1.8	0.5176	1.8	0.99		246	182	0.83	0.04
n2494-10		2757	7	2737	15	2711	34	13.82	1.6	0.5228	1.5	0.96		83	62	0.81	0.04
n2494-11		2729	6	2664	18	2580	40	12.79	1.9	0.4921	1.9	0.98	-2.8	247	171	0.80	0.40
n2494-12		2743	4	2708	20	2662	45	13.40	2.1	0.5112	2.1	0.99		313	226	0.78	0.04
n2494-13		2742	6	2599	16	2420	33	11.93	1.7	0.4556	1.7	0.98	-10.9	206	127	0.63	0.91
~~*n2494-14*~~		~~*2852*~~	~~*13*~~	~~*3071*~~	~~*37*~~	~~*3417*~~	~~*98*~~	~~*19.58*~~	~~*3.7*~~	~~*0.6990*~~	~~*3.7*~~	~~*0.98*~~	~~*15.8*~~	~~*2025*~~	~~*2105*~~	~~*0.88*~~	~~*1.16*~~
n2494-15		2700	3	2683	15	2660	34	13.04	1.5	0.5107	1.5	0.99		591	466	1.34	0.16
n2494-16		2737	7	2681	16	2608	36	13.02	1.7	0.4986	1.7	0.97	-2.1	324	221	0.76	1.93
n2494-17		2742	4	2697	16	2637	37	13.24	1.7	0.5055	1.7	0.99	-1.3	327	232	0.90	0.12
n2494-18		2750	3	2737	15	2719	34	13.81	1.6	0.5246	1.5	0.99		545	416	0.98	0.18
n2494-19		2749	6	2712	15	2662	34	13.45	1.6	0.5112	1.5	0.97	-0.6	209	146	0.71	0.05
n2494-20		2748	8	2726	15	2697	34	13.66	1.6	0.5194	1.5	0.96		223	165	0.91	0.06
n2494-21		2746	5	2709	15	2659	34	13.40	1.6	0.5105	1.5	0.98	-0.7	382	275	0.82	0.19
n2494-22		2749	7	2744	17	2738	38	13.92	1.8	0.5291	1.7	0.97		107	79	0.77	{0.02}
n2494-23		2740	5	2734	16	2726	38	13.77	1.7	0.5262	1.7	0.98		220	164	0.82	0.02
n2494-24		2711	7	2698	15	2681	34	13.26	1.6	0.5157	1.6	0.96		124	89	0.73	0.07
n2494-25		2757	6	2729	15	2692	34	13.70	1.6	0.5183	1.6	0.98		212	158	0.93	0.04
n2494-26		2743	7	2748	17	2754	38	13.97	1.7	0.5331	1.7	0.97		180	130	0.63	0.05
n2494-27		2710	9	2534	16	2320	31	11.13	1.7	0.4333	1.6	0.95	-13.7	101	61	0.96	0.29
n2494-28		2721	7	2629	16	2511	34	12.32	1.7	0.4762	1.6	0.97	-5.9	151	97	0.66	0.09
n2494-29		2751	4	2757	15	2765	35	14.11	1.6	0.5355	1.6	0.99		336	255	0.87	0.02

Appendix 1. cont.

Sample/ spot #	Zircon domain	Derived ages $^{207}Pb/^{206}Pb$	±σ	$^{207}Pb/^{235}U$	±σ	$^{206}Pb/^{238}U$	±σ	Corrected ratios $^{207}Pb/^{235}U$	±σ %	$^{206}Pb/^{238}U$	±σ %	ρ [1]	Disc. % [2]	Elemental data [U] ppm	[Pb] ppm	Th/U meas	f_{206} % [3]
Ilomantsi greenstone belt																	
A221 Hattuvaara Ilomantsi mica gneiss (= n2494). all analyses on mostly oscillatory zoned inner domains																	
n2494-30		2734	3	2664	15	2574	33	12.79	1.6	0.4907	1.5	0.99	-4.1	601	445	1.35	0.06
n2494-31		2749	6	2726	15	2695	34	13.65	1.6	0.5190	1.5	0.97		211	150	0.73	0.02
n2494-32		2730	9	2652	18	2550	37	12.62	1.9	0.4853	1.8	0.95	-4.0	434	296	1.16	0.23
n2494-33		2763	8	2739	16	2707	35	13.84	1.6	0.5219	1.6	0.96		169	119	0.60	{0.01}
n2494-34		2887	10	2890	16	2895	37	16.23	1.7	0.5668	1.6	0.93		64	52	0.95	{0.03}
n2494-35		2735	6	2484	15	2189	29	10.55	1.6	0.4044	1.6	0.97	-20.7	287	159	1.00	0.62
A282-Vehkavaara porphyry dike. Ilomantsi																	
n763-01a	core	3006	4	3024	19	3051	48	18.65	2.0	0.6053	2.0	0.99		500	393	0.29	0.04
n763-02a	core	2971	9	2948	20	2915	47	17.24	2.1	0.5718	2.0	0.96		68	51	0.39	0.34
n763-02b	zoned core	3018	6	2986	19	2938	46	17.93	2.0	0.5773	2.0	0.98		179	138	0.42	0.1
n763-03a	zoned outer	2738	3	2690	19	2625	42	13.14	2.0	0.5027	1.9	0.99	-1.3	571	348	0.08	0.03
n763-04a	core	3237	9	3200	20	3141	49	22.37	2.0	0.6279	2.0	0.96		91	80	0.49	0.22
n763-05a	core	2999	3	2986	19	2966	47	17.92	2.0	0.5843	2.0	0.99		490	390	0.52	0.11
n763-06a	core	3005	5	2943	19	2853	45	17.14	2.0	0.5566	1.9	0.99	-2.4	314	237	0.48	0.2
n763-06b	zoned outer	2751	5	2706	19	2647	43	13.37	2.0	0.5076	2.0	0.99	-0.7	687	416	0.01	0.12
n763-07a	zoned outer	2764	4	2685	19	2581	42	13.07	2.0	0.4925	2.0	0.99	-4.3	643	382	0.05	0.11
n763-08a	zoned core	2978	6	2922	19	2841	46	16.78	2.0	0.5538	2.0	0.98	-1.7	244	180	0.42	0.18
n763-09a	core	2984	3	2896	19	2773	44	16.33	2.0	0.5374	1.9	1.00	-5.1	1068	716	0.10	0.02
n763-10a	core	2986	9	2883	20	2737	44	16.10	2.0	0.5289	2.0	0.96	-6.1	77	55	0.51	0.14
n763-11a	zoned core	3091	8	3005	20	2878	45	18.29	2.0	0.5627	2.0	0.97	-4.5	616	530	1.25	0.05
n763-12a	core	2908	10	2823	21	2704	45	15.12	2.1	0.5212	2.0	0.95	-4.1	151	105	0.47	0.97
A301-Vehkavaara porphyry dike. Ilomantsi																	
n760-01a	core	3100	3	3097	20	3093	50	20.12	2.0	0.6157	2.0	0.99		462	375	0.31	0.03
n760-02b	core	3300	4	3228	20	3115	50	23.04	2.0	0.6214	2.0	0.99	-3.2	577	495	0.44	0.03
n760-03a	zoned core	3103	3	3096	20	3085	50	20.10	2.1	0.6137	2.0	0.99		410	340	0.45	0.05
n760-04a	core	2899	5	2838	20	2753	45	15.37	2.0	0.5328	2.0	0.99	-2.3	262	172	0.09	0.02
n760-04b	zoned outer	2754	3	2857	20	3004	49	15.67	2.0	0.5937	2.0	1.00	6.8	728	522	0.06	0.22
n760-05a	zoned outer	2762	5	2707	20	2634	44	13.38	2.0	0.5047	2.0	0.99	-1.7	612	373	0.05	0.04
n760-05b	core	2996	4	2966	20	2922	49	17.57	2.1	0.5736	2.1	0.99		372	279	0.31	0.05
n760-06a	zoned outer	2753	3	2703	19	2636	44	13.33	2.0	0.5053	2.0	1.00	-1.3	804	489	0.05	0.01
n760-06b	core	3077	3	3023	20	2942	48	18.63	2.0	0.5782	2.0	1.00	-1.6	589	428	0.08	0.05
n760-07a	core	3224	6	3012	20	2706	44	18.43	2.0	0.5216	2.0	0.98	-16.1	660	448	0.19	0.81
n760-07b	zoned outer	2743	7	2750	20	2758	46	14.00	2.1	0.5340	2.0	0.98		653	419	0.04	0.08
n760-08a	zoned outer	2614	4	2550	19	2470	41	11.32	2.0	0.4669	2.0	0.99	-2.7	1624	912	0.09	0.66
n760-8b	core	2702	3	2533	19	2327	39	11.11	2.0	0.4347	2.0	0.99	-13.1	785	411	0.06	0.02
Kovero greenstone belt																	
A1626 Rasisuo#1 gabbro. Ilomantsi																	
n2247-01a	quite homog stubby	2752	6	2759	14	2769	31	14.14	1.4	0.5365	1.4	0.96		129	95	0.66	0.06
n2247-02a	weakly zoned	2759	4	2772	13	2791	31	14.34	1.4	0.5418	1.4	0.98		261	210	1.09	0.04
n2247-03a	weakly zoned	2757	4	2778	13	2807	32	14.42	1.4	0.5455	1.4	0.99		378	312	1.17	0.05
n2247-04a	weakly zoned pale	2747	5	2771	14	2805	33	14.32	1.5	0.5451	1.4	0.98		242	195	1.08	0.03

Appendix 1. cont.

Sample/ spot #	Zircon domain	Derived ages $^{207}Pb/^{206}Pb$	±σ	$^{207}Pb/^{235}U$	±σ	$^{206}Pb/^{238}U$	±σ	Corrected ratios $^{207}Pb/^{235}U$	±σ %	$^{206}Pb/^{238}U$	±σ %	ρ [1]	Disc. % [2]	Elemental data [U] ppm	[Pb] ppm	Th/U meas	f_{206} % [3]
Kovero greenstone belt																	
A1626 Rasisuo#1 gabbro. Ilomantsi																	
n2247-05a	dark zoned inner	2749	6	2764	14	2783	32	14.21	1.5	0.5399	1.4	0.97		133	103	0.92	0.14
n2247-06a	quite homog stubby	2760	6	2778	14	2802	31	14.42	1.4	0.5444	1.4	0.97		144	112	0.88	0.04
n2247-07a	weakly zoned	2759	16	2764	17	2771	33	14.22	1.7	0.5370	1.5	0.83		177	136	0.93	2.01
n2247-08a	quite homog.	2759	4	2776	14	2800	34	14.40	1.5	0.5440	1.5	0.99		429	354	1.23	0.01
n2247-09a	core. altered mantle	2759	3	2788	14	2829	34	14.58	1.5	0.5508	1.5	0.99		393	320	1.09	0.02
n2247-10a	weakly zoned	2757	3	2776	14	2801	33	14.39	1.5	0.5442	1.5	0.99		580	485	1.28	0.02
n2247-11a	weakly zoned	2735	5	2707	13	2671	30	13.39	1.4	0.5134	1.3	0.98		257	190	0.93	0.39
n2247-12a	dark inner zoned	2765	5	2704	13	2622	29	13.33	1.4	0.5020	1.3	0.97	-3.5	203	145	0.82	0.14
n2247-13a	pale core	2764	10	2750	14	2731	31	14.00	1.5	0.5276	1.4	0.91		654	523	1.24	1.46
n2247-13b	dark rim	2768	42	2698	28	2606	31	13.26	3.0	0.4982	1.4	0.48		147	100	0.68	13.98
n2247-14a	quite homog.	2757	4	2757	14	2758	32	14.11	1.4	0.5340	1.4	0.98		224	165	0.73	0.03
n2247-15a	quite homog.	2759	4	2772	13	2791	31	14.34	1.4	0.5418	1.4	0.99		539	438	1.18	0.02
n2247-16a	weakly zoned pale	2749	35	2777	25	2816	32	14.41	2.6	0.5477	1.4	0.54		545	469	1.44	2.52
n2247-16b	dark weakly zoned	2762	5	2733	14	2693	31	13.75	1.4	0.5187	1.4	0.98	-0.1	217	159	0.80	0.10
A1627 Rasisuo#2 felsic tuff. Ilomantsi																	
n2555-01a	weakly zoned	2877	4	2857	8	2830	18	15.68	0.8	0.5510	0.8	0.96	-0.3	222	166	0.55	0.02
~~*n2555-02a*~~	~~*weakly zoned*~~	~~*2832*~~	~~*10*~~	~~*2791*~~	~~*10*~~	~~*2734*~~	~~*19*~~	~~*14.62*~~	~~*1.1*~~	~~*0.5282*~~	~~*0.9*~~	~~*0.80*~~	~~*-1.3*~~	~~*503*~~	~~*354*~~	~~*0.51*~~	~~*2.62*~~
n2555-03a	weakly zoned	2877	5	2876	8	2875	18	15.99	0.8	0.5620	0.8	0.94		174	145	1.05	0.31
n2555-04a	weakly zoned	2874	4	2919	8	2984	19	16.72	0.8	0.5887	0.8	0.94	2.8	390	312	0.61	0.42
n2555-05a	weakly zoned	2879	3	2900	8	2932	19	16.40	0.8	0.5759	0.8	0.97	0.5	382	283	0.31	0.29
n2555-06a	weakly zoned	2878	6	2913	9	2964	19	16.62	0.9	0.5836	0.8	0.90	1.4	186	148	0.59	0.74
n2555-07a	weakly zoned	2855	6	2874	9	2901	19	15.96	0.9	0.5684	0.8	0.90		345	263	0.53	0.13
n2555-08a	weakly zoned	2866	8	2861	9	2854	18	15.73	0.9	0.5569	0.8	0.84		96	75	0.80	0.02
n2555-09a	zoned	2863	5	2878	9	2899	20	16.02	0.9	0.5679	0.9	0.95		243	188	0.64	0.05
n2555-10a	dark inner	2880	4	2872	8	2861	19	15.92	0.9	0.5586	0.8	0.96		242	183	0.57	0.02
n2555-10b	pale rim	2870	3	2881	8	2897	18	16.08	0.8	0.5674	0.8	0.97		460	364	0.75	0.01
n2555-11a	quite homog	2882	6	2886	9	2892	20	16.15	0.9	0.5661	0.9	0.92		121	91	0.44	{0.01}
n2555-12a	quite homog	2870	4	2879	8	2892	19	16.04	0.9	0.5662	0.8	0.95		140	106	0.49	{0.02}
n2555-13a	quite homog	2865	4	2865	8	2865	18	15.81	0.8	0.5597	0.8	0.96		159	118	0.45	0.03
n2555-14a	weakly zoned	2878	3	2892	8	2911	19	16.25	0.8	0.5709	0.8	0.98		246	186	0.42	{0.01}
n2555-15a	dark homog	2882	4	2887	8	2894	19	16.17	0.8	0.5667	0.8	0.95		122	92	0.45	{0.01}
n2555-16a	zoned	2891	7	2876	10	2855	22	15.99	1.1	0.5571	1.0	0.92		389	295	0.59	0.40
~~*n2555-17a*~~	~~*dark homog rim*~~	~~*2866*~~	~~*23*~~	~~*2871*~~	~~*16*~~	~~*2878*~~	~~*20*~~	~~*15.90*~~	~~*1.7*~~	~~*0.5628*~~	~~*0.9*~~	~~*0.52*~~		~~*110*~~	~~*83*~~	~~*0.52*~~	~~*3.93*~~
Pudasjärvi greenstone belt																	
A1782 Käärmevaara gabbro. Ranua																	
n2558-01a#2	pale quite homog (partly corroded)	2791	3	2810	10	2838	25	14.93	1.1	0.5530	1.1	0.98		979	856	1.33	0.01
n2558-02a#2	pale homog (partly corroded)	2798	2	2834	11	2884	28	15.30	1.2	0.5642	1.2	0.99	1.3	525	692	4.16	0.05
n2558-03a#2	darker homog	1845	6	1869	8	1891	15	5.30	0.9	0.3410	0.9	0.94	0.6	275	118	0.51	0.03
n2558-04a#2	pale homog	2803	3	2870	11	2966	26	15.88	1.1	0.5842	1.1	0.99	4.8	492	451	1.38	0.03
n2558-05a#2	darker quite homog	2798	16	2778	18	2750	36	14.42	1.9	0.5321	1.6	0.86		115	117	2.74	0.31
n2558-06a	darker quite homog	2811	7	2830	9	2858	19	15.24	0.9	0.5579	0.8	0.88		123	98	0.80	0.02

Appendix 1. cont.

Sample/ spot #	Zircon domain	Derived ages $^{207}Pb/^{206}Pb$	±σ	$^{207}Pb/^{235}U$	±σ	$^{206}Pb/^{238}U$	±σ	Corrected ratios $^{207}Pb/^{235}U$	±σ %	$^{206}Pb/^{238}U$	±σ %	ρ [1]	Disc. % [2]	Elemental data [U] ppm	[Pb] ppm	Th/U meas	f_{206} % [3]
Pudasjärvi greenstone belt																	
A1782 Käärmevaara gabbro. Ranua																	
n2558-07a	pale homog	2806	2	2842	10	2893	24	15.43	1.0	0.5664	1.0	0.99	1.6	430	455	2.55	0.02
n2558-08a	pale homog	2806	2	2842	9	2894	21	15.43	0.9	0.5666	0.9	0.99	2.0	629	576	1.55	0.02
n2558-09a	dark inner . tiny grain	2704	6	2683	9	2654	20	13.04	1.0	0.5094	0.9	0.93		76	59	1.15	0.04
n2558-10a	hazy small grain	855	9	850	6	848	8	1.309	1.1	0.1405	0.9	0.90		569	90	0.19	0.06
A1783 Puljunlehto dacite. Ranua																	
n2559-01a	homog metam grain	2811	14	2803	11	2792	18	14.81	1.2	0.5420	0.8	0.67		19	13	0.27	0.18
n2559-02a	smoothly zoned (metam?)	2840	12	2837	10	2832	18	15.34	1.1	0.5515	0.8	0.72		22	16	0.60	0.14
n2559-03a	weakly zoned euhedral	2783	11	2808	10	2842	20	14.88	1.1	0.5540	0.9	0.79		24	17	0.25	0.11
n2559-04a	weakly zoned euhedral	2820	6	2818	9	2815	19	15.04	0.9	0.5475	0.8	0.90		98	75	0.71	0.03
n2559-05a	weakly zoned euhedral	2826	11	2841	10	2862	18	15.41	1.0	0.5589	0.8	0.76		31	23	0.50	0.15
n2559-06a	weakly zoned euhedral	2825	8	2797	11	2758	23	14.71	1.1	0.5338	1.0	0.90	-0.2	64	44	0.34	0.07
n2559-07a	homog metam grain	2788	20	2765	14	2735	18	14.23	1.4	0.5284	0.8	0.55		11	8	0.21	0.27
n2559-08a	dark quite homog	2816	9	2786	9	2745	18	14.54	1.0	0.5308	0.8	0.83	-0.4	38	28	0.73	0.13
n2559-09a	weakly zoned/wague euhedral	2832	4	2827	12	2820	28	15.18	1.2	0.5487	1.2	0.98		128	95	0.54	0.04
n2559-10a	dark quite homog	2798	8	2804	9	2811	19	14.82	1.0	0.5467	0.8	0.86		37	27	0.41	0.09
Paragneisses																	
A1814 Pitkäpalo Ranua mica gneiss (= n2129)																	
n2129-03		2847	5	2832	10	2811	24	15.27	1.1	0.5467	1.0	0.96		130	94	0.42	{0.01}
n2129-05		2742	3	2732	10	2718	23	13.74	1.0	0.5245	1.0	0.98		286	202	0.61	{0.01}
n2129-06		2703	6	2229	28	1750	46	7.980	3.0	0.3119	3.0	0.99	-36.3	399	170	1.83	0.73
n2129-07		2745	28	2741	19	2735	23	13.87	2.0	0.5284	1.0	0.52		7	5	0.80	{0.00}
n2129-08		2735	5	2699	10	2652	23	13.27	1.1	0.5089	1.0	0.96	-1.3	207	149	0.96	0.21
n2129-10		2746	2	2744	10	2741	23	13.92	1.0	0.5299	1.0	0.99		662	497	0.82	{0.01}
n2129-11		2730	4	2705	10	2671	22	13.35	1.0	0.5133	1.0	0.97	-0.5	271	200	0.90	0.09
n2129-13		2728	4	2651	10	2550	22	12.61	1.1	0.4853	1.0	0.97	-5.7	366	261	1.16	0.21
n2129-14		2835	5	2837	10	2839	23	15.34	1.0	0.5533	1.0	0.96		173	132	0.64	{0.02}
n2129-15		2846	9	2785	11	2702	23	14.53	1.2	0.5207	1.1	0.89	-3.3	539	382	0.60	{0.02}
n2129-16		2693	10	2377	25	2026	46	9.391	2.7	0.3693	2.6	0.97	-24.4	339	165	1.02	1.22
n2129-17		3166	7	3149	11	3122	25	21.23	1.1	0.6232	1.0	0.92		228	195	0.72	{0.02}
n2129-18		2733	4	2747	10	2766	23	13.96	1.0	0.5358	1.0	0.97		220	157	0.51	{0.01}
n2129-19		2731	5	2686	10	2628	22	13.09	1.1	0.5032	1.0	0.95	-2.3	281	191	0.85	{0.02}
n2129-20		2732	5	2694	11	2643	24	13.20	1.1	0.5068	1.1	0.96	-1.5	157	107	0.70	{0.09}
n2129-21		2784	7	2781	10	2778	23	14.48	1.1	0.5388	1.0	0.92		456	324	0.49	{0.02}
n2129-22		2701	8	2591	10	2452	21	11.82	1.1	0.4629	1.0	0.91	-8.5	218	139	0.74	0.24
n2129-23		2940	6	2845	10	2712	22	15.47	1.1	0.5230	1.0	0.93	-7.1	239	168	0.82	0.05
n2129-24		2719	7	2473	16	2186	32	10.43	1.8	0.4037	1.7	0.97	-19.9	268	145	1.33	0.11
n2129-25		2733	6	2755	10	2784	23	14.07	1.1	0.5402	1.0	0.94		155	112	0.60	0.07
n2129-26		2735	7	2706	11	2668	24	13.37	1.2	0.5127	1.1	0.93	-0.3	171	114	0.45	0.12
n2129-27		2703	5	2615	10	2503	21	12.14	1.1	0.4745	1.0	0.96	-6.7	695	398	0.23	0.28
n2129-29		2725	7	2625	10	2498	21	12.27	1.1	0.4733	1.0	0.93	-7.6	232	141	0.49	0.02
n2129-30		2722	6	2630	10	2512	21	12.33	1.1	0.4764	1.0	0.93	-6.9	287	190	1.18	0.06
n2129-31		2715	7	2603	10	2461	21	11.98	1.1	0.4649	1.0	0.93	-8.8	652	388	0.50	0.01
n2129-33		2694	8	2408	11	2084	19	9.712	1.2	0.3817	1.1	0.90	-23.9	320	162	0.85	0.40

Appendix 1. cont.

		Derived ages						*Corrected ratios*						*Elemental data*			
Sample/		^{207}Pb	±σ	^{207}Pb	±σ	^{206}Pb	±σ	^{207}Pb	±σ	^{206}Pb	±σ	ρ [1]	**Disc.**	**[U]**	**[Pb]**	**Th/U**	f_{206}
spot #	**Zircon domain**	^{206}Pb		^{235}U		^{238}U		^{235}U	%	^{238}U	%		% [2]	**ppm**	**ppm**	**meas**	% [3]
A1842 Jäkälämaa Pudasjärvi mica gneiss (= n2497). all analyses on mostly oscillatory zoned inner domains																	
n2497-01		2714	6	2688	16	2653	35	13.12	1.7	0.5092	1.6	0.98		230	155	0.49	0.23
n2497-02		2798	5	2723	16	2622	34	13.60	1.6	0.5020	1.6	0.98	-4.4	325	206	0.24	0.60
n2497-03		2691	4	2560	15	2398	31	11.44	1.6	0.4505	1.5	0.99	-10.2	362	223	0.65	0.23
n2497-04		2723	3	2726	15	2730	35	13.65	1.6	0.5273	1.6	0.99		1205	986	1.31	0.07
n2497-05		2748	6	2723	16	2689	35	13.60	1.6	0.5175	1.6	0.97		175	127	0.77	0.05
n2497-06		2744	8	2750	17	2757	38	14.00	1.8	0.5337	1.7	0.96		207	146	0.47	0.61
n2497-07		2741	4	2703	15	2653	34	13.33	1.6	0.5092	1.5	0.99	-0.8	365	261	0.75	0.11
n2497-08		2732	6	2745	15	2763	35	13.93	1.6	0.5352	1.5	0.98		218	160	0.63	0.05
n2497-09		2720	4	2708	16	2693	38	13.40	1.7	0.5185	1.7	0.99		681	565	1.43	0.07
n2497-10		2706	6	2701	16	2694	36	13.29	1.6	0.5188	1.6	0.98		334	235	0.60	0.08
n2497-11		2743	6	2724	16	2699	36	13.63	1.6	0.5199	1.6	0.98		219	158	0.71	0.04
n2497-12		2728	6	2571	16	2376	33	11.57	1.7	0.4457	1.7	0.98	-12.3	230	135	0.49	0.41
n2497-13		2705	6	2595	15	2457	32	11.89	1.6	0.4640	1.5	0.97	-7.9	1107	612	0.02	0.10
n2497-14		2748	6	2703	17	2644	38	13.33	1.8	0.5072	1.7	0.98	-1.0	304	232	1.09	0.24
n2497-15		2701	6	2594	16	2459	34	11.86	1.7	0.4643	1.7	0.98	-7.5	644	422	0.79	0.49
n2497-16		2712	13	1877	15	1218	17	5.351	1.7	0.2081	1.5	0.88	-56.7	4059	1216	1.11	0.25
n2497-17		2764	7	2749	17	2728	38	13.98	1.7	0.5267	1.7	0.97		933	685	0.72	0.02
n2497-18		2742	8	2751	15	2765	35	14.03	1.6	0.5355	1.5	0.96		249	206	1.29	0.04
n2497-19		2805	8	2729	16	2627	34	13.69	1.6	0.5032	1.6	0.95	-4.2	357	223	0.16	0.25
n2497-20		2736	4	2755	16	2780	38	14.08	1.7	0.5392	1.7	0.99		412	308	0.71	0.01
n2497-21		2741	6	2731	15	2718	35	13.73	1.6	0.5243	1.6	0.98		271	211	1.06	0.07
n2497-22		2857	3	2831	20	2794	48	15.24	2.1	0.5426	2.1	1.00		684	482	0.35	0.03
n2497-23		2877	29	2886	24	2899	41	16.15	2.5	0.5678	1.7	0.69		253	191	0.48	1.21
n2497-24		2788	4	2652	15	2477	32	12.62	1.6	0.4686	1.6	0.99	-10.5	958	598	0.57	0.05
n2497-25		2967	4	2894	20	2791	47	16.29	2.1	0.5418	2.1	0.99	-3.3	431	332	0.76	0.32
n2497-26		2812	3	2723	15	2605	33	13.61	1.5	0.4979	1.5	0.99	-6.0	1651	1152	0.73	0.08
n2497-27		2765	8	2585	15	2361	30	11.75	1.6	0.4423	1.5	0.96	-14.3	611	344	0.31	1.65
n2497-28		2759	7	2773	16	2791	38	14.34	1.7	0.5418	1.7	0.97		126	92	0.55	0.19
n2497-29		2701	5	2695	15	2688	35	13.22	1.6	0.5174	1.6	0.98		238	158	0.36	{0.01}
n2497-30		2734	10	2574	16	2376	31	11.62	1.7	0.4457	1.5	0.93	-12.1	433	239	0.18	0.50
n2497-31		2892	3	2886	15	2877	36	16.15	1.6	0.5626	1.6	0.99		877	659	0.47	0.07
n2497-32		2888	3	2906	16	2932	38	16.49	1.6	0.5758	1.6	0.99		304	226	0.31	0.01
A1840 Riihivaara Suomussalmi mica gneiss (= n2496). all analyses on mostly oscillatory zoned inner domains																	
n2496-01		2684	7	2621	16	2540	36	12.21	1.7	0.4829	1.7	0.97	-2.9	219	149	0.80	0.55
n2496-02		2797	9	2805	16	2817	37	14.84	1.7	0.5479	1.6	0.95		84	60	0.45	{0.02}
n2496-03		2785	13	2795	23	2808	51	14.68	2.4	0.5459	2.2	0.94		408	301	0.60	0.06
n2496-04		2749	8	2769	16	2797	35	14.29	1.6	0.5433	1.5	0.95		137	116	1.40	{0.01}
n2496-05		2726	3	2752	15	2787	36	14.03	1.6	0.5408	1.6	0.99		546	379	0.36	0.03
n2496-06		2724	5	2724	15	2725	34	13.63	1.6	0.5261	1.5	0.98		560	389	0.52	0.02
n2496-07		2724	7	2608	16	2463	33	12.05	1.7	0.4653	1.6	0.96	-8.2	944	629	0.90	0.76
n2496-08		2970	5	2963	15	2954	37	17.51	1.6	0.5813	1.5	0.98		225	181	0.65	0.35
n2496-09		2950	6	2948	16	2946	37	17.24	1.6	0.5792	1.6	0.97		141	119	0.97	0.05
n2496-10		2742	6	2734	15	2725	34	13.78	1.6	0.5260	1.5	0.97		122	91	0.90	0.16

Appendix 1. cont.

Sample/ spot #	Zircon domain	Derived ages $^{207}Pb/^{206}Pb$	±σ	$^{207}Pb/^{235}U$	±σ	$^{206}Pb/^{238}U$	±σ	Corrected ratios $^{207}Pb/^{235}U$	±σ %	$^{206}Pb/^{238}U$	±σ %	ρ [1]	Disc. % [2]	Elemental data [U] ppm	[Pb] ppm	Th/U meas	f_{206} % [3]
A1840 Riihivaara Suomussalmi mica gneiss (= n2496). all analyses on mostly oscillatory zoned inner domains																	
n2496-11		2730	4	2702	16	2665	36	13.31	1.6	0.5119	1.6	0.99		702	477	0.50	0.06
n2496-12		2702	7	2448	15	2153	28	10.14	1.6	0.3966	1.5	0.97	-21.0	1214	595	0.14	0.04
n2496-13		2717	2	2711	16	2702	37	13.43	1.7	0.5207	1.7	1.00		869	625	0.71	0.02
~~*n2496-14*~~		~~*2637*~~	~~*74*~~	~~*2674*~~	~~*47*~~	~~*2724*~~	~~*37*~~	~~*12.93*~~	~~*4.8*~~	~~*0.5259*~~	~~*1.7*~~	~~*0.34*~~		~~*765*~~	~~*549*~~	~~*0.60*~~	~~*10.94*~~
~~*n2496-15*~~		~~*2684*~~	~~*20*~~	~~*2439*~~	~~*18*~~	~~*2157*~~	~~*28*~~	~~*10.05*~~	~~*2.0*~~	~~*0.3974*~~	~~*1.5*~~	~~*0.78*~~	~~*-17.7*~~	~~*1069*~~	~~*543*~~	~~*0.45*~~	~~*8.48*~~
n2496-16		2807	4	2769	17	2717	38	14.29	1.7	0.5242	1.7	0.99	-0.5	599	413	0.44	0.01
~~*n2496-17*~~		~~*2655*~~	~~*15*~~	~~*2271*~~	~~*20*~~	~~*1870*~~	~~*33*~~	~~*8.365*~~	~~*2.2*~~	~~*0.3366*~~	~~*2.0*~~	~~*0.91*~~	~~*-29.5*~~	~~*170*~~	~~*77*~~	~~*0.77*~~	~~*2.44*~~
n2496-17_8		2753	4	2646	20	2509	45	12.55	2.2	0.4758	2.1	0.99	-6.8	1041	689	0.72	0.08
n2496-18		2737	4	2756	15	2781	36	14.09	1.6	0.5395	1.6	0.99		283	216	0.83	0.02
n2496-19		2840	4	2851	18	2866	43	15.57	1.8	0.5599	1.8	0.99		245	197	0.89	0.04
n2496-20		2771	6	2752	15	2727	34	14.04	1.6	0.5266	1.5	0.97		167	123	0.71	1.67
n2496-21		2724	8	2702	16	2672	35	13.31	1.7	0.5136	1.6	0.95		135	87	0.26	0.47
n2496-22		2759	21	2758	19	2757	35	14.12	2.0	0.5337	1.5	0.77		105	77	0.68	0.51
n2496-23		2805	10	2794	16	2779	36	14.67	1.7	0.5389	1.6	0.93		71	51	0.45	0.06
n2496-24		2733	4	2735	16	2737	37	13.78	1.7	0.5289	1.7	0.99		634	433	0.37	0.30
n2496-25		2835	8	2801	16	2755	36	14.78	1.7	0.5331	1.6	0.96		154	102	0.22	0.10
n2496-26		2729	5	2633	16	2509	34	12.37	1.6	0.4758	1.6	0.99	-6.6	202	130	0.57	0.60
n2496-27		2795	8	2817	16	2848	36	15.03	1.6	0.5555	1.6	0.96		52	40	0.67	0.05
n2496-28		2753	18	2687	21	2600	41	13.10	2.2	0.4968	1.9	0.86	-1.1	84	54	0.32	1.03
n2496-29		2960	4	2884	15	2777	35	16.13	1.6	0.5385	1.5	0.99	-4.6	257	192	0.61	0.14
n2496-30		2780	6	2776	17	2770	38	14.39	1.7	0.5369	1.7	0.98		90	63	0.44	0.05
n2496-31		2763	7	2742	16	2714	36	13.89	1.7	0.5236	1.6	0.97		199	140	0.58	0.33
n2496-32		2726	4	2708	16	2683	37	13.40	1.7	0.5163	1.7	0.99		356	239	0.39	0.05
A1243 Susi-Kervinen Rautavaara mica gneiss (= n2495). all analyses on inner zircon domains																	
n2495-01		2619	6	2320	18	1997	33	8.829	2.0	0.3631	1.9	0.98	-24.4	2862	1241	0.07	0.16
n2495-02		2612	27	2458	22	2277	32	10.26	2.3	0.4236	1.6	0.71	-8.2	1944	980	0.04	1.73
n2495-03		2724	4	2673	15	2605	33	12.90	1.6	0.4980	1.5	0.99	-2.2	506	340	0.57	0.37
n2495-04		2692	6	2621	15	2530	32	12.22	1.6	0.4807	1.5	0.98	-4.1	688	423	0.32	1.32
n2495-05		2613	19	2473	20	2306	34	10.42	2.1	0.4301	1.7	0.83	-8.5	1727	886	0.08	1.57
n2495-06		2661	5	2623	15	2575	33	12.24	1.6	0.4909	1.6	0.98	-0.8	1156	691	0.16	0.01
n2495-07		2630	4	2390	15	2119	28	9.525	1.6	0.3892	1.5	0.99	-20.1	908	431	0.15	0.22
n2495-08		2748	3	2727	15	2698	35	13.66	1.6	0.5197	1.6	0.99		770	535	0.57	0.02
n2495-09		2622	3	2583	15	2533	32	11.72	1.5	0.4812	1.5	0.99	-1.1	928	536	0.10	0.01
n2495-10		2685	3	2642	15	2587	33	12.50	1.5	0.4939	1.5	0.99	-1.4	1497	934	0.33	0.01
n2495-11		2731	5	2501	15	2229	29	10.75	1.6	0.4130	1.5	0.98	-19.0	342	187	0.47	0.14
n2495-12		2741	4	2742	15	2743	34	13.89	1.6	0.5304	1.5	0.98		667	477	0.63	0.02
n2495-13		2595	3	2558	15	2513	32	11.42	1.5	0.4767	1.5	0.99	-0.8	1006	572	0.08	0.05
~~*n2495-14*~~		~~*2778*~~	~~*89*~~	~~*2603*~~	~~*56*~~	~~*2383*~~	~~*32*~~	~~*11.98*~~	~~*5.8*~~	~~*0.4472*~~	~~*1.6*~~	~~*0.27*~~		~~*351*~~	~~*213*~~	~~*0.59*~~	~~*11.68*~~
n2495-15		2675	4	2499	15	2289	30	10.72	1.6	0.4263	1.5	0.99	-14.4	720	387	0.36	0.02
n2495-16		2579	3	2516	15	2439	32	10.92	1.6	0.4599	1.6	0.99	-3.5	1420	773	0.05	0.40
n2495-17		2639	4	2543	15	2425	31	11.24	1.6	0.4567	1.5	0.99	-6.8	1337	742	0.16	0.02
n2495-18		2632	2	2613	15	2590	33	12.11	1.5	0.4944	1.5	1.00		1469	858	0.01	0.01
n2495-19		2624	3	2559	15	2478	32	11.44	1.6	0.4688	1.5	0.99	-3.7	1723	988	0.19	0.14

Appendix 1. cont.

		Derived ages				Corrected ratios							Elemental data				
Sample/		^{207}Pb	±σ	^{207}Pb	±σ	^{206}Pb	±σ	^{207}Pb	±σ	^{206}Pb	±σ	ρ [1]	Disc.	[U]	[Pb]	Th/U	f_{206}
spot #	Zircon domain	^{206}Pb		^{235}U		^{238}U		^{235}U	%	^{238}U	%		% [2]	ppm	ppm	meas	% [3]
A1243 Susi-Kervinen Rautavaara mica gneiss (= n2495). all analyses on inner zircon domains																	
n2495-20		2627	11	2497	18	2341	36	10.70	1.9	0.4378	1.8	0.94	-8.9	1398	733	0.07	0.68
n2495-21		2628	2	2610	15	2588	33	12.07	1.6	0.4940	1.6	1.00		2600	1528	0.05	0.01
n2495-22		2623	2	2591	15	2550	33	11.82	1.5	0.4852	1.5	1.00	-0.4	2597	1494	0.03	0.04
n2495-23		2583	4	2498	15	2396	31	10.71	1.6	0.4501	1.5	0.99	-5.7	1137	607	0.05	0.32
n2495-24		2604	4	2531	17	2440	36	11.09	1.8	0.4601	1.7	0.99	-4.2	2229	1220	0.05	0.21
n2495-25		2634	3	2623	16	2608	36	12.24	1.7	0.4987	1.7	1.00		1329	794	0.08	0.02
n2495-26		2736	4	2723	15	2705	35	13.60	1.6	0.5214	1.6	0.99		415	290	0.63	0.05
n2495-27		2577	4	2413	14	2223	29	9.763	1.6	0.4118	1.5	0.99	-13.4	1992	971	0.03	0.58
n2495-28		2695	4	2627	15	2540	34	12.30	1.6	0.4830	1.6	0.99	-3.8	505	308	0.29	0.77
n2495-29		2603	3	2505	15	2385	32	10.79	1.6	0.4478	1.6	0.99	-7.0	902	482	0.09	0.75
n2495-30		2738	5	2724	15	2706	34	13.63	1.6	0.5216	1.5	0.98		752	516	0.49	0.83
In house zircon standards																	
A382 (n3563) Voinsalmi granite																	
n3563-01		1888	6	1869	7	1852	11	5.301	0.8	0.3327	0.7	0.90	-0.15	198	78	0.21	0.04
n3563-01b		1873	5	1866	8	1860	15	5.282	1.0	0.3344	0.9	0.95		280	112	0.28	0.04
n3563-02	core	1887	2	1942	7	1994	13	5.771	0.8	0.3625	0.8	0.99	4.89	5396	2263	0.13	0.01
n3563-02b	rim	1887	4	1849	7	1815	12	5.177	0.8	0.3252	0.8	0.96	-2.61	524	200	0.20	0.03
n3563-04	core	1875	10	1920	34	1962	65	5.626	3.9	0.3557	3.8	0.99		10162	4498	0.36	0.01
n3563-04b	rim	1874	6	1872	7	1871	11	5.322	0.8	0.3367	0.7	0.91		263	105	0.23	{0.02}
n3563-06	core	1881	1	1948	6	2012	12	5.811	0.7	0.3663	0.7	1.00	6.56	6678	2933	0.29	0.00
n3563-06b	rim	1877	7	1817	7	1766	11	4.988	0.8	0.3151	0.7	0.90	-4.62	205	75	0.19	0.05
n3563-08		1889	7	1876	7	1863	11	5.342	0.8	0.3351	0.7	0.88		148	60	0.33	{0.02}
n3563-09		1870	7	1864	7	1858	12	5.269	0.8	0.3341	0.7	0.87		128	52	0.40	{0.01}
n3563-10		1894	10	1850	8	1811	11	5.183	0.9	0.3244	0.7	0.79	-2.13	71	28	0.41	{0.03}
n3563-11		1879	7	1874	7	1870	12	5.334	0.8	0.3365	0.7	0.88		238	98	0.34	{0.01}
n3563-12		1879	6	1871	7	1863	12	5.310	0.8	0.3351	0.7	0.89		197	79	0.27	0.03
n3563-13		1871	6	1883	7	1894	13	5.388	0.9	0.3415	0.8	0.91		206	87	0.43	0.03
n3563-14		1878	8	1868	7	1859	11	5.296	0.8	0.3343	0.7	0.85		119	50	0.45	{0.05}
n3563-15		1889	8	1865	7	1843	11	5.274	0.8	0.3310	0.7	0.86	-0.41	128	52	0.36	{0.03}
n3563-16		1876	6	1875	7	1875	11	5.341	0.8	0.3376	0.7	0.91		318	122	0.09	0.02
n3563-17		1871	8	1882	7	1891	12	5.380	0.9	0.3409	0.7	0.84		111	48	0.49	{0.04}
n3563-17b		1870	9	1977	10	2080	18	6.007	1.1	0.3809	1.0	0.90	9.96	148	70	0.48	0.12
n3563-18		1871	4	1867	7	1863	12	5.288	0.8	0.3351	0.7	0.95		387	157	0.33	{0.01}
n3563-18b		1884	6	1871	7	1859	11	5.313	0.8	0.3343	0.7	0.91		247	97	0.21	0.04
n3563-20		1884	8	1876	7	1870	11	5.345	0.8	0.3364	0.7	0.85		121	51	0.46	{0.02}
n3563-21		1889	7	1874	9	1860	15	5.333	1.0	0.3345	0.9	0.92		154	62	0.31	{0.03}
n3563-22		1877	5	1890	8	1901	15	5.431	1.0	0.3430	0.9	0.96		351	141	0.20	0.02
n3563-23		1871	7	1878	9	1884	15	5.355	1.0	0.3393	0.9	0.91		140	60	0.48	{0.01}
n3563-24		1871	9	1882	9	1893	15	5.382	1.1	0.3412	0.9	0.88		99	42	0.48	0.06
n3563-25		1873	5	1873	8	1873	15	5.327	1.0	0.3372	0.9	0.96		309	126	0.30	0.03
n3563-26		1877	8	1885	9	1893	15	5.401	1.0	0.3412	0.9	0.89		107	44	0.33	{0.02}
n3563-27		1872	7	1877	9	1882	16	5.350	1.0	0.3390	1.0	0.92		221	91	0.33	0.03
n3563-29		1884	5	1879	8	1875	15	5.365	1.0	0.3376	0.9	0.96		327	134	0.34	0.02

Appendix 1. cont.

		Derived ages						*Corrected ratios*						*Elemental data*			
Sample/		^{207}Pb	±σ	^{207}Pb	±σ	^{206}Pb	±σ	^{207}Pb	±σ	^{206}Pb	±σ	ρ [1]	**Disc.**	**[U]**	**[Pb]**	**Th/U**	f_{206}
spot #	**Zircon domain**	^{206}Pb		^{235}U		^{238}U		^{235}U	%	^{238}U	%		**% [2]**	**ppm**	**ppm**	**meas**	**% [3]**
In house zircon standards																	
A382 (n3563) Voinsalmi granite																	
n3563-30		1859	9	1891	9	1920	15	5.438	1.0	0.3470	0.9	0.89	0.86	248	108	0.49	0.03
n3563-31		1869	5	1889	8	1907	15	5.425	1.0	0.3442	0.9	0.95		282	119	0.40	0.02
n3563-32		1880	6	1870	9	1861	15	5.308	1.0	0.3347	0.9	0.94		211	87	0.40	{0.02}
n3563-33		1878	7	1888	9	1896	15	5.417	1.0	0.3420	0.9	0.92		191	79	0.33	0.04
n3563-34		1883	7	1883	9	1884	15	5.391	1.0	0.3394	0.9	0.92		178	74	0.37	0.04
n3563-35		1877	6	1873	9	1869	15	5.324	1.0	0.3363	1.0	0.95		302	123	0.32	0.02
n3563-36		1880	8	1876	9	1873	15	5.344	1.0	0.3371	0.9	0.91		143	58	0.33	{0.03}
n3563-37		1869	7	1863	9	1858	15	5.266	1.0	0.3340	0.9	0.93		201	84	0.49	{0.02}
n3563-38		1872	6	1885	9	1896	16	5.400	1.0	0.3420	1.0	0.95		244	101	0.34	{0.01}
n3563-39		1877	7	1869	9	1863	16	5.303	1.0	0.3351	1.0	0.94		219	90	0.37	0.03
n3563-40		1871	7	1892	9	1911	16	5.442	1.0	0.3450	0.9	0.92		170	71	0.32	0.05
n3563-41		1886	6	1877	9	1869	15	5.352	1.0	0.3363	0.9	0.93		195	79	0.32	{0.03}
n3563-42		1880	5	1874	8	1868	15	5.330	1.0	0.3361	0.9	0.96		376	156	0.41	0.02
n3563-43		1887	7	1881	9	1876	15	5.377	1.0	0.3377	0.9	0.93		200	81	0.29	{0.02}
n3563-44		1884	7	1887	9	1890	15	5.416	1.0	0.3408	0.9	0.92		172	71	0.30	{0.02}
n3563-45		1881	6	1889	8	1896	15	5.425	1.0	0.3419	0.9	0.94		247	105	0.45	0.03
n3563-46	rim	1875	11	1883	9	1891	15	5.389	1.1	0.3409	0.9	0.84		76	31	0.33	{0.03}
n3563-46b	core	1869	9	1860	9	1852	15	5.245	1.1	0.3328	0.9	0.88		113	45	0.26	0.07
n3563-48		1879	5	1882	8	1884	15	5.381	1.0	0.3395	0.9	0.95		293	116	0.17	0.03
n3563-49		1886	10	1878	9	1871	15	5.357	1.1	0.3367	0.9	0.87		102	42	0.34	0.07
n3563-50		*1857*	*8*	*1845*	*9*	*1835*	*15*	*5.156*	1.0	0.3294	0.9	*0.91*		*177*	*71*	*0.34*	*0.04*
n3563-51		1877	7	1882	9	1886	15	5.379	1.0	0.3398	0.9	0.92		162	67	0.33	{0.03}
n3563-52		1870	5	1871	8	1873	15	5.315	1.0	0.3371	0.9	0.95		298	124	0.41	0.02
n3563-53		*1867*	*8*	*1831*	*10*	*1799*	*18*	*5.070*	1.2	0.3219	1.1	*0.93*	*-1.25*	*158*	*62*	*0.35*	*{0.03}*
n3563-54		1883	5	1864	8	1847	15	5.270	1.0	0.3319	0.9	0.96		327	134	0.41	0.02
n3563-55		1878	6	1872	9	1865	16	5.317	1.0	0.3356	1.0	0.95		275	109	0.24	0.03
A1772 (n3565) Änäkäinen gabbro																	
n3565-01		2713	6	2714	8	2716	16	13.49	0.8	0.5240	0.7	0.89		221	138	0.01	{0.01}
n3565-01b		2712	2	2736	9	2767	21	13.79	0.9	0.5362	0.9	0.99	0.53	624	489	0.98	{0.01}
n3565-02		2715	2	2701	7	2684	16	13.30	0.7	0.5164	0.7	0.98		591	437	0.92	0.01
n3565-02b		2713	2	2691	10	2661	22	13.15	1.0	0.5110	1.0	0.99	-0.30	833	640	1.15	{0.00}
n3565-03		2713	3	2692	7	2664	16	13.17	0.7	0.5116	0.7	0.97	-0.67	572	428	1.03	{0.00}
n3565-03b		2713	4	2694	8	2669	17	13.20	0.8	0.5129	0.8	0.95	-0.18	499	368	0.97	{0.00}
n3565-03c		2711	2	2691	9	2665	20	13.16	0.9	0.5119	0.9	0.99	-0.17	542	402	0.95	0.01
n3565-05		2711	1	2709	7	2707	16	13.42	0.7	0.5218	0.7	1.00		2300	1435	0.03	0
n3565-05b		2715	2	2679	9	2632	20	13.00	0.9	0.5043	0.9	0.99	-1.85	664	478	0.85	0.01
n3565-06		2711	3	2693	7	2669	15	13.18	0.7	0.5129	0.7	0.97	-0.34	413	279	0.48	{0.00}
n3565-07		2714	3	2697	7	2673	15	13.23	0.7	0.5138	0.7	0.96	-0.29	480	331	0.57	{0.01}
n3565-08		2713	2	2697	7	2675	16	13.24	0.7	0.5144	0.7	0.99	-0.18	795	622	1.24	{0.00}
n3565-09		2711	3	2691	7	2664	15	13.16	0.7	0.5116	0.7	0.98	-0.64	500	346	0.61	0.01
n3565-10		2712	2	2708	7	2703	16	13.40	0.7	0.5210	0.7	0.99		939	641	0.46	{0.00}
n3565-10b		2714	2	2720	9	2727	21	13.56	0.9	0.5266	0.9	0.99		636	462	0.68	{0.01}

Appendix 1. cont.

		Derived ages						*Corrected ratios*						*Elemental data*				
Sample/		^{207}Pb	±σ	^{207}Pb	±σ	^{206}Pb	±σ	^{207}Pb	±σ	^{206}Pb	±σ	ρ [1]	**Disc.**	**[U]**	**[Pb]**	**Th/U**	f_{206}
spot #	**Zircon domain**	^{206}Pb		^{235}U		^{238}U		^{235}U	%	^{238}U	%		**% [2]**	**ppm**	**ppm**	**meas**	**% [3]**
A1772 (n3565) Änäkäinen gabbro																	
n3565-11		2711	3	2705	7	2697	16	13.35	0.7	0.5195	0.7	0.97		444	327	0.83	{0.01}
n3565-12		2714	1	2714	7	2714	16	13.48	0.7	0.5235	0.7	0.99		1824	1173	0.16	{0.00}
n3565-13		2715	3	2697	7	2674	15	13.24	0.7	0.5141	0.7	0.98	-0.30	440	330	1.00	{0.00}
n3565-14		2714	2	2701	7	2685	16	13.30	0.7	0.5167	0.7	0.98		616	461	0.96	{0.00}
n3565-15		2704	3	2672	7	2630	15	12.90	0.7	0.5038	0.7	0.97	-1.81	372	239	0.33	0.05
n3565-16		2714	1	2717	7	2722	16	13.53	0.7	0.5254	0.7	0.99		1818	1136	0.01	{0.00}
n3565-16b		2709	2	2713	9	2717	21	13.46	0.9	0.5243	0.9	0.99		1083	719	0.28	0
n3565-17	core	2715	2	2702	7	2684	16	13.31	0.7	0.5164	0.7	0.99		805	548	0.48	0.01
n3565-17b	rim	2711	2	2658	7	2588	15	12.70	0.7	0.4939	0.7	0.99	-4.13	1396	823	0.03	0.03
n3565-19		2713	3	2690	7	2660	15	13.15	0.7	0.5108	0.7	0.97	-0.85	421	301	0.79	0.03
n3565-20		2710	2	2672	7	2623	15	12.90	0.7	0.5021	0.7	0.98	-2.42	542	375	0.70	0.01
n3565-21		2711	4	2708	9	2703	20	13.40	1.0	0.5210	0.9	0.97		535	392	0.78	{0.01}
n3565-22		2706	2	2684	9	2655	20	13.06	0.9	0.5096	0.9	0.99	-0.41	482	324	0.47	0.05
n3565-23		2712	2	2700	9	2683	20	13.28	0.9	0.5161	0.9	0.99		555	382	0.53	{0.00}
n3565-24		2714	2	2707	9	2697	21	13.38	1.0	0.5194	0.9	0.99		460	339	0.84	{0.01}
n3565-25		2707	3	2704	9	2700	21	13.34	1.0	0.5203	1.0	0.99		417	303	0.74	0.01
n3565-26		2711	3	2706	9	2699	20	13.36	0.9	0.5199	0.9	0.98		497	375	0.95	0.01
n3565-27		2713	2	2709	9	2704	22	13.42	1.0	0.5212	1.0	0.99		1841	1247	0.41	{0.00}
n3565-28		2717	2	2709	9	2700	20	13.42	0.9	0.5202	0.9	0.99		729	551	0.95	{0.00}
n3565-29		2712	2	2700	9	2684	21	13.28	0.9	0.5165	0.9	0.99		828	552	0.38	0.01
n3565-30		2711	2	2700	10	2686	22	13.29	1.0	0.5169	1.0	0.99		624	460	0.86	0.01
n3565-31		2708	3	2691	9	2667	20	13.15	0.9	0.5125	0.9	0.98		386	271	0.68	{0.01}
n3565-32		2699	3	2684	9	2664	21	13.06	1.0	0.5117	0.9	0.99		416	257	0.08	0.01
n3565-33		2702	3	2685	9	2661	20	13.07	0.9	0.5111	0.9	0.99		449	281	0.14	0.01
n3565-34		2713	2	2691	9	2661	20	13.15	0.9	0.5111	0.9	0.99	-0.43	530	391	0.92	0.01
n3565-35		2711	2	2698	9	2679	21	13.25	0.9	0.5153	0.9	0.99		795	603	1.02	0.1
n3565-36		2712	3	2684	9	2646	21	13.05	1.0	0.5074	1.0	0.98	-1.01	438	319	0.88	0.04
n3565-37		2707	2	2688	9	2663	21	13.12	1.0	0.5115	1.0	0.99	-0.03	455	282	0.10	0.01
n3565-38		2708	3	2676	9	2634	20	12.95	0.9	0.5046	0.9	0.98	-1.45	392	236	0.06	0.03
n3565-39		2708	2	2693	9	2673	21	13.19	1.0	0.5138	1.0	0.99		558	367	0.34	0.01
n3565-40		2712	2	2698	9	2678	21	13.25	1.0	0.5151	0.9	0.99		593	447	0.98	{0.00}
n3565-41		2715	1	2710	9	2704	21	13.43	0.9	0.5211	0.9	1.00		2363	1508	0.14	0
n3565-42		2710	3	2677	9	2633	20	12.96	0.9	0.5045	0.9	0.98	-1.52	266	159	0.01	0.02
n3565-43		2707	2	2684	9	2655	20	13.06	0.9	0.5095	0.9	0.99	-0.46	518	373	0.81	0.01
n3565-44		2654	2	2630	9	2599	20	12.33	0.9	0.4966	0.9	0.99	-0.62	982	603	0.20	0.01
n3565-47		2714	3	2694	9	2667	21	13.19	1.0	0.5124	0.9	0.99	-0.15	412	292	0.70	{0.01}
n3565-48		2691	2	2686	9	2680	21	13.09	1.0	0.5154	0.9	0.99		483	314	0.29	0.01
n3565-49		2710	2	2701	9	2688	20	13.29	0.9	0.5174	0.9	0.99		813	577	0.67	0.01
n3565-50		2717	2	2698	9	2674	21	13.26	1.0	0.5140	1.0	0.99	-0.02	703	507	0.77	{0.00}
n3565-54		2703	3	2698	9	2693	20	13.26	0.9	0.5185	0.9	0.98		388	245	0.11	0.01
n3565-55		2713	3	2692	9	2664	20	13.17	1.0	0.5116	0.9	0.98	-0.25	487	361	0.94	0.02

All errors are in 1 sigma level. 1) Error correlation in conventional concordia space. 2) Age discordance at closest approach of error ellipse to concordia (2s level).
3) Percentage of common ^{206}Pb in measured ^{206}Pb. calculated from the ^{204}Pb signal assuming a present-day Stacey and Kramers (1975) model terrestrial Pb-isotope composition.
Figures in parentheses are given when no correction has been applied. Some analyses with high common lead are not used in evaluation (strikethrough).A5
homog = homogeneous

Appendix 2. U-Pb TIMS data on zircon. monazite and titanite.

Sample information	Sample	U	Pb	$^{206}Pb/^{204}Pb$	$^{208}Pb/^{206}Pb$	ISOTOPIC RATIOS*				r **	APPARENT AGES / Ma		
density/size (µm)/abraded x hours	weight / mg	ppm	ppm	measured	radiogenic	$^{206}Pb/^{238}U$	$^{207}Pb/^{235}U$	$^{207}Pb/^{206}Pb$	2s%		$^{206}Pb/^{238}U$	$^{207}Pb/^{235}U$	$^{207}Pb/^{206}Pb$
Suomussalmi greenstone belt													
A260 Haaponen metagreywacke													
A260A +4.6/>75	20.1	299	169	6314	0.20	0.4658	13.131	0.2045	0.15	0.98	2465	2689	2862
A260B 4.2-4.6/>75	15.1	496	284	5079	0.20	0.4726	13.052	0.2003	0.15	0.98	2494	2683	2828
A1428 Mesa-aho quartz porphyry													
A1428A +4.3	8.2	161	105	3383	0.28	0.5094	13.850	0.1972	0.15	0.98	2654	2739	2803
A1428B +4.3/abr 5 h	7.5	152	104	4611	0.28	0.5328	14.565	0.1983	0.15	0.98	2753	2787	2812
A1428C +4.3/abr 16 h	7.5	157	108	4854	0.28	0.5351	14.630	0.1983	0.15	0.98	2762	2791	2812
A1429 Kilpasuo meta-andesite													
A1429A +4.0	1.2	501	316	1041	0.26	0.4860	12.834	0.1915	0.15	0.98	2553	2667	2755
A1429B +4.0/abr 5 h	0.5	542	358	2818	0.31	0.5074	13.453	0.1923	0.15	0.98	2645	2712	2762
A1429D +4.0/abr 5 h/tabular	0.3	653	435	2299	0.30	0.5087	13.515	0.1927	0.15	0.98	2651	2716	2765
A1467 Saarikylä felsic volcanic rock													
A1467A +4.3/brownish	0.7	441	210	994	0.15	0.3870	11.582	0.2170	0.16	0.97	2109	2571	2959
A1467B +4.3/pale	0.3	355	143	641	0.21	0.3099	8.705	0.2037	0.15	0.98	1740	2307	2856
A1467C 4.2-4.3/brown/abr 2 h	0.3	514	292	1079	0.13	0.4693	13.920	0.2151	0.15	0.98	2481	2744	2944
A1467D 3.8-4.2/abr 2 h	0.6	812	395	429	0.14	0.3767	11.004	0.2119	0.23	0.95	2061	2524	2920
A1467E +4.2/abr 7 h	0.3	325	201	2383	0.18	0.5061	14.802	0.2121	0.15	0.98	2640	2803	2922
A1593 Saarikylä quartz porphyry													
A1593A Monazite	0.1	2851	13402	2359	8.23	0.5728	16.963	0.2148	0.15	0.98	2920	2933	2942
A1840Palovaara Suomussalmi mica gneiss (west from the greenstone belt)													
A1840A +4.2 >75 a18h	0.49	250	150	18161	0.15	0.5191	13.695	0.1913	0.15	0.98	2695	2729	2754
Kuhmo greenstone belt													
A120 Ruokojärvi dacite													
A120A. +4.6	20	221	59	317	0.29	0.3067	8.355	0.1976	0.30	0.89	1724	2270	2806
A120C 4.2-4.6/<75/abr 1 h	10	443	194	6004	0.08	0.5070	15.238	0.2180	0.15	0.97	2672	2830	2966
A120D 4.2-4.6/>75/abr 3 h	13	458	204	6083	0.09	0.5137	15.574	0.2199	0.15	0.97	2672	2851	2980
A120E 4.2-4.6/<75/abr 5 h	11	439	198	5461	0.09	0.5204	15.737	0.2194	0.15	0.97	2700	2860	2976
A120F 4.0-4.2 <75 a3h	10	488	181	162	0.13	0.2473	6.692	0.1963	0.30	0.93	1424	2071	2796
A120G 3.6-3.8 +150 a	4.0	927	336	109	0.09	0.2187	5.931	0.1967	0.30	0.93	1274	1965	2799
A120I 4.2-4.6 a11h	1.7	459	278	5260	0.09	0.5329	16.230	0.2209	0.15	0.98	2753	2890	2987
A1000 Ruokojärvi dacite													
A1000aA +4.3 dark	3.5	236	135	2168	0.12	0.4951	13.711	0.2008	0.20	0.96	2592	2729	2833
A1000aB +4.3 microgems	8.7	151	89	2397	0.12	0.5121	13.985	0.1981	0.20	0.96	2665	2748	2711
A1000aC +4.2 long	3	294	165	351	0.12	0.4324	11.859	0.1989	0.30	0.91	2316	2593	2817
A1000aD 4.2-4.3 +150 a2h	4	399	220	369	0.10	0.4364	11.942	0.1985	0.30	0.91	2334	2599	2814
A1000bA +4.2 >75 a2h	4.5	290	153	241	0.12	0.3934	10.804	0.1992	0.30	0.91	2138	2506	2820
A1000bB +4.2 +100 a5h	3.5	205	121	392	0.13	0.4561	12.573	0.1999	0.30	0.91	2422	2648	2826
A1000bC +4.2 <75 a5h	2.1	312	179	632	0.12	0.4712	12.945	0.1993	0.30	0.91	2488	2675	2820
A1000bD +4.3 +150 CA**				17679	0.13	0.5396	14.790	0.1988	0.15	0.98	2782	2802	2816
A1346 Lampela andesite													
A1346A +4.5/abr 1 h	4.4	157	86	977	0.12	0.4646	12.205	0.1906	0.20	0.96	2459	2620	2747
A1346B 4.3-4.5/>75/abr 1 h	4.9	208	108	1023	0.13	0.4376	11.300	0.1873	0.20	0.96	2339	2548	2719
A1346C 4.3-4.5/<75/abr 1 h	5.1	266	130	1004	0.14	0.4124	10.461	0.1840	0.20	0.96	2225	2476	2689
A1346D 4.3-4.5/>75/pink	0.6	222	120	1353	0.13	0.4590	11.956	0.1889	0.20	0.96	2435	2601	2733
A1346E 4.3-4.5/<75/pink	0.7	275	136	927	0.14	0.4132	10.513	0.1845	0.30	0.91	2230	2481	2694
A1346F 4.3-4.5 <75 CA***				19630	0.13	0.5377	14.562	0.1964	0.15	0.98	2774	2787	2797

Appendix 2. cont.

Sample information	Sample	U	Pb	$^{206}Pb/^{204}Pb$	$^{208}Pb/^{206}Pb$	ISOTOPIC RATIOS*				r **	APPARENT AGES / Ma		
density/size (µm)/abraded x hours	weight / mg	ppm	ppm	measured	radiogenic	$^{206}Pb/^{238}U$	$^{207}Pb/^{235}U$	$^{207}Pb/^{206}Pb$	2s%		$^{206}Pb/^{238}U$	$^{207}Pb/^{235}U$	$^{207}Pb/^{206}Pb$
A1377 Siivikko felsic fragment in komatiite													
A1377A +4.5/abr 3 h	4.0	325	123	2556	0.19	0.3147	7.835	0.1806	0.15	0.98	1763	2212	2658
A1377B 4.3-4.5/abr 3 h	4.8	351	141	2617	0.21	0.3302	8.249	0.1812	0.15	0.98	1839	2258	2664
A1377C 4.3-4.5	4.5	303	115	2419	0.20	0.3151	7.821	0.1801	0.20	0.96	1765	2210	2654
A1418 Niittylahti gabbro													
A1418A +4.3/>75	6.2	164	101	1027	0.27	0.4717	11.754	0.1807	0.15	0.98	2491	2585	2659
A1418B1 +4.3/>75/abr	6.3	245	154	1177	0.27	0.4843	12.217	0.1830	0.15	0.98	2545	2621	2680
A1418B2 +4.3/>75/abr	6.3	245	154	1215	0.28	0.4846	12.249	0.1834	0.15	0.98	2547	2623	2684
A1418C 4.2-4.3/>75	5.5	356	201	659	0.32	0.4147	9.517	0.1665	0.20	0.96	2236	2389	2523
A1418D 4.0-4.2/>75	6.2	394	202	746	0.34	0.3778	8.169	0.1568	0.20	0.96	2066	2249	2421
A1418E +4.3/>75/abr 16 h	4.8	239	148	1444	0.27	0.4816	12.094	0.1822	0.15	0.98	2534	2611	2673
A1418F 4.2-4.3 turbid CA***				1110	0.28	0.7570	19.170	0.1837	0.20	0.98	3633	3050	2686
A1771 Kellojärvi Kuhmo gabbronorite pegmatoid													
A1771A +4.0 >75 a3h turbid	0.59	260	163	4593	0.23	0.5080	13.248	0.1891	0.15	0.98	2648	2698	2735
A511 Katerma metarhyolite													
A511H +4.2 CA***				23748	0.12	0.5361	14.524	0.1965	0.15	0.98	2767	2785	2797
A788 Polvilampi quartz-feldspar schist													
A788E +4.2 >75 CA***				6292	0.10	0.5284	14.296	0.1962	0.15	0.99	2735	2770	2795
A976 Moisiovaara amphibolite (metavolcanic rock)													
A976J 4.2-4.6 >75 CA***				10368	0.51	0.5342	14.594	0.1982	0.15	0.98	2759	2789	2811
A976K 4.2-4.6 >75 CA***				18807	0.54	0.5407	14.730	0.1976	0.15	0.98	2786	2798	2806
A1213, A1254, N5A Pitkäperä meta-andesite													
A1213A. +3.6	2.2	328.6	173.9	2515	0.11	0.4631	12.424	0.1945	0.15	0.98	2453	2636	2781
A1213B +3.6 CA***				17536	0.10	0.5423	15.041	0.2012	0.15	0.98	2793	2818	2835
A1254A. +4.0/clear	0.3	349.8	182.5	5730	0.10	0.4630	12.512	0.1960	0.15	0.98	2453	2644	2793
A1254B +4.0 CA***				25328	0.11	0.5415	14.934	0.2000	0.15	0.98	2790	2811	2827
N5A. +4.2/abr 1 h/turbid	0.2	373.0	186.3	19511	0.005	0.4886	12.418	0.1843	0.15	0.97	2565	2637	2692
A1560 Huuhilonkylä porphyry													
A1560A +4.3 >75 clear a16h	0.3	131	76.9	2662	0.13	0.5086	13.647	0.1946	0.15	0.98	2651	2726	2782
A1560B +4.3 >75 clear	0.48	169	89.6	5374	0.13	0.4623	12.354	0.1938	0.15	0.98	2450	2632	2775
A1560C 4.2-4.3 a16h	0.37	301	149	3586	0.14	0.4311	11.047	0.1859	0.15	0.98	2311	2527	2706
A1560D 4.0-4.2 <75 a6h	0.55	427	204	3050	0.14	0.4135	10.537	0.1848	0.15	0.98	2231	2483	2697
A1560E +4.3 >75 clear a24h	0.24	134	78.1	6020	0.13	0.5098	13.670	0.1945	0.15	0.98	2656	1727	2781
A1560F +4.3 <75 water-clear a16h	0.07	238	111	9043	0.14	0.4137	9.4426	0.1655	0.15	0.98	2232	2382	2513
A1560G +4.3 >75 CA***				19828	0.11	0.5418	14.683	0.1966	0.15	0.98	2791	2795	2798
A2027 Siivikkovaara porphyry dike													
A2027A +4.2 >75	0.44	147	87	1636	0.14	0.4988	13.137	0.1910	0.15	0.98	2609	2690	2751
A2027B +4.2 >75 a17h	0.56	142	87	7273	0.14	0.5288	14.203	0.1948	0.15	0.98	2736	2763	2783
A2027C +4.2 CA***				17258	0.15	0.5402	14.609	0.1961	0.15	0.98	2785	2790	2794
Naavala 7, amphibolite, metamorphic zircon													
Naa 7 zr +3.6 a2h	0.32	145.0	83.7	22782	0.11	0.5162	13.174	0.1851	0.15	0.98	2683	2692	2699
Tipasjärvi greenstone belt													
A1174 Taivaljärvi felsic volcanic rock (Vaasjoki et al 1999, anal A-D)													
A1174E +4.5 CA***				31736	0.11	0.5417	14.684	0.1966	0.15	0.98	2791	2795	2798
A1886 Tipasjärvi felsic volcanic rock (4322-2005-R305/235-239)													
A1886E +4.3 >75 a17h	0.52	319	200	5200	0.16	0.5334	14.283	0.1942	0.2	0.96	2756	2769	2778
A1886F +4.3 <75 a17h	0.38	288	177	14191	0.13	0.5300	14.200	0.1943	0.15	0.98	2741	2763	2779
A1886G +4.3 >75	0.4	288	170	5262	0.14	0.5101	13.470	0.1915	0.15	0.98	2657	2713	2755
A1886H +4.3 >75 a17h	0.37	242	146	16449	0.13	0.5254	14.060	0.1941	0.15	0.98	2722	2754	2777
A1886I +4.3 >75 CA***				47164	0.12	0.5435	14.699	0.1961	0.15	0.98	2798	2796	2794

Appendix 2. cont.

Sample information	Sample	U	Pb	$^{206}Pb/^{204}Pb$	$^{208}Pb/^{206}Pb$	ISOTOPIC RATIOS*				r **	APPARENT AGES / Ma		
density/size (µm)/abraded x hours	weight / mg	ppm	ppm	measured	radiogenic	$^{206}Pb/^{238}U$	$^{207}Pb/^{235}U$	$^{207}Pb/^{206}Pb$	2s%		$^{206}Pb/^{238}U$	$^{207}Pb/^{235}U$	$^{207}Pb/^{206}Pb$
A1377 Siivikko felsic fragment in komatiite													
A1921A +3.3 CA***				7146	0.3	0.5375	14.416	0.1945	0.15	0.98	2773	2778	2781
A1922 Tipasjärvi volcanic rock, agglomerate (4322-2006-R337/138.55-139.75)													
A1922A +4.0 a17h	0.21	62.9	40.1	12216	0.16	0.5429	15.007	0.2005	0.15	0.98	2796	2816	2830
A1922B +4.0 CA***				38708	0.16	0.5446	15.023	0.2001	0.15	0.98	2802	2817	2827
A1748 Aarreniemi Tipasjärvi greywacke													
A1748A +4.2 a4h	0.58	333	198	3473	0.19	0.4938	12.965	0.1904	0.15	0.98	2587	2677	2746
Kovero greenstone belt													
A1624 Hämälänniemi felsic volc.													
A1624A +4.3 >75 a4h pale	0.59	248	157	4264	0.19	0.5244	14.701	0.2033	0.3	0.91	2718	2796	2853
A1624B +4.3 >75 a5h red	0.36	315	201	6874	0.19	0.5287	14.756	0.2024	0.15	0.98	2736	2800	2846
A1624C +4.3 <75 pale	0.46	301	189	1220	0.19	0.5043	14.014	0.2016	0.15	0.98	2632	2751	2839
A1624D +4.3 <75 red	0.3	288	179	1276	0.19	0.5023	13.963	0.2016	0.3	0.91	2624	2747	2839
A1624E +4.3 <75 a4h pale	0.42	197	124	1418	0.19	0.5072	14.104	0.2017	0.15	0.98	2645	2757	2840
A1624F +4.3 >75 a16h	0.57	223	145	5770	0.18	0.5388	15.083	0.2030	0.15	0.98	2779	2821	2851
A1624G 4.2-4.3 “bulk”	0.51	515	291	699	0.21	0.4413	11.762	0.1933	0.15	0.98	2356	2586	2771
A1624H +4.3 >75 a16h	0.44	307	194	5283	0.18	0.5260	14.687	0.2025	0.15	0.98	2725	2795	2847
A1624I +4.3 >75 CA***		(“69”)		10689	0.16	0.5604	15.939	0.2063	0.12	0.99	2868	2873	2877
A1625 Rasisuo pl-porphyry dyke													
A1625A +4.3 >75 a16h long	0.45	262	159	5095	0.18	0.5118	13.343	0.1891	0.15	0.98	2665	2704	2734
A1625B +4.3 >75 long	0.3	291	171	1932	0.16	0.4940	12.791	0.1878	0.15	0.98	2588	2664	2723
A1625C +4.3 <75 a1h long	0.3	343	201	1261	0.17	0.4826	12.445	0.1871	0.2	0.96	2538	2639	2716
A1625D +4.3 <75 long	0.28	354	205	2750	0.18	0.4854	12.498	0.1867	0.15	0.98	2551	2643	2714
A1625E +4.3 >75 a16h clear	0.42	177	111	6730	0.20	0.5204	13.623	0.1899	0.15	0.98	2701	2724	2741
A1625F +4.3 >75 CA***		(“100”)		26367	0.19	0.5274	13.936	0.1916	0.15	0.98	2731	2745	2756
A1626 Rasisuo gabbro													
A1626A +4.3 >75 a16h	0.46	488	285	2884	0.28	0.4566	11.408	0.1812	0.15	0.98	2424	2557	2664
A1626B +4.3 >75	0.46	385	233	1374	0.27	0.4673	12	0.1863	0.15	0.98	2472	2604	2709
A1626C +4.3 <75 a1h	0.24	321	200	1380	0.27	0.4809	12.457	0.1879	0.15	0.98	2531	2640	2723
A1626D +4.3 <75	0.17	331	200	1178	0.27	0.4647	12.002	0.1873	0.25	0.99	2460	2605	2719
A1626F +4.3 >75 a21h	0.46	398	254	3822	0.27	0.5032	13.007	0.1875	0.15	0.98	2628	2680	2720
A1627 Rasisuo felsic tuff													
A1627A +4.3 >75 a4h dark euh	0.43	360	218	6309	0.13	0.5237	14.469	0.2004	0.15	0.98	2715	2781	2829
A1627B +4.3 <75	0.54	381	196	2674	0.11	0.4524	11.749	0.1884	0.15	0.98	2406	2585	2728
A1627C +4.3 <75 a16h	0.52	221	138	10519	0.15	0.5380	14.891	0.2007	0.15	0.98	2775	2808	2832
A1627D +4.3 >75 a16h	0.48	283	174	8717	0.14	0.5301	14.62	0.2000	0.15	0.98	2742	2791	2826
A1627E +4.3 >75 a32h	0.55	243	152	10090	0.14	0.5389	14.967	0.2014	0.15	0.98	2779	2813	2838
A1627F +4.3 >75 CA***		(“97”)		36972	0.14	0.5584	15.898	0.2065	0.15	0.98	2860	2871	2878
A1520 Kiukoinvaara (granitic-granodioritic vein)													
A1520A +4.3/stubby/abr 6 h	0.44	363	287	122	0.15	0.4805	12.365	0.1867	0.43	0.84	2529	2633	2713
A1520B +4.3/longish/abr 2 h	0.46	466	301	230	0.14	0.463	11.820	0.1852	0.3	0.92	2453	2590	2700
A1520C +4.3/<75/euhedral	0.15	503	327	158	0.14	0.4302	10.891	0.1836	0.33	0.91	2307	2514	2686
A1520D 4.2-4.3/>75/abr 6 h	0.49	496	339	146	0.15	0.4409	11.161	0.1836	0.36	0.89	2355	2537	2686
A1520E 4.2-4.3/>75/long	0.23	766	429	159	0.14	0.3723	9.235	0.1799	0.34	0.91	2040	2362	2652
A1520F +4.3 >75 CA**		(“97”)		28504	0.16	0.5273	13.881	0.1909	0.12	0.99	2730	2742	2750
A1155 Linnasuo porphyry													
A1155G +4.3 >75 CA***		(“67”)		25584	0.13	0.5376	14.2560	0.1923	0.12	0.99	2774	2767	2762

Appendix 2. cont.

Sample information	Sample	U	Pb	$^{206}Pb/^{204}Pb$	$^{208}Pb/^{206}Pb$	ISOTOPIC RATIOS*				r **	APPARENT AGES / Ma		
density/size (µm)/abraded x hours	weight / mg	ppm	ppm	measured	radiogenic	$^{206}Pb/^{238}U$	$^{207}Pb/^{235}U$	$^{207}Pb/^{206}Pb$	2s%		$^{206}Pb/^{238}U$	$^{207}Pb/^{235}U$	$^{207}Pb/^{206}Pb$
A1377 Siivikko felsic fragment in komatiite													
A1749D +4.2 >75 CA***		(“98”)		26695	0.12	0.5415	14.765	0.1978	0.12	0.99	2790	2800	2808
Pudasjärvi complex													
A1490 Tuore Ristisuonpalo granodiorite													
A1490A +4.2	0.49	453	197	5714	0.15	0.3803	9.150	0.1745	0.15	0.98	2078	2353	2601
A1490B +4.2 a6h	0.19	284	151	7347	0.13	0.4693	11.791	0.1822	0.15	0.98	2480	2588	2673
A1490C 4.0-4.2	0.25	601	220	2096	0.12	0.3241	7.503	0.1679	0.15	0.98	1810	2173	2537
A1490D 4.0-4.2 a6h	0.22	281	257	5084	0.11	0.3959	9.578	0.1755	0.15	0.98	2150	2395	2610
A1490E +4.2 CA***		(“87”)		17350	0.15	0.5313	14.429	0.1970	0.12	0.99	2747	2778	2801
A1533 Surmakumpu porphyry													
A1533A +4.3 a18h	0.22	222	101	2368	0.23	0.3692	9.070	0.1782	0.15	0.98	2026	2345	2636
A1533B +4.3	0.48	422	114	233	0.46	0.1641	3.635	0.1607	0.3	0.93	979	1557	2463
A1533C 4.2-4.3 a18h	0.27	396	113	1619	0.29	0.2223	5.237	0.1709	0.15	0.98	1294	1859	2566
A1533D 4.0-4.2	0.53	784	114	339	0.49	0.0925	1.836	0.1439	0.3	0.91	570	1058	2275
A1533E +4.3 a23h	0.15	125	64	6496	0.2	0.4336	10.768	0.1801	0.15	0.98	2322	2503	2654
A1533F +4.3 CA***		(“99”)		43514	0.19	0.5127	13.015	0.1841	0.15	0.98	2668	2681	2690
A1534 Keväpalo tonalite													
A1534A +4.2 >75 a18h	0.46	204	119	5987	0.11	0.5173	13.847	0.1941	0.15	0.98	2688	2739	2778
A1534B +4.2 >75	0.45	238	120	1162	0.08	0.4412	11.610	0.1909	0.15	0.98	2356	2573	2750
A1534C +4.2 <75 a20h	0.06	366	213	3161	0.11	0.515	13.742	0.1935	0.15	0.98	2678	2732	2773
A1534D +4.2 <75	0.35	244	127	792	0.09	0.4512	11.933	0.1918	0.2	0.96	2400	2599	2758
A1534E +4.2 >75 CA***		(“58”)		11208	0.08	0.5304	14.200	0.1942	0.15	0.98	2743	2763	2778
A1534sphene	9.52	31	20	791	0.17	0.5205	13.427	0.1871	0.2	0.96	2701	2710	2717
A1553 Pitkäkumpu tonalite													
A1553A +4.0>75 a18h	0.42	244	120	4633	0.1	0.4397	11.287	0.1862	0.15	0.98	2357	2551	2709
A1553B +4.0 >75	0.45	405	144	1297	0.09	0.3134	7.855	0.1818	0.15	0.98	1758	2215	2669
A1553C +4.0 <75 a4h	0.25	214	106	4495	0.1	0.4448	11.351	0.1851	0.15	0.98	2372	2552	2699
A1553D +4.0 <75	0.52	322	123	2052	0.1	0.3399	8.523	0.1819	0.15	0.98	1886	2288	2670
A1553E +4.0 <75 a20h	0.17	217	116	2729	0.11	0.4723	12.160	0.1867	0.15	0.98	2494	2617	2714
A1553F +4.0 >75 CA***		(“68”)		26356	0.09	0.5242	13.672	0.1892	0.15	0.98	2717	2727	2735
A1731 Palomaa granite													
A1731A +4.2 <75 a15h	0.09	1172	622	2313	0.1	0.4726	11.832	0.1816	0.15	0.98	2495	2591	2667
A1731B +4.2 <75	0.56	657	338	589	0.11	0.4271	10.552	0.1792	0.15	0.98	2293	2485	2645
A1731C +4.2 >75 a14h	0.53	1067	544	1380	0.09	0.4521	11.252	0.1805	0.15	0.98	2404	2544	2658
A1731D +4.2 >75 a2h	0.41	856	433	1161	0.09	0.4451	11.048	0.18	0.15	0.98	2374	2527	2653
A1731E +4.0 CA***		(“51”)		19927	0.08	0.5112	13.051	0.1852	0.15	0.98	2662	2683	2700
A1739 Veskanmaa granodiorite													
A1739A +4.2 a3h long clear euhedral	0.57	871	464	10559	0.09	0.4845	12.266	0.1836	0.15	0.98	2547	2625	2686
A1739B +4.2 >75 euhedral turbid	0.45	788	394	3355	0.10	0.4472	11.298	0.1832	0.15	0.98	2383	2548	2682
A1739C +4.2 <75 a17h euh	0.52	908	487	10196	0.09	0.4873	12.327	0.1835	0.15	0.98	2559	2630	2685
A1739D titanite 3.3-3.6 abr	1.5	259	167	2725	0.32	0.4910	12.001	0.1773	0.15	0.98	2575	2605	2628
A1739E +4.2 CA***		(“54”)		13444	0.09	0.5237	13.877	0.1922	0.15	0.98	2715	2741	2761
A1740 Palomaa monzonite													
A1740A +4.0 >75 a16h long euh	0.46	2441	1429	22497	0.23	0.4816	11.901	0.1792	0.15	0.98	2534	2597	2646
A1740B +4.0 >75 a5h long euh	0.44	1886	1097	19323	0.22	0.4824	11.937	0.1795	0.15	0.98	2538	2600	2648
A1740C +4.0 <75 a5h long euh	0.43	675	384	8408	0.16	0.4915	12.311	0.1817	0.15	0.99	2577	2628	2668
A1740D +4.0 <75 a16h	0.35	444	259	12085	0.17	0.4992	12.495	0.1815	0.15	0.98	2610	2642	2667
A1740E +4.0 >75	0.47	1162	682	11893	0.22	0.4851	12.042	0.1800	0.15	0.98	2550	2608	2653
A1740F +4.0 <75 a17h	0.44	862	502	21403	0.17	0.4979	12.479	0.1818	0.15	0.98	2605	2641	2669
A1740G +4.0 >75 CA***		(“63”)		26707	0.12	0.5128	12.876	0.1821	0.15	0.98	2668	2671	2672

Appendix 2. cont.

Sample information	Sample	U	Pb	$^{206}Pb/^{204}Pb$	$^{208}Pb/^{206}Pb$	ISOTOPIC RATIOS*				r **	APPARENT AGES / Ma		
density/size (µm)/abraded x hours	weight / mg	ppm	ppm	measured	radiogenic	$^{206}Pb/^{238}U$	$^{207}Pb/^{235}U$	$^{207}Pb/^{206}Pb$	2s%		$^{206}Pb/^{238}U$	$^{207}Pb/^{235}U$	$^{207}Pb/^{206}Pb$
A1377 Siivikko felsic fragment in komatiite													
A1741A +4.2 a5h	0.54	226	110	232.2	0.14	0.3492	9.1559	0.1902	0.4	0.90	1931	2354	2744
A1741B +4.2	0.47	511	133	243.9	0.15	0.1893	4.7372	0.1815	0.4	0.90	1117	1774	2667
A1741C 4.0-4.2	0.39	838	179	193.3	0.16	0.1480	3.5822	0.1756	0.4	0.90	890	1546	2611
A1741D +4.2 a17h	0.4	145	58.2	1002	0.13	0.3395	8.7446	0.1868	0.3	0.93	1884	2312	2714
A1741E +4.2 CA***		(“49”)		17571	0.10	0.5235	13.841	0.1918	0.15	0.98	2714	2739	2757
A1742 Viitakangas granite													
A1742A 3.6-4.0 a2h turbid	0.49	2260	517	204.1	0.33	0.1493	2.532	0.123	0.4	0.90	897	1281	2000
A1742B +4.0 a2h	0.56	1386	430	215.2	0.33	0.2016	3.7896	0.1363	0.4	0.90	1184	1591	2181
A1842 Jäkälämaa Pudasjärvi mica gneiss													
A1842A monazite +4.3 magn a20min	0.26	2981	4580	91080	2.33	0.5073	12.431	0.1777	0.15	0.98	2645	2637	2632
A1842B Zr +4.3 a17h	0.44	174	104	8241	0.14	0.5216	13.704	0.1906	0.15	0.98	2706	2729	2747
***Iisalmi complex*, A1243 Susi-Kervinen mica gneiss**													
A1243A +4.3	5.0	529	276	3927	0.06	0.4811	11.929	0.1798	0.15	0.98	2532	2598	2651
A1243B 4.2-4.3	5.1	702	351	3732	0.05	0.4679	11.508	0.1784	0.15	0.98	2474	2565	2638
A1243C 4.0-4.2	5.3	932	459	2956	0.04	0.4631	11.315	0.1772	0.15	0.98	2453	2549	2627
A1243D 3.8-4.0	5.0	1262	554	1654	0.03	0.4110	9.941	0.1755	0.15	0.98	2219	2429	2610
JVP-II +3.3	5.3	749	348	4493	0.07	0.4293	10.460	0.1767	0.15	0.98	2302	2476	2622
Loso sanukitoids													
A331I Loso 4.2-4.3 <75 CA***				12409	0.17	0.5194	13.292	0.1856	0.15	0.98	2697	2701	2703
A1926 Ansosuo diorite													
A1926A +4.2 >75	0.52	325	191	271	0.21	0.4163	10.561	0.1840	0.3	0.94	2244	2485	2689
A1926B +4.2 >75 a17h	0.47	307	190	265	0.21	0.4362	10.991	0.1827	0.3	0.94	2334	2522	2678
A1926C +4.2 >75 CA***				32628	0.19	0.5213	13.43	0.1869	0.15	0.98	2705	2710	2715
In house zircon standards:													
A382 Voinsalmi granite (for A382F-I concordia age 1877±2 Ma)													
A382F +4.6 >75 a17h	0.45	172	61	6867	0.10	0.3375	5.3366	0.1147	0.15	0.98	1874	1875	1875
A382G +4.6 >75 a5h	0.49	167	59.1	8642	0.10	0.3377	5.3467	0.1148	0.15	0.98	1876	1876	1877
A382H +4.6 <75 a17h	0.52	165	58.2	9801	0.10	0.3368	5.3326	0.1148	0.15	0.98	1871	1874	1877
A382I +4.6 >75	0.57	189	66.1	8579	0.09	0.3363	5.3284	0.1149	0.15	0.98	1869	1874	1879
A382J +4.6 >75 CA***		(“85”)		16502	0.09	0.3363	5.3521	0.1154	0.15	0.98	1869	1877	1886
A382K +4.6 >75 CA***		(“97”)		75302	0.09	0.3365	5.3522	0.1154	0.15	0.98	1870	1877	1885
A382L +4.6 <75 CA***		(“105”)		13697	0.08	0.3356	5.3196	0.1150	0.15	0.98	1866	1872	1879
A1772 Änäkäinen gabbro (upper intercept age 2711±3 Ma)													
A1772A +4.0 >75 a17h	0.58	567	342	11241	0.17	0.5146	13.2140	0.1862	0.15	0.98	2676	2695	2709
A1772B +4.0 >75 a9h	0.53	655	401	18816	0.19	0.5149	13.2135	0.1861	0.15	0.98	2678	2695	2708
A1772C +4.0 <75 a3h	0.4	522	310	6372	0.19	0.4959	12.6781	0.1854	0.15	0.98	2596	2656	2702

*) Isotopic ratios corrected for fractionation, blank and age related common lead (Stacey & Kramers 1975).
For most analyses 2-sigma errors in Pb/U ratios are estimated at 0.7%.
Pb-blank 10-50 pg except 100 pg for A1428 and A120 and 500 pg for A260.
**) Error correlation for 207Pb/235U vs. 206Pb/238U ratios.
***) Pre-treated using chemical abrasion (CA, Mattinson 2005), final sample weight in analysis was not obtained.
For CA analyses number in “U ppm” calculated using original sample wt (ca. 0.4 mg), thus not real concentration, but a signal of the amount of material in the analysis
Most zircons were hand-picked and chemically processed by Tuula Hokkanen. Mass-spectrometry mostly by Arto Pulkkinen.
Sample locations are given by Huhma et al. (this volume)

Appendix 3. LA-MC-ICPMS analyses on zircon

	ppm			*Ratios*								*Discordance*		*Ages (Ma)*					
Name	**U**	**^{206}Pb**	**^{206}Pb$_c$(%)**	**^{206}Pb/^{204}Pb**	**^{207}Pb/^{206}Pb***	**1s**	**^{207}Pb/^{235}U***	**1s**	**^{206}Pb/^{238}U***	**1s**	**Rho**	**Central (%)**	**^{207}Pb/^{206}Pb**	**1s**	**^{207}Pb/^{235}U**	**1s**	**^{206}Pb/^{238}U**	**1s**
A1429 Kilpasuo, Tormua andesite (analyzed 20100812)																			
A1429-3b	105	79	0.38	3783	0.2022	0.0015	14.57	0.47	0.5227	0.0165	0.98	-6	2844	12	2788	31	2711	70
A1429-4b	491	370	0.16	9500	0.2005	0.0013	14.97	0.44	0.5415	0.0156	0.98	-2	2830	10	2813	28	2790	65
A1429-5b	505	385	2.30	621	0.2003	0.0014	15.07	0.43	0.5458	0.0151	0.97	-1	2828	11	2820	27	2808	63
A1429-21a	568	436	0.00	37394	0.1998	0.0013	15.27	0.44	0.5543	0.0156	0.98	1	2824	10	2832	28	2843	65
A1429-7b	533	415	0.00	21148	0.2001	0.0013	15.39	0.45	0.5578	0.0161	0.98	1	2827	10	2839	28	2857	67
~~A1429-22a~~	~~162~~	~~123~~	~~3.50~~	~~386~~	~~0.2068~~	~~0.0020~~	~~15.37~~	~~0.45~~	~~0.5389~~	~~0.0149~~	~~0.95~~	~~-4~~	~~2881~~	~~15~~	~~2838~~	~~28~~	~~2779~~	~~63~~
A1429-23a	258	207	0.61	10091	0.1984	0.0013	15.70	0.45	0.5739	0.0161	0.97	5	2813	11	2858	28	2924	66
A1429-24a	737	548	0.12	15507	0.1970	0.0012	14.64	0.41	0.5390	0.0147	0.98	-1	2802	10	2792	27	2779	62
A1429-25a	404	305	0.00	31484	0.1991	0.0013	14.80	0.45	0.5391	0.0161	0.98	-2	2819	10	2803	29	2780	67
A1429-26a	311	247	0.00	16987	0.1991	0.0013	15.51	0.56	0.5650	0.0202	0.98	3	2818	10	2847	35	2887	83
A1429-27a	144	115	0.00	8207	0.1982	0.0013	15.92	0.47	0.5824	0.0168	0.98	7	2812	10	2872	28	2959	69
A1191 Ala-Luoma Suomussalmi metasediment (20101220, 35µm spot, GJ1 and A1772 standards)																			
A382-1 control	131	63	0.00	4260	0.1143	0.0013	5.432	0.28	0.3447	0.0170	0.98	3	1869	20	1890	43	1909	82
A382-2 control	119	57	0.00	2796	0.1142	0.0011	5.429	0.39	0.3447	0.0248	0.99	3	1868	17	1889	62	1909	119
A382-3 control	176	83	0.00	6440	0.1130	0.0011	5.245	0.38	0.3367	0.0243	0.99	1	1848	18	1860	62	1871	117
A1191-1a (=n759-01)	223	174	0.40	9439	0.1975	0.0023	15.87	0.93	0.5828	0.0336	0.98	7	2806	18	2869	56	2960	137
A1191-2a (=n759-02)	596	447	0.20	7846	0.2133	0.0025	17.39	1.02	0.5913	0.0338	0.98	3	2931	19	2957	56	2995	137
A1191-3a	647	543	0.00	14803	0.2220	0.0031	20.16	1.25	0.6586	0.0398	0.97	11	2995	22	3099	60	3262	155
A1191-4a	338	269	0.68	2410	0.2187	0.0026	18.36	1.11	0.6090	0.0361	0.98	4	2971	18	3009	58	3066	145
A1191-5a	392	338	0.20	13599	0.2161	0.0029	20.38	1.17	0.6840	0.0382	0.97	18	2952	21	3109	56	3359	146
A1191-6a	284	222	0.16	7518	0.2190	0.0030	19.47	1.06	0.6448	0.0340	0.97	10	2973	22	3065	53	3208	133
A1191-7a	198	133	0.55	3984	0.2202	0.0031	17.39	0.86	0.5726	0.0272	0.96	-3	2982	22	2956	47	2919	111
A1191-8a	326	258	0.14	10850	0.2198	0.0031	20.29	1.09	0.6693	0.0349	0.97	14	2979	22	3105	52	3303	135
A1191-9a	199	154	0.36	4171	0.2099	0.0029	19.14	1.05	0.6614	0.0350	0.97	16	2905	22	3049	53	3272	136
A1191-10a	550	410	0.13	9735	0.2107	0.0029	18.29	0.96	0.6296	0.0318	0.97	10	2911	22	3005	50	3148	126
A1191-11a	167	126	0.08	19887	0.2194	0.0031	20.12	1.04	0.6648	0.0331	0.96	13	2977	22	3097	50	3286	128
A1191-12a	782	536	0.09	17144	0.2102	0.0029	17.92	0.91	0.6182	0.0301	0.96	9	2907	22	2985	49	3103	120
A1191-13a	475	279	1.60	1027	0.2056	0.0037	14.81	0.74	0.5224	0.0244	0.93	-7	2871	29	2803	48	2709	103
A1191-14a	358	260	0.34	5950	0.2119	0.0026	18.37	1.03	0.6287	0.0344	0.98	10	2920	19	3009	54	3144	136
A1191-15a	471	342	0.35	9638	0.2165	0.0033	19.45	1.05	0.6518	0.0338	0.96	12	2955	24	3064	52	3235	132
A1191-16a	464	323	0.31	7470	0.2080	0.0031	18.08	0.91	0.6306	0.0304	0.96	12	2890	23	2994	49	3152	120
A1191 Ala-Luoma Suomussalmi metasediment (sessio #2, 20101220, GJ1 and A1772 standards)																			
A1191-17a	199	266	0.21	8976	0.2162	0.0025	18.57	0.62	0.6228	0.0195	0.94	7	2953	18	3020	32	3121	78
A1191-18a	329	445	0.25	6649	0.2146	0.0025	18.44	0.63	0.6235	0.0203	0.94	8	2940	17	3013	33	3124	80
A1191-19a (=n759-10)	264	339	0.29	5086	0.1971	0.0022	16.32	0.59	0.6005	0.0207	0.95	10	2803	17	2896	35	3032	83
A1191-20a	304	360	0.48	76733	0.2085	0.0024	15.99	0.50	0.5561	0.0163	0.93	-2	2894	19	2876	30	2851	68
A1191-21a	330	439	0.55	5964	0.2186	0.0033	18.59	0.95	0.6168	0.0302	0.96	5	2971	25	3021	49	3097	120
A1191-22a	421	568	0.00	17023	0.2184	0.0030	19.10	0.97	0.6343	0.0310	0.96	8	2969	23	3047	49	3166	122
A1191-23a	121	156	0.36	12027	0.2127	0.0026	17.56	0.91	0.5989	0.0304	0.97	4	2926	20	2966	50	3026	122
A1191-24a	238	308	0.26	4480	0.2168	0.0026	17.89	0.95	0.5984	0.0310	0.97	3	2957	19	2984	51	3024	125
A1191-25a	58	74	0.92	1309	0.2101	0.0026	16.91	0.91	0.5836	0.0307	0.97	3	2906	20	2930	52	2964	125
A1191-26a	503	653	0.15	10760	0.2169	0.0026	18.23	0.63	0.6097	0.0199	0.94	5	2958	18	3002	33	3069	80

Appendix 3. cont.

	ppm				*Ratios*							*Discordance*		*Ages (Ma)*					
Name	**U**	**^{206}Pb**	**^{206}Pb$_c$(%)**	**^{206}Pb/^{204}Pb**	**^{207}Pb/^{206}Pb***	**1s**	**^{207}Pb/^{235}U***	**1s**	**^{206}Pb/^{238}U***	**1s**	**Rho**	**Central (%)**	**^{207}Pb/^{206}Pb**	**1s**	**^{207}Pb/^{235}U**	**1s**	**^{206}Pb/^{238}U**	**1s**
A1429 Kilpasuo, Tormua andesite (analyzed 20100812)																		
A976-1	435	244	0.04	81060	0.2004	0.0014	14.91	0.72	0.5395	0.0259	0.99	-2	2830	11	2810	46	2782	108
A976-2a	246	136	0.08	30257	0.1996	0.0014	14.68	0.70	0.5332	0.0252	0.99	-3	2823	11	2794	45	2755	106
A976-3a	252	142	0.15	38587	0.1998	0.0014	14.93	0.72	0.5422	0.0260	0.99	-1	2824	11	2811	46	2793	109
A976-4a	232	127	0.00	43591	0.1992	0.0014	14.63	0.69	0.5328	0.0247	0.99	-3	2819	12	2792	45	2753	104
A976-4b	288	159	0.29	5333	0.1995	0.0014	14.61	0.69	0.5314	0.0250	0.99	-3	2822	11	2790	45	2747	105
A976-6a	229	117	0.24	14933	0.1983	0.0014	13.71	0.62	0.5014	0.0222	0.99	-8	2812	11	2730	42	2620	95
A976-7a	394	213	0.00	114942	0.2011	0.0014	14.67	0.65	0.5289	0.0233	0.99	-4	2836	11	2794	42	2737	98
A976-8a	327	182	0.83	2431	0.1997	0.0015	14.81	0.67	0.5378	0.0240	0.99	-2	2824	12	2803	43	2774	101
A976-9a	286	154	0.00	108612	0.1995	0.0014	14.47	0.66	0.5261	0.0238	0.99	-4	2822	12	2781	44	2725	101
A976-11a	328	176	0.00	52564	0.1999	0.0015	14.47	0.66	0.5250	0.0237	0.99	-5	2826	12	2781	43	2720	100
A976-12a	398	210	0.00	991859	0.1999	0.0015	14.26	0.66	0.5176	0.0236	0.99	-6	2825	12	2767	44	2689	100
A976-15a	338	173	0.27	38742	0.1994	0.0015	13.89	0.63	0.5055	0.0225	0.99	-8	2821	12	2742	43	2637	96
A976-5a	235	127	0.22	8701	0.1961	0.0013	14.16	0.66	0.5238	0.0242	0.99	-4	2794	11	2761	44	2715	102
A976-1b	429	232	0.00	2474	0.2039	0.0015	14.73	0.68	0.5241	0.0239	0.99	-6	2858	12	2798	44	2717	101
A976-10a	369	185	0.41	3809	0.1895	0.0014	12.87	0.54	0.4928	0.0202	0.98	-7	2737	12	2670	39	2583	87
A976-13a	341	184	0.57	2675	0.1997	0.0015	14.49	0.68	0.5263	0.0245	0.99	-4	2823	12	2782	45	2726	103
A1346 Lampela, Kuhmo, andesite (anal. 20091218)																		
A1346-1a	194	96	0.43	2784	0.1959	0.0015	13.39	0.52	0.4957	0.0188	0.98	-9	2793	13	2708	36	2595	81
A1346-2a	178	91	0.42	4565	0.1961	0.0014	13.70	0.59	0.5066	0.0216	0.99	-7	2794	12	2729	41	2642	92
A1346-3a	128	65	0.28	6304	0.1951	0.0014	13.55	0.58	0.5036	0.0213	0.99	-7	2786	12	2719	41	2629	91
A1346-4a	155	78	0.39	4503	0.1965	0.0015	13.50	0.57	0.4982	0.0208	0.99	-8	2798	11	2715	40	2606	89
A1346-5a	350	182	0.10	19749	0.1993	0.0015	14.25	0.62	0.5186	0.0223	0.99	-6	2820	11	2766	41	2693	95
A1346-6a	284	134	2.40	453	0.1975	0.0021	12.73	0.52	0.4677	0.0183	0.97	-14	2805	17	2660	38	2473	80
A1346-7a	173	87	0.38	3433	0.1977	0.0022	13.74	0.62	0.5043	0.0219	0.97	-8	2807	18	2732	42	2632	94
A1346-8a	127	64	0.04	36935	0.1942	0.0015	13.41	0.59	0.5008	0.0216	0.99	-7	2778	12	2709	41	2617	93
A1346-9a	149	76	0.27	33300	0.1965	0.0015	13.67	0.61	0.5049	0.0221	0.99	-7	2797	12	2727	42	2635	95
A1346-10a	121	59	0.48	7553	0.1939	0.0015	13.08	0.56	0.4892	0.0208	0.98	-9	2776	12	2685	41	2567	90
A2027 Siivikkovaara, Kuhmo, porphyry dike (20100820)																		
A2027-1a	119	119	0.00	12881	0.1961	0.0014	14.47	0.44	0.5352	0.0160	0.97	-1	2794	12	2781	29	2763	67
A2027-2a	56	53	0.00	7472	0.1974	0.0015	14.50	0.56	0.5328	0.0202	0.98	-2	2805	12	2783	37	2753	85
A2027-3a	99	98	0.00	15478	0.1961	0.0015	14.36	0.43	0.5312	0.0154	0.97	-2	2794	12	2774	28	2747	65
A2027-4a	147	147	0.00	20915	0.1977	0.0015	14.42	0.41	0.5292	0.0147	0.97	-3	2807	12	2778	27	2738	62
A2027-5a	209	205	0.00	25355	0.1964	0.0014	14.27	0.52	0.5272	0.0187	0.98	-3	2796	11	2768	34	2729	79
A2027-6a	99	98	0.00	11463	0.1978	0.0015	14.31	0.41	0.5246	0.0147	0.97	-4	2808	12	2770	28	2719	62
A2027-6b	112	111	0.00	12643	0.1968	0.0015	14.20	0.41	0.5231	0.0144	0.97	-4	2800	12	2763	27	2712	61
A2027-7a	160	159	0.00	27251	0.1971	0.0015	14.25	0.43	0.5242	0.0153	0.97	-4	2802	12	2766	29	2717	65
A2027-7b	103	103	0.00	16505	0.1979	0.0015	14.49	0.45	0.5312	0.0161	0.97	-3	2809	12	2783	30	2747	68
A2027-8a	93	95	0.10	10520	0.2012	0.0015	15.13	0.56	0.5453	0.0199	0.98	-1	2836	12	2823	35	2805	83
A2027-9a	141	141	0.00	16750	0.1973	0.0015	14.24	0.43	0.5236	0.0152	0.97	-4	2804	12	2766	28	2714	64
A2027-10a	131	131	0.00	22100	0.1963	0.0015	14.16	0.41	0.5234	0.0145	0.97	-4	2795	12	2761	27	2713	61
A2027-11a	133	135	0.00	21964	0.1961	0.0015	14.34	0.42	0.5304	0.0150	0.97	-2	2794	12	2773	28	2743	63
A2027-12a	95	93	0.00	13561	0.1972	0.0015	14.19	0.44	0.5219	0.0156	0.97	-4	2803	12	2763	29	2707	66
A2027-13a	50	48	0.00	5098	0.2005	0.0016	13.98	0.46	0.5055	0.0160	0.97	-8	2830	13	2748	31	2637	68

Appendix 3. cont.

	ppm			Ratios								Discordance		Ages (Ma)					
Name	U	^{206}Pb	$^{206}Pb_c$(%)	$^{206}Pb/^{204}Pb$	$^{207}Pb/^{206}Pb^*$	1s	$^{207}Pb/^{235}U^*$	1s	$^{206}Pb/^{238}U^*$	1s	Rho	Central (%)	$^{207}Pb/^{206}Pb$	1s	$^{207}Pb/^{235}U$	1s	$^{206}Pb/^{238}U$	1s
A2027 Siivikkovaara, Kuhmo, porphyry dike (20100820)																		
A2027-14a	117	117	0.00	17914	0.1954	0.0015	14.17	0.44	0.5260	0.0158	0.97	-3	2788	13	2761	29	2725	67
A2027-15a	103	101	0.00	15936	0.1959	0.0015	14.04	0.47	0.5196	0.0168	0.97	-4	2792	13	2752	32	2697	71
A2027 Siivikkovaara, Kuhmo, porphyry dike (20100820)																		
A2027-16a	65	65	0.00	7398	0.1958	0.0015	14.18	0.48	0.5254	0.0172	0.97	-3	2791	12	2762	32	2722	73
A2027-17a	76	75	0.10	7174	0.1949	0.0015	13.84	0.41	0.5153	0.0146	0.96	-5	2784	12	2739	28	2679	62
A2027-18a	107	106	0.00	12125	0.1965	0.0015	14.26	0.42	0.5264	0.0151	0.97	-3	2797	12	2767	28	2726	64
A2027-19a	236	232	0.00	30601	0.1959	0.0015	14.11	0.46	0.5225	0.0165	0.97	-4	2792	12	2757	31	2710	70
A2027-20a	106	105	0.00	11259	0.1958	0.0015	14.08	0.41	0.5217	0.0148	0.96	-4	2791	12	2755	28	2706	63
A1254 Pitkäperä, Kuhmo, andesite (anal. 20100812)																		
A1254-3b	161	107	0.08	5036	0.1969	0.0013	13.35	0.34	0.4916	0.0122	0.97	-10	2801	11	2705	24	2577	53
A1254-9b	90	71	0.18	4101	0.2009	0.0013	15.69	0.45	0.5664	0.0159	0.97	3	2834	11	2858	28	2893	66
A1254-41a	354	284	0.00	19762	0.2037	0.0013	16.33	0.47	0.5814	0.0163	0.98	4	2856	10	2896	27	2955	66
A1254-8b	385	298	0.06	11692	0.2032	0.0013	15.81	0.44	0.5643	0.0152	0.97	1	2852	10	2865	26	2884	63
A1254-5b	222	175	0.00	10186	0.2028	0.0013	15.84	0.46	0.5667	0.0160	0.98	2	2849	11	2867	28	2894	66
A1254-42a	155	124	0.00	11138	0.2027	0.0013	16.26	0.46	0.5817	0.0161	0.97	5	2848	11	2892	27	2956	66
A1254-11b	103	82	0.00	12703	0.2016	0.0014	15.96	0.47	0.5741	0.0163	0.97	4	2839	11	2874	28	2925	67
A1254-12b	289	233	0.00	14730	0.2022	0.0013	16.06	0.47	0.5764	0.0165	0.98	4	2844	10	2881	28	2934	68
A1254-15b	248	188	0.01	9094	0.2030	0.0013	15.30	0.44	0.5465	0.0155	0.98	-2	2851	10	2834	28	2811	64
A1174 Tipasjärvi (Taivaljärvi) felsic volcanic rock (anal. 20091217)																		
~~A1174-02-1a~~	~~239~~	~~121~~	~~2.00~~	~~766~~	~~0.1929~~	~~0.0026~~	~~13.41~~	~~0.94~~	~~0.5043~~	~~0.0348~~	~~0.98~~	~~-6~~	~~2767~~	~~22~~	~~2709~~	~~66~~	~~2632~~	~~149~~
A1174-02-2a	102	52	0.00	36931	0.1962	0.0027	13.95	1.00	0.5156	0.0365	0.98	-5	2795	22	2746	68	2680	155
A1174-02-3a	59	29	0.00	19243	0.1956	0.0027	13.32	0.98	0.4938	0.0356	0.98	-9	2790	22	2703	69	2587	154
A1174-02-3b	48	24	0.00	14626	0.1958	0.0027	13.60	0.90	0.5035	0.0325	0.98	-7	2792	22	2722	62	2629	139
A1174-02-3c	137	68	0.00	44188	0.1978	0.0027	13.67	0.94	0.5013	0.0339	0.98	-8	2808	22	2727	65	2619	146
A1174-02-4a	204	102	0.00	81869	0.1972	0.0027	13.88	0.93	0.5105	0.0333	0.98	-6	2803	22	2742	63	2659	142
A1174-02-5a	64	32	0.00	34986	0.2008	0.0028	14.19	0.95	0.5124	0.0336	0.98	-7	2833	22	2762	64	2667	143
A1174-02-6a	84	43	0.04	25268	0.2008	0.0028	14.30	0.96	0.5166	0.0340	0.98	-6	2833	23	2770	64	2685	144
A1174-02-7a	51	25	0.09	18842	0.1946	0.0027	13.46	0.88	0.5016	0.0322	0.98	-7	2782	23	2713	62	2621	138
A1174-02-8a	42	20	0.00	24455	0.1953	0.0027	13.55	0.89	0.5032	0.0324	0.98	-7	2787	21	2719	62	2628	139
A1174-02-9a	85	43	0.00	31549	0.1957	0.0027	13.93	0.94	0.5165	0.0341	0.98	-5	2790	21	2745	64	2684	145
A1174-02-10a	66	32	0.01	24093	0.1954	0.0027	13.49	0.88	0.5007	0.0320	0.98	-8	2788	22	2715	62	2617	137
A1174-02-11a	78	44	0.00	13284	0.2008	0.0012	14.62	0.25	0.5281	0.0086	0.94	-4	2833	10	2791	17	2734	36
A1174-02-12a	103	57	0.00	34585	0.1965	0.0012	14.05	0.23	0.5187	0.0081	0.93	-5	2797	10	2753	16	2694	34
A1174-02-7b	44	24	0.00	8030	0.1965	0.0013	13.93	0.24	0.5142	0.0082	0.93	-5	2797	10	2745	16	2674	35
A1174-02-13a	72	40	0.00	10295	0.1963	0.0013	14.09	0.24	0.5207	0.0084	0.93	-4	2795	10	2756	16	2702	36
A1174-02-14a	88	50	0.00	14709	0.1963	0.0013	14.39	0.27	0.5319	0.0092	0.93	-2	2795	11	2776	18	2749	39
A1174-02-14b	269	152	0.00	32782	0.1987	0.0014	14.58	0.29	0.5323	0.0100	0.94	-3	2815	11	2788	19	2751	42
A1174-02-15a	48	29	0.00	14515	0.1957	0.0019	14.69	0.30	0.5443	0.0099	0.88	1	2790	15	2795	20	2802	41
A1174-02-15b	40	24	0.00	12085	0.1957	0.0019	14.54	0.30	0.5389	0.0097	0.88	-1	2790	16	2786	20	2779	41
A1174-02-15c	85	52	0.21	18887	0.1960	0.0019	14.80	0.30	0.5478	0.0099	0.88	1	2793	16	2803	20	2816	41
A1174-02-16a	64	38	0.20	12707	0.1954	0.0019	14.41	0.29	0.5349	0.0096	0.88	-1	2788	16	2777	19	2762	40
A1174-02-16b	56	33	0.00	16537	0.1966	0.0020	14.25	0.30	0.5257	0.0096	0.88	-3	2798	16	2766	20	2723	41
A1174-02-17a	79	43	0.07	19103	0.1959	0.0020	13.32	0.27	0.4929	0.0087	0.87	-9	2792	16	2702	19	2583	37

Appendix 3. cont.

	ppm				*Ratios*							*Discordance*		*Ages (Ma)*					
Name	**U**	**^{206}Pb**	**^{206}Pb$_c$(%)**	**^{206}Pb/^{204}Pb**	**^{207}Pb/^{206}Pb***	**1s**	**^{207}Pb/^{235}U***	**1s**	**^{206}Pb/^{238}U***	**1s**	**Rho**	**Central (%)**	**^{207}Pb/^{206}Pb**	**1s**	**^{207}Pb/^{235}U**	**1s**	**^{206}Pb/^{238}U**	**1s**
A1174 Tipasjärvi (Taivaljärvi) felsic volcanic rock (anal. 20091217)																		
A1174-02-18a	80	48	0.00	23646	0.1966	0.0020	14.57	0.30	0.5374	0.0096	0.87	-1	2798	16	2787	20	2772	40
~~A1174-02-19a~~	~~48~~	~~31~~	~~7.70~~	~~194~~	~~0.1820~~	~~0.0026~~	~~13.40~~	~~0.30~~	~~0.5343~~	~~0.0094~~	~~0.78~~	~~4~~	~~2671~~	~~23~~	~~2709~~	~~21~~	~~2759~~	~~39~~
A1174-02-20a	116	68	0.00	51844	0.1964	0.0020	14.28	0.30	0.5276	0.0096	0.88	-3	2796	16	2769	20	2731	40
A1174-02-21a	46	28	0.00	12352	0.1956	0.0020	14.45	0.29	0.5359	0.0093	0.86	-1	2790	16	2780	19	2766	39
A1886 Tipasjärvi felsic volcanic rock (anal. 20091218)																		
A1886-1a	192	99	0.46	2965	0.1957	0.0014	14.08	0.61	0.5220	0.0225	0.99	-4	2790	11	2755	41	2708	95
A1886-3a	363	184	0.00	79887	0.1981	0.0014	14.20	0.61	0.5200	0.0220	0.99	-5	2810	11	2763	41	2699	93
A1886-5a	173	86	0.08	24619	0.1962	0.0014	13.80	0.59	0.5102	0.0214	0.99	-6	2794	11	2736	40	2658	92
A1886-6a	139	69	0.14	21233	0.1953	0.0014	13.79	0.60	0.5122	0.0219	0.99	-5	2787	11	2736	41	2666	93
A1886-7a	149	77	0.00	54562	0.1960	0.0014	14.35	0.64	0.5311	0.0235	0.99	-2	2794	12	2773	43	2746	99
A1886-9a	166	82	0.28	9039	0.1962	0.0014	13.84	0.59	0.5116	0.0215	0.99	-6	2795	11	2739	40	2663	92
A1886-10a	172	86	0.02	30776	0.1968	0.0014	13.99	0.60	0.5157	0.0218	0.99	-5	2800	11	2749	41	2681	93
A1886-11a	239	121	0.06	40690	0.1970	0.0014	14.19	0.62	0.5224	0.0224	0.99	-4	2802	11	2763	41	2710	95
A1886-2a	114	52	0.01	27092	0.1935	0.0014	12.65	0.51	0.4741	0.0189	0.99	-12	2772	11	2654	38	2501	83
A1886-8a	104	50	0.00	32563	0.1957	0.0014	13.54	0.57	0.5018	0.0208	0.99	-7	2790	12	2718	40	2622	89
A1921 Tipasjärvi felsic volcanic rock (anal. 20100816)																		
A1921-3c	513	435	0.01	19153	0.1999	0.0018	15.33	0.41	0.5562	0.0139	0.94	1	2825	14	2836	25	2851	58
A1921-12b	196	161	0.05	9753	0.1973	0.0018	14.48	0.44	0.5323	0.0153	0.96	-2	2804	14	2781	29	2751	65
A1921-20b	292	239	0.00	12322	0.1986	0.0018	14.86	0.41	0.5429	0.0143	0.95	-1	2814	14	2806	27	2795	60
A1921-23b	283	255	0.00	18054	0.1982	0.0018	16.42	0.45	0.6009	0.0154	0.94	10	2812	14	2902	26	3034	62
A1921-26c	252	207	0.00	9533	0.1985	0.0018	14.88	0.41	0.5437	0.0140	0.95	-1	2814	15	2808	26	2799	58
A1921-27b	398	345	0.00	22948	0.1974	0.0018	15.57	0.43	0.5719	0.0149	0.95	5	2805	14	2851	26	2916	61
A1921-30a	318	268	0.00	13195	0.1971	0.0017	14.91	0.39	0.5488	0.0137	0.94	1	2802	14	2810	25	2820	57
A1921-31a	404	335	0.00	19253	0.1957	0.0017	14.67	0.39	0.5437	0.0135	0.94	0	2791	13	2794	25	2799	57
A1921-32a	487	369	0.00	16286	0.1984	0.0018	13.50	0.37	0.4935	0.0129	0.95	-10	2813	14	2715	26	2586	56
A1921-33c	267	228	0.00	17460	0.1984	0.0018	15.17	0.43	0.5547	0.0148	0.95	1	2813	14	2826	27	2845	61
A1921-34c	239	196	0.00	18436	0.1987	0.0018	14.54	0.42	0.5306	0.0147	0.95	-3	2815	14	2785	28	2744	62
A1921-18a monazite	512	198	0.01	52944	0.1121	0.0008	5.309	0.17	0.3434	0.0109	0.97	4	1834	13	1870	28	1903	52
A1922 Tipasjärvi felsic volcanic rock (anal. 20100816)																		
A1922-7c	139	121	0.12	5028	0.2000	0.0018	15.46	0.43	0.5606	0.0148	0.95	2	2826	14	2844	27	2869	61
A1922-8b	100	85	0.00	29147	0.2009	0.0018	15.18	0.42	0.5481	0.0144	0.95	-1	2833	14	2826	26	2817	60
A1922-12b	406	343	0.00	29487	0.2015	0.0017	15.01	0.41	0.5402	0.0142	0.95	-2	2838	13	2816	26	2784	59
A1922-13b	133	108	0.22	5636	0.2039	0.0018	14.42	0.41	0.5129	0.0139	0.95	-8	2858	14	2778	27	2669	59
A1922-14c	45	38	0.00	2351	0.2000	0.0019	14.62	0.42	0.5299	0.0145	0.95	-4	2827	15	2791	28	2741	61
A1922-15c	120	102	0.07	4333	0.1999	0.0017	14.48	0.44	0.5255	0.0152	0.96	-5	2825	14	2782	29	2722	64
A1922-20b	80	69	0.00	6709	0.2000	0.0018	15.41	0.44	0.5587	0.0151	0.95	2	2826	14	2841	27	2861	62
A1922-23b	152	126	0.00	6921	0.1999	0.0017	14.63	0.41	0.5308	0.0142	0.95	-4	2825	14	2791	27	2745	60
A1922-28a	160	134	0.00	14099	0.1997	0.0017	14.55	0.41	0.5285	0.0144	0.95	-4	2824	14	2786	27	2735	61
A1922-29a	64	54	0.00	2627	0.1995	0.0018	14.59	0.41	0.5304	0.0143	0.95	-3	2822	14	2789	27	2743	60
A1922-30a	116	98	0.00	8588	0.1991	0.0018	15.07	0.41	0.5487	0.0143	0.95	.	2819	14	2819	26	2820	59
83-PGN-90 Rakennuslahti, Kuhmo, metagreywacke (anal. 20100816)																		
83-PGN-90-1b	301	262	0.00	13978	0.1914	0.0012	13.73	0.52	0.5201	0.0196	0.99	-2	2755	10	2731	36	2699	83
83-PGN-90-2b	109	97	0.00	4587	0.1914	0.0013	14.05	0.53	0.5324	0.0196	0.98	-0	2754	11	2753	35	2752	82

Appendix 3. cont.

	ppm			Ratios								Discordance		Ages (Ma)				
Name	U	^{206}Pb	$^{206}Pb_c$(%)	$^{206}Pb/^{204}Pb$	$^{207}Pb/^{206}Pb^*$	1s	$^{207}Pb/^{235}U^*$	1s	$^{206}Pb/^{238}U^*$	1s	Rho	Central (%)	$^{207}Pb/^{206}Pb$	1s	$^{207}Pb/^{235}U$	1s	$^{206}Pb/^{238}U$	1s
83-PGN-90 Rakennuslahti, Kuhmo, metagreywacke (anal. 20100816)																		
83-PGN-90-5b	196	176	0.00	9982	0.1921	0.0013	14.39	0.54	0.5433	0.0200	0.99	2	2760	10	2776	36	2797	84
83-PGN-90-3b	163	163	0.00	10171	0.1891	0.0013	15.75	0.60	0.6041	0.0227	0.99	14	2734	11	2862	36	3046	91
83-PGN-90-4b	615	557	0.00	32502	0.1935	0.0012	14.51	0.54	0.5441	0.0200	0.99	1	2772	10	2784	35	2801	83
83-PGN-90-6b	306	301	0.00	20989	0.1917	0.0012	15.81	0.61	0.5981	0.0227	0.99	12	2757	10	2865	37	3022	91
83-PGN-90-7b	114	101	0.00	39762	0.1920	0.0013	14.17	0.52	0.5355	0.0194	0.98	0	2759	11	2761	35	2764	81
83-PGN-90-10b	245	224	0.00	13915	0.1910	0.0012	14.73	0.54	0.5594	0.0201	0.98	5	2751	10	2798	35	2864	83
83-PGN-90-11b	288	250	0.01	11409	0.1920	0.0013	13.81	0.52	0.5216	0.0194	0.99	-2	2760	10	2737	36	2706	82
83-PGN-90 Rakennuslahti metagreywacke (anal. 20100312)																		
83-PGN-90-1a	163	106	0.00	27230	0.1905	0.0021	14.11	0.60	0.5373	0.0223	0.97	1	2747	17	2757	41	2772	93
83-PGN-90-2a	143	94	0.07	12549	0.1901	0.0021	14.31	0.61	0.5457	0.0224	0.97	3	2743	18	2770	40	2807	93
83-PGN-90-3a	346	219	0.07	25432	0.1853	0.0018	13.71	0.51	0.5368	0.0194	0.97	3	2701	15	2730	35	2770	81
83-PGN-90-4a	218	148	0.00	18002	0.1933	0.0020	15.03	0.67	0.5638	0.0245	0.97	5	2770	16	2817	42	2882	101
83-PGN-90-5a	127	83	0.00	13600	0.1905	0.0019	14.30	0.61	0.5446	0.0227	0.97	3	2746	16	2770	41	2803	95
83-PGN-90-6a	273	189	0.00	20472	0.1947	0.0020	15.33	0.69	0.5712	0.0250	0.97	6	2782	17	2836	43	2913	103
83-PGN-90-7a	163	112	0.00	18522	0.1908	0.0023	14.64	0.71	0.5566	0.0263	0.97	5	2749	19	2792	46	2852	109
83-PGN-90-8a	326	224	0.00	38472	0.2030	0.0025	15.65	0.69	0.5594	0.0237	0.96	1	2850	19	2856	42	2864	98
83-PGN-90-9a	223	169	0.00	24617	0.2308	0.0031	19.45	0.95	0.6113	0.0286	0.96	1	3057	21	3064	47	3075	114
83-PGN-90-10a	185	122	0.00	15079	0.1900	0.0022	14.35	0.61	0.5479	0.0225	0.96	3	2742	18	2773	40	2816	93
83-PGN-90-11a	47	30	0.00	4268	0.1906	0.0023	14.14	0.59	0.5380	0.0215	0.96	1	2747	19	2759	40	2775	90
83-PGN-90-12a	252	166	0.15	13184	0.2020	0.0025	15.23	0.65	0.5471	0.0225	0.96	-1	2842	20	2830	41	2813	94
83-PGN-90-13a	120	64	0.00	10789	0.1911	0.0022	12.19	0.46	0.4627	0.0164	0.95	-13	2752	19	2619	35	2451	72
83-PGN-90-14a	163	109	0.00	11234	0.1904	0.0022	14.51	0.63	0.5527	0.0230	0.96	4	2746	18	2784	41	2836	96
83-PGN-90-15a	133	87	0.00	11494	0.1905	0.0022	14.30	0.60	0.5447	0.0220	0.96	3	2746	19	2770	40	2803	92
83-PGN-90-16a	84	55	0.00	6540	0.1913	0.0023	14.50	0.61	0.5497	0.0223	0.96	3	2753	19	2783	40	2824	93
83-PGN-90-17a	176	115	0.00	16729	0.1902	0.0022	14.17	0.60	0.5404	0.0221	0.96	2	2744	19	2761	40	2785	92
83-PGN-90-18a	288	178	0.00	19904	0.1900	0.0022	13.52	0.56	0.5160	0.0205	0.96	-3	2742	18	2717	39	2682	87
83-PGN-90-19a	86	60	0.00	7707	0.2059	0.0026	16.41	0.73	0.5783	0.0247	0.96	3	2873	20	2901	43	2942	101
83-PGN-90-20a	83	67	0.00	7672	0.2560	0.0038	22.95	1.18	0.6503	0.0319	0.96	0	3222	22	3225	50	3229	125
83-PGN-90-21a	82	66	0.16	5784	0.2604	0.0039	23.29	1.20	0.6489	0.0320	0.96	-1	3249	24	3239	50	3224	125
83-PGN-90-22a	178	124	0.00	12956	0.2068	0.0026	16.34	0.72	0.5733	0.0244	0.96	2	2881	19	2897	42	2921	100
83-PGN-90-23a	161	116	0.00	14275	0.2158	0.0028	17.69	0.81	0.5946	0.0261	0.96	3	2950	20	2973	44	3008	106
83-PGN-90-24a	42	26	0.00	3231	0.1844	0.0021	13.13	0.52	0.5165	0.0197	0.96	-0	2693	18	2689	38	2684	84
83-PGN-90-24b	66	42	0.08	4727	0.1899	0.0023	13.98	0.57	0.5338	0.0210	0.96	1	2741	19	2748	39	2758	88
83-PGN-90-25a	68	45	0.00	6660	0.2268	0.0031	17.27	0.75	0.5524	0.0228	0.95	-8	3029	21	2950	42	2835	95
83-PGN-90-26a	206	133	0.00	14420	0.1892	0.0022	14.15	0.60	0.5424	0.0219	0.96	3	2736	19	2760	40	2794	92
83-PGN-90-27a	101	65	0.00	8713	0.1910	0.0023	14.32	0.60	0.5437	0.0217	0.96	2	2751	19	2771	40	2799	91
83-PGN-90-28a	60	40	0.00	63602	0.2060	0.0024	16.08	0.72	0.5662	0.0244	0.97	1	2874	18	2882	43	2892	100
83-PGN-90-29a	156	104	0.00	11858	0.2133	0.0026	16.48	0.73	0.5604	0.0238	0.96	-3	2931	18	2905	42	2868	98
83-PGN-90-30a	102	62	0.24	5194	0.1894	0.0021	13.50	0.56	0.5171	0.0205	0.96	-2	2737	18	2715	39	2687	87
83-PGN-90-31a	101	73	0.21	7257	0.2154	0.0024	17.74	0.84	0.5974	0.0275	0.97	3	2947	18	2976	46	3019	111
83-PGN-90-32a	76	58	0.00	7634	0.2518	0.0032	21.91	1.12	0.6309	0.0314	0.97	-2	3196	21	3180	50	3153	124
83-PGN-90-33a	155	102	0.00	12761	0.2038	0.0022	15.63	0.69	0.5563	0.0238	0.97	-0	2857	17	2854	42	2851	99
83-PGN-90-34a	110	73	0.00	8369	0.2034	0.0022	15.81	0.70	0.5639	0.0244	0.97	1	2854	17	2866	43	2883	100

Appendix 3. cont.

	ppm				*Ratios*							*Discordance*		*Ages (Ma)*					
Name	**U**	**^{206}Pb**	**^{206}Pb$_c$(%)**	**^{206}Pb/^{204}Pb**	**^{207}Pb/^{206}Pb***	**1s**	**^{207}Pb/^{235}U***	**1s**	**^{206}Pb/^{238}U***	**1s**	**Rho**	**Central (%)**	**^{207}Pb/^{206}Pb**	**1s**	**^{207}Pb/^{235}U**	**1s**	**^{206}Pb/^{238}U**	**1s**
83-PGN-90 Rakennuslahti metagreywacke (anal. 20100312)																		
83-PGN-90-35a	103	67	0.02	7383	0.1900	0.0020	14.38	0.63	0.5491	0.0232	0.97	4	2742	16	2775	41	2822	97
83-PGN-90-36a	128	83	0.00	19525	0.1895	0.0020	14.30	0.63	0.5475	0.0233	0.97	4	2738	16	2770	42	2815	97
83-PGN-90-37a	156	100	0.01	21636	0.1893	0.0019	14.27	0.62	0.5468	0.0230	0.97	3	2736	16	2768	41	2812	96
83-PGN-90-38a	117	83	0.00	12578	0.2151	0.0024	17.42	0.81	0.5875	0.0266	0.97	2	2944	17	2958	45	2979	108
83-PGN-90-39a	64	41	0.00	5489	0.1903	0.0020	14.25	0.61	0.5429	0.0226	0.97	2	2745	17	2766	41	2796	94
83-PGN-90-40a	78	53	0.00	7705	0.2050	0.0022	16.13	0.73	0.5706	0.0249	0.97	2	2866	17	2884	43	2910	102
83-PGN-90-41a	237	172	0.05	18111	0.2200	0.0025	18.24	0.88	0.6014	0.0281	0.97	2	2980	18	3002	46	3035	113
83-PGN-90-42a	211	135	0.07	44542	0.1897	0.0020	14.32	0.63	0.5477	0.0233	0.97	3	2739	16	2771	42	2816	97
83-PGN-90-43a	169	111	0.07	13189	0.1892	0.0019	14.57	0.64	0.5587	0.0238	0.97	6	2735	16	2788	42	2861	99
83-PGN-90-44a	171	123	0.00	16501	0.2155	0.0025	17.85	0.85	0.6005	0.0279	0.97	4	2948	19	2982	46	3032	112
83-PGN-90-45a	67	45	0.04	4904	0.2038	0.0022	15.96	0.72	0.5681	0.0248	0.97	2	2857	17	2875	43	2900	102
A1533 Surmakumpu porphyry dike, Pudasjärvi complex (anal. 20100812&16)																		
A1533-1a	85	61	0.20	4978	0.1810	0.0012	12.82	0.34	0.5138	0.0134	0.97	1	2662	11	2667	25	2673	57
A1533-1b	71	61	0.00	5082	0.1818	0.0013	11.97	0.45	0.4774	0.0175	0.98	-7	2670	12	2602	35	2516	76
A1533-2a	74	55	0.00	71713	0.1821	0.0012	13.30	0.36	0.5297	0.0138	0.97	3	2672	11	2701	25	2740	58
A1533-2b	79	75	0.00	4087	0.1821	0.0013	13.33	0.51	0.5308	0.0199	0.98	3	2672	11	2703	36	2745	84
A1533-3a	165	121	0.15	12029	0.1817	0.0012	13.12	0.36	0.5239	0.0138	0.97	2	2668	10	2689	26	2716	58
A1533-4a	84	61	0.13	5853	0.1818	0.0012	13.05	0.37	0.5207	0.0142	0.97	2	2669	10	2683	26	2702	60
A1533-5a	73	51	0.21	4205	0.1819	0.0012	12.64	0.34	0.5042	0.0133	0.97	-2	2670	11	2654	26	2632	57
A1533-6a	89	63	0.00	4166	0.1822	0.0012	12.62	0.35	0.5025	0.0134	0.97	-2	2673	11	2652	26	2624	58
A1533-7a	1473	114	2.10	1286	0.0620	0.0011	0.378	0.02	0.0442	0.0017	0.91	-60	675	39	325	12	279	11
A1533-8a	759	49	5.20	628	0.0688	0.0014	0.336	0.01	0.0354	0.0012	0.85	-76	892	43	294	10	224	7
A1533-9a	1593	65	0.30	12161	0.0521	0.0004	0.180	0.01	0.0250	0.0007	0.97	-46	290	17	168	5	159	5
~~A1533-10a~~	~~605~~	~~88~~	~~16.00~~	~~92~~	~~0.1291~~	~~0.0020~~	~~1.242~~	~~0.07~~	~~0.0697~~	~~0.0040~~	~~0.97~~	~~-82~~	~~2086~~	~~26~~	~~820~~	~~33~~	~~435~~	~~24~~
A331 Loso quartz diorite (sanukitoid) (20100824)																		
A331-6a	665	510	0.06	23417	0.1599	0.0006	9.468	0.65	0.4295	0.0297	1.00	-7.3	2454	6	2384	63	2303	134
A331-21a	453	383	0.75	7725	0.1626	0.0008	10.24	0.84	0.4566	0.0373	1.00	-2.8	2483	8	2456	76	2425	165
A331-6b	138	111	0.78	3396	0.1661	0.0018	10.76	0.76	0.4698	0.0329	0.99	-1.7	2519	18	2503	66	2483	144
A331-8a	483	392	0.00	26653	0.1716	0.0012	11.02	0.82	0.4658	0.0343	1.00	-5	2573	11	2525	69	2465	151
A331-24a	319	279	1.20	8806	0.1722	0.0008	11.67	0.89	0.4917	0.0373	1.00	.	2579	8	2578	71	2578	161
A331-9a	324	291	0.00	13059	0.1791	0.0007	12.26	0.90	0.4964	0.0364	1.00	-2.1	2644	6	2624	69	2598	157
A331-22a	417	370	0.00	15463	0.1803	0.0007	12.30	0.95	0.4949	0.0382	1.00	-2.9	2655	6	2628	73	2592	165
A331-13a	437	402	0.00	11647	0.1811	0.0007	12.83	0.94	0.5138	0.0376	1.00	0.4	2663	6	2667	69	2673	160
A331-7a	336	300	0.00	15695	0.1823	0.0007	12.55	0.93	0.4994	0.0370	1.00	-2.9	2674	6	2647	70	2611	159
A331-10b	275	233	0.47	4560	0.1823	0.0009	11.88	0.87	0.4725	0.0344	1.00	-8.1	2674	8	2595	68	2495	151
A331-1a	146	135	0.69	2331	0.1825	0.0009	12.11	0.93	0.4815	0.0368	1.00	-6.4	2675	8	2613	72	2534	160
A331-10a	343	317	0.03	18503	0.1834	0.0007	12.92	0.97	0.5111	0.0383	1.00	-1	2683	6	2674	71	2661	163
A331-15a	282	253	0.76	1815	0.1837	0.0007	12.56	0.91	0.4960	0.0358	1.00	-4.1	2686	6	2647	68	2596	154
A331-16a	522	465	0.10	9519	0.1842	0.0008	12.64	0.95	0.4978	0.0374	1.00	-3.9	2691	7	2653	71	2604	161
A331-14a	373	357	0.00	18424	0.1849	0.0007	13.56	1.02	0.5320	0.0398	1.00	2.4	2697	6	2720	71	2750	168
A331-2a	169	152	0.00	14558	0.1852	0.0007	12.47	0.93	0.4885	0.0364	1.00	-6.1	2700	6	2641	70	2564	158
A331-23a	143	134	0.00	16806	0.1853	0.0011	13.60	0.83	0.5323	0.0322	1.00	2.3	2700	9	2722	57	2751	135
A331-25a	606	565	0.18	13906	0.1855	0.0007	13.29	1.06	0.5199	0.0413	1.00	-0.2	2702	6	2701	75	2699	175

Appendix 3. cont.

	ppm			Ratios									Discordance		Ages (Ma)				
Name	U	^{206}Pb	$^{206}Pb_c$(%)	$^{206}Pb/^{204}Pb$	$^{207}Pb/^{206}Pb^*$	1s	$^{207}Pb/^{235}U^*$	1s	$^{206}Pb/^{238}U^*$	1s	Rho	Central (%)	$^{207}Pb/^{206}Pb$	1s	$^{207}Pb/^{235}U$	1s	$^{206}Pb/^{238}U$	1s
A331 Loso quartz diorite (sanukitoid) (20100824)																		
A331-17a	208	194	0.23	9860	0.1856	0.0011	13.21	1.02	0.5164	0.0399	1.00	-0.9	2703	9	2695	73	2684	170
A331-4a	178	173	0.04	6991	0.1856	0.0016	13.78	1.04	0.5382	0.0405	0.99	3.3	2704	14	2734	72	2776	170
A331-19a	255	237	0.00	10790	0.1860	0.0009	13.25	1.02	0.5167	0.0399	1.00	-1	2707	8	2697	73	2685	170
A331-11a	222	210	0.00	8907	0.1861	0.0007	13.45	1.01	0.5244	0.0393	1.00	0.5	2708	6	2712	71	2718	166
A331-5a	430	423	0.00	14522	0.1866	0.0007	13.78	1.04	0.5358	0.0403	1.00	2.4	2712	6	2735	71	2766	169
A331-12a	256	238	0.00	15372	0.1876	0.0007	13.46	1.00	0.5206	0.0386	1.00	-0.9	2721	6	2713	70	2702	163
A331-18a	191	186	0.00	12294	0.1881	0.0009	14.09	1.12	0.5433	0.0432	1.00	3.2	2726	8	2756	75	2797	180
A331-20a	131	122	0.00	5262	0.1897	0.0010	13.62	1.05	0.5209	0.0402	1.00	-1.6	2739	8	2724	73	2703	171
A331-3a	197	195	0.00	5228	0.1985	0.0009	15.26	1.27	0.5576	0.0464	1.00	1.9	2814	7	2832	79	2857	192
A1926 Ansosuo diorite (Loso sanukitoid) (20100824)																		
A1926-5b	87	73	0.16	2034	0.1803	0.0011	11.62	0.87	0.4674	0.0347	1.00	-8.3	2655	10	2574	70	2472	152
A1926-5a	269	248	0.00	8251	0.1821	0.0008	12.92	1.00	0.5148	0.0396	1.00	0.3	2672	7	2674	73	2677	169
A1926-20a	391	365	0.12	8026	0.1840	0.0009	13.30	1.08	0.5242	0.0427	1.00	1.3	2689	7	2701	77	2717	181
A1926-9a	109	105	0.52	2333	0.1845	0.0009	13.54	1.07	0.5320	0.0420	1.00	2.5	2694	8	2718	75	2750	177
A1926-11a	270	231	0.00	8924	0.1848	0.0008	12.08	0.91	0.4744	0.0356	1.00	-8.6	2696	7	2611	70	2503	155
A1926-13a	280	269	0.00	10232	0.1851	0.0008	13.64	1.08	0.5343	0.0422	1.00	2.7	2700	7	2725	75	2759	177
A1926-15a	402	401	0.00	32352	0.1855	0.0007	14.05	1.13	0.5493	0.0443	1.00	5.5	2703	6	2753	77	2822	184
A1926-1a	42	39	0.00	1966	0.1856	0.0012	13.29	1.08	0.5191	0.0421	1.00	-0.4	2704	10	2700	77	2696	179
A1926-16a	474	448	0.00	17166	0.1860	0.0008	13.48	1.06	0.5258	0.0414	1.00	0.8	2707	7	2714	74	2724	175
A1926-6a	151	146	0.00	6994	0.1861	0.0008	13.67	1.08	0.5329	0.0420	1.00	2.1	2708	7	2727	75	2754	177
A1926-19a	211	213	0.77	2297	0.1863	0.0009	14.32	1.17	0.5573	0.0454	1.00	6.6	2710	8	2771	77	2855	188
A1926-3a	117	114	0.00	7069	0.1871	0.0009	13.77	1.09	0.5340	0.0422	1.00	1.9	2716	7	2734	75	2758	177
A1926-12b	184	182	0.00	5532	0.1871	0.0009	14.11	1.14	0.5471	0.0440	1.00	4.4	2717	8	2757	76	2813	183
A1926-8a	189	182	0.00	10990	0.1872	0.0008	13.85	1.09	0.5365	0.0424	1.00	2.3	2718	7	2739	75	2769	178
A1926-12a	118	118	0.00	4754	0.1874	0.0009	14.28	1.16	0.5528	0.0448	1.00	5.3	2719	7	2769	77	2837	186
A1926-16b	100	100	0.00	3008	0.1874	0.0009	14.43	1.18	0.5584	0.0454	1.00	6.4	2719	8	2778	77	2860	188
A1926-12c	195	199	0.00	7650	0.1874	0.0007	14.51	1.18	0.5613	0.0456	1.00	6.9	2720	6	2783	77	2872	188
A1926-7a	238	223	0.09	6464	0.1877	0.0009	13.34	1.04	0.5152	0.0403	1.00	-2	2722	7	2704	74	2679	171
A1926-4a	262	247	0.01	6395	0.1878	0.0009	13.63	1.07	0.5265	0.0412	1.00	0.2	2723	7	2724	74	2727	174
A1926-18a	416	417	0.00	15644	0.1878	0.0008	14.43	1.18	0.5574	0.0454	1.00	6.1	2723	7	2779	77	2856	188
A1926-2a	180	173	0.00	6551	0.1880	0.0009	13.81	1.08	0.5329	0.0418	1.00	1.3	2724	7	2737	74	2754	176
A1926-17a	105	108	0.00	6052	0.1880	0.0009	14.78	1.22	0.5704	0.0470	1.00	8.5	2724	8	2801	78	2910	193
A1926-10a	382	399	0.00	14307	0.1885	0.0008	15.06	1.24	0.5796	0.0476	1.00	10	2729	7	2819	78	2947	194
A1926-14a	189	183	0.00	6382	0.1887	0.0009	14.00	1.12	0.5383	0.0428	1.00	2.1	2730	7	2750	76	2776	179

LA-MCICPMS measurements were made using 35µm laser spot and GJ1 (609 Ma) and A382 (1877 Ma) standards (before June 2010) or 25µm spot and GJ1 and A1772 (2712 Ma) standards (after June 2010)
$^{206}Pb_c$(%): percentage of common 206Pb in measured 206Pb calculated from the 204Pb signal using age-related common lead after model by Stacey&Kramers (1975)
Errors are 1-sigma absolute
Rho: Correlation of Pb/U errors
Some analyses with high common lead are not used in evaluation (strikethrough).

Appendix 4. SIMS U-Th-Pb data.

Sample	Spot	% $^{206}Pb_c$	ppm U	ppm Th	$^{232}Th/^{238}U$	ppm $^{206}Pb^*$	(1) $^{206}Pb/^{238}U$ Age		(1) $^{207}Pb/^{206}Pb$ Age		% Dis-cordant	(1) $^{207}Pb^*/^{206}Pb^*$	±%	(1) $^{207}Pb^*/^{235}U$	±%	(1) $^{206}Pb^*/^{238}U$	±%	err corr
A788 Polvilampi felsic rock																		
	A788.1.1	0.14	231	103	0.46	103	2686	25	2791	7	4	0.1957	0.45	13.95	1.2	0.5169	1.1	0.93
	A788.2.1	0.27	217	85	0.41	94	2632	22	2786	8	6	0.1951	0.48	13.57	1.1	0.5043	1	0.91
	A788.3.1	0.41	192	68	0.37	80	2550	22	2770	9	8	0.1933	0.53	12.93	1.2	0.4852	1.1	0.89
	A788.4.1	0.24	235	81	0.36	101	2604	22	2800	7	7	0.1969	0.45	13.51	1.1	0.4977	1	0.92
	A788.5.1	0.30	165	83	0.52	74	2702	24	2801	9	4	0.1970	0.54	14.14	1.2	0.5205	1.1	0.89
	A788.6.1	0.30	95	28	0.30	44	2776	26	2779	11	0	0.1944	0.7	14.42	1.4	0.5383	1.2	0.86
	A788.7.1	0.07	483	186	0.40	213	2667	22	2786	5	4	0.1952	0.29	13.79	1	0.5124	1	0.96
	A788.8.1	0.17	215	93	0.45	97	2728	23	2767	8	1	0.1929	0.46	14.01	1.1	0.5268	1	0.92
	A788.9.1	0.18	259	177	0.71	110	2591	22	2791	9	7	0.1957	0.56	13.35	1.2	0.4947	1.1	0.88
	A788.10.1	0.57	153	55	0.38	67	2649	25	2772	12	4	0.1935	0.75	13.56	1.4	0.5083	1.1	0.83
	A788.11.1	0.31	122	43	0.37	55	2700	25	2803	10	4	0.1972	0.63	14.15	1.3	0.5203	1.1	0.87
	A788.12.1	0.77	181	115	0.65	80	2649	24	2783	10	5	0.1948	0.6	13.65	1.2	0.5082	1.1	0.88
	A788.13.1	0.29	198	82	0.43	89	2698	24	2788	8	3	0.1953	0.48	14.00	1.2	0.5196	1.1	0.91
	A788.14.1	0.24	250	106	0.44	109	2629	22	2786	7	6	0.1952	0.43	13.55	1.1	0.5036	1	0.92
	A788.15.1	0.17	140	47	0.35	62	2699	24	2801	9	4	0.1969	0.56	14.11	1.2	0.5199	1.1	0.89
	A788.16.1	0.15	108	32	0.30	50	2773	26	2790	10	1	0.1956	0.64	14.49	1.3	0.5374	1.1	0.87
A1748 Aarreniemi. Tipasjärvi metagreywacke																		
	A1748.1.1	0.02	121	112	0.95	55	2737	30	2752	9	1	0.1911	0.6	13.94	1.4	0.529	1.3	0.92
	A1748.2.1	0.03	514	151	0.30	233	2730	26	2746	5	1	0.1905	0.3	13.85	1.2	0.527	1.2	0.97
	A1748.3.1	0.34	171	127	0.76	72	2559	29	2744	14	7	0.1903	0.9	12.78	1.6	0.487	1.4	0.85
	A1748.4.1	1.30	191	176	0.95	87	2701	44	2741	21	1	0.1899	1.3	13.62	2.4	0.520	2.0	0.85
	A1748.5.1	0.56	301	155	0.53	132	2642	28	2827	12	7	0.2001	0.7	13.98	1.5	0.507	1.3	0.87
	A1748.6.1	-0.00	63	40	0.66	30	2847	40	2746	18	-4	0.1905	1.1	14.58	2.1	0.555	1.7	0.84
	A1748.7.1	1.35	188	175	0.96	82	2613	30	2737	22	5	0.1894	1.3	13.05	1.9	0.500	1.4	0.73
	A1748.8.1	1.21	216	172	0.83	92	2560	28	2750	15	7	0.1909	0.9	12.84	1.6	0.488	1.3	0.84
	A1748.9.1	0.95	209	116	0.57	92	2633	30	2747	25	4	0.1906	1.5	13.26	2.1	0.505	1.4	0.67
	A1748.10.1	0.37	346	177	0.53	141	2496	27	2707	12	8	0.1860	0.7	12.12	1.5	0.473	1.3	0.87
	A1748.11.1	0.46	380	296	0.81	171	2703	28	2728	10	1	0.1883	0.6	13.53	1.4	0.521	1.3	0.90
	A1748.12.1	1.46	177	94	0.55	79	2655	31	2726	19	3	0.1882	1.1	13.22	1.8	0.510	1.4	0.79
	A1748.12.2	2.09	293	256	0.90	110	2278	26	2710	17	19	0.1863	1.0	10.89	1.7	0.424	1.4	0.81
A1753 Arola quartzite (55-PTP-03)																		
	55.11.1	0.17	408	341	0.86	170	2550	43	2680	6	5	0.1830	0.38	12.25	2.1	0.485	2	0.98
	55.13.1	0.53	100	72	0.74	45	2694	45	2683	16	-0	0.1833	0.98	13.11	2.3	0.519	2.1	0.90
	55.21.1	0.28	286	213	0.77	115	2462	40	2686	8	8	0.1836	0.47	11.77	2	0.465	2	0.97
	55.4.1	0.49	127	92	0.74	57	2674	44	2693	13	1	0.1845	0.8	13.08	2.2	0.514	2	0.93
	55.16.1	0.18	260	145	0.58	114	2663	43	2697	8	1	0.1849	0.49	13.04	2	0.511	2	0.97
	55.3.1	0.37	283	217	0.79	113	2457	40	2699	9	9	0.1850	0.52	11.83	2	0.464	2	0.97
	55.2.1	0.20	178	49	0.29	80	2714	44	2700	10	-1	0.1852	0.58	13.37	2.1	0.523	2	0.96
	55.8.1	0.65	161	113	0.73	64	2433	41	2701	12	10	0.1853	0.72	11.71	2.1	0.459	2	0.94
	55.7.1	0.19	208	109	0.54	93	2699	44	2707	9	0	0.1860	0.51	13.33	2	0.520	2	0.97
	55.18.1	0.66	68	26	0.40	31	2743	47	2716	18	-1	0.1870	1.1	13.67	2.4	0.530	2.1	0.89
	55.12.1	0.48	103	58	0.58	47	2732	46	2729	14	-0	0.1885	0.83	13.72	2.2	0.528	2	0.93
	55.5.1	0.69	40	40	1.01	18	2730	50	2748	26	1	0.1906	1.6	13.86	2.7	0.527	2.3	0.82

Appendix 4. cont.

Sample	Spot	% $^{206}Pb_c$	ppm U	ppm Th	$^{232}Th/^{238}U$	ppm $^{206}Pb^*$	(1) $^{206}Pb/^{238}U$ Age		(1) $^{207}Pb/^{206}Pb$ Age		% Dis-cordant	(1) $^{207}Pb^*/^{206}Pb^*$	±%	(1) $^{207}Pb^*/^{235}U$	±%	(1) $^{206}Pb^*/^{238}U$	±%	err corr
A1753 Arola quartzite (55-PTP-03)																		
	55.17.1	0.21	200	54	0.28	92	2774	45	2795	8	1	0.1962	0.5	14.54	2	0.538	2	0.97
	55.20.1	0.27	177	140	0.82	85	2849	46	2807	9	-1	0.1977	0.55	15.15	2.1	0.556	2	0.96
	55.6.1	0.17	529	422	0.82	239	2720	43	2809	5	3	0.1980	0.31	14.32	2	0.525	1.9	0.99
	55.9.1	0.56	84	116	1.42	41	2877	54	2932	14	2	0.2135	0.86	16.55	2.5	0.562	2.3	0.94
	55.15.1	0.14	397	113	0.29	201	2982	46	2952	5	-1	0.2161	0.32	17.52	2	0.588	1.9	0.99
	55.22.1	0.34	161	217	1.39	85	3079	52	3195	7	4	0.2517	0.46	21.25	2.2	0.612	2.1	0.98
	55.19.1	0.20	164	90	0.57	89	3160	50	3196	7	1	0.2518	0.45	21.96	2.1	0.633	2	0.98
	55.1.1	0.11	275	234	0.88	146	3105	49	3200	6	3	0.2525	0.36	21.54	2	0.619	2	0.98
	55.10.1	0.16	130	150	1.19	72	3175	51	3211	8	1	0.2541	0.52	22.30	2.1	0.636	2	0.97
	55.14.1	0.10	315	153	0.50	189	3414	52	3450	4	1	0.2960	0.29	28.50	2	0.698	2	0.99

Errors are 1-sigma; Pb_c and Pb^* indicate the common and radiogenic portions. respectively.
Error in Standard calibration was 0.5-0.9%(not included in above errors but required when comparing data from different mounts).
(1) Common Pb corrected using measured ^{204}Pb.
Analysed at VSEGEI. St. Petersburg